

# Investigations on the formation of porous membranes during non-solvent induced phase separation

Von der Naturwissenschaftlichen Fakultät  
der Gottfried Wilhelm Leibniz Universität Hannover

zur Erlangung des Grades  
**Doktorin der Naturwissenschaften**  
*Dr. rer. nat.*

genehmigte Dissertation  
von

Catharina Kahrs, M. Sc.

2020

Die vorliegende Arbeit wurde im Zeitraum von Januar 2017 bis Januar 2020 im Arbeitskreis von Professor Dr. Thomas Scheper am Institut für Technische Chemie der Gottfried Wilhelm Leibniz Universität Hannover in Kooperation mit der Firma Sartorius Stedim Biotech GmbH angefertigt.

**Referent:** Professor Dr. Thomas Scheper  
Institut für Technische Chemie  
Gottfried Wilhelm Leibniz Universität Hannover

**Korreferent:** PD Dr. Sascha Beutel  
Institut für Technische Chemie  
Gottfried Wilhelm Leibniz Universität Hannover

**Tag der Promotion:** 18. Juni 2020

## Danksagung

An dieser Stelle möchte ich mich recht herzlich bei allen bedanken, die mich während der Promotion und der Anfertigung dieser Arbeit unterstützt haben.

Mein besonderer Dank gilt Professor Dr. Thomas Scheper für die Eröffnung der Möglichkeit dieses hochinteressantes Thema zu bearbeiten, sowie für die Übernahme der Betreuung, die hilfreiche Unterstützung und jegliche Ratschläge. Außerdem möchte ich mich bei PD Dr. Sascha Beutel für die Übernahme des Korreferats bedanken. Darüber hinaus danke ich PD Dr. Ulrich Krings für die Übernahme des Drittgutachtens und des Vorsitzes der Prüfungskommission, sowie Dr. Janina Bahnmann für das kurzfristige Einspringen als Prüferin für die Disputation.

Weiterhin möchte ich mich herzlichst bei Jan Schwellenbach für die exzellente Betreuung und die großartige Unterstützung während meiner Zeit bei der Sartorius Stedim Biotech GmbH bedanken. Insbesondere möchte ich ihm für die kritischen Diskussionen und die hilfreichen Anregungen danken, die maßgeblich zur Anfertigung dieser Arbeit beigetragen haben. Hervorzuheben sind außerdem sein einzigartiger Humor und die aufbauenden Worte, die mir vor allem in kritischen Phasen zum nötigen Durchhaltevermögen und einer positive Einstellung verholfen haben.

Ein herzlicher Dank geht an die Kollegen der Firma Sartorius und insbesondere an die Mitarbeiter der Abteilung SMFE für das hervorragende Arbeitsklima, die Hilfsbereitschaft und Unterstützung, sowie für die angenehme Atmosphäre im Labor. Ganz besonders möchte ich dabei Sandra Otto und Rebekka Schmidt für die tolle Zusammenarbeit innerhalb der Ultrafiltrationsgruppe danken. Ich bedanke mich bei Heike Hepprich und Wulf Linke für die Unterstützung bei der Anfertigung der REM-Aufnahmen, bei Joachim König für die zahlreichen Gaschromatografie-Messungen sowie bei Björn Hansmann und Michael Metze für die Zeit und Mühe, Teile der Arbeit Korrektur zu lesen. Außerdem möchte ich den Doktoranden bei Sartorius für die anregenden Diskussionen und die stets gute Arbeitsatmosphäre im Büro danken.

Ein außerordentlicher Dank gilt den Studenten, die ich im Rahmen von Praktika und Abschlussarbeiten betreuen durfte. Dazu zählen Christian Fricke, Thorben Gühlstorf, Pascal Kircher, Lasse Guericke, Chiara Knoblich, Kristina Eisfeld, Sarah Therre, Anika Mahler und Lisa Schick.

Nicht zuletzt möchte ich mich bei meiner Familie und insbesondere bei Magnus bedanken. Die bedingungslose Unterstützung und der ständige Zuspruch haben mir die Kraft und Motivation gegeben, mein Ziel nicht aus den Augen zu verlieren.

## Zusammenfassung

Eine gängige Methode zur Herstellung von Membranen ist das Fällbadverfahren. Dabei wird ein Polymer in einem geeigneten Lösungsmittel gelöst und anschließend in einem Fällbad mit einem geeigneten Nichtlösungsmittel wieder ausgefällt. Während dieses Prozesses findet eine Phasenseparation statt, die zur Ausbildung einer porösen Struktur führt. Diese poröse Struktur ermöglicht die selektive Trennung von Stoffgemischen nach dem Größenausschlussprinzip. Die zurzeit hierbei verwendeten Lösungsmittel haben den Nachteil, dass sie als bedenklich für Mensch und Umwelt eingestuft sind. Daher besteht ein großes Interesse darin, die konventionellen Lösungsmittel bei der Membranherstellung durch ungefährlichere Stoffe zu ersetzen. Die Herausforderung hierbei ist, dass trotz einer Lösungsmittelumstellung die Membraneigenschaften weiterhin kontrollierbar sein müssen. Um die Kontrolle der Eigenschaften durch die Anpassung der beeinflussenden Faktoren zu gewährleisten, ist deshalb ein gutes Verständnis des Prozesses nötig.

Im ersten Teil der Arbeit wurde eine Methode zur Charakterisierung der Mischphasenthermodynamik von Polymerlösungen entwickelt. Im Zuge einer Validierung dieser Methode konnte gezeigt werden, dass die Methode verlässliche und reproduzierbare Daten liefert, welche im Vergleich zur bisher gängigen Methode einen höheren Informationsgehalt haben. Zudem wurde die Methode zur Charakterisierung eines gängigen Polymerlösungssystems zur Herstellung von Polymermembranen angewandt und die Ergebnisse mit denen der bisher verwendeten Trübungstiteration verglichen.

Im zweiten Teil dieser Arbeit wurde eine vergleichende Untersuchung des Einflusses von polymeren Additiven auf die Membranbildung und die resultierenden Membraneigenschaften durchgeführt. Dabei lag der Fokus insbesondere auf dem Vergleich zwischen konventionellen und alternativen Lösungsmitteln, um eine Umstellung auf umweltverträglichere Lösungsmittel zu ermöglichen. Es konnte gezeigt werden, dass es in Abhängigkeit des Lösungsmittels Unterschiede in den zu beobachtenden Effekten gibt. Jedoch können durch das erlangte mechanistische Verständnis Anpassungen im Herstellungsprozess vorgenommen werden, sodass die Membraneigenschaften kontrollierbar bleiben.

Im dritten Teil dieser Arbeit wurden ebenfalls die Einflüsse verschiedener Parameter auf den Fällbadprozess mit verschiedenen Lösungsmitteln untersucht. Um ein Gesamtbild der Einflussfaktoren zu erhalten, wurden die Auswirkungen von verschiedenen Nichtlösungsmitteln in der Lösung sowie von unterschiedlichen Polymerkonzentrationen und Fällungsbedingungen untersucht. Es konnte gezeigt werden, dass alle drei Faktoren in den untersuchten Lösungsmitteln eine Auswirkung auf die Eigenschaften der hergestellten Membran haben. Zusätzlich konnte erneut demonstriert werden, dass die Wahl des Lösungsmittels eine große Auswirkung auf die Ausprägung der jeweiligen Effekte hat.

**Schlagwörter:** Phasenseparation, Membranherstellung, alternative Lösungsmittel, Fällbadverfahren, Membraneigenschaften

## Abstract

A common method for the production of membranes is immersion precipitation. For this, a polymer is dissolved in a suitable solvent and then precipitated by immersing it into a precipitation bath consisting of a proper non-solvent. Induced by an exchange between the solvent and the non-solvent phase separation occurs, which leads to the formation of a porous structure. The resulting structure allows the selective separation of a mixture of substances, which is based on a size exclusion mechanism. At the moment, the disadvantage of the commonly used solvents for membrane fabrication is their classification as being hazardous for humans and the environment. This is the reason why there is an increased interest in replacing the conventional solvents by less harmful alternatives. However, the challenge is that despite changing the solvent, the membrane properties must still be controllable. In order to ensure the required control of the resulting membrane properties by adjusting the influencing parameters, it is essential that the membrane fabrication process is well understood.

In the first part of this work a method for the characterization of the thermodynamics of polymer solution phase equilibria was developed. In course of the validation of this method, it could be shown that the method provides reliable and reproducible data, which in comparison to the previously established method provides a higher information content. Furthermore, the method was applied for the characterization of a polymer solution system, which is commonly used for membrane preparation, and the results were compared to those of the previously used cloud point titration method.

In the second part of this work a comparative study on the influences of polymeric additives on the membrane formation process and the resulting membrane properties was conducted. The focus was particularly laid on the comparison between conventional and alternative solvents in order to allow a substitution of hazardous solvents through less harmful alternatives. It could be shown that there are differences in the observed effects in dependence of the applied solvent. However, it could also be demonstrated that the gained mechanistic understanding can be used for adjusting the membrane preparation process, so that the properties of the fabricated membranes remain controllable.

The third part of this work also focused on the influence of variations during the immersion precipitation process using different solvents. In order to obtain an overall picture of the influencing factors on membrane formation, the effects of non-solvent additives in the solution, of variations in the polymer concentration and of altered precipitation conditions were investigated. It could be shown that all three factors have an influence on the characteristics of the fabricated membranes in the investigated solvent systems. In addition, it was repeatedly demonstrated that the choice of the solvent is of high importance for the manifestation of the respective effects.

**Key words:** Phase separation, membrane production, alternative solvents, immersion precipitation, membrane characteristics

## Table of contents

Danksagung .....	I
Zusammenfassung .....	II
Abstract .....	III
Table of contents .....	IV
1 Introduction .....	1
2 Scope of the Research .....	3
3 Theoretical Background .....	4
3.1 Membranes.....	4
3.1.1 Definition and function .....	4
3.1.2 Classification .....	5
3.1.3 Ultrafiltration membranes .....	6
3.1.4 Membrane production methods .....	8
3.2 Immersion precipitation .....	9
3.2.1 Principle of immersion precipitation.....	9
3.2.3 Technical implementation .....	10
3.3 Structure forming mechanisms.....	11
3.3.1 Phase diagram .....	11
3.3.2 Demixing mechanisms .....	14
3.3.3 Coarsening mechanisms .....	16
3.3.4 Formation of the skin layer of ultrafiltration membranes .....	17
3.3.5 Formation of macrovoids.....	18
3.3.6 Solidification .....	19
3.4 Sustainable membrane processes .....	20
3.4.1 REACH regulations .....	20
3.4.2 Green Chemistry in membrane technology.....	20
3.5 State-of-the-Art .....	22
3.5.1 Characterization of polymer solution thermodynamics.....	22
3.5.2 Influences of the polymer solution composition .....	22
3.5.3 Increasing membrane sustainability .....	26
4 Experimental Part .....	27
4.1 Thermodynamic analysis of polymer solutions.....	30
4.2 Influences of polymeric additives in different solvent systems .....	49
4.3 Influences of casting solution composition and precipitation conditions.....	75
5 Summary and Conclusion .....	101

6	References .....	103
7	Appendix.....	113
7.1	List of Abbreviations .....	113
7.2	List of Figures.....	114
8	List of Publications .....	115
8.1	Journal Articles.....	115
8.2	Conference Contributions.....	116
9	Curriculum Vitae .....	117

# 1 Introduction

Nowadays, an increasing number of pharmaceuticals is manufactured by means of biotechnology. By definition, biotechnology is the use of living organisms, biological processes or biological system for the manufacturing of agricultural, industrial or medical products. Hence, any biotechnologically manufactured pharmaceuticals like antibodies, vaccines or biosynthetic proteins are derived from biological sources such as cell lines or blood plasma. For this reason, biopharmaceuticals have to be purified before use to remove any hazardous contaminants. Furthermore, the target molecule has to be concentrated and formulated into the final product form. Consequently, different methods are applied after the actual production step to concentrate, sterilize and finalize the product. Several of these purification steps involve the application of membranes. Especially for the removal of impurities and the concentration of the product polymeric membranes are frequently used.

Polymeric membranes are filters made of synthetic polymers. They have a porous structure and are capable of separating mixtures of substances. This selective separation of particles is based on a sieving effect, so that the separation of different types of particles is dependent on the size of the membrane pores and the particles. Depending on the size of the product and the substances to be separated, the pore sizes have to be strictly controlled during membrane fabrication.

For the production of polymeric membranes with various pore sizes different methods are available. However, one of the most commonly applied methods is the immersion precipitation process. In preparation for this process, a selected polymer is dissolved in a suitable solvent. Subsequently, the resulting homogeneous solution is applied to a support with a defined thickness and immersed into a precipitation bath consisting of an appropriate non-solvent. Through the exchange between the solvent from the polymer film and the non-solvent from the precipitation bath the composition of the polymer solution changes. When a certain composition is reached, the homogeneous solution separates into two phases, which finally leads to the formation of the porous membrane structure. One of the phases mainly consists of the polymer and is therefore responsible for the formation of the membrane matrix. In contrast, the other phase mainly consists of solvent and non-solvent and is responsible for the formation of the pores.

The resulting membrane structure ultimately determines the properties of the membrane. The most important membrane characteristics include the flux rate, the separation efficiency for the molecule of interest, as well as the mechanical and chemical stability. All of these properties are dependent on the conditions during immersion precipitation and can be regulated by controlling the influencing variables. These include the precipitation conditions as well as the polymer solution composition.



As mentioned, in dependence on the application certain demands are placed on the membrane. In order to specifically obtain the required features, the control parameters during membrane fabrication have to be defined and the mechanisms behind them well understood. However, since the membrane formation process by immersion precipitation is very complex, it is still not fully understood and in some points even controversially discussed. Therefore, there is still a high need for improving the understanding of the membrane formation via immersion precipitation and its underlying mechanisms. Furthermore, as part of regulatory assessments of existing and new chemicals, the common solvents for membrane production have recently been classified as hazardous to humans and the environment. This is why there is an increased interest in replacing the existing solvents with less hazardous ones without changing the relevant membrane properties. Since each solvent has its individual properties, a one-by-one exchange is not possible. To hold the membrane properties constant when replacing the solvent, other control parameters have to be adjusted instead. This once again requires an excellent understanding of membrane formation and appropriate investigations on potentially new alternative solvents.

## 2 Scope of the Research

The aim of this work is to gain an improved understanding of the mechanisms, which impact the membrane formation during immersion precipitation. In addition, the work shall contribute to the creation of a holistic picture on non-solvent induced membrane formation, which in particular includes the identification of the significant control parameters of the process and their mutual interaction.

Since membrane formation via non-solvent induced phase separation is dependent on both, the thermodynamics of the polymer solution for the production of polymeric membranes and the kinetics of the solvent exchange in the precipitation bath, these two aspects will be focused in this work. For this purpose, a method is developed, which allows an informative characterization of the polymer solution thermodynamics. Based on a conventional polymer solution system the developed method is validated and applied for creating the phase diagram of this system at different experimental conditions. Furthermore, various controllable parameters are varied during the manufacturing of polyethersulfone membranes in order to study their influences on the membrane formation process. Therefore, two comparative studies are conducted which investigate the impact of variations in concentration and type of polymeric additives on one hand, and on concentration and type of non-solvent additives, polymer concentration and precipitation conditions on the other hand. Additionally, both studies include a comparison between different applied solvent systems where both, conventional and alternative solvents are used. Apart from monitoring the polymer solution viscosity and the solution thermodynamics in dependence of the different applied variables, the membrane properties to be investigated include the permeability, the protein retention capacity, the surface characteristics and the cross-section structure of each membrane prototype.

All in all, the main goals of this work are to improve the understanding of the membrane formation mechanisms and to evaluate potential alternative solvents for membrane fabrication in comparison to conventional solvents. Therefore both, the thermodynamic and kinetic aspects of membrane formation are addressed in this work.

### 3 Theoretical Background

#### 3.1 Membranes

##### 3.1.1 Definition and function

A membrane is defined as a thin selective barrier between two different fractions [1,2]. On one hand, a membrane enables the spatial segregation of one or more components from each other. It can for instance separate a compartment from an external environment as it is the case in a biological cell [3]. On the other hand, a membrane can also be used for the selective separation of different components from a mixture of substances. An application example is the selective separation of particles from a suspension during a biotechnological purification process. In this case the aim is the removal of small molecules such as proteins, viruses or bacteria from an aqueous solution containing the desired target molecule [4]. The selectivity of the membrane defines for which substances the membrane is permeable and for which it is impermeable. If the membrane is permeable for at least one component of the filtration medium, the presence of an adequate driving force enables the separation of the substances within the feed as it is schematically depicted in Figure 1 [1,5].

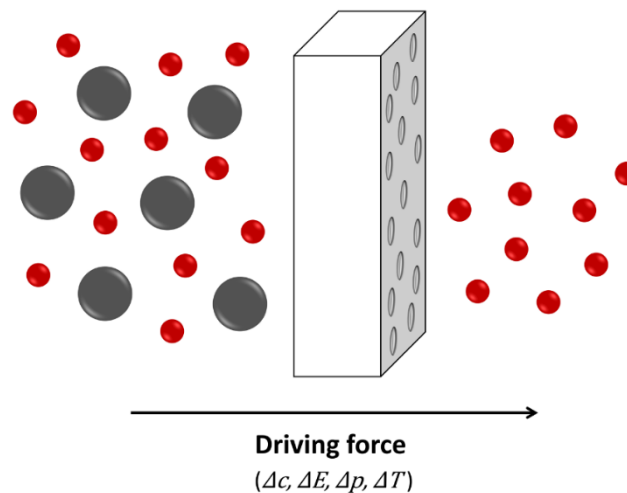


Figure 1 Schematic illustration of a membrane separation process (adapted from Mulder) [1].

The driving force determines the flow direction of the feed stream as well as the duration of the filtration [6]. Depending on the application of the process different driving forces can be applied [7]. The most prevalent driving force in membrane technology is a pressure difference ( $\Delta p$ ) between both sides of the membrane. Pressure-driven membrane processes are applied for water purification and desalination, for the downstream processing of pharmaceuticals, as well as for sterilization of drugs and foods [8]. In contrast, processes with concentration gradients ( $\Delta c$ ) or differences in the electrochemical potential ( $\Delta E$ ) as driving force are mainly used for dialysis. At last, temperature differences ( $\Delta T$ ) are commonly applied as driving force in membrane distillation [5–7].

### 3.1.2 Classification

In general, membranes can be classified based on their origin. They can have a biological source, as it is the case for cell membranes, or they can be technically derived synthetic products [3,9]. This work focuses exclusively on synthetic membranes. Due to the diversity of synthetic membranes, they can be further classified with respect to different characteristics. These include the bulk material they are made of, the separation properties such as the mean pore size or the molecular weight cut-off, and the morphological structure of the membrane cross-section [2,10].

With respect to the bulk material membranes can be divided up into two main categories: Organic and inorganic membranes [1]. Inorganic membranes include products consisting of oxides, metals, or ceramics. In comparison to organic membranes, the use of inorganic membranes enables higher selectivity and higher permeability during filtration. Additionally, they are much more resistant towards extreme filtration conditions such as extremely high temperatures or extreme pH values [11,12]. Nonetheless, in industrial production the dominating materials for the production of filtration membranes are different organic polymers [13]. Cellulose derivatives, polyethersulfone (PES) and polysulfone (PSf), as well as polyamide (PA) and polyvinylidene fluoride (PVDF) are among the most commonly applied organic membrane materials [14]. Compared to inorganic compounds, the advantages of polymeric materials are their broad availability, the lower material prices and a larger range of application possibilities. However, the downside of polymeric membranes is their limited resistance to extreme temperatures, pH conditions and certain organic solvents [12,15,16].

Another possibility to classify membranes is based on their cross-sectional morphology (Figure 2). In general, membranes can have a dense or a porous morphology [1]. In case of porous membranes one can further distinguish between a symmetric and an asymmetric pore size gradient. An additional variant is the composite membrane. It consists of both, a dense top layer responsible for the separation efficiency as well as a porous support responsible for an increased stability [12,13,17].

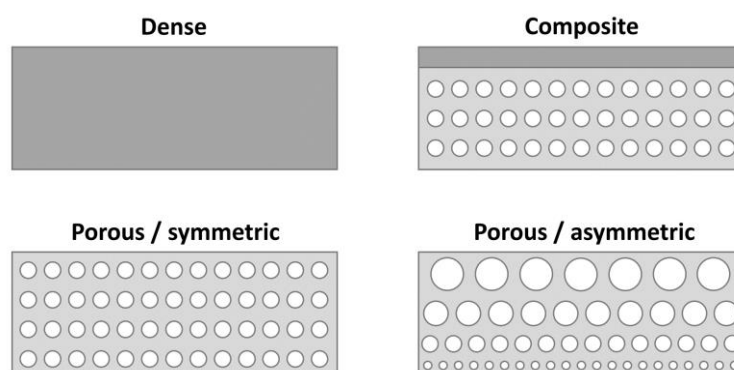


Figure 2 Schematic illustration of membrane cross-section morphologies (adapted from Rösler) [18].

While the separation mechanism of dense membranes is based on a solution-diffusion model, as it is for example applied in pervaporation or gas separation, the separation of mixtures using porous membranes is mainly based on the principle of size exclusion [19–22]. However, the sieving effect of porous membranes may be supported by adsorptive effects [23,24]. Furthermore, it may also be completely based on adsorptive effects as it is the case for membrane adsorbers [13,21,25].

Since the application area of size-exclusion based porous membranes strongly depends on the separation properties of the filter, these membranes are commonly further classified by their pore size or their molecular weight cut-off [22]. Depending on the range of the pore sizes and on the respective molecules which shall be separated from each other, one can distinguish between reverse osmosis, nanofiltration, ultrafiltration, virus filtration and microfiltration (Figure 3) [1,4].

Reverse osmosis	Nanofiltration	Ultrafiltration	Virus filtration	Microfiltration	
Amino acids Salts Sugar	Divalent Ions Amino acids Antibiotics	Colloids Peptides Proteins	Bacteria Viruses	Bacteria Cell debris Intact cells	<b>Feed / Retentate</b>
.....					
Water	Salts Water	Amino acids Buffer components	Buffer components Proteins	Colloids Proteins Salts Viruses	<b>Permeate</b>
<b>&lt; 0.1 nm</b>	<b>0.1 - 1 nm</b>	<b>1 - 100 nm</b>	<b>20 - 200 nm</b>	<b>&gt; 0.1 µm</b>	

Figure 3 Classification of size-exclusion based membrane processes (adapted from van Reis and Zydney) [4].

The areas of applications for reverse osmosis and nanofiltration mainly include the purification of wastewater, water desalination and drinking water purification [2,8]. In contrast, ultrafiltration, virus filtration and microfiltration are primarily applied for the purification of biotechnologically manufactured drugs such as antibodies or vaccines, as well as for the clarification and sterilization of beverages and other foods [21,26].

### 3.1.3 Ultrafiltration membranes

This work addresses the production of porous polymeric membranes. The focus was laid on the manufacturing of ultrafiltration membranes, since it was chosen as model process for all investigations. Ultrafiltration membranes typically feature a separation range of molecule sizes varying from 1 nm up to 100 nm [17]. Furthermore, they can be characterized by a porous asymmetric structure consisting of a dense separation layer and a porous support layer (Figure 4) [16].

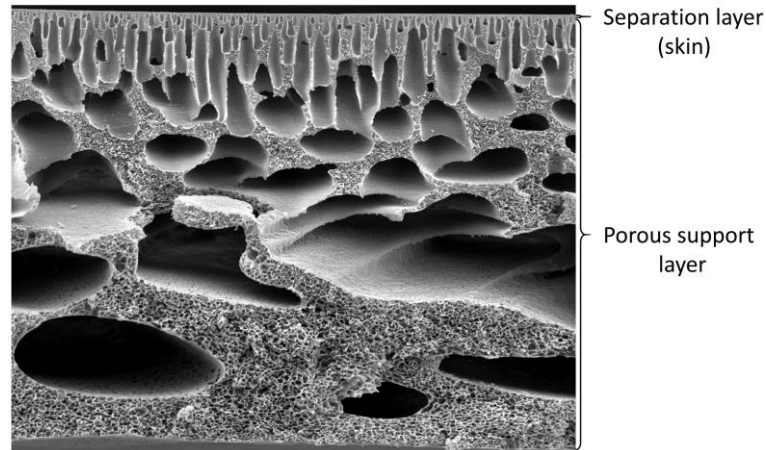


Figure 4 Scanning electron microscopy image showing the typical structure of an ultrafiltration membrane.

The so-called skin is located on the air-facing side of the membrane, where the side refers to the orientation of the membrane during the production process. It is the selective layer, which is responsible for the separation performance of the filter and which is mainly contributing to the flow resistance of the filter [16,27]. The skin is supported by a porous sublayer, which can be characterized by an increasingly growing pore size gradient towards the support-facing side of the membrane [28,29]. It serves as a mechanical support for the skin layer, which typically has a thickness of only a few nanometers. However, at the same time it is also contributing to the flow resistance of the membrane and therefore influences the membrane permeability [4,5,30]. In general, the substructure can exhibit one of two different morphologies. On one hand it can consist of a complete sponge-like structure, which has a visible pore size gradient towards the bottom of the membrane. On the other hand, the structure can be dominated by a finger-like morphology, where the sponge-like regions are repeatedly interrupted by large holes, the so-called macrovoids [31–33]. The macrovoids significantly reduce the flow resistance of the membrane, but at the same time they also lower the mechanical stability of the filter [34,35]. The two typical cross-section morphologies are exemplary shown in Figure 5.

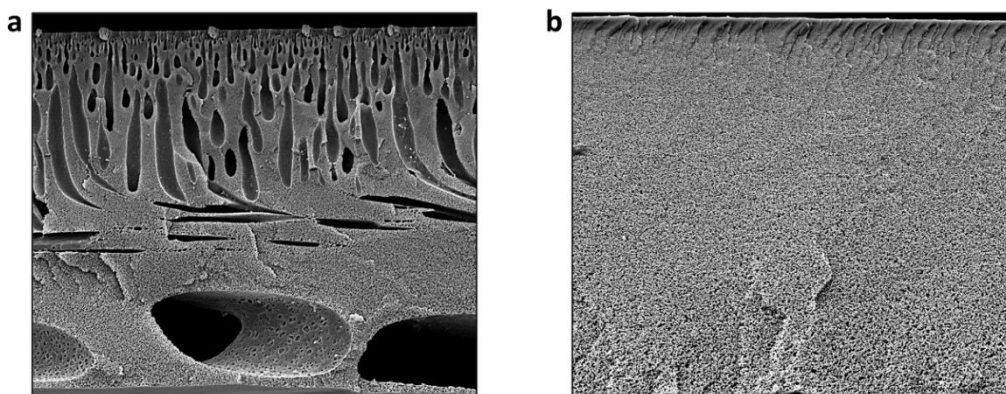


Figure 5 Scanning electron microscopy image of an ultrafiltration membrane with a finger-like (a) and a sponge-like (b) morphology.

Apart from applications in the food industry, such as for the clarification of juices, wine and beer, the purification of biopharmaceutical products is one of the main areas of application for ultrafiltration membranes [36–38]. Depending on the membrane characteristics and the respective process design, an ultrafiltration membrane may be used for concentration of the product or for the replacement of buffers and cell media [21,25]. According to the particular application area and to the size of the particles to be filtrated membranes with certain characteristics are required, especially with regard to their separation behavior [30].

In order to meet the requirements of the user as well as of regulatory agencies like the Food and Drug Association (FDA), the production process of ultrafiltration membranes has to be strictly controlled [39,40]. Therefore, it is essential that the process is very well known and understood [41]. In order to improve the understanding of the membrane formation process a lot of studies were conducted in the last decades [31,42]. However, for the basic understanding of the membrane formation mechanisms there is still room for improvement, since some of the past studies demonstrated contradictory results [43]. Furthermore, many studies on the production ultrafiltration membranes are limited to only one or at most a few single aspects, so that to date a holistic picture of membrane formation via immersion precipitation is missing.

### 3.1.4 Membrane production methods

There are several methods, which can be applied for the production of membranes. The selection of the appropriate production method depends on the starting material as well as on the desired product properties [44,45]. In case of inorganic materials, the starting material is often pressed from a powder to a plate and the pores are subsequently generated by sintering [11,22]. The same procedure can also be applied for the production of specific polymer membranes [44]. Furthermore, intentionally induced leaching of chemically less resistant components of the raw material is another possibility for producing inorganic membranes [11].

In addition to sintering of pressed polymer powder, polymeric membranes can also be produced by stretching or extruding films [21]. However, currently the most commonly applied method for the production of porous polymer membranes is based on phase separation of polymer solutions [46–48]. There are essentially four different mechanisms, which can be used to induce the phase separation: Non-solvent induced phase separation (NIPS), vapor induced phase separation (VIPS), evaporation induced phase separation (EIPS) and thermally induced phase separation (TIPS) [33,47]. During NIPS the contact of a homogeneous polymer solution to a suitable liquid non-solvent causes an exchange between the solvent in the polymer film and the precipitant in the so-called precipitation bath. In turn, this results in a compositional change, which ultimately leads to the phase separation of the polymer

solution [49–51]. In contrast, during VIPS the precipitant is absorbed from a gas phase containing the non-solvent. Therefore, the compositional change leading to phase separation is solely resulting from an uptake of the non-solvent [52,53]. In the case of EIPS, the change of the polymer film composition is caused by an evaporation of the volatile solvent from the polymer solution [54]. Finally, the TIPS method is based on the fact that the solvent is only able to dissolve the polymer at high or low temperatures. Consequently, a reduction or an increase of the temperature can induce the separation of the phases [32,49].

This work solely focuses on NIPS, which is one fundamental process step of the immersion precipitation method. Therefore, in the following this technique will be described in more detail.

## 3.2 Immersion precipitation

### 3.2.1 Principle of immersion precipitation

Among the different phase inversion techniques, immersion precipitation is one of the most commonly applied processes for the production of porous polymer membranes in industry [1,47]. It can be described as a combination of VIPS and NIPS, where a precise control of both mechanisms allows the production of membranes with a wide range of different properties [53,55]. The immersion precipitation process is schematically represented in Figure 6.

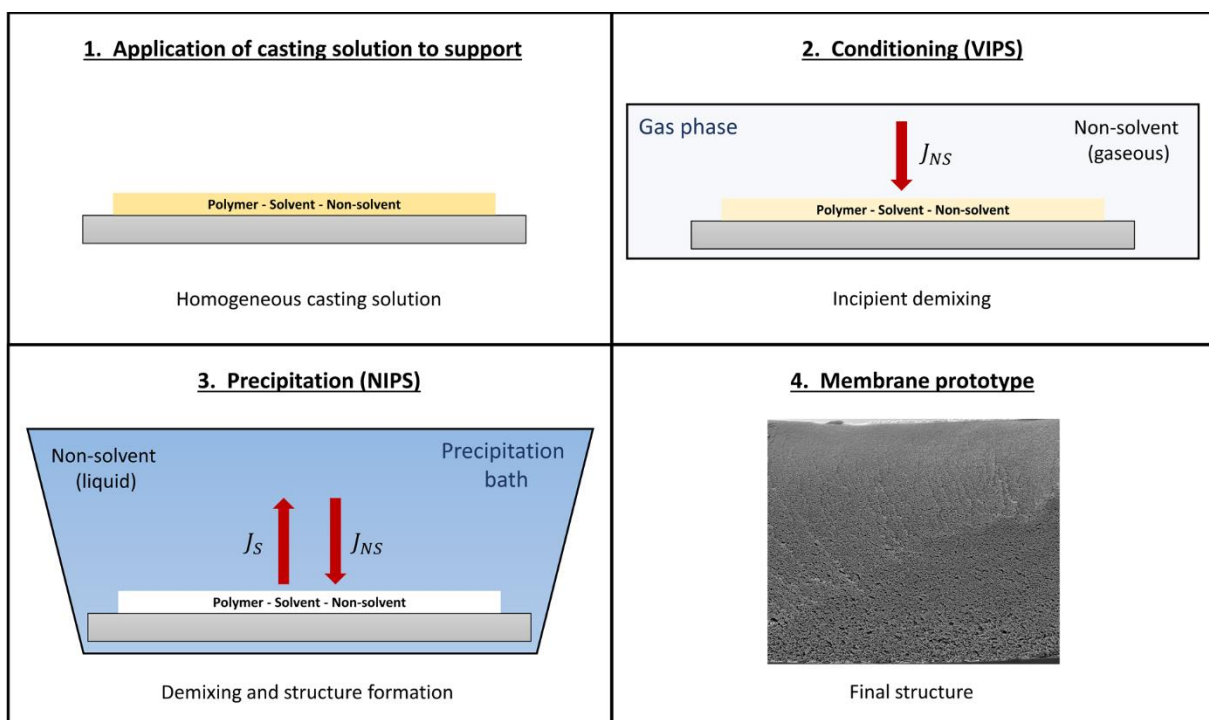


Figure 6 Schematic illustration of the different steps during the immersion precipitation process.



In the first step of the immersion precipitation process a previously prepared homogeneous polymer solution is applied to an appropriate support with a defined thickness [56]. For the production of membranes with coarser pore structures, as it is for example the case for microfiltration membranes, a so-called preconditioning step is implemented, which is based on the VIPS mechanism [53,57]. During this step the phase separation is induced from the top of the polymer film by introduction of the non-solvent from a gaseous phase into the polymer film [52]. The duration of this preconditioning step can be varied to control the porosity and the pore size of the resulting membrane [52,58]. However, after the VIPS step the phase separation process is usually not completely finished in a large part of the film. This is why the preconditioning is followed by an actual precipitation step [53]. Therefore, the support with the polymer film is immersed into a bath of non-solvent, so that NIPS can occur [51]. The exchange between the solvent from the polymer film and the non-solvent from the precipitation bath induces phase separation throughout the complete polymer film [59–61]. This results in the development of the structure until solidification sets in, which ultimately defines the final membrane morphology [62,63]. A prerequisite for the precipitation process is the insolubility of the membrane-forming polymer in the precipitation medium. In contrast, the solvent and the precipitating agent have to be miscible with each other in order to enable a bilateral diffusive mass transfer between non-solvent and solvent [42,49,64]. This diffusional exchange is driven by a gradient in the chemical potential [65]. When the solubility limit of the polymer in the polymer film is exceeded, so that an unstable composition in the film is achieved, phase separation occurs [66]. Thus, the combination of mass transport and phase separation determines the final membrane structure.

### 3.2.3 Technical implementation

For the technical implementation in an industrial scale the immersion precipitation process is realized by application of special membrane casting lines, which allow a continuous production process [1]. A schematic representation of an immersion precipitation casting line is shown in Figure 7.

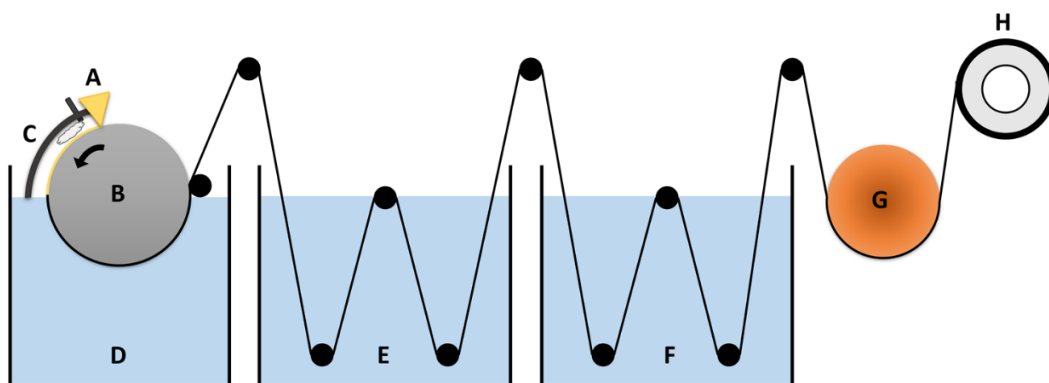


Figure 7 Schematic illustration of a membrane casting line for membrane production via immersion precipitation (adapted from Strathmann) [44].

For large scale implementation the casting solution is prepared in a large vessel. This solution usually consists of the polymer, the solvent, a small amount of the non-solvent and possibly additives. These raw materials are mixed in a temperature-controlled vessel with an engine-driven stirrer until a homogeneous solution is obtained. Afterwards, the solution is degassed in order to prevent defects within the membranes through air bubbles [67]. After pumping the casting solution from the vessel to the casting line, the solution is filtered over a filter cartridge to ensure the removal of any disturbing particles. Following that, the solution is applied onto a steel belt or drum (B) by a nozzle or a doctor blade system (A) with a defined thickness. Depending on the desired membrane properties, the film is then exposed to the preconditioning atmosphere (C), which contains a defined amount of the non-solvent. In case of membranes which have to be produced without any preconditioning, the VIPS step is omitted. After preconditioning, the medium with the polymer film is immersed into the precipitation bath (D), which is filled with liquid non-solvent. Within this bath the actual phase separation takes place. Subsequently, the membrane is moved through one or more rinsing tanks (E) and extraction reservoirs (F) via several deflection pulleys. This ensures the removal of possible extractables and leachables. Finally, the membrane is dried (G) and then winded up (H) for further processing [1,44,68].

### 3.3 Structure forming mechanisms

#### 3.3.1 Phase diagram

In general, a phase diagram is used to describe the behavior of a mixture of substances when either composition, pressure or temperature is changed, while the other two factors remain constant [69]. Therefore, a phase diagram can be used to display the thermodynamic state of a ternary polymer solution for membrane preparation, which consists of the membrane-forming polymer, an appropriate solvent and a proper non-solvent at constant pressure and temperature (Figure 8) [1,31].

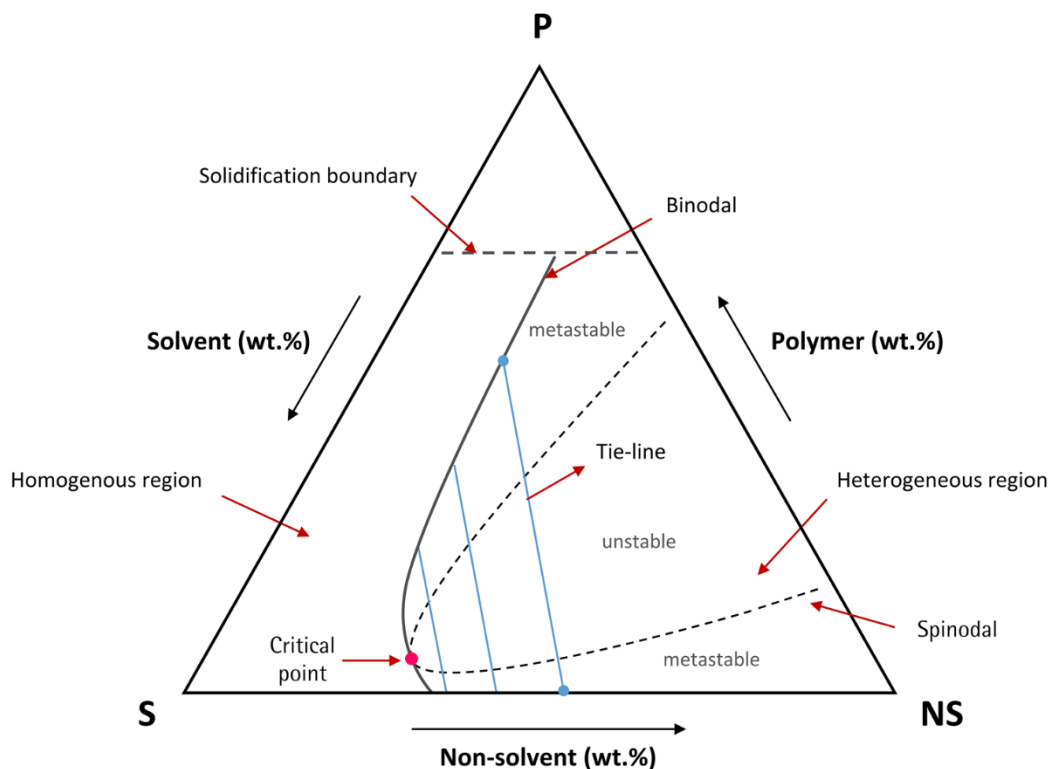


Figure 8 Representative phase diagram for the thermodynamic description of a ternary polymeric system at constant pressure and temperature (adapted from Mulder) [1].

While the corners of the ternary diagram represent the pure components, the sides of the triangle show the composition of binary mixtures. In case of binary mixtures, lines which run parallel to the opposite side of the triangle represent a constant share of one component. On the other hand, any thermodynamic state lying within the phase diagram indicates the mass fractions of all three components at this point [10,70].

The production of membranes is based on the circumstance that the phase diagram of the respective polymer solution features a two-phase region. By transforming the originally stable state of the mixture into a thermodynamically unstable condition, two coexisting phases are formed. These two phases are in a thermodynamic equilibrium [59,71]. Phase separation occurs because the thermodynamically unstable condition causes an achievement of the minimum of the free enthalpy of mixing (Gibbs energy), so that a new thermodynamic equilibrium is reached. The function of the free enthalpy within the heterogeneous region of a polymer solution exhibits two minima. These minima represent the compositions of the two phases at equilibrium (Figure 9) [1,72].

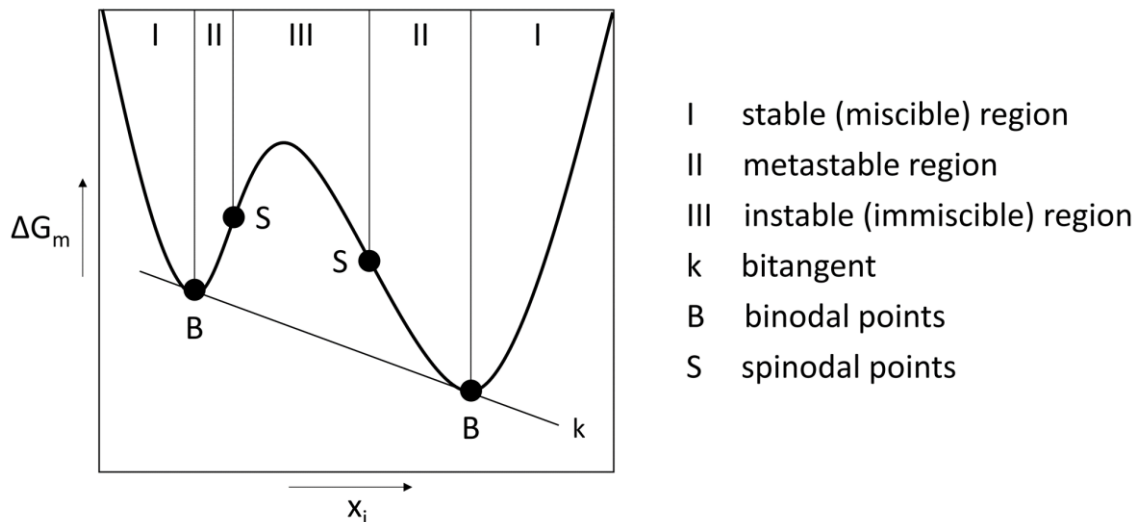


Figure 9 Free enthalpy of mixing as a function of the substance amount fraction in a phase diagram [72].

The minima of the enthalpy of mixing are the endpoints of each tie-line, which represent the connecting line between the two phases in equilibrium [1,70]. The boundary between the thermodynamically stable and unstable region is limited by a connection line, which links all minima of the free enthalpy function of the polymer across the complete compositional range. This connection line is the so-called binodal. It thus represents the boundary between the homogeneous one-phase and the heterogeneous two-phase region, which is synonymously also referred to as miscibility gap or liquid-liquid equilibrium [1]. If the binodal is crossed during the membrane manufacturing process, a polymer-poor and a polymer-rich phase is forming, with both phases being in an equilibrium. The polymer-rich phase is responsible for the formation of the membrane matrix, whereas the polymer-poor phase accounts for the formation of the porous network [50,60].

The heterogeneous region can be further divided up into a metastable and an unstable region. The unstable region is located between the two inflection points of the enthalpy function (Figure 9) and can therefore be identified through the maximum of the free enthalpy of mixing. This region is surrounded by the spinodal curve, which therefore separates the metastable from the unstable region [15]. The area between the binodal and the spinodal curve, which lies in-between the minimum and the inflection point of the enthalpy function, is the metastable region [73]. The point where both, binodal and spinodal intersect, is known as the critical point. At this point the solution exists as a single phase and therefore exhibits a homogeneous condition [1]. Another crucial element of the phase diagram is the solidification boundary. It represents the border in the phase diagram at which the single phase of a homogeneous solution or the polymer-rich phase of a heterogeneous solution reaches a viscosity, which is so high that the solution passes into a gel-like state. Therefore, the structure formation is finalized as soon as the solidification boundary is crossed [74–76].

### 3.3.2 Demixing mechanisms

A major challenge in the fabrication of membranes is the reproducibility and controllability of the segregation mechanisms occurring during the phase separation process. However, due to the large number of influencing variables and dependencies of the mechanisms, a prediction of the final membrane structure is challenging and therefore only partially possible. In turn, this means that the reproducibility of the membrane structure cannot be completely controlled. Although membrane formation via phase separation has repeatedly been in focus of research during the last decades in the field of membrane technology, the discussions about specific influences are still controversial [31,77]. The segregation mechanisms, which have already been discussed and are widely accepted, are summarized in the following.

The mechanisms which are responsible for the structure formation depend on two factors. On one hand, the kinetics of the phase separation process play an important role for the membrane properties, since they influence the mass transfer during precipitation. Therefore, the kinetics affect the compositional changes and thus are crucial for the path through the phase diagram [43,78]. On the other hand, the underlying structure formation mechanism ultimately depends on the entry point into the miscibility gap [15]. One can differentiate between four different precipitation paths, which can be associated with different separation mechanisms (Figure 10) [79].

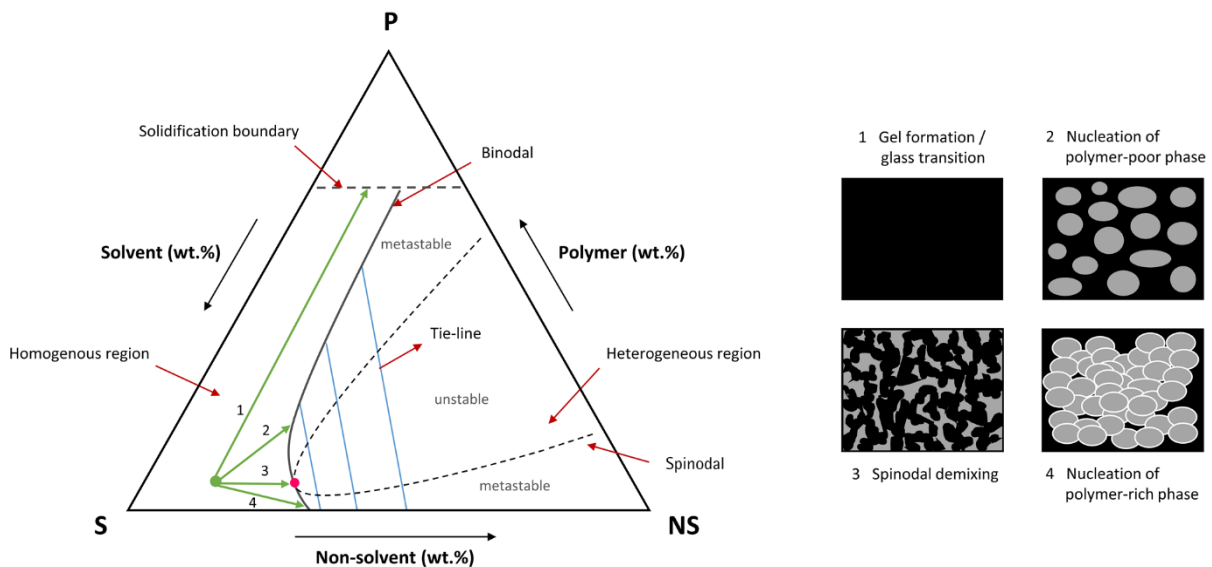


Figure 10 Schematic illustration of structure forming mechanism in dependence of the point of entry into the heterogeneous region of the ternary phase diagram (adapted from Stropnik et al.) [79].

In case of the first path, the composition of the casting solution does not enter the miscibility gap at all. Nonetheless, at some point of the process the solidification boundary is crossed. In turn, this results in the gelation of the polymer solution and therefore in the formation of a foil [1,79]. In contrast, the other three mechanisms result from a path through the miscibility gap, with different structures

developing in dependence of the entry point. The second and the fourth precipitation path of Figure 10 enter the heterogeneous area directly into the metastable region, either above or below the critical point. In both cases the structure formation is based on a nucleation and growth mechanism [15]. Although the polymer solution is stable towards small compositional fluctuations, segregation of the solution occurs when a critical radius of the fluctuations is reached. The reason for this is that the formation of a stable nuclei of one phase within the matrix of the other phase leads to a decrease in the free enthalpy of the polymer solution [1,2]. The critical radius  $r^*$  is necessary to induce phase separation and can be described by the following equation [80]:

$$r^* = - \frac{2 \cdot \sigma}{\Delta g} \quad (1)$$

The necessary radius for the formation of a stable nuclei is thus dependent on the surface energy  $\sigma$  and on the change in the free enthalpy per volume  $\Delta g$  [80]. The rate of the nuclei formation, however, is dependent on the number of nuclei, which have already reached the critical radius. The higher the number, the higher the probability that an unstable nucleus will absorb another particle and consequently will become stable [1,2].

As soon as the binodal is crossed, the formation of homogeneous nuclei starts [66]. If the entry point lies above the critical point, the nuclei consist of the polymer-poor phase, which is predominantly composed of the solvent and the non-solvent. The individual nuclei are enclosed by a polymer-rich matrix, which is the basis for the backbone of the membrane. In contrast, the polymer-poor domains are washed out during the immersion precipitation process, so that a porous network within the membrane backbone is formed [61]. The pore size structure is determined by different coarsening mechanisms, which take place until solidification sets in [81,82].

If the entry point into the metastable region is located below the critical point, however, the nuclei are formed from the polymer-rich phase. In this case the nuclei are surrounded by a polymer-poor matrix. However, this mechanism usually does not result in a usable membrane, but rather in a polymer dust, a polymer granulate or at best in a globularly defective structure [44,79].

The third precipitation path enters the miscibility gap near or through the critical point directly into the unstable region. In this case spinodal segregation occurs. In comparison to the nucleation and growth mechanism, the smallest composition variations result in a reduction of the free enthalpy of mixing [1,15]. As a consequence instantaneous demixing without nucleation occurs, which results in a bicontinuous structure [66]. Spinodal segregation can be divided up into three phases. In the early phase, which begins with the crossing of binodal and spinodal near or through the critical point, the composition fluctuations are small and the structure growth begins. In the intermediate phase the structure growth stagnates and spinodal demixing finishes. In the last stage different coarsening

mechanisms such as Ostwald ripening or coalescence occur, which lead to further structural changes [83]. Due to these structural changes, which are similar to those appearing during growth and coalescence, the structure might no longer be distinguishable from a structure that developed through growth and coalescence [52]. Thus, a direct fixation of the structure after non-solvent induced demixing results in the typical morphologies shown in Figure 10. However, if subsequent coarsening mechanisms occur, it is nearly impossible to attribute the final structure to the structure-forming mechanisms which have occurred [2,84].

### 3.3.3 Coarsening mechanisms

As mentioned, until solidification sets in the structure is subject to further structure-forming effects. This is why the originally formed structure cannot be regarded as static [85]. The effects significantly contributing to the coarsening of the forming membrane matrix include coalescence and Ostwald ripening [73].

Coalescence describes the merging of dispersed droplets of one phase, so that it results in the fusion of several small nuclei to a larger nucleus. The driving force of this process is the minimization of the interfacial tension between the polymer-rich and the polymer-poor phase [64,68]. Significant influencing factors are the time and the viscoelastic properties of the coalescing phase. The following equation was derived by Matsuyama *et al.* and can be used to describe coalescence [73]:

$$d^3 = \frac{8 \cdot k \cdot T \cdot \nu}{\mu \cdot \pi} \cdot t \quad (2)$$

Here  $d$  is the diameter of the nucleus,  $k$  is the Boltzmann constant,  $T$  is the temperature,  $\nu$  is the volume fraction of the nuclei,  $\mu$  is the viscosity of the medium,  $\pi$  is the circle number and  $t$  is the time.

It was experimentally shown that coalescence does not only influence the structure during the nucleation and growth mechanism, but also after spinodal segregation. Tsai *et al.* demonstrated that a prolonged time of coalescence results in the change from a bicontinuous structure of the spinodal segregation to a cellular nuclei morphology. The observed structural transition was not only dependent on the time, but also on the viscoelastic properties of the polymer solution. Thus it could be shown that an increase of the solution viscosity, for example as a result of using another solvent, can retain the original bicontinuous structure, although the time in the coalescence area is high [52].

In contrast to coalescence, Ostwald ripening is a coarsening mechanism where the small nuclei shrink in favor of the larger nuclei [86]. This effect results from the circumstance that the surface concentration of the nucleating phase is larger for smaller nuclei, than it is for the larger ones. This results from the greater curvature of the small nuclei in comparison to the large nuclei. Consequently, the internal pressure in the small nuclei is higher and a passage of the particles from the nuclei into

the surrounding phase is favored. Furthermore, the concentration difference between small and large nuclei causes an attraction and therefore a diffusive transport of the small nuclei towards the larger ones [87]. In the course of this movement the small nuclei shrink in size, until they reach a radius smaller than the critical radius (Equation 1). Finally, an instantaneous dissolving of the small nuclei is provoked, whereas at the same time the large nuclei can enhance their growth rate. Coarsening by Ostwald ripening can be describe mathematically with the following equation [73]:

$$d^3 = \frac{64 \cdot \sigma \cdot D \cdot \chi \cdot V_m}{9 \cdot R \cdot T} \cdot t \quad (3)$$

Here  $d$  is the diameter of the nucleus,  $\sigma$  is the interfacial energy between the nucleating and the surrounding phase,  $D$  is the diffusion coefficient of the nucleating phase,  $\chi$  is the substance amount fraction of the nucleating phase within the matrix,  $V_m$  is the molar volume of the nucleating phase,  $R$  is the ideal gas constant,  $T$  is the temperature of the nucleating phase and  $t$  is the time.

#### 3.3.4 Formation of the skin layer of ultrafiltration membranes

The so-called skin layer is mainly responsible for the retention capacity of asymmetric ultrafiltration membranes. The separation efficiency of the skin is strongly influenced by the manufacturing process, since the separation performance is mainly dependent on the polymer concentration at which the phase separation is induced through the entry of the miscibility gap [19,88]. The separation layer is generated on the air-facing side of the polymer film, since this side comes into contact with the non-solvent first when the film is immersed into the precipitation bath [44]. The resulting diffusive exchange between solvent and non-solvent at the top of the polymer film induces the phase separation from the top. This is why the structure is first solidified at the top of the polymer film [19]. Consequently a diffusion barrier is created, which significantly slows down the diffusive exchange between the precipitation bath and the lower layers of the polymer film. Therefore, below the diffusion barrier less solvent can diffuse out of the polymer solution, so that the onset of the phase separation occurs at lower polymer concentrations. As a result, the pore structures become more open towards the support-facing side of the developing membrane, which leads to the typical asymmetric structure [41,89]. In contrast to the formation of the support layer, which is developing from nucleation and growth or spinodal segregation, the formation of the skin layer is not fully understood. On one hand, the skin layer can be formed by a direct passage of the homogeneous polymer solution to a gel-like state, so that the solution does not even reach the two-phase region. Since a phase separation is not induced, a non-porous structure is resulting. In this case, the retention capacity is determined by the arrangement of the polymer chains within the gel at a molecular level [75,89,90]. On the other hand, the skin can also be formed by phase separation. However, in contrast to the case



of the porous support, the entry point into the two-phase region is located at very high polymer concentrations and therefore close to the solidification boundary. Consequently, solidification is reached quickly and a structure coarsening is almost impossible, so that a thin narrow layer is formed, which is responsible for the separation capability [74,91].

### 3.3.5 Formation of macrovoids

The mechanisms for the formation of cavities within the membrane cross-section, which are also known as macrovoids or finger-like structures, are controversially discussed [85,92–94].

One theoretical explanation for the formation of macrovoids is based on the assumption that they appear at the skin-side of the membrane and that they therefore result from interfacial phenomena between the casting solution and the precipitation bath [92,94]. One interfacial phenomenon, which could be responsible for macrovoid formation, is the Marangoni effect. It induces the formation of convection cells, which act as an initiator for the growth of the finger-like structures. In this case the driving force for the macrovoid development is the increased polymer concentration in the selective separation layer, since it causes an increased surface tension [94].

Another possible interfacial mechanism could be the mechanical force during the shrinkage of the polymer film, which causes the occurrence of defects within the skin. These defects allow a locally increased inflow of the non-solvent. In turn, the onset of phase separation within one horizontal film layer is locally retarded, so that the formation and growth of larger nuclei is promoted [92].

However, an argument against these mechanisms is the occurrence of macrovoids considerably below the skin layer. Therefore, another theory implies that a rapid demixing process (instantaneous demixing) below the skin layer is responsible for formation of the voids [93]. As previously described, the formed skin layer acts as a diffusion barrier, which slows down the diffusional exchange between polymer film and precipitation bath. While the structure formation in the separation layer has already been completed, the demixing process in the underlying layer has only just begun [41]. Consequently, there is another section below the skin layer, which is still in a thermodynamically stable state. Hence, the phase separation is locally delayed (delayed demixing) and does not occur instantaneously after immersion into the precipitation bath across the complete cross-section of the polymer film [93]. As a result, the polymer-poor phase nuclei can grow by the diffusive inflow of solvent from the still homogeneous polymer solution of the underlying layers. This diffusive transport is driven by a concentration gradient [93,95]. The diffusion-based growth is additionally enhanced through coalescence of the polymer-poor domains. If the phase separation front is moving slower through the cross-section of the polymer film than the diffusion front of the non-solvent, the formation of voids extending to the support-facing side of the film is favored (Figure 11) [1].

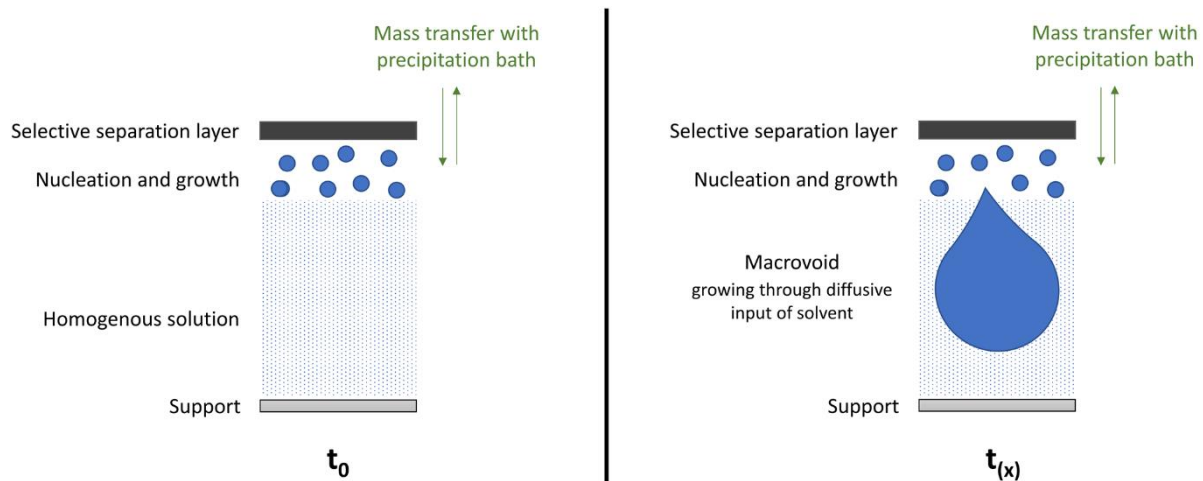


Figure 11 Schematic illustration of the development of macrovoids (adapted from Mulder) [1].

If the extended solvent-rich domains are outrun by the phase separation front, new nuclei can form below the already growing domains. In turn, this leads to the termination of the nucleus growth. Thus, the rate of the solvent diffusion and the locally delayed onset of phase separation are critical factors for the presence and the morphology of macrovoids within the membrane [1,78,93].

### 3.3.6 Solidification

After onset of phase separation the composition of the two phases cannot be considered to be static, since there is a steady mass transfer during membrane formation [85]. The removal of solvent from the polymer-rich phase leads to an increase in the polymer concentration within this phase. If a critical polymer concentration is exceeded, a three-dimensional network is formed. This can be mainly attributed to intermolecular interactions between the polymer chains, such as hydrogen bonds, dipole-dipole interactions and hydrophobic interactions [74,76,85]. Because of these interactions the viscosity is increasing. At some point the viscosity increase results in a complete immobilization of the formed structures, so that the polymer solution passes into a gel-like state [82]. As soon as the so-called solidification boundary (Figure 8) is exceeded, a coarsening of the structure is no longer possible and the matrix solidifies, which finally determines the essential membrane performance properties [19]. Due to the lack of knowledge on the exact mechanisms of gel formation during immersion precipitation, there is no precise definition for the exact location of the solidification boundary. A main reason for this is the short duration of the solidification process. However, the solidification boundary is often referred to as the state of infinite viscosity or it is declared to be higher than  $10^6$  mPa·s [1,2,96].

### 3.4 Sustainable membrane processes

#### 3.4.1 REACH regulations

The European Union's system for regulation, evaluation and authorization of chemicals (REACH) is a strategy which specifies different rules for the application and handling of existing and new chemicals [97]. In particular, this strategy involves regulatory restrictions on the use of substances of high concern for human health and the environment. Therefore, the intention of the regulations is to make chemical processes safer for humans and the environment [98]. In order to fulfill the regulatory function, the work of REACH includes the classification and the proper labeling of existing and new chemicals. Furthermore, the tasks involve the registration and evaluation of all existing chemicals with respect to their properties, as well as the determination of limitations in the manufacturing and application of substances in industry. In addition, REACH regulates the information transfer by creating and sharing reports and technical documents, so that the users are informed about relevant changes. This shall help the user to look for potential alternatives when a used substance is of high concern [99]. To conclude these tasks, the general objectives of REACH involve the protection of environment and human health, the increase of the competitiveness of the European chemical industry, the prevention of animal testing in industry and the integration of international objectives [100].

#### 3.4.2 Green Chemistry in membrane technology

Green chemistry is a concept for reducing or eliminating the application or generation of hazardous substances in chemical processes, in order to make these processes less harmful for humans and the environment [49]. In order to reach this goal, the design of chemical processes and the implementation of chemical reactions or components has to follow certain principles, which are known as the twelve principles of green chemistry [101–103]. These twelve principles formulated by Paul Anastas and John C. Warner [102] are summarized in Figure 12.

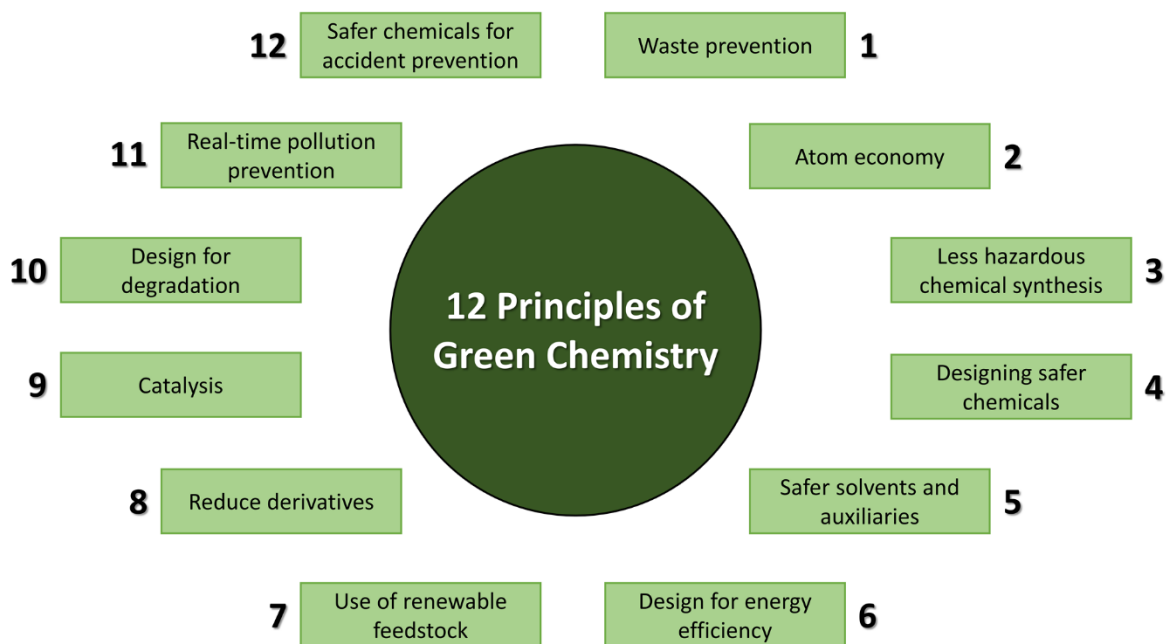


Figure 12 Depiction of the twelve principles of green chemistry.

In general, the application of these principles shall reduce or even completely avoid the use of harmful substances. In this context, the safety improvement refers to both, the manufacture of new or existing chemicals and the application of chemicals in a process. In particular, the focus of the improvement is laid on the influence of a chemical or a process on human health and on the environment [103,104].

In order to follow the principles of green chemistry and to comply with the REACH regulations, the adaption of membrane production and membrane application processes is currently an important issue in membrane technology [105–107]. It shall increase the membrane sustainability, so that membrane processes remain competitive.

One of the most important principles of green chemistry for reaching the environmental and economic goals is the use of safer solvents and auxiliaries [103]. Since most of the conventionally used solvents for membrane preparation via phase inversion are hazardous and considered to be carcinogenic or toxic, their substitution is one of the main tasks to increase the safety of the fabrication processes [8,49]. However, the replacement of the currently used solvents for membrane preparation is also one of the main challenges. The reason for this is that product specifications, customer requirements and competitive properties have to remain similar, despite of the solvent exchange [108]. The difficulty at this are the different characteristics of the individual solvents, which make a one-to-one exchange impossible. This is the reason why recently a lot of different solvents have been studied for their potential to substitute conventional solvents in membrane production by immersion precipitation [106,107,109–111]. The better the fabrication process and the influencing factors are understood, the more feasible is a solvent substitution while maintaining the previous membrane characteristics.

### 3.5 State-of-the-Art

#### 3.5.1 Characterization of polymer solution thermodynamics

The currently used methods for studying the polymer solution thermodynamics include the theoretical calculation of a system's phase diagram on one hand, as well as an experimental determination of the binodal curve on the other hand. In this context, the theoretical calculation of the phase diagram is based on the Flory-Huggins theory [112–114]. The Flory-Huggins theory has been adapted by several groups in order to be able to apply the solubility parameter of the respective polymer and solvent for the calculation of the miscibility gap [71,115–117]. On the other hand, the currently established experimental method for the investigation of the polymer solution thermodynamics is the cloud point titration [48,59,118]. By determining several cloud points of the system at different solution compositions with low polymer concentrations, the binodal curve can be extrapolated for the complete polymer concentration range [48].

Although these two methods allow the determination of critical phase diagram components, they have several limitations. In case of the Flory Huggins based calculations, the interpolated results can deviate from the real thermodynamics. This can be caused by several assumptions that have to be supposed to be able to apply the Flory Huggins theory for the phase diagram calculation. In contrast, the limitations of the cloud point titration method are of experimental nature. During one experimental run only one single composition can be determined, which lies on the binodal curve. Furthermore, a relatively low solution viscosity is required in order to obtain reliable results. Therefore, cloud point titrations can only be performed for solutions with a low polymer concentration. Consequently, the binodal curve has to be extrapolated from a few single measurements, which might lead to deviations from the reality. Apart from the experimental limitations, cloud point titration experiments do not provide direct information on the phase equilibria and therefore they do not allow the direct determination of the compositions of the co-existing phases [119]. This is why there is a demand for an improved method, which minimizes the limitations the currently available methods bring along.

#### 3.5.2 Influences of the polymer solution composition

In the past various studies were conducted to investigate the influence of varying polymer solution compositions on membrane performance and structure. However, as the membrane formation process is very complex and strongly depends on the combination of several different variables, there is still a huge interest to further enhance the knowledge on the fundamentals of the formation mechanisms [31,42,43,47]. Furthermore, if the existing studies are compared to each other, the results

are contradictory. Especially in case of studies on the influences of polymeric additives on membrane formation, the reported results disagree among each other.

For polyvinylpyrrolidone (PVP) it has been shown that the pure water flux increases with a raising concentration of PVP in the casting solution, while the retention decreases at the same time [120–124]. Most research groups reported a maximum of the flux at a certain PVP concentration, although the location of this maximum differs between the studies of the different groups. Following the observed maximum, it was found that the water flux starts to decrease when the PVP concentration is further increased [120,121,125]. In contrast, two other groups could not observe a flux minimum or maximum at a certain PVP concentration within the examined concentration range. Instead they found that the flux is constantly rising with an increasing PVP concentration, until it reaches a plateau at which the flux remains more or less constant with a further increase in the PVP concentration [124,126]. Yet another study reveals that an increase of the PVP concentration results in a constant rise of the pure water flux, without reaching a point at which the flux starts to stagnate [127].

A similar inconsistency of the results can be noted for variations of the PVP molecular weight. Most studies indicate that the water flux and the molecular weight cut-off decline when PVP with a higher molecular weight is applied [43,62,128–131]. However, there is also one study showing the contrary trend for the application of PVP with different molecular weights [132]. On top of that, the critical molecular weight, which is necessary to induce a significant flux decline, varies between the different investigations [128–131].

Apart from the impact on the membrane performance data, some research groups reported that the addition of PVP to the casting solution can suppress the formation of macrovoids. In these studies it has been shown that the effect is independent of the molecular weight of the additive [43,126,130,131,133,134]. In contrast, other studies report opposite results, since the presence of PVP in the casting solution resulted in an increased growth of macrovoids [121,135]. Again other researcher reported that the opposing effects can be explained by the choice of the solvent, as well as by the molecular weight and concentration of the PVP [125,135–137].

Contradictory results have also been reported for polyethylene glycol (PEG) as additive. It has repeatedly been shown that the flux can be enhanced by increasing the PEG concentration [138–141]. In contrast to this, one research group found that this increase can only be observed until a certain PEG concentration is reached. The group showed that after this critical concentration has been reached, a further enlargement of the PEG content in the casting solution results in a flux decrease [142].

Similar observations were reported for variations of the PEG molecular weight. Most research groups observed a constant flux increase with a rising PEG molecular weight [138,139,143]. However, there is also one study revealing that the flux increase has a maximum at a certain molecular weight. By further elevating the length of the PEG molecules, a flux reduction could be observed after reaching this

maximum [144]. The same research group has also reported that the pore size decreases with an increase of the PEG molecular weight. This shows that at some point the pore forming characteristics of PEG, which lead to the observed flux increase, are overcome. In turn, this would explain the observed flux reduction [145]. Furthermore, it could be shown by several groups that the porosity of the membranes can be increased through an addition of PEG to the casting solution [139,142,144]. However, again other research groups found slightly different results. Their results imply that the increase of the porosity can only be achieved until a critical concentration is reached, whereas a further rise of the PEG concentration leads to a decline of the porosity [146,147].

Further inconsistencies were found for the effect of PEG on the formation of macrovoids. Several studies indicate that the addition of PEG to the polymer solution can hinder the formation of macrovoids or finger-like structures [144,145,147]. In contrast, other works imply that the addition of PEG to the casting solution induces the formation of macrovoids and finger-like structures [138,140,141]. Yet one other research group reported that PEG does not influence the formation of macrovoids or finger-like structures at all [148].

Contradictory results have also been reported for the combined correlations between membrane structure and performance in dependence of variations in concentration or molecular weight of PVP or PEG. While some studies showed a direct correlation between the porosity and the permeability of membranes prepared from solutions with different additive variations [140,147,149], other studies could not confirm these relationships between membrane structure and performance at varying additive conditions [62,124,127,144].

In comparison to polymeric additives, the influences of non-solvent additives, polymer concentration and precipitation bath conditions have received far less attention. Although all three variables have already been investigated and are known to have an impact on membrane formation via phase inversion, the existing studies are only limited to single solvent systems or a distinct polymer.

With respect to non-solvent additives, there are only a few studies which focus on the influence of adding different alcohols or water to PES casting solutions prepared with either dimethylacetamide (DMAc) or *N*-methyl-2-pyrrolidone (NMP) as solvents [51,150]. Furthermore, there is one other study which investigates the influence of maleic acid on PES membrane formation, using dimethylformamide (DMF) as solvent [151]. These studies reveal that the precipitation speed and consequently the membrane performance can be influenced by adding non-solvents to the casting solution. However, the present studies do not compare the influences between different solvent systems. Furthermore, the impact of a non-solvent addition to casting solutions prepared with ecologically less harmful solvents has not been tested so far. Since these alternative solvents often have different characteristics in comparison to conventional solvents, a change of the solvent could alter the impact of non-solvent additives. This is why there is still potential for further investigations.

In case of the polymer concentration, there are also only a limited number of previous investigations, which all focus on systems consisting of PSf dissolved in either NMP or DMAc [33,152]. These studies indicate that an increase of the polymer concentration can suppress the formation of macrovoids, independently of the solvent which is applied. However, differences on the extent of the studied effects can already be observed when comparing the results between the two conventional solvents NMP and DMAc. Therefore, the combination of solvent and polymer seems to be an important point to be considered when substituting an existing solvent through another one and thus should be studied in more detail.

The precipitation bath conditions have also been studied previously by several different research groups [121,123,147,153,154]. However, these studies are again limited to single ternary or quaternary systems and to solutions prepared with the hazardous solvents NMP, DMAc and DMF. This is why there is still potential to increase the knowledge on the precipitation variables when using ecologically less harmful solvents. In contrast to the contradictory results which could be observed for the other preparation parameters, the effects of varying precipitation bath conditions were the same for all previously studied systems. In all cases, it was shown that a higher temperature of the precipitation bath raises the water flux of the resulting membrane and that higher precipitation temperatures favor the formation of macrovoids.

The past studies reveal that the prediction of the impacts of polymer solution composition and precipitation conditions on membrane formation via phase inversion is not straightforward. The results rather show that there are many influencing factors and that the combination of these factors during the membrane formation process is critical for the final membrane characteristics. This is supported by the significant heterogeneity of the results from the previous studies. As most previous studies only focused on one polymer, one solvent system, and often on the influence of one additive alone, there is still a high potential to improve the understanding of the membrane formation mechanisms and their influencing parameters. In particular, there is a lack of comparative studies, which consider the interaction of several factors.



### 3.5.3 Increasing membrane sustainability

Commonly applied solvents for the preparation of membrane casting solutions include NMP, DMAc, DMF and dioxane [31,49]. However, all of the named solvents bring up different safety, health and environmental issues during transport, storage and handling [8,106,110]. Furthermore, the disposal of these solvents can be problematic because their reuse is often limited due to certain quality requirements and regulatory demands [155,156].

For the production of PES membranes the most commonly used solvents are NMP and DMAc, which are both regarded as concerning for human health and the environment [55]. Consequently, there is a high interest in replacing these commonly applied solvents through less harmful alternatives. If possible, this substitution shall comply with the principles of green chemistry as far as possible. Due to the increasing interest in meeting the criteria of green chemistry, several different solvents have been tested for their suitability to replace hazardous solvents in the recent past.

Until now, the most frequently studied alternative solvent is dimethyl sulfoxide (DMSO). It has been reported by different research groups that DMSO is a suitable alternative for NMP and DMAc, which among other membrane-forming polymers is able to dissolve PES [107,157–160]. Another substance which has been frequently studied with respect to its ability for replacing toxic solvents is Rhodiasolv®Polarclean (Polarclean). Different scientific works reveal that Polarclean can be regarded as a safer alternative, which is able to dissolve PSf, PVDF and PES [55,105,109,161]. More recently, Marino *et al.* reported that Cyrene™ can also be used as an alternative solvent for the preparation of PVDF and PES membranes [111]. In comparison to DMSO, the solvents Polarclean and Cyrene™ can even be declared as green solvents. Both these solvents are not only non-toxic and biodegradable, but they additionally stand out due to their bio-derived source [106,162]. Another suitable bio-derived solvent for membrane fabrication is  $\gamma$ -Valerolactone (GVL). It has been shown that GVL is not only capable of dissolving PES, but also other polymers such as PSf, cellulose acetate and polyimide [109,110]. Beyond the already mentioned alternatives, Rasool and Vankelecom named different other bio-based solvents that can be used to prepare membranes with different membrane-forming polymers. They all have in common that they are basically different derivatives of glycerol [110].

As the REACH regulations and the concept of green chemistry has just recently attracted more attention, the knowledge on the potential of less harmful solvents and on the comparison of these alternatives to the currently applied hazardous solvents is still limited. In turn, there is a high interest in gaining more information about potential new alternative solvents and their suitability for substituting hazardous solvents such as NMP and DMAc.

## 4 Experimental Part

In order to improve the understanding of the membrane formation mechanisms via NIPS, this doctoral thesis has been divided up into three different parts. Taken together, these closely related parts provide a holistic picture on the membrane formation mechanisms via NIPS. They identify the relevant influencing variables and prove that it is possible to substitute toxic solvents through less harmful alternatives, while the ability to control the desired properties of the fabricated membranes is maintained. Each single part was published separately in a peer-reviewed journal.

The first part of the work focuses on the thermodynamic aspects, which are relevant for the fabrication of polymeric membranes. The location of the miscibility gap of a polymer solution system has a significant impact on the membrane formation mechanisms and therefore on the resulting membrane structure. Consequently, the determination of the system's phase diagram at constant pressure and temperature is a crucial step for understanding the underlying mechanisms of the structure formation process. The information gained from the phase diagram allow the adjustment of the polymer solution composition and enable a regulation of the entry point into the miscibility gap, so that the respective membrane formation mechanisms can be controlled [1,31].

In the past, the determination of the binodal curve was either based on theoretical calculations, or it was experimentally determined by means of cloud point measurements [114,116]. This still commonly used experimental method was already described in 1993 by Boom *et al.* [48]. However, the cloud point method has several drawbacks and further it only provides limited information about the essential elements of the phase diagram [119]. Therefore, the aim of the first part of this thesis was to develop a new method for characterizing the polymer solution thermodynamics. In comparison to the commonly used cloud point method, it shall provide a higher information content and additionally overcome the drawbacks of the cloud point approach.

Consequently, the publication "Thermodynamic analysis of polymer solutions for the production of polymeric membranes" (Journal of Molecular Liquids, 2019) focuses on the development of an improved method for characterizing the polymer solution thermodynamics [165]. This method is based on the induction of phase separation and a following segregation of the demixed polymer solution in a test tube. At this, the separation is based on density differences between the two phases, which enable a division of both phases by centrifugation. Subsequently, the exact composition of the single phases can be determined by using a set of analytical methods. Thus, the method does not only enable the determination of the binodal curve, but it also provides valuable information about the tie-lines. The publication focuses on the validation of the method, which was performed to determine its reproducibility as well as the reliability of the results. Furthermore, this part of the work focuses on a comparison between the commonly applied cloud point method and the newly developed procedure.

It demonstrates the advantages of the novel method in comparison to cloud point titrations and emphasizes the additional information, which can be obtained by application of the novel procedure. Apart from the polymer solutions thermodynamics, the kinetics of the phase separation process play a significant role for the resulting membrane features [43,116]. Therefore, a good understanding of the existing control parameters is crucial for regulating the final membrane properties.

The kinetics of the NIPS process are strongly influenced by the temperature of the precipitation bath. The reason for this is a strong influence of the temperature on the diffusion speed in the non-solvent bath, and therefore on the exchange between the solvent from the polymer film and the non-solvent from the bath [121,147]. Beyond that, it can also be strongly impacted by the polymer solution composition. A change of the dope solution composition can significantly alter the solution viscosity. Since the viscosity influences the diffusional speed, it also has an impact on the exchange rate between the solvent and the non-solvent [146,163]. Apart from other components of the membrane dope solution, such as solvent and non-solvent additives, especially the concentration of the membrane-forming polymer and of polymeric additives can significantly alter the viscosity and therefore the membrane formation kinetics [47]. However, previously reported results on these aspects are contradictory and further limited to single systems or variables [43].

Furthermore, an emerging topic in membrane technology is the substitution of currently used solvents for the production of membranes via phase inversion. Since most of these solvents feature several environmental and health risks, it is of high interest to find appropriate more ecologically harmless alternatives, which make the membrane production more sustainable [49]. However, the choice of the combination of solvent and non-solvent has a high impact on the exchange rate that leads to phase separation. In dependence of the affinity and miscibility between solvent and non-solvent, the exchange rate can be modified. This in turn impacts the resulting membrane properties [31]. In order to gain the desired membrane properties, an understanding of the similarities and differences between the membrane formation mechanisms in conventional and alternative solvent systems is necessary, where a focus should be the combination of solvent system and other preparation variables. This is why the second publication “Membrane formation via non-solvent induced phase separation using sustainable solvents: A comparative study” (Polymer, 2020) presents a comparative study on the influences of polymeric additives in four different solvent systems on the membrane formation mechanisms during immersion precipitation [166]. The work focuses on the polymeric additives PVP and PEG, since these are the two most commonly used additives to modify the membrane surface. In addition, this part of the work investigates the effects of the additives in dependence of the applied solvent. Among these are the two commonly applied solvents NMP and DMAc, as well as the two less harmful alternatives 2-pyrrolidone (2P) and dimethylactamide (DML), which have been chosen as they are non-carcinogenic and have not been tested in the context of PES membrane formation before.

One focus in this part is laid on the influence of the variables on the polymer solution viscosity. On top of that it emphasizes the effects of the variations on several different membrane characteristics, which include the membrane permeability, the protein retention capacity, as well as the structure. Furthermore, it involves the effects of the variables on the membrane surface characteristics, which are evaluated by the unspecific protein binding capacity, the surface contact angle and the specific surface area of the membrane prototypes. This part of the thesis demonstrates that the combination of the studied parameters is crucial for the effects on the resulting membrane properties. Depending on the chosen membrane preparation variables, the resulting membrane properties can be adjusted in a controlled manner. Furthermore, this part of the work proves that 2P and DML are suitable alternative solvents for PES membrane preparation instead of using NMP and DMAc as solvents.

As mentioned, the applied solvent and polymer additives are not the only solution components influencing the membrane formation process. Other relevant solution components include the membrane-forming polymer and its concentration, as well as different non-solvent additives and their concentration [31]. Additionally, the precipitation conditions can significantly impact the membrane formation process. These conditions include the precipitation bath composition, since the miscibility of the non-solvent in the bath and the solvent in the polymer solution determines the exchange speed of those two components [164]. On top of that, they also involve the precipitation temperature, as it strongly affects the diffusion speed during the mass transfer between the polymer solution and the precipitation bath [121].

In order to complete the holistic picture of the membrane formation process via NIPS and to complement the impacting parameters studied in the parts before, the third publication named "Influences of different preparation variables on polymeric membrane formation via non-solvent induced phase separation" (Journal of Applied Polymer Science, 2019) focuses on the influence of polymer concentration and the concentration of different non-solvent additives in the dope solution, as well as on the precipitation conditions on the characteristics of the fabricated membranes [167]. Similar as in the previous part, this includes a comparison between the membrane prototypes prepared with NMP as a conventional solvent and with 2P as a less harmful alternative solvent. On one hand, this publication focuses on the polymer solution characteristics in terms of viscosity and the location of the binodal curve. On the other hand, the work demonstrates the influence of the variables on several different membrane characteristics. These include the membrane structure, the membrane permeability and the retention capability for lysozyme as model protein. This part of the thesis again demonstrates that 2P is a suitable alternative for substituting hazardous solvents such as NMP or DMAc. Furthermore, it shows that the studied variables have to be taken into account for controlling the membrane formation process and that they can be used for adjusting the resulting membrane features.

#### 4.1 Thermodynamic analysis of polymer solutions

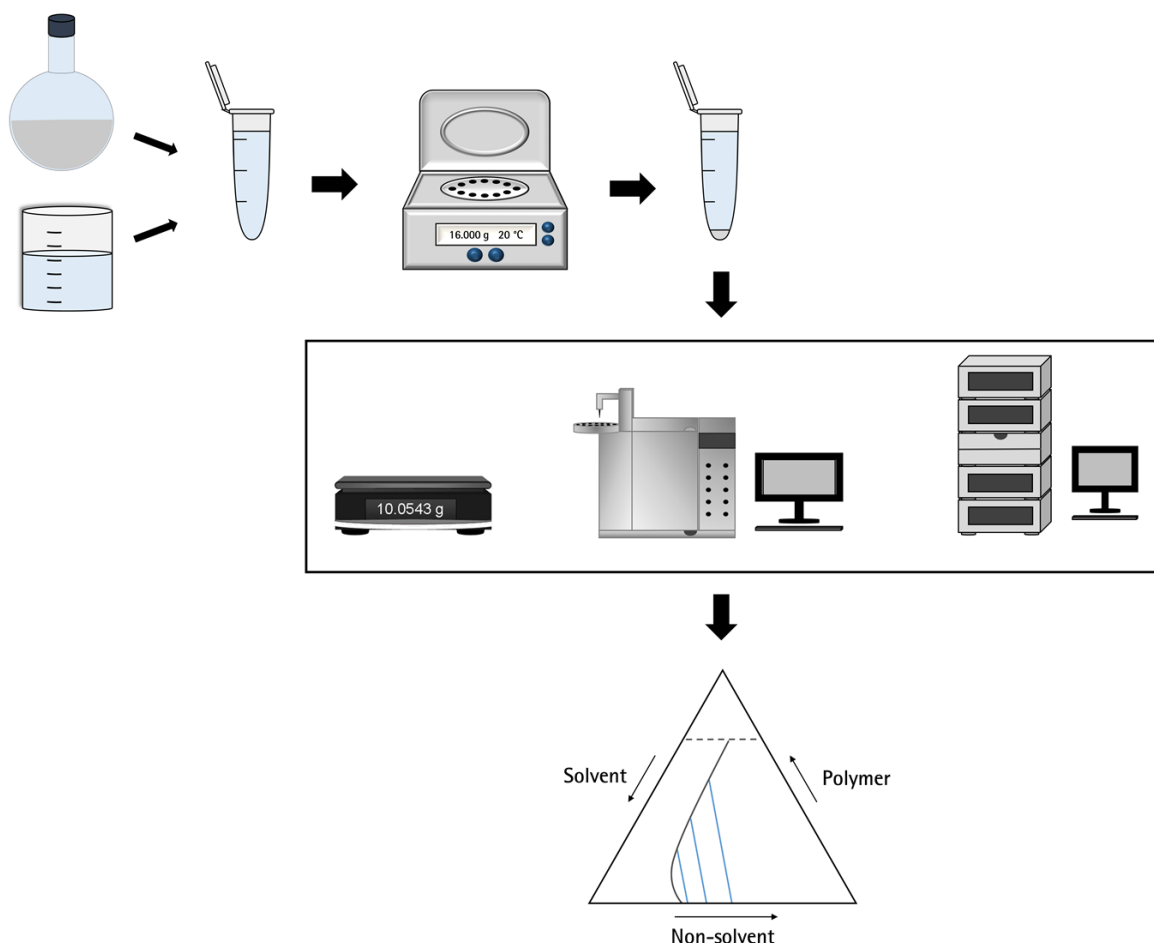


Figure 13 Graphical abstract of the publication “Thermodynamic analysis of polymer solutions for the production of polymeric membranes” [165].

The knowledge of the polymer solution thermodynamics is crucial to understand and adapt the membrane formation process during the fabrication of porous membranes [114]. The most important thermodynamic properties of a polymer solution system are described by its phase diagram. Especially the location of the miscibility gap, which is one of the essential parts of a phase diagram, is of high interest for guiding the membrane production process [1,79].

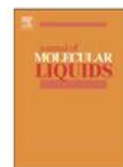
In the past, the experimental determination of the miscibility gap boundary, which is also known as binodal curve, has been done by cloud point titrations [59,118]. Since a large number of titration experiments are necessary to obtain the complete binodal curve, usually only a few experiments were conducted and used to extrapolate the remaining part of the curve. However, the method has several drawbacks. It is time-intensive and limited by the viscosity of the solution, so that it is only applicable for solutions with low polymer concentrations. Furthermore, the extrapolation might result in a curve progression that deviates from the real course of the curve, especially at higher polymer

concentrations. Another disadvantage is that the method does not give any information about the composition of the co-existing phases, which are responsible for the formation of the membrane matrix and the pore network [119].

Therefore, in this part of the work a novel method was developed, which overcomes the drawbacks of the cloud point method. It is based on the induction of phase separation in a test tube by mixing the polymer solution and the non-solvent in an appropriate ratio. Due to a density difference, the resulting phases can then be separated by centrifugation. Afterwards, each single phase composition can be determined by a combination of analytical measurements. Finally, the results can be used to create the tie-lines and several tie-lines can be employed for the construction of the binodal curve.

This publication focuses on the description of the developed method and presents its validation, which is based on an exemplary ternary system consisting of NMP, PES and water. As part of the method validation it could be shown that the application of the novel method enables the generation of reproducible and reliable results with very low deviations. At three different temperatures, the determination of replicate samples with the same polymer solution to non-solvent ratios resulted in the same phase compositions. Furthermore, a comparison to the cloud point method at three different temperatures is presented. It could be shown that up to a certain polymer concentration the determination of the binodal curve by both methods provides similar results. In case of the exemplary studied system, the thermodynamics were in both cases independent of the phase separation temperature. However, at higher polymer concentrations the results of the two methods deviated from each other. The observed deviations can be attributed to the additional information content which is provided by the novel method. It was concluded that in case of the novel method the solidification boundary is indicated in the deviating area, whereas it is not possible to obtain these information from cloud point titrations. While the indicated solidification boundary was found to be below 50 wt.% PES at 10 °C, it was found to be above 50 wt.% PES at 20 °C and at around 60 wt.% at 40 °C. Therefore, although the location of the binodal curve was not found to be temperature-dependent, the onset of the solidification can be influenced by the temperature. Another factor, which was found to be temperature-dependent, is the distribution of the PES chain sizes in the polymer-poor phase. This is also an additional information, which can only be gained from the novel procedure. It was found that the average molecular weight in the polymer-poor phase increased from around 6 kDa to above 10 kDa when the temperature was raised from 10 °C to 40 °C.

To conclude, it was possible to develop and validate a novel method for the characterization of the polymer solution thermodynamics. In contrast to the commonly applied cloud point method, it enables an improved characterization and provides a higher information content. The information can be used to develop new casting solutions and to improve the process control of membrane production.



## Thermodynamic analysis of polymer solutions for the production of polymeric membranes

Catharina Kahrs<sup>a,b,\*</sup>, Michael Metze<sup>a</sup>, Christian Fricke<sup>c</sup>, Jan Schwellenbach<sup>a</sup>

<sup>a</sup> Sartorius Stedim Biotech GmbH, 37079 Goettingen, Germany

<sup>b</sup> Leibniz University Hannover, Institute for Technical Chemistry, 30167 Hannover, Germany

<sup>c</sup> Georg-August-University Goettingen, Institute for Physical Chemistry, 37073 Goettingen, Germany



### ARTICLE INFO

#### Article history:

Received 18 March 2019

Received in revised form 11 June 2019

Accepted 10 July 2019

Available online 11 July 2019

#### Keywords:

Phase diagram

Tie-lines

Phase inversion

Polyether sulfone

N-methyl-2-pyrrolidone

### ABSTRACT

Phase separation is a commonly used mechanism for the preparation of porous filtration membranes. In order to control the membrane structures for obtaining required membrane characteristics and performances, the examination of the thermodynamics of the membrane formation mechanisms is essential. This is why several studies have already been conducted to determine the phase diagrams of polymeric casting solution systems. However, most of the commonly used methods have certain limitations. This is the reason why a new method for the investigation of ternary polymeric systems was developed and evaluated in this study. The new method provides reproducible data which does not only provide information on the position of the binodal curve but also on the compositions of the phases which are formed after the phase separation. The tie-lines of the ternary system polyethersulfone/N-methyl-2-pyrrolidone/water were determined at different temperatures and compared to cloud point titrations conducted under the same experimental conditions. It could be shown that the location of the miscibility gap of the examined system is not visibly dependent on the phase separation temperature within the examined temperature range, especially in the region of the polymer-poor phases. This finding was comparable in all experiments, irrespectively of the method which was used. However, in the region of the polymer-rich phases within the phase diagram, the results of both methods differ from each other as the binodal determined by the tie-line method showed a temperature-dependent shift which cannot be found for the binodal curves extrapolated from cloud point measurements. Apart from determining the binodal curves, the molecular weight distributions of the polymer in the polymer-poor and the polymer-rich phases were determined in the frame of the tie-line determination. Hereby it was found that the distribution in the polymer-poor phase shows a temperature-dependence, as the average molecular weight raised from around 6 kDa at 10 °C to above 10 kDa at 40 °C.

© 2019 Elsevier B.V. All rights reserved.

### 1. Introduction

Membrane filtration is a widely used method to separate small molecules such as salts, viruses, bacteria, or proteins from fluids [1–7]. Apart from applications in the food industry, for the recycling of wastewater, or for medical purposes, membranes are frequently used in the pharmaceutical industry. Especially for the production of biopharmaceuticals they are an integral part of the downstream processing as they serve as tools for different clarification, sterilization and buffer exchange steps [1,5–11]. Concerning the implementation of these membranes into processes of the biomedical industry, the filters have to meet specific requirements in order to ensure the biological safety of the final

product [1]. This in turn requires that the production process of the membranes is well understood in order to be able to control the resulting membrane features [12–14].

Currently, one of the most commonly applied methods for the production of porous membranes is based on the phase separation of polymer solutions [9,15]. The demixing of these so-called casting solutions can be induced by different mechanisms, e.g. non-solvent induced phase separation (NIPS), evaporation induced phase separation (EIPS), thermally induced phase separation (TIPS) and vapor induced phase separation (VIPS) [13,16–18]. The focus in this study was laid on the phase separation by the commonly used membrane precipitation process which is particularly used for the production of polymeric ultrafilters, virus filters and microfiltration membranes [19,20]. The dominating mechanism during the immersion precipitation process is NIPS. However, in order to generate more open pore structures for example in case of microfiltration membrane production, VIPS can also

\* Corresponding author at: Sartorius Stedim Biotech GmbH, 37079 Goettingen, Germany.

E-mail address: [catharina.kahrs@sartorius.com](mailto:catharina.kahrs@sartorius.com) (C. Kahrs).

be applied previously to the final formation of the structure by NIPS [13,18].

Among other process parameters such as the precipitation temperature, the composition of the casting solution is a fundamental aspect for the production of macroporous membranes as it influences the features of the resulting membrane [21–27]. It has been repeatedly shown that in addition to different available polymers as the main component of the forming membrane, a broad range of solvents, non-solvents, and polymeric additives are available which can be used to affect the kinetics and thermodynamics of the membrane formation process [23,26,28–40]. This will enable the control of the resulting membrane characteristics, if the effects of each variable on the kinetic and thermodynamics of the processes are well understood.

In the past decades many empiric studies on different polymeric solution systems were conducted to get a better understanding of the influencing factors. The results of these empiric studies were then used to determine the composition of casting solution receipts aiming to improve the membrane structures and performances [22,35,38,40–50]. However, as the membrane formation process is very complex, there is still a high interest in further improving the understanding of the formation mechanisms during immersion precipitation and therefore the need for developing new methods which are suitable for gaining new insights into the kinetics and thermodynamics of the process [16,20,51–53].

In this study, the focus was laid on the development of a new method for examining the thermodynamics of casting solutions. The behavior of these casting solutions with changing compositions and at constant pressure and temperature can be described by a ternary phase diagram (Fig. 1).

The crucial areas of a ternary system include the homogenous and heterogeneous phase regions which are separated from each other by the binodal, the tie-lines which connect the co-existing phases, and the solidification boundary which indicates the transition from liquid-liquid demixing to the formation of gel-like structures. These areas have already been discussed in the literature to be essential for the structure formation process [17,40,53–57].

In the past the polymer solutions for membrane preparation were often determined by theoretical calculations based on the Flory-Huggins theory [46,50,55,58–66]. Apart from theoretical calculations, the binodal can also be investigated by experimental means. For experimental examinations of polymer solution thermodynamics an established method is the cloud point titration [15,50,54,60,65–67]. From the experimental determination of several cloud points with low polymer concentrations, the binodal curve can be extrapolated in

order to calculate compositions with higher polymer concentrations [15]. Therefore both, theoretical calculations and experimental studies enabled the study of phase diagrams for several different systems by giving information on the binodal and spinodal curves [15,48,50,54,58,68].

Nonetheless, theoretical calculations and cloud point measurements have several limitations. It is possible that calculations can deviate from the reality as several assumptions have to be done in order to calculate the important components of a phase diagram. In case of cloud point titrations the experimental measurement enables the determination of exact compositions on the binodal. However, in one experiment only the composition of one single point on the binodal curve can be determined and only of solution compositions which have a low polymer content. If the binodal curve shall also be investigated at higher polymer contents, an extrapolation of a few measurements is necessary which cannot reflect the exact reality. Furthermore, it does not give direct information on the phase equilibrium and it does not enable the direct determination of the exact compositions of the co-existing phases.

Therefore, in contrast to previous studies this work shall contribute to a more detailed experimental determination of the thermodynamic properties of polymer solution systems. This shall enable a more precise prediction of resulting membrane structures and performances from certain solution compositions. For this reason, a method was developed which includes the separation of the demixed phases by centrifugation and a following analysis of the phases after inducing the phase separation. A combination of analytic techniques (size-exclusion chromatography (SEC) and gas chromatography (GC)) was used to determine the exact composition of the phases. In this case polyethersulfone (PES) was chosen as the membrane-forming polymer because it is one of the most commonly chosen raw materials for the preparation of membranes by immersion precipitation in academia and industry [31]. In addition to locating the binodal curve and the miscibility gap, the newly developed method allows the determination of the exact composition for each of the two phases generated by the addition of non-solvent to a defined initial composition. This enables to define the tie-lines within the phase diagram and therefore generates information on the phase equilibrium.

After evaluating the method and ensuring its reproducibility, initial experiments were conducted to determine the phase equilibrium in dependence on temperature and casting solution composition of a ternary system consisting of PES, water and N-Methyl-2-pyrrolidone (NMP). In order to evaluate the results which were generated with the tie-line determination method, the resulting binodal curves were then compared to additionally conducted cloud point experiments under the same conditions, as this technique was chosen as a reference method due to its widespread acceptance.

## 2. Experimental

### 2.1. Materials

Commercial PES was purchased from BASF (Ludwigshafen, Germany) and applied as the reference polymer for immersion precipitation casting solutions. In order to prepare these casting solutions, an appropriate solvent was needed. The chosen solvent for PES was NMP (Carl Roth, Karlsruhe, Germany). Furthermore, reverse-osmose (RO) water (Sartorius Stedim Biotech GmbH, Goettingen, Germany) was applied as the non-solvent.

### 2.2. Preparation of polymer solutions

For the studies, non-volatile polymer solutions with different PES concentrations (2.5 wt% to 15 wt%) were prepared for studying a commonly applied system in the membrane precipitation process. Therefore, NMP was pre-filled into a 500 mL twin-neck flask (Carl Roth, Karlsruhe, Germany) and 0.5 wt% of RO-water were added. Then the

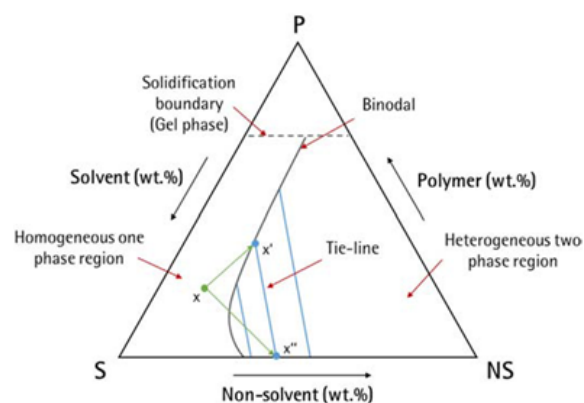


Fig. 1. Schematic drawing of a phase diagram for a ternary system consisting of polymer, solvent and non-solvent.



solution was stirred and tempered to 60 °C. Finally, the desired amount of polymer was added and the mixture was stirred at 150 rpm (IKA overhead stirrer RW20, IKA, Staufen, Germany) over night, until a homogenous solution was generated. Finally, the solutions were degassed at 50 °C in an oven.

### 2.3. Cloud point determination

The cloud points of the polymer solutions were determined by measuring the turbidity while constantly adding non-solvent to the sample. Therefore, the solution was filled into a tempered reactor (HWS, Mainz, Germany) and stirred at 300 rpm (IKA overhead stirrer RW20, IKA, Staufen, Germany) at a constant temperature using a KPG mixer (Bola, Gruensfeld, Germany). A photometric sensor (Metrohm 662 Photometer, Metrohm GmbH and Co. KG, Filderstadt, Germany) was dipped into the solution and the light transmittance of the starting solution was set to 95%. Then an automatic titration tip was applied to the lid of the reactor and connected to a bottle containing water as non-solvent. The experiment was started by set up the titration unit (Metrohm 900 Touch Control, Metrohm 846 Dosing Interface, Metrohm 807 Dosing Unit and Metrohm 800 Dosino, Metrohm GmbH and Co. KG, Filderstadt, Germany) which added 0.03 mL/min of the non-solvent into the polymer solution under constant stirring. During this procedure the light transmittance was recorded as a function of time by a computer connected to the titration unit. Experiments were conducted at 10 °C, 20 °C and 40 °C. The measurement was stopped when the light transmittance dropped below a value of 5%. The recorded data were analyzed with the software *Origin 2018b* (Northampton, MA, USA) by determining the inflection point of the titration curve which represents the cloud point of the solution. This enables the determination of the composition on the demixing point. For each system five different starting solutions were investigated to gain different points on the binodal curve. In order to obtain a complete binodal curve, the measurement data were extrapolated using a linearized fit as described by the group around Smolders [15]:

$$\ln \frac{\phi_{NS}}{\phi_P} = b \cdot \ln \frac{\phi_S}{\phi_P} + a \quad (1)$$

where  $\phi_{NS}$  is the weight fraction of the non-solvent,  $\phi_P$  is the weight fraction of the polymer,  $\phi_S$  is the weight fraction of the solvent, and  $a$  and  $b$  are the constants which result from the equation of the linear regression from the experimentally determined data of the cloud point measurements.

### 2.4. Tie-line determination

As an alternative procedure for the cloud point titration, a new method was developed. In order to determine the tie-lines, an empty 2 mL Eppendorf tube (Eppendorf, Hamburg, Germany) was weighed on an analytical balance (Sartorius AG, Goettingen, Germany). Afterwards, the polymer solution was filled into the tube and the weight of the filled tube was recorded. Finally, the tube was filled up with water to approximately 2 mL and the final weight was determined. It had to be ensured that the amount of added non-solvent was high enough to induce the demixing of the casting solution. By preparing samples with different ratios of polymer solution and non-solvent, different data points within the phase diagram could be determined. After the preparations of the tubes the solution was homogenized using a vortexer (Heidolph Instruments, Schwabach, Germany) and placed in a tempered centrifuge (Hereaus Primo R, Thermo Fisher Scientific, Waltham, MA, USA). The samples were centrifuged at  $16,000 \times g$  for 24 h at a defined temperature. Due to the different densities of the two developing phases, the phases could be separated in the centrifuge. The polymer-rich, gel-like phase accumulates at the bottom of the tube and the polymer-poor, liquid phase accumulates above it. The next

steps of the procedure are depended on the volatility of the solvents. In case of a polymeric systems with non-volatile solvents follow Section 2.4.1. In case of polymeric systems with volatile solvents follow Section 2.4.2.

#### 2.4.1. Non-volatile solvents

The polymer-poor phase was directly transferred to a new tube and its mass was determined. Additionally, the weight of the polymer-rich phase was measured. Then the tube with the remaining polymer rich phase was placed into a 100 mL Schott flask (Schott AG, Mainz, Germany) and 5 mL of HPLC-grade *N,N*-Dimethylacetamide (DMAc) (VWR, Radnor, PA, USA) were added to the flask. The exact addition of DMAc was determined on an analytical balance (Sartorius AG, Goettingen, Germany). During this step it should be checked that the Eppendorf tube is not floating in the solution. If necessary, the lid from the Eppendorf tube was removed before placing it into the flask. Then the Schott flask with the Eppendorf tube was placed on a horizontal shaker (Certomat® U, B. Braun, Melsungen, Germany) until the polymer-rich phase was completely solved. After the samples have been separated from each other they could be prepared for further analyses, whereby the amount of the solid components were determined via size exclusion chromatography (SEC), whereas the amount of solvent and non-solvent was determined via gas chromatography (GC). For the determination of the composition of the polymer-poor phase, 1 mL of the polymer-poor phase was added to 1 mL of HPLC-grade DMAc (VWR, Radnor, PA, USA). Subsequently the mixture was transferred to a crimp vial (Agilent, Santa Clara, CA, USA) and used for the SEC analysis (for details see Section 2.5). The remaining polymer-poor phase was then diluted 1:10 with pure 1,4-dioxane (Merck KGaA, Darmstadt, Germany). Afterwards a sample of this mixture was filled into a screw cap vial (Agilent, Santa Clara, CA, USA) and used for the GC analysis (for details see Section 2.6). In contrast, for determination of the composition of the polymer rich phase the dissolved sample could be directly filled into a crimp vial for the SEC analysis. The remaining part of the prepared samples were 1:10 diluted with 1,4-dioxane (Merck KGaA, Darmstadt, Germany) and a sample of this mixture was filled into a screw cap vial (Agilent, Santa Clara, CA, USA) for the GC analysis. The combination of SEC and GC results finally gave the composition of both analyzed phases.

#### 2.4.2. Volatile solvents

10 mL of 1,3-Dioxolane (Merck KGaA, Darmstadt, Germany) were placed into a 100 mL Schott flask and the weight of solvent and flask was determined. A flask is prepared for each phase to be examined. Subsequently the upper polymer-poor phase was added to the first flask and the weight was recorded again. Afterwards the weight of the lower polymer-rich phase was determined as well. The tube containing the polymer-rich phase was placed into the second flask. During this step it should be checked that the Eppendorf tube is not floating in the solution. If necessary, the lid from the Eppendorf tube was removed before placing it into the flask. Then the Schott flask with the Eppendorf tube was placed on a horizontal shaker (Certomat® U, B. Braun, Melsungen, Germany) until the polymer-rich phase was completely solved. After the phases have been separated from each other they could be prepared for further analyses. The amount of the solid components was determined gravimetrically, the volatile components were determined via GC (for details see Section 2.6). For the determination of the solid components the empty weight of drying trays (e.g. aluminum pans for moisture balances) was determined for each of the two phases. The empty weight of a syringe was determined as well and the syringe was used to completely absorb the sample. Approximately 1 mL of each sample was filled into a screw cap vial (Agilent, Santa Clara, CA, USA) for the GC analysis. The weight of the remaining solution was determined and then the complete remaining solution was placed onto the drying tray. The tray was left at room temperature under a fume hood in order to allow the evaporation of the volatile solvent.

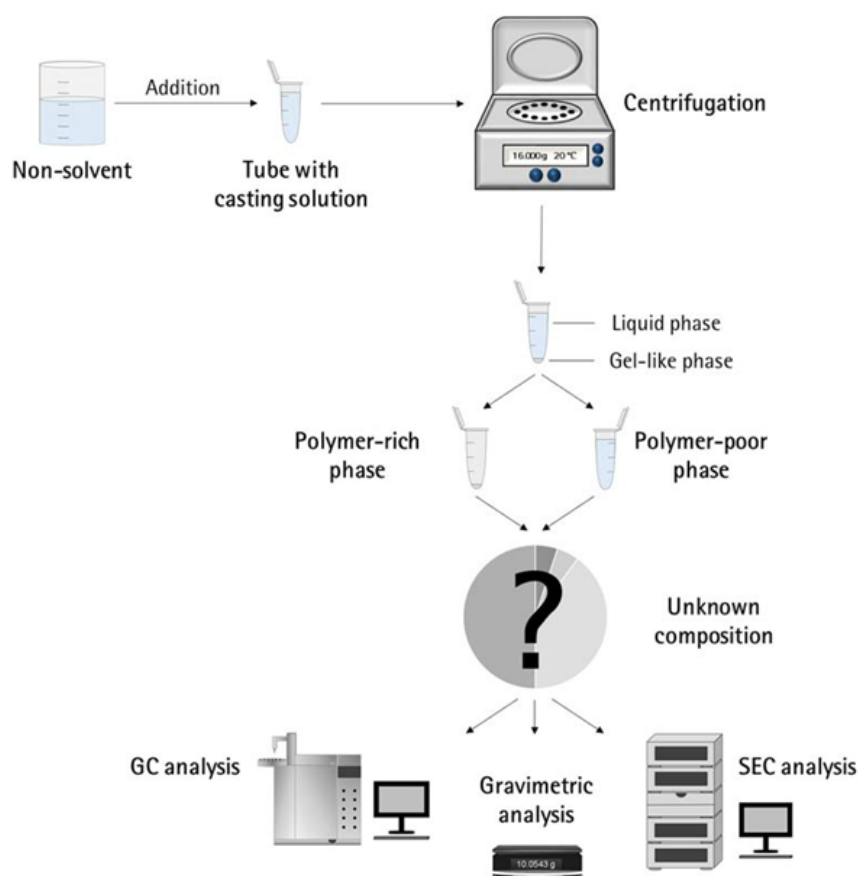


Fig. 2. Schematic depiction of the experimental steps applied for the tie-line determination method.

Afterwards, they were placed into a drying oven at 60 °C to ensure the complete evaporation of all liquid components of the sample. Finally, the weight of the drying tray was determined. The combination of the gravimetric measurement and the GC result gave the composition of both analyzed phases.

An overview of the tie-line determination method is depicted in Fig. 2.

In this study the focus was laid on non-volatile systems so that the following results show examples for the study of non-volatile polymeric solutions.

### 2.5. Size exclusion chromatography (SEC)

In case of polymeric systems with non-volatile solvents, the polymer concentration in both phases was determined via SEC. Therefore, a PES calibration series was prepared by dissolving different concentrations of PES in HPLC-grade DMAc (HiPerSolve CHROMANORM®, VWR, Darmstadt, Germany) which was also used as the eluent for the SEC analyses with 4.35 g/L lithium chloride (VWR, Darmstadt, Germany) added to it. The concentrations used for determining the PES calibration curve ranged from 0,036 wt% PES up to 1 wt% PES. For the determination of the molecular weight distributions, a polystyrene ReadyCal Kit (PSS Polymer Standards, Mainz, Germany) was used. The commercial polystyrene standards were dissolved in the eluent and used for the molecular weight calibration curve. The polystyrene standards, the PES

calibration samples, as well as the samples with an unknown PES concentration, prepared as stated in Section 2.4, were measured with the SEC system Infinity II (Agilent Technologies, Santa Clara, CA, USA). The measurements were conducted with a flow rate of 1 mL/min and a column temperature of 50 °C. The column used for separating the polymer chains by size was the PSS GRAM column combination medium (PSS Polymer Standards, Mainz, Germany). The detection of PES was done by a UV-Vis detector (Agilent, Santa Clara, CA, USA) which was set to 280 nm. The resulting chromatograms were recorded and analyzed by calculating the peak area of each sample with the software *PSS WinGPC® UniChrom V 8.20* (PSS Polymer Standards, Mainz, Germany).

### 2.6. Gas chromatography (GC)

GC was used to determine the relative proportions of solvent and non-solvent in the samples. The measurements of the in 1,4-dioxan diluted samples were performed with the 7890A gas chromatographic system (Agilent Technologies, Santa Clara, CA, USA) using helium as the carrier gas. The capillary column J&W CP-PoraPLOT Q52 (Agilent Technologies, Santa Clara, CA, USA) was used for separation and the components of the samples were detected with a thermal conductivity detector. The parameters for GC analyses are summarized in Table 1.

A calibration for the GC was conducted by using three defined standards containing different ratios of non-solvent and solvent. Afterwards the samples with unknown compositions were measured in duplicates.

**Table 1**  
Programming parameters of the GC measurements.

Injector		Oven	
Temperature	150 °C	Starting temperature	200 °C
Hold time	0.01 min	Hold time	5 min
Split rate	1:10	Heating rate	120 °C/min
Injection volume	0.5 µL	Hold time	21 min

The analysis of the chromatograms was conducted with the software EZChrom Elite.

### 3. Results and discussion

#### 3.1. Reference method - cloud point titration

As the cloud point titration is an accepted method for the examination of the binodal curve of polymer solutions, it was applied as the reference method for the tie-line determination procedure. Cloud point measurements of PES casting solutions containing up to 15 wt% of PES could successfully be conducted. However, the cloud points of samples with higher polymer contents could not be determined. The limiting factor of samples with higher polymer concentrations was the increasing viscosity. When the non-solvent drops entered the solution, a locally higher water concentration was caused for a short time, resulting in a local phase separation event at the point where the drop entered the solution. At lower viscosities, stirring of the solution quickly resulted in re-dissolving of the precipitated area so that good quality data were recorded where the inflection point of the curve could be easily determined (Fig. S1a, supporting information). However, at higher viscosities the mixing of the polymer solution was aggravated so that the re-dissolving of particles took longer. As a result of this, the precipitated particles disturbed the photometric measurements and caused high fluctuations in the measured values making the evaluation of the data impossible (Fig. S1b, supporting information).

Six different cloud points of the binodal curve were determined at three different temperatures (Fig. 3a). The data were then used to extrapolate the complete binodal curve (Fig. 3b) by the application of linearized cloud point curve correlations at higher polymer concentrations as described by Boom et al. [15]. This extrapolation technique is an

accepted avenue to gain the full phase diagram of a ternary system. This is why it is repeatedly applied by other groups [67,69,70], although the extrapolated curve may not reflect the real course of the binodal.

It has been previously shown that the miscibility gap of other ternary systems used for the preparation of porous membrane is strongly dependent on the temperature at which phase separation takes place [68,71,72]. However, the results in this study show that the miscibility gap of the PES/NMP/H<sub>2</sub>O system is only slightly dependent on the temperature of the investigated range from 10 °C up to 40 °C. At all examined temperatures the measured cloud points and therefore the extrapolated binodal curves were found to be nearly at the same ternary compositions. There are several measurements of PES/NMP/H<sub>2</sub>O cloud points as well as theoretically calculated binodal curves reported in literature [17,50,54,58,73–75]. Often these studies do not include temperature variations but focus on one selected temperature. Since in this study it has been shown that the temperature has barely an influence on the location of the binodal curve, as expected the results of previously reported studies match the findings of this work.

As mentioned before, at higher polymer concentrations the method did not work as the addition of non-solvent resulted in locally precipitated particles, which then disturbed the photometric measurements. This is why a linear extrapolation was conducted to work around this problem. The disadvantage of this extrapolation is that it is based on the assumption that the binodal follows a linear function which can be calculated from a few measuring points only. However, this assumption might not reflect the real course of the binodal leading to inaccurate projection of the miscibility gap. Due to the method, binodal curves extrapolated from cloud point measurements tend to result in a progression towards the solvent-axis [15,50,54,60].

However, there are indications in the literature that the binodal curve at higher polymer concentrations rather drifts towards the polymer axis due to the set-in of the solidification [58,76]. Apart from the fact that viscosity is a limiting factor leading to a small measurement range, further disadvantages of the cloud point measurements are that it is time-consuming. From one measurement only one point on the binodal is obtained. Furthermore the measurements can be disturbed by precipitated particles and air entering to the solution through stirring of the solution. Cloud point titrations provide no information about the phase equilibrium of the coexisting phases, which results from the phase separation event. These disadvantages should be overcome by the development of the tie-line determination method which is presented in Section 2.4 and discussed in detail in the following.

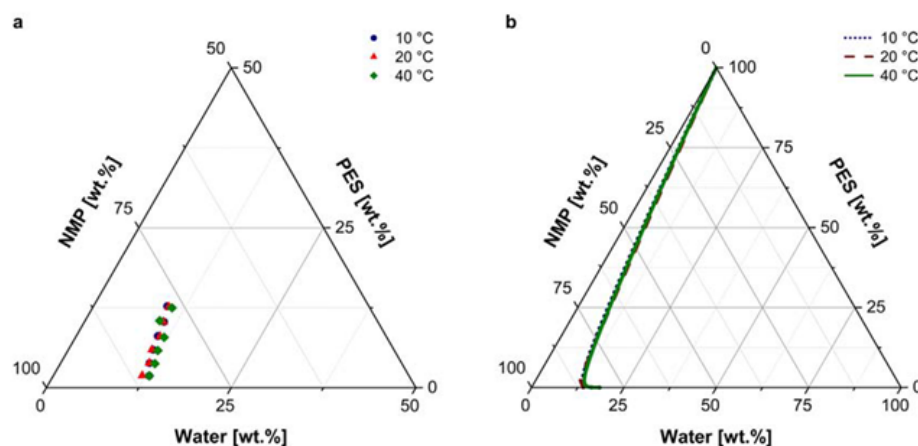


**Fig. 3.** Cloud points of polymer solutions with different starting concentrations determined by turbidity measurements (a) and the extrapolated binodal curves from these cloud points (b) in dependence of the phase separation temperature (10 °C, 20 °C and 40 °C).

### 3.2. Tie-line determination

#### 3.2.1. Centrifugation time

In order to ensure a complete separation of the polymer-poor phase from the polymer-rich phase during centrifugation, the influence of the centrifugation time on the phase proportions was studied, with the aim to set an appropriate centrifugation time for the tie-line determination. A separate experiment was conducted in the frame of the method development in which nine identical samples were prepared as described above with each sample having the same proportions of polymer solution and non-solvent. Referring to the previously described method, the samples were placed into the centrifuge which was set to 20 °C and 16,000  $\times$ g. Then each sample was centrifuged for a different duration including the time points 2 h, 6 h, 12 h, 16 h, 24 h, 48 h, 96 h, 120 h and 144 h. The experiment was run in duplicates for each time point. After centrifugation, the phases were directly separated from each other and the mass of each phase was determined with an analytical balance. The proportions of the phases were then compared between the samples in order to determine the time point where the phase separation was completed, indicated by a constant mass for both phases.

While at centrifugation durations below 24 h the masses in both phases differed between the distinct time points, it could be shown that they did not change visually by choosing centrifugation times ranging from 24 h up to 166 h (Fig. 4a and b). The polymer-poor phase

consistently showed a mass of approximately  $1.63 \text{ g} \pm 0.01 \text{ g}$  at all time points between 24 h and 166 h while the polymer-rich phase had a weight of around  $0.30 \text{ g} \pm 0.005 \text{ g}$ , regardless of the centrifugation duration in the investigated time range (Fig. 4c). By performing a linear regression on the data of both phases it could also be demonstrated that the masses did not change significantly within this time range as the slopes in case of both phases was close to zero. Furthermore, the average weight percentage composition of each phase of the five studied centrifugation times exhibited a very low standard deviation which indicates the constant masses in both phases over the time (Fig. 4d). The deviations can rather be explained by slight variations in the sample preparation. For all following experiments a centrifugation time of 24 h is used.

#### 3.2.2. Evaluation of the method

In the following the evaluation of the method in terms of its precision and reproducibility is shown. For this purpose, four identical samples were prepared using an analytical balance which all contained the same proportions of polymer solution and non-solvent. The samples were equally processed and analyzed as described before (see Section 2.4), and the results were used to construct the phase diagram of the system. Additionally, the average and the standard deviation of the four single measurements were calculated for each component in both phases in order to evaluate the reproducibility. Furthermore, a mass balance was calculated by putting the input masses which were

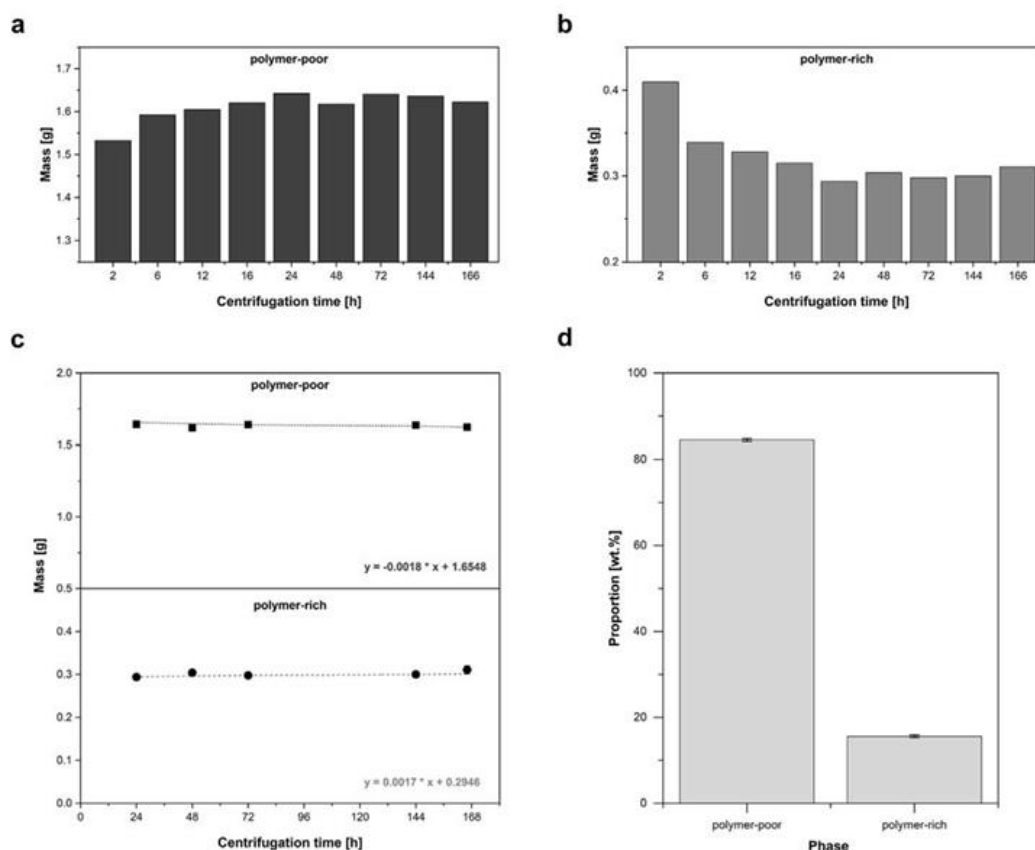


**Fig. 4.** Mean masses of polymer-poor (a) and polymer-rich phases (b) for all investigated time points ( $n = 2$ ), mean masses of both phases with a linear fit (dotted lines) after phase separation and centrifugation in dependence of the centrifugation time from 24 h to 166 h (c) and mean proportion  $\pm$  standard deviation ( $n = 5$ ) of each phase averaged over all time points from 24 h to 166 h (d).

tracked by gravimetric measurements in relation to the output masses which were determined by SEC and GC. Furthermore, the validation was conducted at three different temperatures and the samples were compared among each other to prove that the method gives reproducible results regardless of the temperature (Fig. S2, supporting information).

At all examined temperatures (10 °C, 20 °C and 40 °C) the four independently prepared and analyzed samples resulted in similar phase compositions and therefore in equivalent tie-lines which proceed almost exactly one on top of the other with only small deviations at high polymer concentration (Fig. S2, supporting information). In order to confirm this, the reproducibility was illustrated by averaging the composition of the four different samples and by then calculating their deviations (Fig. 5).

Especially the consistency of the polymer-poor phase was in all cases highly reproducible. This is particularly evident from the standard deviations and the thereof resulting relative deviations of the four individual measurements from the average composition of each component (Table S1, supporting information). To prove that the method delivers reliable results the determined standard deviations of the average compositions were compared to the expected variations. It could be found

that in all cases the standard deviations of the average compositions were in the same order of magnitude or even lower than the expected deviations caused by experimental inaccuracies such as the weighing error and the deviations of the analytical methods used during the tie-line determination procedure (Table S2, supporting information).

Furthermore, the average composition result does also show that the measurement precision for the determination of the percentage phase compositions is very high. As already assumed from the phase diagrams, the reproducibility in the polymer-poor phase is even higher than the one of the polymer-rich phase. A reason for this could be that the polymer-rich phase exists in a gel-like state after centrifugation. In order to re-dissolve the phase the tubes are put in a bottle with DMAc and shaken overnight. The larger differences between the four replicates in the polymer-rich phase might result from the sample processing in this additional step. In general, the deviations found in both phases between the replicate samples are rather due to small fluctuations in the proportion of polymer solution and non-solvent during sample preparation, resulting as a cause of the balance error than to imprecise results from the analytic determination of the compositions itself. Another reason for the inaccuracies could be that a small fraction of the polymer-poor phase remains in the polymer-rich phase when

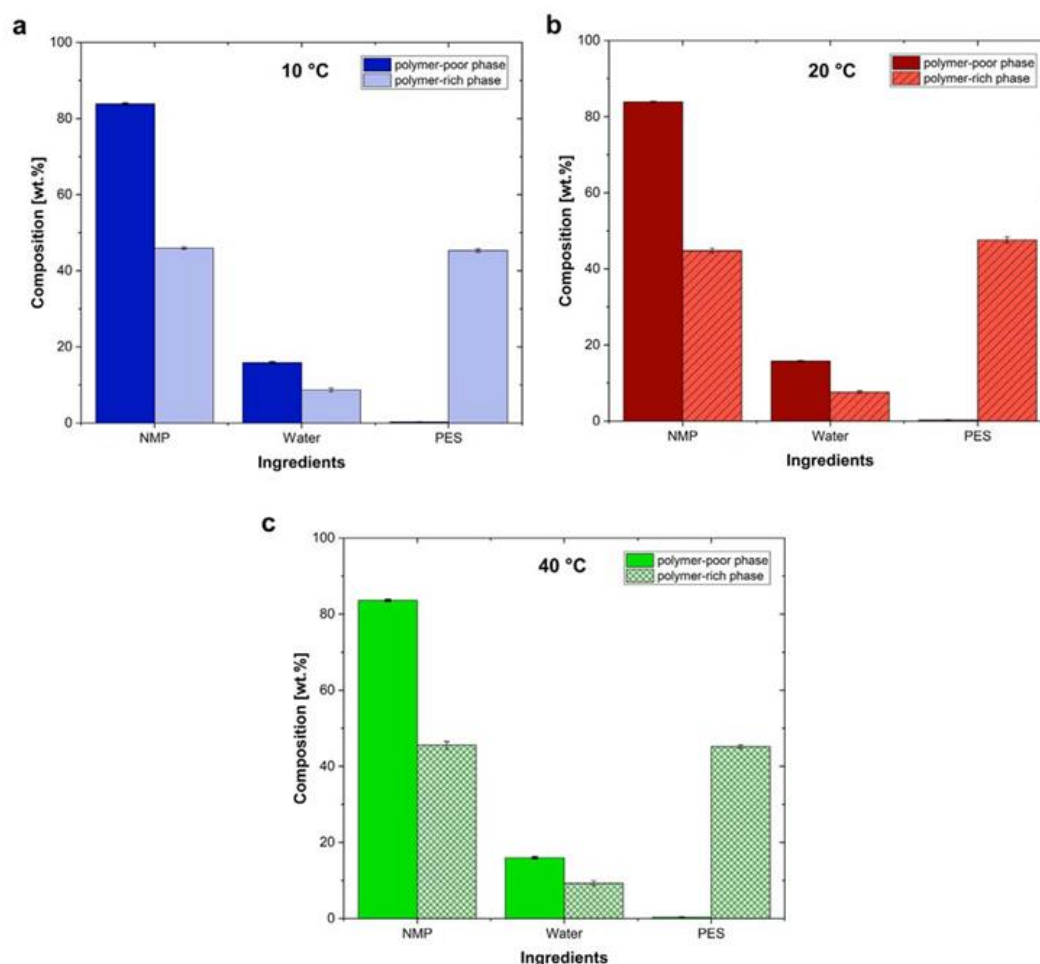


Fig. 5. Averaged composition  $\pm$  standard deviation ( $n = 4$ ) of the polymer-poor and the polymer-rich phases determined via SEC and GC after phase separation by centrifugation of the fourfold repeated tie-line determination at different temperatures of 10 °C (a), 20 °C (b) and 40 °C (c).

both phases are separated after centrifugation as a complete transfer of the liquid phase into the separate tube is not possible.

On top of the reproducibility, it was checked if the amounts of all ingredients added in the beginning can be retrieved from the analytical measurements in the end. Therefore, the mass balance was calculated for all samples and averaged for each ingredient at all examined temperatures (Fig. S3, supporting information). The mass balance could be solved with deviations below 10% for all substances at all studied temperatures. Taking into consideration that the method involves several weighing steps and analytical analyses which all have certain measurement errors, this is still a precise and therefore acceptable result as the deviations caused by the experimental error are in the same order of magnitude as the expected deviations (Table S2, supporting information). In particular the proportions of the solvent and the non-solvent which have been identified by GC only exhibit very small deviations from the mass balance. In contrast, the share of the polymer PES which was determined by SEC exhibit higher deviations which could be explained by a higher measurement accuracy of the GC method compared to the SEC procedure.

### 3.2.3. Tie-lines of the NMP/PES/water system at different temperatures

As the method has been proven to deliver reproducible and accurate results, tie-lines of the NMP/PES/water system were determined at three different temperatures and plotted into a phase diagram (Fig. 6). In order to get different points on the binodal curve, the ratios of

polymer solution and non-solvent during the sample preparation were varied.

Comparable to the results of the cloud point titrations, the tie-lines measured at different temperatures indicate that the course of the binodal curve in the area of lower polymer concentrations is not visibly dependent on the temperature. This reveals that the location of the miscibility gap barely changes when the temperature is changed within the examined temperature range, especially in the area of the polymer-poor phases. However, in the region of the polymer-rich phases in the phase diagram, slight variations between the measurements at different temperatures could be found.

This finding deviates from the results which were found by the cloud point titrations in this study as well as from previous findings based on turbidity measurements or theoretical calculations of the binodal [50,58,60,67,73]. Equivalent methods for the determination of polymer solution thermodynamics and especially of the position of the tie-lines in the phase diagram are barely published in the literature. One example from the literature for determining the tie-lines of a ternary polymeric system is based on the exact determination of the composition of the polymer-poor phase. By applying the so called lever rule, the composition of the concentrated polymer-rich phase could be calculated from a mass balance using the previously experimental examined composition of the other phase [50]. Similarly to this work, the tie-lines of the ternary system PES/NMP/water were calculated, however at 25 °C instead of 20 °C. Nonetheless, the composition of the phases which were

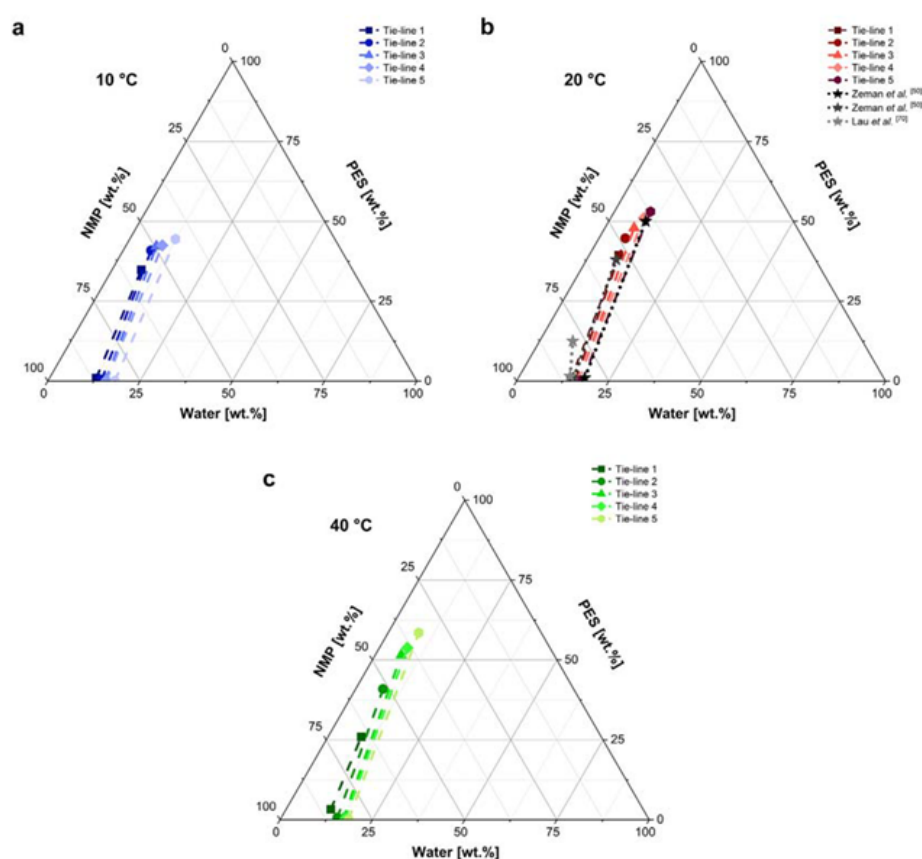


**Fig. 6.** Tie-line determination of differently composed samples at 10 °C (a), 20 °C (including two reference data sets [50,73], measured at 25 °C) (b) and 40 °C (c) by determining the compositions of polymer-poor and polymer-rich phase after phase separation by centrifugation via SEC and GC. The symbols indicate the phase compositions, the dotted lines the respective tie-lines.

determined in that work corresponds to the data from the data recorded using the newly developed method [50]. Apart from the experimental tie-line determination, the same group used the Flory-Huggins theory in order to simulate the course of the binodal curve at high polymer concentrations. Similar to the results which could be seen for the linearly extrapolated binodal in this study, the via Flory-Huggins calculated binodal deviates from the result of the experimentally established tie-lines [50].

Yet there is another example where the compositions of the polymer-poor and the polymer-rich phases of PES/NMP/water were determined at 25 °C. In that case the phases were also separated in a tube, but instead of using a centrifugation step the method was based on time-dependent diffusion processes. Again the tie-lines they identified are similar to the ones of this study [73]. However, in comparison to the method presented in this study, the disadvantage of the diffusion based procedure is that the phase separation especially for more viscous solutions is very time-consuming as diffusion based separation takes much longer than the phase division by centrifugation.

### 3.2.4. Comparison of the binodal curves from the two different methods

In order to compare the results of both methods at different temperatures, the course of the binodal curves were derived from the tie-lines (Fig. 7b) and used to compare their course with the ones of the extrapolated curves from the cloud point experiments (Fig. 7a).

At all temperatures with both methods, the binodal curves at lower polymer concentrations (until 40%) converge towards the solvent-axis. In case of the extrapolated curves the binodal continues to converge towards the solvent-axis in the area of higher polymer concentrations. The course of the binodal curves derived from the tie-lines show a different progress. At a certain point within the phase diagram the polymer-rich phase tends to shift towards polymer axis. The binodal curve based on the determined tie-lines in this work represents a more realistic position of the binodal since the course is not based on assumptions but on reproducible measured values.

There are several previous works which also indicate that the binodal does not continue to converge towards the solvent axis but that it shifts towards the polymer axis at a critical polymer concentration in the polymer-rich phase [58,76].

As shown in Fig. 7b this shift seems to be dependent on the temperature as at lower temperature the polymer-rich phase tends to drift earlier to the polymer axis than at higher temperatures. Therefore, it can be concluded that the higher the temperature, the later the tie-lines start to shift. This means that the polymer-rich phases contain higher polymer

concentrations at higher temperatures compared to those of lower temperatures.

A reason for this could be that at high concentrations the polymer undergoes a solidification process called gelation. It is well known that ternary polymeric systems exhibit a solidification boundary at which the liquid-liquid demixing process is overcome by the formation of a gel-like structure [17,53,58,77,78]. This gelation involves the formation of a three-dimensional network by physical cross-linking of the polymeric chains which is caused by the formation of micro-crystallites or due to chain entanglement [79–81]. As chain entanglement sets in at higher polymer concentrations when the temperature is increased due to a higher mobility of the polymer chains, it can be assumed that the equilibrium is shifted from solidification towards liquid-liquid separation when the temperature is raised.

Another reason for this finding could be that the viscosity of the homogenous solution and therefore in the resulting phases is decreased when the phase separation temperature is raised as it is also dependent on the degree of the chain entanglement. As a result the mass transport, simplified as the Brownian motion, is faster which leads to a higher diffusion rate of the polymer into the polymer-rich phase. If it is assumed that the viscosity is the critical factor for the solidification of the polymeric structure, more polymer is needed at raised temperatures to reach the critical viscosity in the polymer-rich phase that leads to the solidification. In literature the solidification boundary is also described as a condition of infinite viscosity which would support this assumption [2,57].

### 3.2.5. Determination of the polyethersulfone molecular weight distributions

The determination of the polymer concentration by SEC not only enables the absolute polymer content in each phase but it also provides an insight into the molecular weight distribution of the polymer in each of the phases. Common methods to determine the polymer concentrations which have been published previously are based on gravimetric determination of the polymer content in a ternary system [50,73]. However, this does not give any information on the molecular weight distributions of the polymer in each phase. It has been shown on a binary system that the polymer-poor phase contains predominantly the short-chained polymer while the longer polymer chains accumulate in the polymer-rich phase [82]. These findings could also be proven for the ternary system investigated in this work. Fig. 8 shows that the molecular weight distribution of the polymer-poor phase consists of shorter polymer chains while the larger ones can be found in the polymer-rich phase. This can be explained by the chemical nature of polymer and its end groups, which in case of PES are hydroxyl groups. In contrast

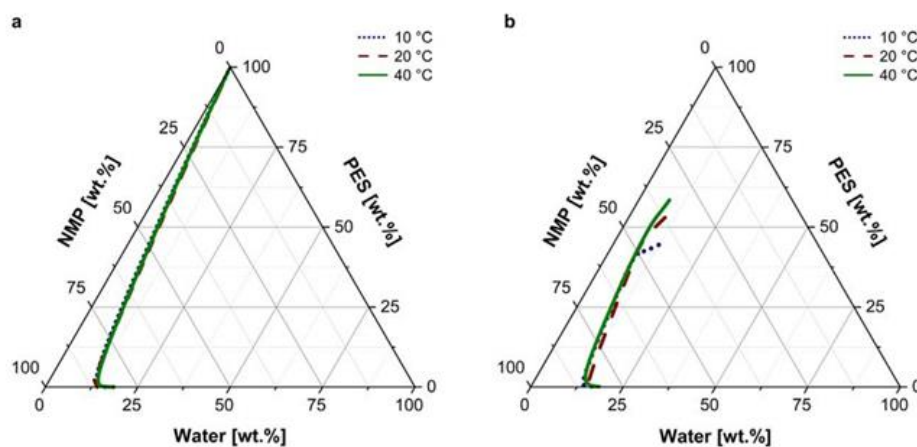
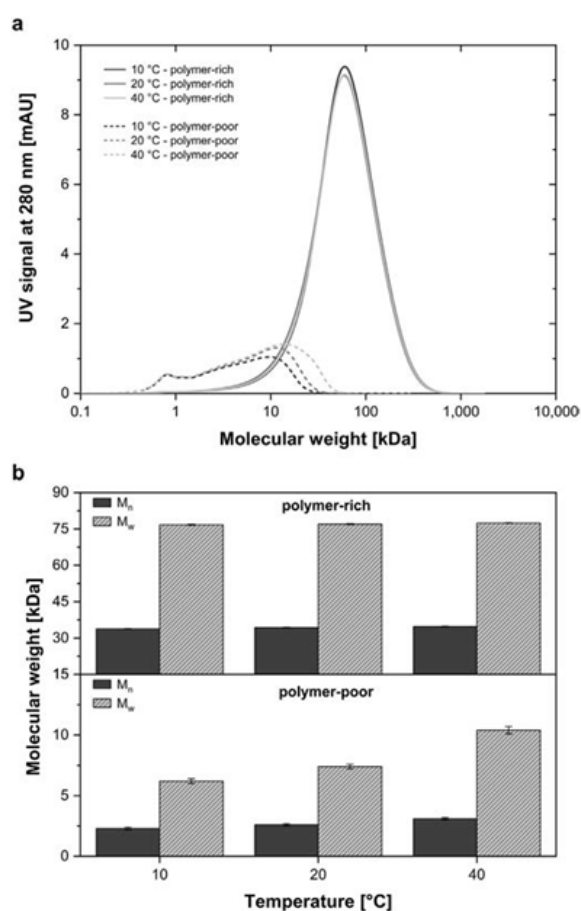


Fig. 7. Binodal curves in dependence of the phase separation temperature determined by cloud point measurements (a) and the tie-line determination method (b).

10

C. Kahrs et al. / Journal of Molecular Liquids 291 (2019) 111351



**Fig. 8.** Number and weight means of the molecular weight distributions of PES in the polymer-poor and polymer-rich phases at different temperatures determined via SEC analyses with the application of a polystyrene standard mix for the molecular weight determination.

to the hydrophilic end group, the rest of the PES is quite hydrophobic [83]. Therefore, the longer the polymer chains, the more hydrophobic is the molecule as the share of the hydrophobic part increases. Hence, as it has been shown in the determination of the phase compositions, due to its low solubility in water, the polymer accumulates in the polymer-rich phase as this phase mainly consists of the solvent. As the polymer-poor phase contains a larger fraction of water compared to the polymer-rich phase, only a few polymers with a low molecular weight are able to dissolve and therefore persist in this phase as the short polymer chains are less hydrophobic than the longer chains due to the hydrophilic nature of the hydroxyl end groups. This is underlined by the calculation of the number and the weight average of the molecular weight distributions which were calculated on the basis of a polystyrene standard. While the number mean of the molecular weight in the polymer-rich phase lies around 40 kDa, the number mean in the polymer-poor phase only averages out at around 2.5 kDa. The same trend can be seen from the results of the weight average in both phase as it lies around 75 kDa in the polymer-rich phase and only around 5 kDa to 10 kDa in the polymer-poor phase. The chromatograms as well as the result of the weight mean of the polymer-poor phase molecular weight distribution indicate that the molecular weights in the polymer-poor phase are also broader distributed in comparison to the

ones in the polymer-rich phase. This could be explained by a high number of different low-molecular components in the raw material while the high-molecular components in the basic polymer is more equally distributed. This assumption is underlined by the polydispersity index of the SEC measurements which was found to be slightly higher at all temperatures for the polymer-poor phase in comparison to the one of the polymer-rich phase.

While the temperature does not visibly affects the distribution of the molecular weights in the polymer-rich phase, a trend can be seen for the distributions in the polymer-poor phase although the distribution has to be in an equilibrium. The higher the temperature during phase separation, the higher the amount of longer polymer-chains could be found in the polymer-poor phase. A reason for observing an effect in one phase but not in the other phase could be that the polymer concentration in the polymer-rich phase is generally higher than in the polymer-poor phase. As a result the effect does not become as obvious as in the other phase. The finding of a shift in size with rising temperature in the polymer-poor phase is underlined by the trend which arises from the illustration of the molecular weight mean of the size distribution in this phase (Fig. 8b).

A reason for the temperature-dependent size shift could be that the solubility of the polymer is increased at higher temperatures. As a result also a larger share of the high-molecular weight chains could dissolve in the polymer-poor phase leading to the drift of the size distribution as seen from the results of the weight mean of the molecular weight in the polymer-poor phase. This assumption is supported by the fact that the difference between 10 °C and 20 °C is less pronounced than the difference between 20 °C and 40 °C.

#### 4. Conclusion

It was possible to develop a new method for the examination of polymer solution thermodynamics. The procedure can be applied for systems containing either volatile or non-volatile solvents. It could be shown that the method provides reproducible data as well as reliable results which were comparable to previous investigations based on experimental measurements or theoretical calculations. Beyond delivering information on the position of the binodal and thus the location of the miscibility gap, the method also enables the determination of the tie-lines. This gives information on the composition of all formed phases as well as the phase equilibria. The evaluation of the method showed that the deviations are in an acceptable range which proves that the analytical methods are suitable for determining the exact phase compositions.

In contrast, determinations of the phase boundary by cloud point measurements lead to results deviating from those of the tie-line experiments. Cloud point titrations only allow a small measurement range, as the viscosity is a limiting factor. When the viscosity gets to high the measurement is disturbed by precipitated particles through inappropriate mixing and air-inclusion during stirring. This leads to the necessity of an extrapolation which might not reflect the real course of the binodal as the extrapolation tends to underestimate the water content of the polymer-rich phase. The deviations from the real compositions in the polymer-rich phases can be avoided by determining the binodal curve via the tie-line determination. Therefore, the newly developed method is suitable for substituting the conventional cloud point titration.

Another benefit of the tie-line method is the number of measurement points which can be determined at the same time as several samples can be processed simultaneously whereas one cloud point experiment only delivers one phase composition at a time.

Furthermore, the newly developed method gives also information on the polymer size distributions in the separated phases when the polymer concentration is determined via SEC. The application of the method for the investigation of the ternary polymeric system PES/NMP/water shows that the location of the miscibility gap within the



studied temperature range is barely dependent on the temperature. However, the temperature at which phase separation was conducted influenced the molecular weight distribution in the phases and above that it caused differences in the location of a shift of the binodal towards the polymer axis. It is assumed that this shift might represent the solidification boundary, however, this has to be proven in suitable future experiments. Another option for further experiments is the expansion of the method for the examination of systems containing more than three components such as polymeric additives.

### Acknowledgements

The authors would like to thank Joachim Koenig from the Sartorius membrane development team for his support conducting the gas chromatography analyses.

### Appendix A. Supplementary data

Supplementary data to this article can be found online at <https://doi.org/10.1016/j.molliq.2019.111351>.

### References

- [1] R. van Reis, A. Zydney, Bioprocess membrane technology, *J. Membr. Sci.* 297 (2007) 16–50.
- [2] M. Mulder, *Basic Principles of Membrane Technology*, Kluwer Academic Publishers, Dordrecht, Boston, London, 1996.
- [3] H. Strathmann, *Introduction to Membrane Science and Technology*, Wiley, 2011.
- [4] T. Matsuura, *Synthetic Membranes and Membrane Separation Processes*, CRC Press, 1993.
- [5] R. van Reis, A. Zydney, Membrane separations in biotechnology, *Curr. Opin. Biotechnol.* 12 (2001) 208–211.
- [6] R.W. Baker, *Membrane Technology and Applications*, 3rd ed. John Wiley & Sons, Ltd, 2012.
- [7] H. Strathmann, The use of membranes in downstream processing, *Food Biotechnol.* 4 (1990) 253–272.
- [8] A.F. Jozala, D.C. Gerales, L.L. Tundisi, V.d.A. Feitosa, C.A. Breyer, S.L. Cardoso, P.G. Mazzola, L.d. Oliveira-Nascimento, C.d.O. Rangel-Yagui, P.d.O. Magalhães, M.A.d. Oliveira, A. Pessoa, *Biopharmaceuticals from microorganisms: from production to purification*, *Braz. J. Microbiol.* 47 (2016) 51–63.
- [9] J.T. Jung, J.F. Kim, H.H. Wang, E. Di Nicolò, E. Drioli, Y.M. Lee, Understanding the non-solvent induced phase separation (NIPS) effect during the fabrication of microporous PVDF membranes via thermally induced phase separation (TIPS), *Int. Symp. Prog. Membr. Sci. Technol.* 514 (2016) 250–263.
- [10] A.S. Rathore, A. Shirke, Recent developments in membrane-based separations in biotechnology processes: review, *Prep. Biochem. Biotechnol.* 41 (2011) 398–421.
- [11] P. Gronemeyer, R. Ditz, J. Strube, Trends in upstream and downstream process development for antibody manufacturing, *Bioengineering (Basel, Switzerland)* 1 (2014) 188–212.
- [12] H. Strathmann, K. Kock, The formation mechanism of phase inversion membranes, *Desalination* 21 (1977) 241–255.
- [13] J.-F. Li, Z.-L. Xu, H. Yang, Microporous polyethersulfone membranes prepared under the combined precipitation conditions with non-solvent additives, *Polym. Adv. Technol.* 19 (2008) 251–257.
- [14] Dongliang Wang, K. Li, S. Sourirajan, W.K. Teo, Phase separation phenomena of polysulfone/solvent/organic nonsolvent and polyethersulfone/solvent/organic nonsolvent systems, *J. Appl. Polym. Sci.* 50 (1993) 1693–1700.
- [15] R.M. Boom, T. van den Boomgaard, J.W.A. van den Berg, C.A. Smolders, Linearized cloudpoint curve correlation for ternary systems consisting of one polymer, one solvent and one non-solvent, *Polymer* 34 (1993) 2348–2356.
- [16] A.K. Holda, I.F.J. Vankelecom, Understanding and guiding the phase inversion process for synthesis of solvent resistant nanofiltration membranes, *J. Appl. Polym. Sci.* 132 (2015).
- [17] J. Barzin, B. Sadatnia, Correlation between macrovoid formation and the ternary phase diagram for polyethersulfone membranes prepared from two nearly similar solvents, *J. Membr. Sci.* 325 (2008) 92–97.
- [18] E.Y. Astakhov, S.F. Zhironkin, I.M. Kolganov, E.R. Klinshpont, P.G. Tsarin, Study of the formation of the porous structure of membranes during phase separation of a poly(ester sulfone) solution, *Polym. Sci. Ser. A* 53 (2011) 613–620.
- [19] G.R. Guillen, Y. Pan, M. Li, E.M.V. Hoek, Preparation and characterization of membranes formed by nonsolvent induced phase separation: a review, *Ind. Eng. Chem. Res.* 50 (2011) 3798–3817.
- [20] B.S. Lalia, V. Kochkodan, R. Hashaikh, N. Hilal, A review on membrane fabrication: structure, properties and performance relationship, *Desalination* 326 (2013) 77–95.
- [21] M. Amirilargani, E. Sajjoughi, T. Mohammadi, M.R. Moghbeli, Effects of coagulation bath temperature and polyvinylpyrrolidone content on flat sheet asymmetric polyethersulfone membranes, *Polym. Eng. Sci.* 50 (2010) 885–893.
- [22] Q.-Z. Zheng, P. Wang, Y.-N. Yang, Rheological and thermodynamic variation in polysulfone solution by PEG introduction and its effect on kinetics of membrane formation via phase-inversion process, *J. Membr. Sci.* 279 (2006) 230–237.
- [23] H. Susanto, M. Ulbricht, Characteristics, performance and stability of polyethersulfone ultrafiltration membranes prepared by phase separation method using different macromolecular additives, *J. Membr. Sci.* 327 (2009) 125–135.
- [24] E. Sajjoughi, M. Sadrzadeh, T. Mohammadi, Effect of preparation variables on morphology and pure water permeation flux through asymmetric cellulose acetate membranes, *J. Membr. Sci.* 326 (2009) 627–634.
- [25] A. Akbari, R. Yegani, Study on the impact of polymer concentration and coagulation Bath temperature on the porosity of polyethylene membranes fabricated via TIPS method, *J. Membr. Sep. Technol.* 1 (2012) 100–107.
- [26] C. Barth, M.C. Gonçalves, A.T.N. Pires, J. Roeder, B.A. Wolf, Asymmetric polysulfone and polyethersulfone membranes: effects of thermodynamic conditions during formation on their performance, *J. Membr. Sci.* 169 (2000) 287–299.
- [27] J. Peng, Y. Su, W. Chen, Q. Shi, Z. Jiang, Effects of coagulation bath temperature on the separation performance and antifouling property of poly(ether sulfone) ultrafiltration membranes, *Ind. Eng. Chem. Res.* 49 (2010) 4858–4864.
- [28] S.M. Mousavi, A. Zadhoush, Investigation of the relation between viscoelastic properties of polysulfone solutions, phase inversion process and membrane morphology: the effect of solvent power, *J. Membr. Sci.* 532 (2017) 47–57.
- [29] S.H. Yoo, J.H. Kim, J.Y. Jho, J. Won, Y.S. Kang, Influence of the addition of PVP on the morphology of polyimide phase inversion membranes: effect of PVP molecular weight, *J. Membr. Sci.* 236 (2004) 203–207.
- [30] S.A. Al Malek, M.N. Abu Seman, D. Johnson, N. Hilal, Formation and characterization of polyethersulfone membranes using different concentrations of polyvinylpyrrolidone, *Desalination* 288 (2012) 31–39.
- [31] M. Amirilargani, T. Mohammadi, Synthesis and characterization of asymmetric polyethersulfone membranes: effects of concentration and polarity of nonsolvent additives on morphology and performance of the membranes, *Polym. Adv. Technol.* 22 (2011) 962–972.
- [32] J. Barzin, S.S. Madaeni, H. Mirzadeh, M. Mehrabzadeh, Effect of polyvinylpyrrolidone on morphology and performance of hemodialysis membranes prepared from polyether sulfone, *J. Appl. Polym. Sci.* 92 (2004) 3804–3813.
- [33] B. Chakrabarty, A.K. Ghoshal, M.K. Purkait, Preparation, characterization and performance studies of polysulfone membranes using PVP as an additive, *J. Membr. Sci.* 315 (2008) 36–47.
- [34] K.A. Gebru, C. Das, Effects of solubility parameter differences among PEG, PVP and CA on the preparation of ultrafiltration membranes: impacts of solvents and additives on morphology, permeability and fouling performances, *Chin. J. Chem. Eng.* 25 (2017) 911–923.
- [35] M.-J. Han, S.-T. Nam, Thermodynamic and rheological variation in polysulfone solution by PVP and its effect in the preparation of phase inversion membrane, *J. Membr. Sci.* 202 (2002) 55–61.
- [36] A. Idris, N. Mat Zain, M.Y. Noordin, Synthesis, characterization and performance of asymmetric polyethersulfone (PES) ultrafiltration membranes with polyethylene glycol of different molecular weights as additives, *Desalination* 207 (2007) 324–339.
- [37] I.-C. Kim, K.-H. Lee, Effect of various additives on pore size of polysulfone membrane by phase-inversion process, *J. Appl. Polym. Sci.* 89 (2003).
- [38] K.-W. Lee, B.-K. Seo, S.-T. Nam, M.-J. Han, Trade-off between thermodynamic enhancement and kinetic hindrance during phase inversion in the preparation of polysulfone membranes, *Desalination* 159 (2003) 289–296.
- [39] Y. Ma, F. Shi, J. Ma, M. Wu, J. Zhang, C. Gao, Effect of PEG additive on the morphology and performance of polysulfone ultrafiltration membranes, *Desalination* 272 (2011) 51–58.
- [40] M. Sadrzadeh, S. Bhattacharjee, Rational design of phase inversion membranes by tailoring thermodynamics and kinetics of casting solution using polymer additives, *J. Membr. Sci.* 441 (2013) 31–44.
- [41] H.J. Kim, R.K. Tyagi, A.E. Fouda, K. Jonasson, The kinetic study for asymmetric membrane formation via phase-inversion process, *J. Appl. Polym. Sci.* 62 (1996) 621–629.
- [42] H. Matsuyama, M. Teramoto, T. Uesaka, M. Goto, F. Nakashio, Kinetics of droplet growth in the metastable region in cellulose acetate/acetone/nonsolvent system, *J. Membr. Sci.* 152 (1999) 227–234.
- [43] J. Han, W. Lee, J.M. Choi, R. Patel, B.-R. Min, Characterization of polyethersulfone/polyimide blend membranes prepared by a dry/wet phase inversion: precipitation kinetics, morphology and gas separation, *J. Membr. Sci.* 351 (2010) 141–148.
- [44] S.K. Yong, J.K. Hyo, Y.K. Un, Asymmetric membrane formation via immersion precipitation method. I. Kinetic effect, *Int. Symp. Prog. Membr. Sci. Technol.* 60 (1991) 219–232.
- [45] Q.-Z. Zheng, P. Wang, Y.-N. Yang, D.-J. Cui, The relationship between porosity and kinetics parameter of membrane formation in PSF ultrafiltration membrane, *J. Membr. Sci.* 286 (2006) 7–11.
- [46] S.S. Madaeni, L. Bakhtiari, Thermodynamic-based predictions of membrane morphology in water/dimethylsulfoxide/polyethersulfone systems, *Polymer* 53 (2012) 4481–4488.
- [47] S. Mohsenpour, A. Safekordi, M. Tavakolmoghdam, F. Rekabdar, M. Hemmati, Comparison of the membrane morphology based on the phase diagram using PVP as an organic additive and TiO<sub>2</sub> as an inorganic additive, *Polymer* 97 (2016) 559–568.
- [48] S. Mohsenpour, F. Esmaeilzadeh, A. Safekordi, M. Tavakolmoghdam, F. Rekabdar, M. Hemmati, The role of thermodynamic parameter on membrane morphology based on phase diagram, *J. Mol. Liq.* 224 (2016) 776–785.
- [49] L. Shuguang, J. Chengzhang, Z. Yuanqi, The investigation of solution thermodynamics for the polysulfone–DMAC–water system, *Desalination* 62 (1987) 79–88.

- [50] L. Zeman, G. Tkacik, Thermodynamic analysis of a membrane-forming system water/N-methyl-2-pyrrolidone/polyethersulfone, *J. Membr. Sci.* 36 (1988) 119–140.
- [51] H. Strathmann, K. Kock, P. Amar, R.W. Baker, The formation mechanism of asymmetric membranes, *Desalination* 16 (1975) 179–203.
- [52] A.J. Reuvers, C.A. Smolders, Formation of membranes by means of immersion precipitation: part II. The mechanism of formation of membranes prepared from the system cellulose acetate-acetone-water, *J. Membr. Sci.* 34 (1987) 67–86.
- [53] J.G. Wijmans, J. Kant, M.H.V. Mulder, C.A. Smolders, Phase separation phenomena in solutions of polysulfone in mixtures of a solvent and a nonsolvent: relationship with membrane formation, *Polymer* 26 (1985) 1539–1545.
- [54] K.-J. Baik, J.Y. Kim, H.K. Lee, S.C. Kim, Liquid-liquid phase separation in polysulfone/polyethersulfone/N-methyl-2-pyrrolidone/water quaternary system, *J. Appl. Polym. Sci.* 74 (1999) 2113–2123.
- [55] L. Keshavarz, M.A. Khansary, S. Shirazian, Phase diagram of ternary polymeric solutions containing nonsolvent/solvent/polymer: theoretical calculation and experimental validation, *Polymer* 73 (2015) 1–8.
- [56] J.G. Wijmans, J.P.B. Baaij, C.A. Smolders, The mechanism of formation of microporous or skinned membranes produced by immersion precipitation, *International Symposium Progress in Membrane Science and Technology*, 14, 1983, pp. 263–274.
- [57] T.-H. Young, L.-W. Chen, Pore formation mechanism of membranes from phase inversion process, *Desalination* 103 (1995) 233–247.
- [58] J. Barzin, B. Sadatnia, Theoretical phase diagram calculation and membrane morphology evaluation for water/solvent/polyethersulfone systems, *Polymer* 48 (2007) 1620–1631.
- [59] T. Lindvig, M.L. Michelsen, G.M. Kontogeorgis, A Flory-Huggins model based on the Hansen solubility parameters, *Fluid Phase Equilib.* 203 (2002) 247–260.
- [60] A. Ghasemi, M. Asgarpour Khansary, M.A. Aroon, A comparative theoretical and experimental study on liquid-liquid equilibria of membrane forming polymeric solutions, *Fluid Phase Equilib.* 435 (2017) 60–72.
- [61] A.L. Medina-Castillo, J.F. Fernandez-Sanchez, A. Segura-Carretero, A. Fernandez-Gutierrez, Micrometer and submicrometer particles prepared by precipitation polymerization: thermodynamic model and experimental evidence of the relation between Flory's parameter and particle size, *Macromolecules* 43 (2010) 5804–5813.
- [62] M.L. Huggins, Some properties of solutions of long-chain compounds, *J. Phys. Chem.* 46 (1942) 151–158.
- [63] P.J. Flory, *Principles of Polymer Chemistry*, Cornell University Press, 1953.
- [64] P.T.P. Aryanti, D. Ariono, A.N. Hakim, I.G. Wenten, Flory-Huggins based model to determine thermodynamic property of polymeric membrane solution, *J. Phys. Conf. Ser.* 1090 (2018) 12074.
- [65] M. Metzke, Untersuchungen zur Bildung von porösen Membranen aus Cellulosederivaten nach dem Verdunstungsverfahren, (Dissertation, Hannover) 2014.
- [66] M. Roericht, M. Metzke, A. Reiche, G. Niño-Amézquita, Demixing model for the production of cellulose acetate membranes, *Euromembrane* (2015).
- [67] L. Xu, F. Qiu, Simultaneous determination of three Flory-Huggins interaction parameters in polymer/solvent/nonsolvent systems by viscosity and cloud point measurements, *Polymer* 55 (2014) 6795–6802.
- [68] F.W. Altana, Phase Separation Phenomena in Cellulose Acetate Solutions in Relation to Asymmetric Membrane Formation, 1982.
- [69] S. Mazinani, S. Darvishmanesh, A. Ehsanzadeh, B. van der Bruggen, Phase separation analysis of Extem/solvent/non-solvent systems and relation with membrane morphology, *J. Membr. Sci.* 526 (2017) 301–314.
- [70] C. Yin, J. Dong, Z. Li, Z. Zhang, Q. Zhang, Ternary phase diagram and fiber morphology for nonsolvent/DMAc/polyamic acid systems, *Polym. Bull.* 72 (2015) 1039–1054.
- [71] M. Liu, Y.-M. Wei, Z.-L. Xu, R.-Q. Guo, L.-B. Zhao, Preparation and characterization of polyethersulfone microporous membrane via thermally induced phase separation with low critical solution temperature system, *J. Membr. Sci.* 437 (2013) 169–178.
- [72] P. van de Witte, P.J. Dijkstra, J.W.A. van den Berg, J. Feijen, Phase behavior of polylactides in solvent-nonsolvent mixtures, *J. Polym. Sci. B Polym. Phys.* 34 (1996) 2553–2568.
- [73] W.W.Y. Lau, M.D. Guiver, T. Matsuura, Phase separation in polysulfone/solvent/water and polyethersulfone/solvent/water systems, *J. Membr. Sci.* 59 (1991) 219–227.
- [74] L. Shen, L. Li, J. Chen, H. Hong, H. Yu, Z. Hou, H. Lin, X. Lu, Effects of molecular weight distribution (M<sub>d</sub>) on the performances of the polyethersulfone (PES) ultrafiltration membranes, *J. Membr. Sci.* 490 (2015) 220–226.
- [75] H.J. Lee, B. Jung, Y.S. Kang, H. Lee, Phase separation of polymer casting solution by nonsolvent vapor, *J. Membr. Sci.* 245 (2004) 103–112.
- [76] A. Idris, Z. Man, A.S. Maulud, M.S. Khan, S. Suetsugu, Effects of phase separation behavior on morphology and performance of polycarbonate membranes, *Membranes* 7 (2017) 21.
- [77] S.-G. Li, T. van den Boomgaard, C.A. Smolders, H. Strathmann, Physical gelation of amorphous polymers in a mixture of solvent and nonsolvent, *Macromolecules* 29 (1996) 2053–2059.
- [78] J.Y. Kim, Y.D. Kim, T. Kanamori, H.K. Lee, K.-J. Baik, S.C. Kim, Vittrification phenomena in polysulfone/NMP/water system, *J. Appl. Polym. Sci.* 71 (1999) 431–438.
- [79] M. Mulder, Membrane preparation|phase inversion membranes, in: I.D. Wilson (Ed.), *Encyclopedia of Separation Science*, Academic Press, Oxford 2000, pp. 3331–3346.
- [80] P. van de Witte, P.J. Dijkstra, J.W.A. van den Berg, J. Feijen, Phase separation processes in polymer solutions in relation to membrane formation, *J. Membr. Sci.* 117 (1996) 1–31.
- [81] J. Maitra, V.K. Shukla, Cross-linking in hydrogels-a review, *Am. J. Polym. Sci.* 4 (2014) 25–31.
- [82] R.S. Shrestha, R.C. McDonald, S.C. Greer, Molecular weight distributions of polydisperse polymers in coexisting liquid phases, *J. Chem. Phys.* 117 (2002) 9037–9049.
- [83] N.A. Alenazi, M.A. Hussein, K.A. Alamry, A.M. Asiri, Modified polyether-sulfone membrane: a mini review, *Des. Monomers Polym.* 20 (2017) 532–546.

## Supporting information

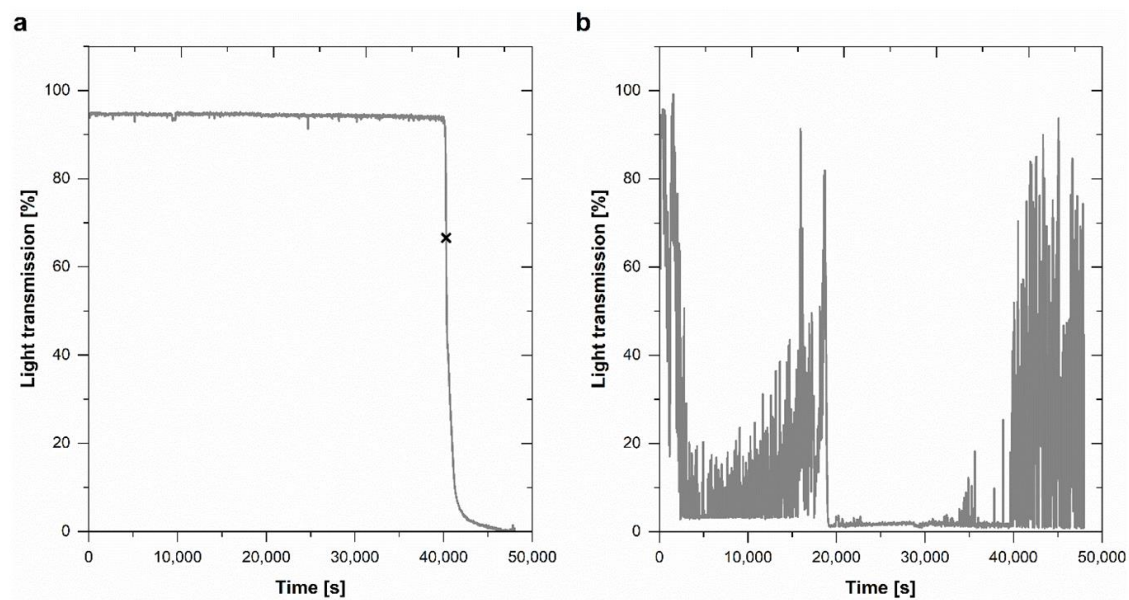


Figure S1 Exemplary data record of a cloud point measurement of a 2.5 wt.% PES solution in NMP with the cloud point indicated by a black cross (a), and of a cloud point measurement of 17 wt.% PES in NMP where the determination of the cloud point is not possible due to the poor data quality (b).

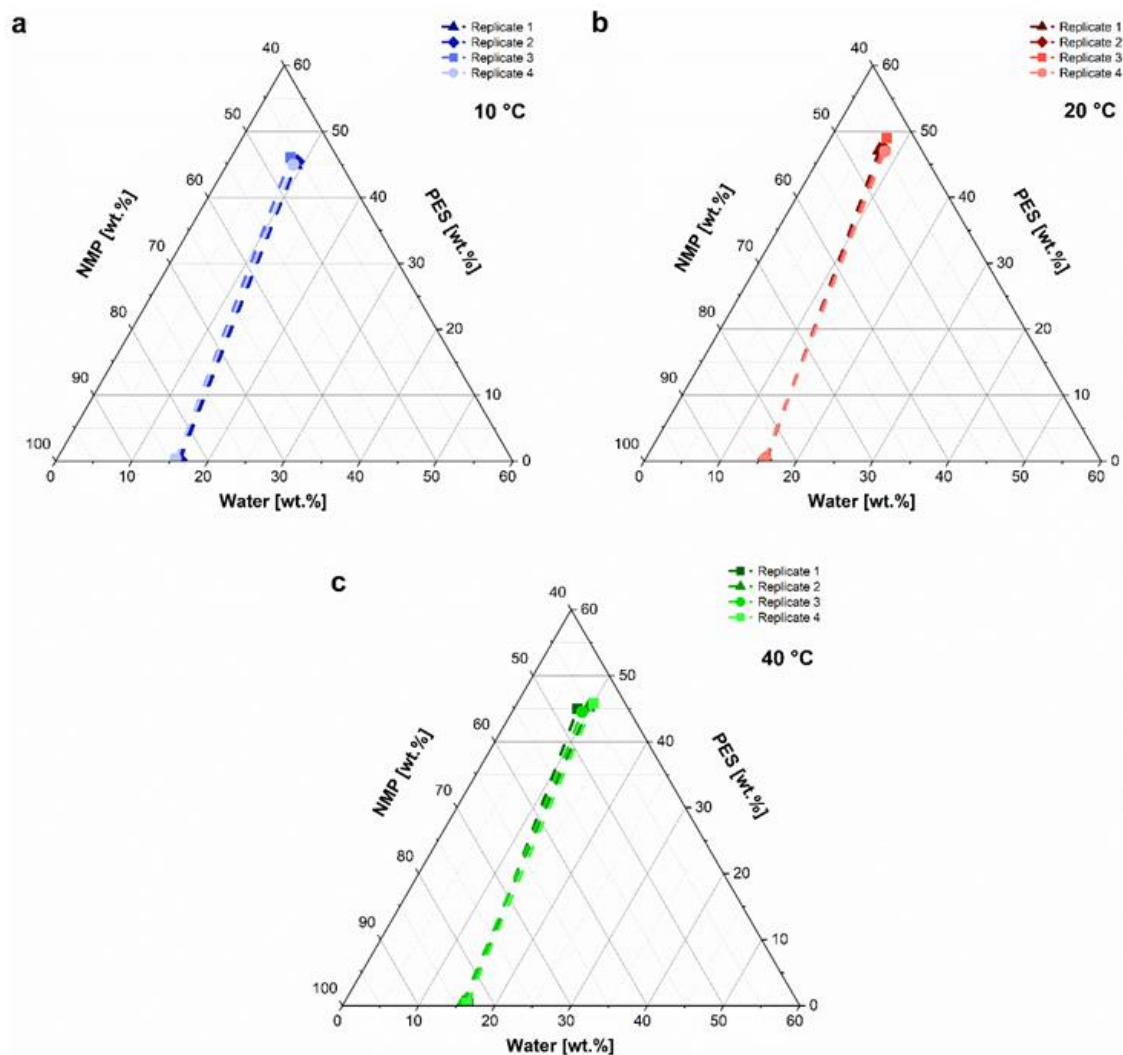


Figure S2 Reproducibility of the tie-line determination based on the fourfold repetition of the same measurement point. The phases of each samples were separated by centrifugation and their compositions analyzed via SEC and GC. The results were plotted in a phase diagram at different temperatures of 10 °C (a), 20 °C (b) and 40 °C (c).

**Table S1** Standard deviations and expected deviations from the average share of each component of the ternary system NMP/PES/water in the polymer-lean and the polymer-rich phases at 10 °C, 20°C and 40 °C.

Ingredient	Temperature [°C]	Phase	Standard deviation [wt.%]	Expected deviation [wt.%]
NMP	10	lean	0.22	1.00
		rich	0.29	1.35
	20	lean	0.09	1.11
		rich	0.66	1.64
	40	lean	0.27	0.98
		rich	0.98	1.61
Water	10	lean	0.22	0.29
		rich	0.43	0.35
	20	lean	0.09	0.40
		rich	0.34	0.58
	40	lean	0.28	0.28
		rich	0.63	0.63
PES	10	lean	0.01	0.02
		rich	0.43	1.51
	20	lean	0.01	0.02
		rich	0.78	1.60
	40	lean	0.02	0.03
		rich	0.46	1.51

**Table S2** Average composition with standard and relative deviation of the polymer-poor and the polymer-rich phases after phase separation of the fourfold repeated tie-line determination at different temperatures.

Temperature	Ingredient	polymer-poor phase			polymer-rich phase		
		Proportion [wt.%]	SD [wt.%]	RD [%]	Proportion [wt.%]	SD [wt.%]	RD [%]
10 °C	NMP	83.86	0.22	0.26	45.99	0.29	0.62
	Water	15.87	0.22	1.40	8.66	0.49	5.64
	PES	0.26	0.01	3.71	45.35	0.43	0.95
20 °C	NMP	83.92	0.09	0.10	44.78	0.66	1.48
	Water	15.77	0.09	0.58	7.62	0.34	4.41
	PES	0.32	0.01	3.60	47.61	0.78	1.65
40 °C	NMP	83.63	0.27	0.32	45.55	0.98	2.15
	Water	15.98	0.28	1.77	9.29	0.63	6.76
	PES	0.39	0.02	4.28	45.15	0.46	1.02

The expected experimental inaccuracies were calculated by

$$\Delta w_i = \frac{100\%}{m_A} \times \Delta m_i + \frac{m_i \times 100\%}{m_A^2} \times \Delta m_B$$

where  $\Delta w_i$  is the expected experimental deviation in wt.%,  $m_A$  is the mass of the sample which was applied for the analytical determination of the component by GC or SEC,  $m_i$  is the mass of the ingredient which was measured, and  $\Delta m_B$  is the mass deviation caused by the inaccuracies of the balance. Furthermore,  $\Delta m_i$  is the mass deviation of the respective component which was calculated by

$$\Delta m_i = \frac{w_i}{100\%} \times \Delta m_B + \frac{m_t}{100\%} \times \sigma_A$$

where  $w_i$  is the determined proportion of the component in wt.%,  $\Delta m_B$  is the inaccuracy caused by the weighing steps,  $m_t$  is the total sample amount in case of PES, or the total sample amount without the polymer content for NMP and water, and  $\sigma_A$  is the standard deviation of the analytical steps. For the SEC  $\sigma_A$  was calculated from the deviations of the slope and the y-intercept of calibration regression, while for the GC  $\sigma_A$  was calculated from the deviations of the double determination.

At all temperatures the standard deviation of every single component was lower than the expected deviation due to measuring inaccuracies, which takes into consideration that the method involves several gravimetric and analytical steps. Although the polymer-rich phase showed slightly higher deviations in comparison to the other phase, a good reproducibility was still given as the deviations between the four samples were in an acceptable range. This can be concluded from that fact that the expected deviations which can arise from experimental inaccuracies were again higher than the actual measured deviations (Table S2).

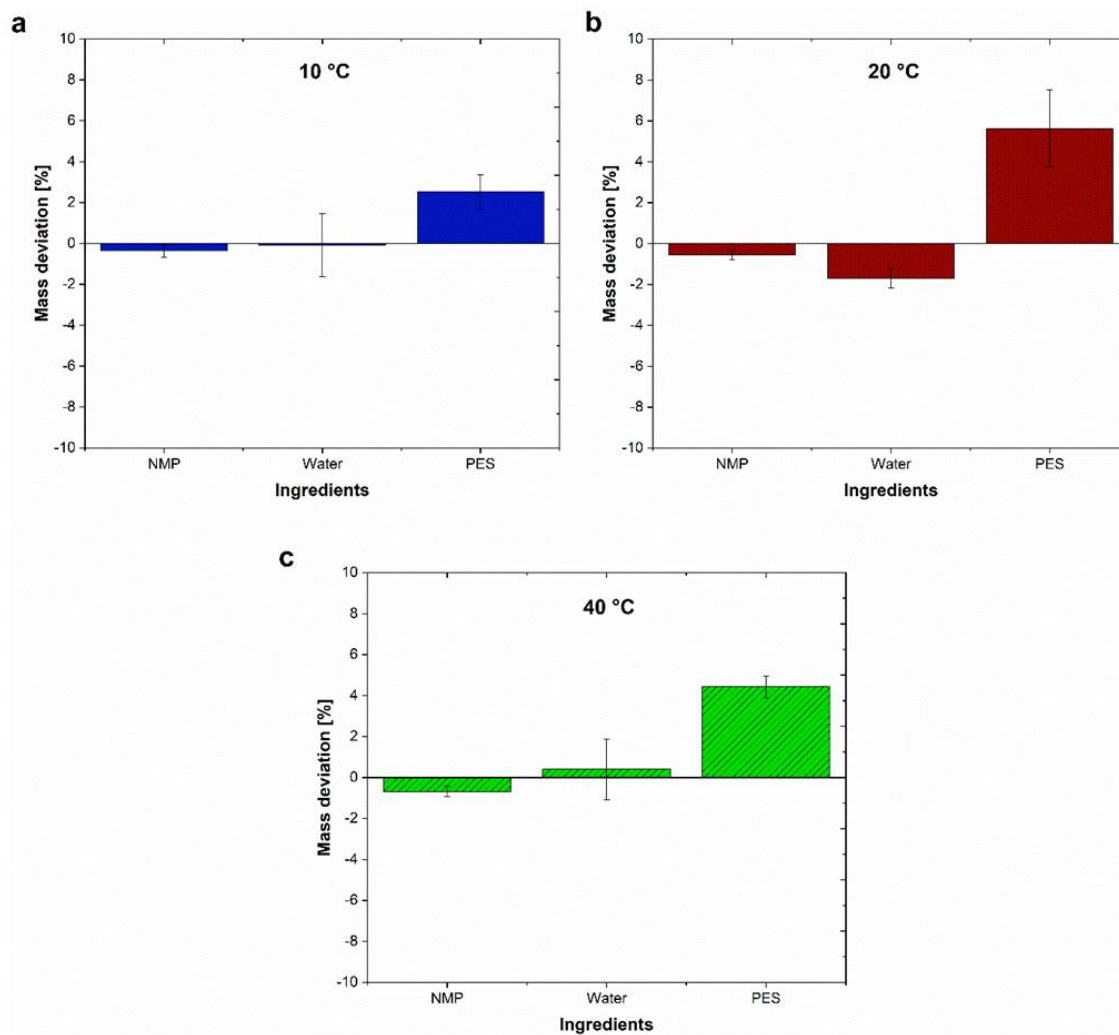


Figure S3 Mean mass deviation of N-methyl-2-pyrrolidone, water and polyethersulfone (n=4)  $\pm$  standard deviation in the validation samples based on the mass balance of the tie-line determination at 10 °C (a), 20 °C (b) and 40 °C (c).

## 4.2 Influences of polymeric additives in different solvent systems

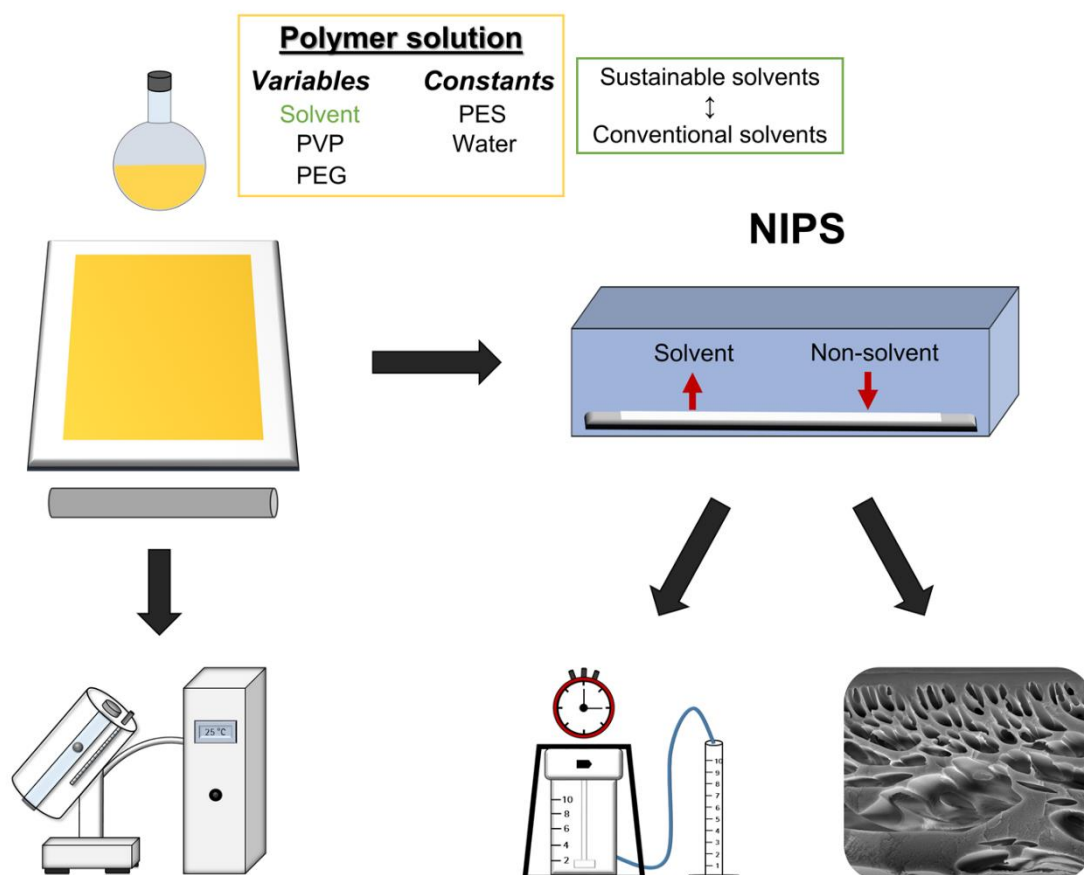


Figure 14 Graphical abstract of the publication “Membrane formation via non-solvent induced phase separation using sustainable solvents: A comparative study” [166].

The previous section focused on the thermodynamic aspects of the membrane formation process. However, the fabrication of membranes via NIPS is not only dependent on the thermodynamics of the system, but it is also significantly affected by the kinetics of the process [43]. One important set of parameters for controlling the thermodynamics and kinetics of the NIPS process is the composition of the membrane dope solution. Apart from the polymer, the solvent and the non-solvent, the addition of polymeric additives can be used to alter the characteristics of the resulting membranes [31].

In order to improve the understanding of the underlying mechanisms of NIPS and the effects of the dope solution composition on the characteristics of PES membranes, this part of the work focuses on the influences of the two commonly applied polymeric additives PVP and PEG in four different solvent systems. Among the four studied solvents are the two commonly applied solvents NMP and DMAc. Since they are both toxic and environmentally unfriendly, it is highly desirable to substitute them through ecologically less harmful alternatives. However, a substitution of the solvent, whilst achieving the same desired membrane characteristics, is very challenging. This is why 2P and DML were tested



for their potential to substitute the currently used toxic solvents. These particular solvents were chosen as they are considered to be non-carcinogenic and have not been tested with respect to their suitability to substitute NMP and DMAc in PES membrane fabrication before. As discussed previously, the reason for examining the effects of the polymeric additives in these solvents systems is that previously reported results in the literature on this topic are contradictory. Especially among different dope solution systems the effects observed by different groups are conflicting.

To gain a holistic picture on both variables in combination, the additive influences and the choice of the solvent, systematic variations of PVP and PEG were carried out in each of the four different solvents. The dope solutions with varying compositions were used to prepare PES membranes via NIPS and the resulting membrane characteristics were investigated. The studied membrane properties include the structure, the permeability, the lysozyme retention capability and the surface characteristics of the membrane prototypes. Among the surface characteristics, the applied characterization methods involve the unspecific lysozyme binding to the membrane surface, the surface contact angle and the specific surface area of the membrane. Additionally, the viscosity of each dope solution was determined, since it can impact the exchange speed of solvent and non-solvent, which finally leads to the demixing of the solution. Another reported result is the comparison of the needed water amount in each of the four solvent systems to induce the phase separation in a 5 wt.% PES solution.

It was found that the dope solution viscosity is influenced by increasing the concentration or the molecular weight of PVP and PEG. Since the increased viscosity slows down the diffusional exchange between solvent and non-solvent, the membrane formation process is altered. This is especially indicated by the observed changes in the membrane characteristics. It was found that structure, permeability, protein retention capability and surface properties of the membranes were strongly influenced by changes in additive concentrations or molecular weights. Especially the PVP variations strongly impacted the membrane characteristics, which can be explained by the greater influence of the PVP variations on the solution viscosity. In case of PEG, the effects were much less pronounced or even not present, which can arise from the observed lower effect of PEG on the solution viscosity. Furthermore, it could be found that the effects partially differed between the conventional and the alternative solvents. The influences of the additive variations were found to be higher in case of the application of the chosen alternative solvents. Therefore, the adjustment of the polymeric additives is an appropriate controlling parameter for obtaining the desired membrane properties.

To conclude, the results of the experiments indicate that both, solvents and polymeric additives, can significantly impact the membrane properties. The reason for this is that they can alter the mass transfer during NIPS, which in turn leads to modified kinetics of the membrane formation process. Furthermore, the comparative study proves that 2P and DML are suitable more ecologically harmless alternatives for replacing NMP and DMAc as solvents for the preparation of PES membranes.



## Membrane formation via non-solvent induced phase separation using sustainable solvents: A comparative study

Catharina Kahrs<sup>a,b,\*</sup>, Jan Schwellenbach<sup>a</sup>

<sup>a</sup> Sartorius Stedim Biotech GmbH, 37079, Goettingen, Germany

<sup>b</sup> Leibniz University Hannover, Institute for Technical Chemistry, 30167, Hannover, Germany

### ARTICLE INFO

#### Keywords:

Sustainable solvents  
Polyethersulfone (PES)  
Ultrafiltration membranes

### ABSTRACT

Non-solvent induced phase separation (NIPS) is a frequently used technique for the production of polymeric membranes. It enables the production of membranes with a broad range of different characteristics. Current solvents used in membrane preparation are often toxic, environmentally unfriendly and prepared from non-sustainable resources. This is why a replacement of solvents like *N*-methyl-2-pyrrolidone (NMP) and dimethylacetamide (DMAc) is highly desirable. In order to substitute a solvent whilst achieving the same desired membrane properties, it is necessary to understand the formation mechanisms and its influencing factors. One important set of parameters for controlling the membrane features is the polymer solution composition. This is why the aim of this study was to improve the understanding of membrane formation by gaining a holistic picture of the influences of systematic additive variations, focusing on the comparison between conventional and alternative sustainable solvent systems. Thus, 72 different polyethersulfone (PES) membrane prototypes were produced by immersion precipitation from polymer solutions prepared in NMP and DMAc, as well as in the sustainable alternatives 2-pyrrolidone (2P) and dimethylacetamide (DML). In all four solvent systems varying concentrations and molecular weights of the polymeric additives polyvinylpyrrolidone (PVP) and polyethylene glycol (PEG) were applied. The viscosity of the polymer solutions was determined, and thereof formed membranes were analyzed in terms of permeability, protein retention, surface properties, mechanical stability and morphology. The results indicate that both, solvents and additives, significantly impact the membrane properties. It was shown that the influences of the additives on all investigated membrane features were strongly dependent on the applied solvent. The observed effects were similar for the conventional solvents NMP and DMAc, but differed from those found for the alternative solvents 2P and DML, which among themselves also showed comparable outcomes. In conclusion, this study proves that it is possible to obtain desired membrane properties with 2P or DML as long as the solution composition is chosen appropriately.

### 1. Introduction

Filtration describes a mechanical separation process which is used to remove small particles or molecules from an aerosol or a fluid stream [1–4]. Typical areas of application are the purification of products in the food industry, the treatment of waste water, drinking water purification, the use for medical purposes such as dialysis, and the purification of pharmaceutical products [4–7]. In order to fulfill the requirements for different applications, filtration membranes have to meet certain criteria in terms of structure and performance [1]. Apart from determining these criteria through adjusted process parameters, the desired membrane characteristics such as pore size distribution, permeability, rejection

capability and surface properties can be controlled during the production process [8–10]. Due to their good capability of forming membranes with different morphologies and different performances, polymeric membranes are frequently chosen for filtration purposes [6,11–13].

A commonly applied manufacturing method for producing polymeric membranes is the phase separation of polymer solutions with a defined composition [14,15]. In this context one of the most applied approaches is the non-solvent induced phase separation (NIPS) [16–18]. It involves the formation of two phases through an exchange of the solvent from the polymer solution through a non-solvent from a precipitation bath. One of the phases contains a high polymer solution and is responsible for the formation of the membrane matrix, whereas the

\* Corresponding author. August-Spindler-Straße 11, 37079, Goettingen, Germany.  
E-mail address: [catharina.kahrs@sartorius.com](mailto:catharina.kahrs@sartorius.com) (C. Kahrs).

<https://doi.org/10.1016/j.polymer.2019.122071>

Received 9 August 2019; Received in revised form 18 November 2019; Accepted 6 December 2019

Available online 7 December 2019

0032-3861/© 2019 Elsevier Ltd. All rights reserved.

second phase contains only a very small proportion of the polymer and is washed out during the membrane formation process. This causes the development of the pore network within the matrix of the membrane until structure solidification sets in Refs. [19–21].

For controlling the membrane morphology, many factors have to be considered. Apart from the process conditions the composition of the initial polymer solution has a major impact on the thermodynamics and kinetics of the membrane formation process [19,22–24]. In this context, different membrane-forming polymers, different solvents and various non-solvent or polymeric additives can be used to alter the fundamental progress of phase inversion [8,25,26].

Among different membrane-forming polymers such as polysulfone (PSf), polyvinylidene fluoride (PVDF), polyamide (PA), or cellulose acetate (CA), polyethersulfone (PES) is one of the most commonly applied polymers for membrane preparation [8,27–29]. PES features favorable characteristics, which include a high thermal, chemical, and mechanical stability, as well as a high glass transition temperature and a good processability [30–32].

In order to prepare a membrane casting solution, the polymer and potential non-solvent or polymeric additives have to be dissolved in an appropriate solvent. Currently, common solvents which are used for preparing membrane casting solutions include *N*-methyl-2-pyrrolidone (NMP), dimethylacetamide (DMAc), dimethylformamide (DMF) and dioxane [8,19,33]. However, all these solvents have in common that they bring up several issues regarding safety, health and environmental sustainability during transport, storage and handling [33–35]. Another concern with these solvents is their disposal. They often cannot be reused due to certain quality requirements and regulatory demands [36, 37]. Therefore, the listed solvents implicate environmental issues and are further regarded as dangerous for human health [38–40].

In case of PES the most frequently used solvents are NMP and DMAc, which both belong to the list of the hazardous solvents. Consequently, there is a high interest in replacing these harmful solvents through sustainable alternatives, which at best meet the criteria of green chemistry [41–43]. A fundamental principle of green chemistry is the promotion of applying non-toxic and eco-friendly solvents in order to replace the conventionally used ones [19]. Furthermore, it requires the development of sustainable processes and products in order to minimize the risk factors, which emanate from the applied materials and in particular from chemicals such as solvents [37]. Finally, the replacement of conventional solvents through more sustainable ones shall reduce the environmental impact and simultaneously increase the sustainability of membrane fabrication [34,37,44–48].

As a result of the raising interest to improve the sustainability of membrane production, several different solvents have been investigated in the recent past with respect to their suitability for replacing harmful solvents. The non-toxic and biodegradable solvents which have been tested so far for their ability to form PES ultrafiltration membranes include dimethyl sulfoxide (DMSO), as well as the bio-derived solvents Rhodiasolv®Polarclean,  $\gamma$ -Valerolactone (GVL) and Cyrene™ [21,33, 35,41,42,48–51]. Furthermore, it has been reported that several other bio-based solvents, which are basically different derivatives of glycerol, can be used to prepare membranes with different polymers [35].

Apart from dissolving the selected polymer, the membrane which is formed from the prepared polymer solution has to be adjustable with regard to structure and performance. For polymeric systems with NMP and DMAc the control parameters have been frequently studied [8,20, 32,52–64]. The main parameters which have been found to influence the resulting membrane features include the casting solution composition and the precipitation conditions, since both affect the kinetics and thermodynamics of the formation process [8,19,22,60,65–70]. In addition to polymer, solvent and non-solvent, polymeric or non-solvent additives can be used to alter the thermodynamic and kinetic properties of polymer solution and membrane formation process [8,32,70,71]. Two of the most commonly used polymeric additives are polyvinylpyrrolidone (PVP) and polyethylene glycol (PEG) [20]. Apart from creating a more

hydrophilic membrane surface when the membrane-forming polymer has a quite hydrophobic character, PVP and PEG can impact the viscosity of the casting solution and therefore the diffusive exchange rate during NIPS. As a consequence it affects the resulting pore sizes as well as the formation of macrovoids in the sub-structure of the membrane. This is based on the change in coalescence of the polymer-poor phase and therefore on the alteration of the sizes of the remaining holes within the membrane matrix when the viscosity is altered [14,20,22,72]. Furthermore, PVP and PEG are designated as pore-forming agents because both additives have been shown to influence the permeability, the rejection properties, the stability and the structure of the resulting membranes [53,56,58,60,61,73,74].

In the past various studies were conducted which investigate the influence of varying concentrations and molecular weights of PVP and PEG on membrane structure and performance to understand their impact on the membrane formation process. However, as this process is very complex and strongly depends on the combination of several different variables, there is still a huge interest to further enhance the knowledge of the fundamentals of the formation mechanisms [8,20,25, 26]. On top of that, the studies on polymeric additives are limited to polymer solutions prepared with hazardous solvents. If the existing studies are compared among each other, the results are somewhat contradictory as well [20].

This is why in this work a comparative study is presented, which on one hand investigates the effects of polymeric additive variations in the conventional solvents NMP and DMAc, and on the other hand compares the outcomes of the conventionally used systems to those of the alternative solvents 2-pyrrolidone (2P) and dimethylacetamide (DML). These two alternative solvents exhibit similar characteristics to the conventional ones with regard to their physicochemical properties, which are summarized for all four solvents in Table 1.

In contrast to NMP and DMAc, 2P and DML are not classified as substances of very high concern. Instead, they are both regarded as non-toxic solvents and are readily biodegradable, which is why they have been categorized into the lowest water pollution class. Therefore, 2P and DML can be considered as sustainable solvents, which are safe for human health [75,76]. In contrast to 2P, which is mainly produced from  $\gamma$ -butyrolactone [77], DML can even be regarded as a bio-derived substance. It is the dimethylamide of natural lactic acid and therefore meets the principles of green chemistry, since it is produced from renewable sources [76].

2P was chosen as it has previously been shown that it is a suitable sustainable alternative for PSf membrane preparation [59,78]. However, until now no studies have been conducted which address the production of PES membranes with 2P as solvent. Furthermore, the effects caused by addition of additives have also not been studied so far for a 2P-based system. In contrast, DML was chosen as alternative solvent because to date it has not been presented as solvent in the context of membrane fabrication at all. However, DML has been reported to be a suitable non-toxic alternative for hazardous solvents in other application areas [79]. This is why a first trial was conducted to use DML for the production of PES membranes.

**Table 1**  
Physicochemical properties of the applied solvents.

Characteristics	NMP	DMAc	2P	DML
Molar mass	99.13 g/mol	87.12 g/mol	85.11 g/mol	117.2 g/mol
Density (at 20 °C)	1.03 g/mol	0.94 g/cm <sup>3</sup>	1.11 g/cm <sup>3</sup>	1.05 g/cm <sup>3</sup>
Melting point	- 24 °C	- 20 °C	25 °C	- 2 °C
Boiling point	204 °C	166 °C	250 °C	223 °C
Miscibility with water	completely miscible	completely miscible	completely miscible	completely miscible
Substance of very high concern	yes	yes	no	no

Consequently, the aim of this comparable study was to prove that 2P and DML are suitable for substituting NMP and DMAc in PES membrane production via NIPS. This shall contribute to the reduction of the environmental impact of the production process and therefore to the increase of the membrane process sustainability. Furthermore, a holistic picture of the influences on membrane formation during immersion precipitation should be gained by comparing additive influences among all four solvent systems. Therefore, concentration variations as well as the influences of different molecular weights of both additives, PVP and PVP, were studied in the four different solvent systems which have different affinities for dissolving the solution components as well as varying physical and chemical properties. A row of different casting solutions was prepared and used to produce PES membrane prototypes. Finally, the effects of the variables on the membrane properties were studied by determining the polymer solution viscosity, by evaluating the membrane structure and by determining the membrane performance in terms of permeability, retention capacity, mechanical stability and surface characteristics.

## 2. Experimental

### 2.1. Materials

Commercial PES Ultrason® E6020 with a molecular weight of 75,000 g/mol was purchased from BASF (Ludwigshafen, Germany) and applied as the membrane-forming polymer. The different solvents which were applied included the two conventional solvents NMP and DMAc (Carl Roth, Karlsruhe, Germany), as well as the two alternative solvents 2P (Carl Roth, Karlsruhe, Germany) and DML (BASF, Ludwigshafen, Germany). Different types of PVP Luvitec® powder with molecular weights of 9 kDa (Luvitec® K17), 50 kDa (Luvitec® K30) and 1400 kDa (Luvitec® K90) were acquired from BASF (Ludwigshafen, Germany), while PEG with molecular weights of 400 Da, 1500 Da, and 6000 Da were supplied by Sigma-Aldrich (St. Louis, MO, USA). Reverse-osmosis (RO) water (Sartorius Stedim Biotech GmbH, Goettingen, Germany) was used as non-solvent. For measurements of the membrane permeability 0.9 wt% sodium chloride (Merck, Darmstadt, Germany) in RO-water was used. In case of the protein retention measurements lysozyme (Carl Roth, Karlsruhe, Germany) was applied as model molecule, whereas the used diluent potassium phosphate buffer with a pH of 7.0 (Carl Roth, Karlsruhe, Germany).

### 2.2. Polymer solution preparation

In order to study the influence of the polymeric additives in different solvent systems, membranes with varying concentrations and molecular weights of PVP and PEG were prepared, while the PES concentration was constantly held at 15 wt%. Since the water content can influence the final membrane characteristics, it was also held at a constant level. Therefore, the water proportion in all raw materials and their contribution to the final water amount in the polymer solution was determined using a moisture analyzer (Sartorius Lab Instruments GmbH & Co. KG, Goettingen, Germany) for solids, and a Karl Fischer Titrando (Metrohm, Herisau, Switzerland) for liquids. The necessary amount of RO-water was calculated to reach a final concentration of 0.5 wt% water in each casting solution. The compositions of the polymer solutions for preparing different membrane prototypes are listed in Table 2. All specified solution compositions were applied with each of the four chosen solvents so that in total 72 different membrane prototypes were produced. Each prototype was assigned with a code consisting of a letter and a number. The letter refers to the respectively applied solvent, where A stands for DMAc, N for NMP, M for DML and P for 2P. The number refers to the casting solution composition as it is listed in Table 2.

In order to prepare the polymer solutions, the defined amounts of RO-water and the respective solvent were filled into a 500 mL twin-neck flask (Carl Roth, Karlsruhe, Germany). The flask was placed into a

**Table 2**

Casting solution compositions for the preparation of PES membrane prototypes with variations in additive concentrations and molecular weights.

Composition	Components [wt.%]				
	PES	PVP 50 kDa	PEG 400 Da	Water	Solvent
1	15	0	0.0	0.5	84.5
2	15	1	0.0	0.5	83.5
3	15	2	0.0	0.5	82.5
4	15	3	0.0	0.5	81.5
5	15	4	0.0	0.5	80.5
6	15	5	0.0	0.5	79.5
7	15	1	0.0	0.5	83.5
8	15	1	2.5	0.5	81.0
9	15	1	5.0	0.5	78.5
10	15	1	7.5	0.5	76.0
11	15	1	10.0	0.5	73.5
12	15	1	12.5	0.5	71.0
13	15	1	15.0	0.5	68.5

Composition	Components				
	15 wt %	2.5 wt%	7.5 wt%	0.5 wt %	74.5 wt %
14	PES	PVP 9 kDa	PEG 400 Da	Water	Solvent
15	PES	PVP 50 kDa	PEG 400 Da	Water	Solvent
16	PES	PVP 1400 kDa	PEG 400 Da	Water	Solvent

Composition	Components				
	15 wt %	1.0 wt%	7.5 wt%	0.5 wt %	76.0 wt %
17	PES	PVP 50 kDa	PEG 1500 Da	Water	Solvent
18	PES	PVP 50 kDa	PEG 6000 Da	Water	Solvent

heated oil bath and tempered to 60 °C. Under constant stirring at 250 rpm (IKA overhead stirrer RW20, IKA, Staufen, Germany), the respective additives and finally the membrane-forming polymer were added to the flask. In case of all four solvents the mixture was then stirred overnight at 60 °C to dissolve the PES in the respective solvent, so that finally a homogenous casting solution was obtained. In a last step each solution was degassed in an oven at 50 °C for at least 2 h.

### 2.3. Preparation of membrane prototypes

In order to produce membrane prototypes, the previously prepared polymer solutions were cooled to 25 °C, poured onto a glass plate and evenly spread with a casting rake (AWU Precision Slovakia k.s., Prešov, Slovakia). The casting rake was made of stainless steel and had a defined casting thickness of 250 µm. Subsequently, the glass plate with the casting film was immediately immersed into a precipitation bath, which consisted of the non-solvent (RO-water) tempered to 25 °C. In order to allow the complete exchange of solvent and non-solvent, which resulted in a self-initiated detaching of the membrane from the glass support and the formation of the final membrane structure, the samples were left in the precipitation bath for 5 min. Subsequently, the membrane sheets were impregnated with 40 wt% glycerol in RO-water to prevent the collapse of the pore structure during storage of the samples. Finally, the samples were dried in an oven at 50 °C for 10 min and stored in airtight sealed bags until used for further investigation.

### 2.4. Characterization

#### 2.4.1. Dynamic solution viscosity

The dynamic viscosity of each casting solution was determined using a HAAKE™ falling ball viscometer (ThermoFisher Scientific, Waltham, MA, USA). Therefore, the casting solution and an appropriate nickel-steel ball were filled into the viscometer tube and then tempered to 25 °C for at least 15 min using a thermostat (Lauda, Lauda-

Koenigshofen, Germany) connected to the viscometer. Finally, the falling time of the ball was measured in a fivefold determination and the dynamic viscosity was calculated as follows:

$$\eta = \frac{t_m \cdot (\phi_B - \phi_S) \cdot K}{1000} \quad (1)$$

where  $\eta$  is the dynamic viscosity (Pa·s),  $t_m$  is the mean falling time of the ball (sec),  $\phi_B$  is the density of the ball (g/cm<sup>3</sup>),  $\phi_S$  is the density of the solution (g/cm<sup>3</sup>), and  $K$  the constant of the ball (mPa·cm<sup>3</sup>·g<sup>-1</sup>), which is determined through the calibration of the ball.

#### 2.4.2. Cloud point titration

Cloud point measurements were conducted to compare the amount of water which can be added to the four different solvent systems until demixing is induced. For each solvent a 5 wt% PES solution was prepared and filled into a reactor (HWS, Mainz, Germany) tempered to 25 °C. Under constant stirring at 300 rpm (IKA overhead stirrer RW20, IKA, Staufen, Germany), 0.03 g/min of water were added to the polymer solution using an automatic titration unit (Metrohm900 Touch Control, Metrohm846 Dosing Interface, Metrohm 807 Dosing Unit and Metrohm800 Dosino, MetrohmGmbH and Co. KG, Filderstadt, Germany). During the titration experiment, the light transmittance was recorded as a function of time, until the transmittance dropped below a value of 5%. Finally, the inflection point of the function, which represents the cloud point of the solution, was determined with Origin 2018b (Northampton, MA, USA).

#### 2.4.3. Scanning electron microscopy

In order to wash out the glycerol from the membrane structure, a small piece of each membrane sample was cut and flushed with RO-water for at least 15 min. Subsequently, the wet membranes were immersed into liquid nitrogen and cross-section samples were prepared by creating smooth breaks of the frozen membranes using a razor blade. The samples were placed into specimen stubs, marginal coated with conductive silver and sputter coated with a thin film of argon. Finally, the images were recorded using a FEI Quanta 200 ESEM (ThermoFisher Scientific, Waltham, MA, USA) under high vacuum and at a potential of 12.5 kV.

#### 2.4.4. Sponge layer thickness

The recorded cross-section images were used to determine the thickness of the sponge-like layer on the skin-side of each membrane. The sponge layer was defined as the layer from the surface of the membrane to the first appearance of finger-like voids [80]. The software Image J (National Institutes of Health, Bethesda, MD, USA) was used as an image analysis tool.

#### 2.4.5. Membrane permeability

The permeability of the manufactured membrane prototypes was determined with a solution of 0.9 wt% sodium chloride diluted in RO-water. Together with a fibrous support, a round membrane sample with a diameter of 26 mm was integrated into a 10 mL stirred cell (Sartorius Stedim Biotech GmbH, Goettingen, Germany), which was then filled with the previously prepared salt solution. The lid of the stirred cell was connected to a pressure supply and the measurement module was exposed to a pressure of 1 bar. By doing so, the salt solution was filtrated over the membrane sample with an effective filtration area of 3.8 cm<sup>2</sup>, and the time which was needed to collect 10 mL of the filtrate was stopped. During the filtration run the solution was stirred on a magnetic stirrer at 1100 rpm (IKA color squid, IKA, Staufen, Germany). Finally, the membrane permeability was calculated as follows:

$$J = \frac{V_F}{A_M \cdot t \cdot p} \quad (2)$$

where  $J$  is the membrane permeability (L·m<sup>-2</sup>·h<sup>-1</sup>·bar<sup>-1</sup>),  $V_F$  is the

filtration volume (L),  $A_M$  is the effective filtration area of the membrane (m<sup>2</sup>),  $t$  is the filtration time (h) and  $p$  is the applied pressure (bar).

#### 2.4.6. Protein retention

The protein retention of the membrane prototypes was determined by applying lysozyme (Lot. 235225855, Carl Roth, Karlsruhe, Germany) as model protein. Using a 20 mM potassium phosphate buffer (pH 7.0) as diluent, a lysozyme solution with a concentration of 0.2 g/L was prepared and mixed at 250 rpm on a magnetic stirrer (IKA color squid, IKA, Staufen, Germany), until the protein was completely dissolved. The prepared modules from the permeability measurements were emptied and filled with 10 mL of the lysozyme solution. Then the filtration was started by applying a pressure of 1 bar to the stirring cell. During the filtration the solution within the cell was constantly stirred at 1100 rpm on a magnetic stirrer (IKA color squid, IKA, Germany) to simulate cross-flow filtration, and the filtrate was collected in a test tube. After collecting 9.5 mL of the filtrate, the filtration was stopped and the cell was flushed twice with the pure salt solution. Subsequently, the cell was filled with the salt solution and the filtration at 1 bar and 1100 rpm was continued to a final filtrate volume of 12 mL in order to collect the remaining protein filtrate from the dead volume of the module. Finally, the lysozyme concentrations in the feed solution and the filtrates were measured by a UV-Vis spectrophotometer (Infinite® 200 PRO, Tecan, Maennedorf, Switzerland) at a wavelength of 280 nm. As the protein concentration is proportional to the extinction of the protein solution, the lysozyme rejection was calculated as follows:

$$R = 1 - \frac{c_p}{c_f} \cdot 100 \quad (3)$$

where  $R$  is the protein rejection (%),  $c_p$  is the protein concentration in the filtrate (g/L) and  $c_f$  is the protein concentration in the feed solution (g/L).

#### 2.4.7. Bursting pressure

In order to evaluate the mechanical stability of the membrane prototypes, the bursting pressure was determined. The bursting pressure is defined as the pressure which is needed to rupture the membrane. First the membrane samples were wetted with water and then placed with the skin-side facing down into the bursting pressure device. The actual measurement was started by moving the plunger of the device directly onto the membrane sample. A continuously raising pressure was applied to the membrane sample until the bursting pressure was reached, which was indicated through an audible rupture of the membrane. Finally, the reached pressure was read from the meter of the device.

#### 2.4.8. Water contact angle

The hydrophilicity of the membrane surface was evaluated by measurements of the contact angle, which was determined by application of the sessile drop method using an OCA 15 EC contact angle system (DataPhysics Instruments GmbH, Filderstadt, Germany). For the measurement a drop of 10 µL RO-water was injected onto the surface of a dry membrane sample with a micro-syringe. The drop was visualized with the integrated camera of the measurement system and the contact angle was determined at room temperature 10 s after placing the water drop onto the membrane surface. Three measurements of different locations on the membrane sample were recorded and averaged.

#### 2.4.9. Unspecific protein binding

An indirect method to analyze the surface hydrophilicity is the measurement of the unspecific protein binding to the membrane surface. Therefore, 10 mm membrane blanks were placed into a 48-well plate. A protein solution of 3 g/L lysozyme (Lot. 235225855, Carl Roth, Karlsruhe, Germany) was prepared with 20 mM potassium phosphate buffer (pH 7.0) as diluent. Each well containing a membrane sample was supplied with 200 µL of the protein solution and the plate was incubated

for 16 h at room temperature on a Heidolph Titramax 100 plate shaker (Heidolph Instruments, Schwabach, Germany) at 300 rpm. After 16 h the protein solution was removed and the samples were washed twice for 20 min and once for 3 h with the phosphate buffer. In the meantime, a calibration standard row was prepared by serial dilution of the protein stock solution and 30  $\mu\text{L}$  of each standard was added in duplicates to empty wells of the plate. 300  $\mu\text{L}$  of the BCA reagent (ThermoFisher, Waltham, MA, USA) were added to each well and the plate was incubated at 300 rpm on the plate shaker for 1 h. Afterwards, 200  $\mu\text{L}$  of each well were transferred into a new well plate and finally the absorbance was measured at 562 nm using a Infinite M2000 well-plate reader (Tecan, Männedorf, Switzerland). A calibration curve was created from the absorbance data and used to calculate the concentration of the protein concentration bound to the membrane samples.

#### 2.4.10. Specific surface area

The specific surface area was determined by application of a normal BET procedure with a Gemini V device (Micromeritics, Norcross, GA, USA). In preparation for the measurement the samples were heated at 120  $^{\circ}\text{C}$  and under vacuum for at least 3 h. The weight of the dry samples was determined and finally the specific surface area was determined using the 11 point method of the Gemini device. The BET method detects the specific surface area on the basis of nitrogen gas adsorption to the membrane sample [81]. It can be described as follows:

$$S_{\text{BET}} = \frac{N_A \cdot A_M \cdot V_{\text{Mono}}}{m_{\text{ges}} \cdot V_M} \quad (4)$$

where  $N_A$  is the Avogadro constant,  $A_M$  is the area of the adsorbed nitrogen molecules,  $V_{\text{Mono}}$  is the volume of the adsorbed monolayer,  $m_{\text{ges}}$  is the mass of the sample and  $V_M$  is the molar volume of adsorbed nitrogen

molecules.

### 3. Results and discussion

#### 3.1. Dynamic solution viscosity

The viscosity is an important variable with regard to the processability of the casting solution. In all cases, the viscosities of the polymer solutions was dependent on the additive type which was added to the solution (Fig. 1).

Furthermore, the viscosity showed a dependence on the respective additive concentration and molecular weight (Fig. 1). Although the magnitude of the viscosities differed between the four solvent systems, the main trends which were found for the tested variables were the same, independently of the solvent which was used. Therefore, the results show that the solvent which is applied for dissolving polymer and additives has an important impact on the final casting solution viscosity. Regardless of the type of additive and its respective concentration or molecular weight, the use of DMAc always resulted in the lowest solution viscosity when it is compared to one of those having the same composition, but were prepared in one of the other three solvents. In case of DMAc the viscosities ranged from 0.2 Pa-s to around 2 Pa-s. In comparison to casting solutions prepared with DMAc, polymer solutions which were prepared with NMP exhibited viscosities which were only slightly higher, as they ranged from 0.4 Pa-s to approximately 4 Pa-s. In contrast to these two commonly used solvents, polymer solutions which were prepared with 2P or DML showed significantly higher viscosities. In general, the use of 2P resulted in the highest viscosity values. While the viscosities of polymer solutions with DML ranged from around 3 Pa-s up to 28 Pa-s, the solutions prepared with 2P exhibited viscosities

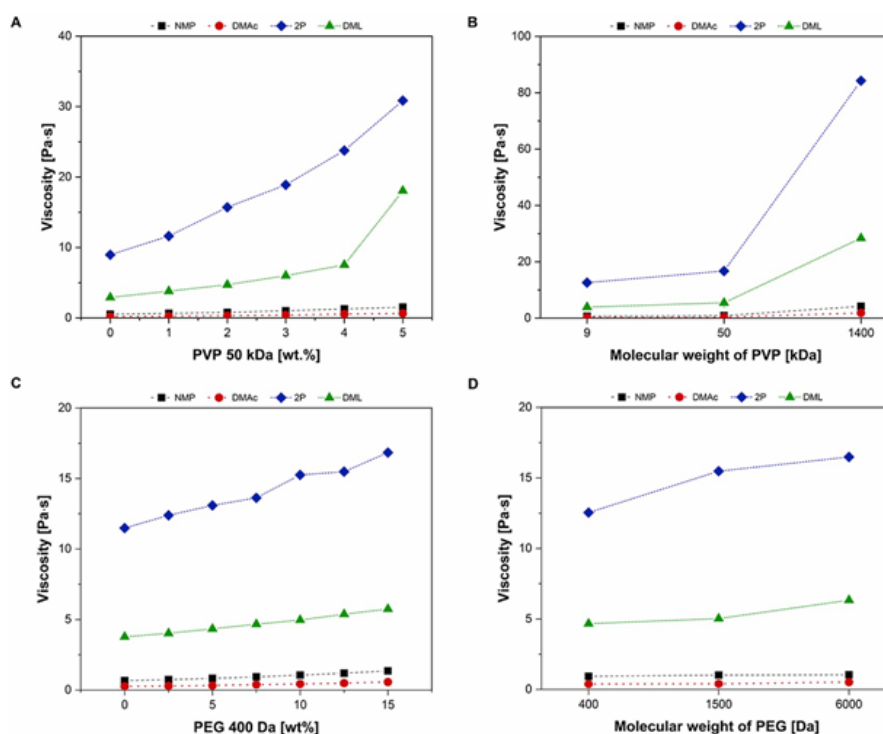


Fig. 1. Dynamic viscosity of polyethersulfone casting solutions at 25  $^{\circ}\text{C}$  in dependence of the PVP 50 kDa concentration (A), the PVP molecular weight (B), the concentration of PEG 400 Da (C), and the PEG molecular weight (D), determined with a falling ball viscometer.

ranging from 9 Pa·s up to 84 Pa·s. Comparing the viscosity ranges of the four systems among each other it becomes evident that the upper value in all cases is approximately ten times higher than the lower value. This implies that the increase of the viscosity caused by the additive variations lies in the same order of magnitude for all solvents.

Similarly to the results found after the polymers have been dissolved, sole DMAc exhibits the lowest viscosity, followed by NMP, which has almost twice the viscosity of DMAc. The viscosity of pure DML is about five times higher in comparison to DMAc, while 2P is even above 13 times higher (Table 3).

If the relation of the values for the pure solvents are compared to the relations of the complete viscosity range for each solvent after polymer and additives have been dissolved in it, it becomes apparent that the viscosities of the pure solvents NMP and DMAc differ by a factor of two. The range for NMP is also twice as high as the one of DMAc. This correlation between the pure solvent viscosity and the viscosity of the final casting solution could not be found for the other two solvents. While the viscosity of pure DML is only about five times higher than the one of DMAc, the range which was found for the whole set of casting solutions prepared in DML was approximately 15 times higher than the range determined for solutions in DMAc. In case of 2P this range was roughly 45 times higher in comparison to the one found for DMAc. An explanation for this could be that the viscosity is influenced by the interaction between solvent and polymer. The interaction of each solvent to another solvent or to a certain polymer can be characterized by their Hansen solubility parameters (HSP). The HSP data can be used to predict the affinity between two solvents, as well as the affinity between a polymer and a solvent. These affinities can be expressed by a so called distance value, which indicates how likely a polymer will dissolve in a certain solvent as the rule applies that like dissolves like. Hereby a low distance value indicates a good solubility of the polymer within the solvent, while a high distance value indicates that the solubility is rather poor [84]. The HSP for the four chosen solvents and their distance values to PES can be taken from Table 4.

The affinity between solvent and polymer affects the viscosity because the shape of the dissolved polymer chains has an influence on the resulting solution viscosity. Therefore both, the shape of the polymer molecules, as well as their arrangement and their behavior within the solvent play an important role. Depending on the interaction between polymer and solvent, the conformation of the polymer can change and the solvent can either be immobilized due to high interaction, or move about freely due to low interaction, which in turn changes the solution viscosity [85].

For both examined additives a rising concentration or the use of higher molecular weight additives resulted in an increase of the polymer solution viscosity. This trend could be observed for all four solvents, however, the magnitude of the final viscosity was solvent-dependent. Nonetheless, the proportions of the effects were similar in all four solvents, as the multiplication factor between the lowest and the highest viscosities, which yields the total viscosity interval, was the same for all tested systems.

The viscosity enlargement which was seen for an increase in PVP or PEG molecular weight is based on the general fundamentals of polymer physics. The viscosity increases when the polymer chains of the additives become longer because the internal friction between the coiled and swollen macromolecules becomes stronger, so that the chains interact which each other and cause polymer entanglement [86–88].

**Table 3**  
Dynamic viscosities of the pure applied solvents at 25 °C.

Solvent	Dynamic viscosity at 25 °C [mPa·s]	Reference
<i>N</i> -methyl-2-pyrrolidone	1.7	[82]
<i>N,N</i> -dimethylacetamide	0.9	[83]
2-pyrrolidone	13.3	[82]
<i>N,N</i> -dimethylactamide	5.1	[76]

**Table 4**

Hansen solubility parameters of polymer and solvents which were applied for membrane preparation, including the calculated distance values between the polymer and each solvent.

Solvent/Polymer	$\delta_d$ [MPa <sup>0.5</sup> ]	$\delta_p$ [MPa <sup>0.5</sup> ]	$\delta_h$ [MPa <sup>0.5</sup> ]	Distance value to PES
Polyethersulfone	19.6	10.8	9.2	–
<i>N</i> -methyl-2-pyrrolidone	18.0	12.3	7.2	2.97
<i>N,N</i> -dimethylacetamide	16.8	11.5	10.2	3.05
2-pyrrolidone	18.0	16.6	7.4	6.28
<i>N,N</i> -dimethylactamide	18.4	12.9	15.9	7.12

Furthermore, the larger the hydrodynamic size of the molecules, the more they slow down their movement. In turn, these circumstances result in a more confined position of the polymers and therefore in a more viscous solution. This also explains why the results for solutions with variations of PVP molecular weights showed a more pronounced effect in comparison to the variations with PEG because the molecular weight range which was tested in case of PVP was much higher than in case of PEG. An elevation of the viscosity could also be observed when the concentration of PVP or PEG was increased. Again this can be explained by the movement of the molecules within the solution as well as by the interactions between the polymer molecules. When the amount of polymeric additives in the solution rises, the polymer molecules more likely tend to interact with each other, which consequently favors the entanglement of the polymer chains. As a result, the position of the polymer molecules becomes more inflexible and in turn the viscosity of the solution increases [87,88]. This is also the reason why the viscosity raised at higher concentrations of polymeric additives, since the movement of the molecules becomes more restricted when their quantity increases. Again, the observed effect on the viscosity with increasing PVP concentration was more pronounced in comparison to the effect seen in case of PEG. Again, the chain length of the used PVP was higher than the one of PEG, which as discussed before influences the solution viscosity.

The trends which were observed in this study agree to the findings other groups made with similar systems or systems containing other solvents or polymers, as well as a different combination of both [14,62,64,71,72,89].

### 3.2. Cloud point titration

The cloud points of 5 wt% PES solutions prepared in the four different solvents NMP, DMAc, 2P and DML were determined and compared to each other. The compositions at the determined cloud points of each solution are shown in Table 5.

It was found that the ternary system with NMP has the highest water tolerance, so that in comparison to the other three solvents the most water is needed to induce precipitation. In contrast, a solution containing the same starting concentration of PES but DMAc as solvent tolerates around 2.5 wt% less water than the NMP solution. The reason for this could be the better solubility of PES in NMP, which in turn results in a larger miscibility gap. Similar observations for PES in NMP and DMAc were previously reported in literature [90,91].

**Table 5**  
Cloud points of 5 wt% PES solutions prepared with NMP, DMAc, 2P and DML as solvents.

Solvent system	Water [wt.%]	Polymer [wt.%]	Solvent [wt.%]
NMP	12.01	3.86	83.43
DMAc	9.54	4.19	86.27
2P	5.91	4.47	89.62
DML	3.81	4.71	91.48

However, no phase diagrams have been reported for PES-2P or PES-DML so far. Therefore, a first trial was made in this study to compare the water tolerance of the alternative solvents to the conventional ones. It was found that both alternative solvent systems tolerate less water than the conventional ones, so that less water is needed to induce membrane formation. This can be explained by a lower solvent power of 2P and DML for PES [90].

From these results can be concluded that in case of the same PES concentration different membrane characteristics will be obtained when changing the solvents. The higher the water tolerance, the lower the polymer concentration in the solution when demixing sets in. As a consequence the proportion of solvent in the matrix-forming phase is reduced after onset of phase separation. This is why the nascent pore size after demixing is strongly influenced because higher polymer concentrations lead to tighter pore structures. It has been previously shown that higher polymer concentrations in the dope solution, which also cause an entry into the miscibility gap at higher polymer concentrations, result in tighter membranes [55]. Consequently membranes prepared with the same polymer concentration but with different solvents should exhibit different performances with respect to permeability and retention capability.

### 3.3. Membrane structure

In order to evaluate the influence of the additive and solvent variations on the membrane structure, cross-sections of each membrane prototype were recorded. It was found that all membranes had an asymmetric structure with a dense retentive layer on the top-side, which is commonly known as skin, and a porous sublayer below the skin. This sublayer can either contain macrovoids, finger-like cavities, or a sponge-

like morphology. These typical structural characteristics have been frequently published in literature [23,61,92–96].

Although the membranes had the asymmetric structure in common, the thickness of the dense top layer and the morphology of the sublayer differed in dependence of the type, concentration and molecular weight of the additive which was used. Furthermore, the resulting structure was strongly dependent on the applied solvent. The structures of the membranes prepared with the low viscosity solvents NMP and DMAc were similar, and differed to those of the membranes prepared with the high viscosity solvents 2P and DML, which on the other hand also exhibited similar morphological properties among each other.

If the structures of these two groups are compared to each other, it is striking that the sponge-like layer on the skin side of the membranes become thicker when a more viscous solvent is used. While the thickness of the sponge-like layer of the NMP and DMAc membranes is in the nanometer range (Fig. 2), its thickness is rather in the micrometer range for 2P and DML membranes (Fig. 3).

Apart from the sponge layer thickness, the substructures of the resulting membranes from both solvent groups differed as well. The morphology which was observed directly below the thin sponge-like layer can be distinguished between the different systems, as the cavities in the porous sublayer differ in size and shape in dependence of the applied solvent.

The influences of solvents and additives variations on the membrane morphology are in the following discussed based on selected representative membrane samples. For the whole set of cross-section images refer to Figs. S1–S4 in the supplementary material.

The left half of Fig. 4 depicts the sole influences of the respective solvent on the membrane morphology. The figure shows membrane cross-sections which were prepared without any additives. It was found

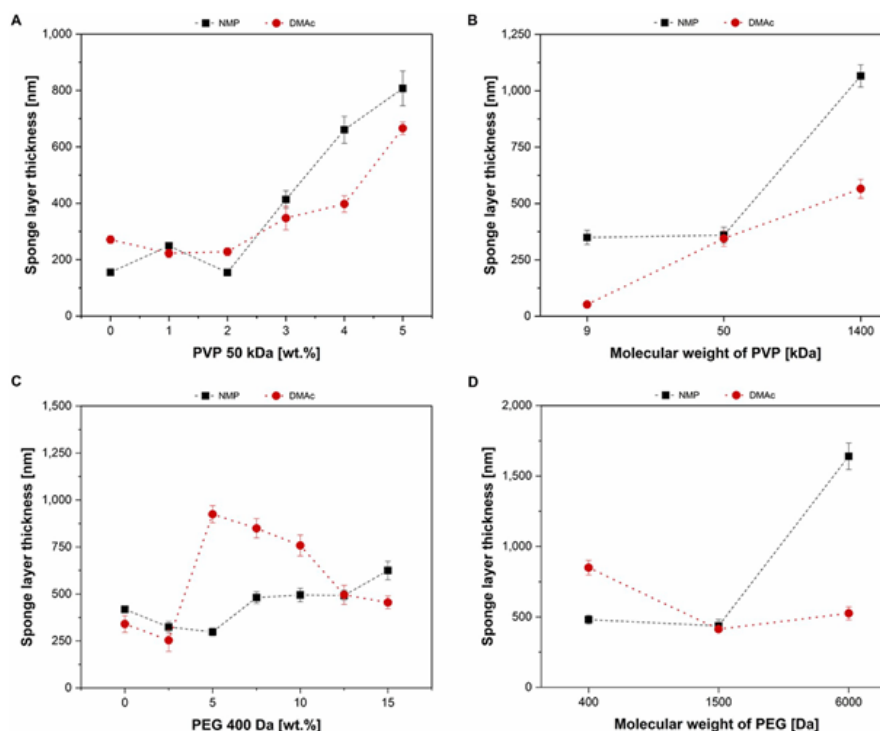


Fig. 2. Average sponge layer thickness  $\pm$  standard deviation ( $n = 5$ ) in dependence of the PVP 50 kDa concentration (A), the PVP molecular weight (B), the concentration of PEG 400 Da (C), and the PEG molecular weight (D) of membrane prototypes prepared by immersion precipitation using NMP and DMAc as solvents.



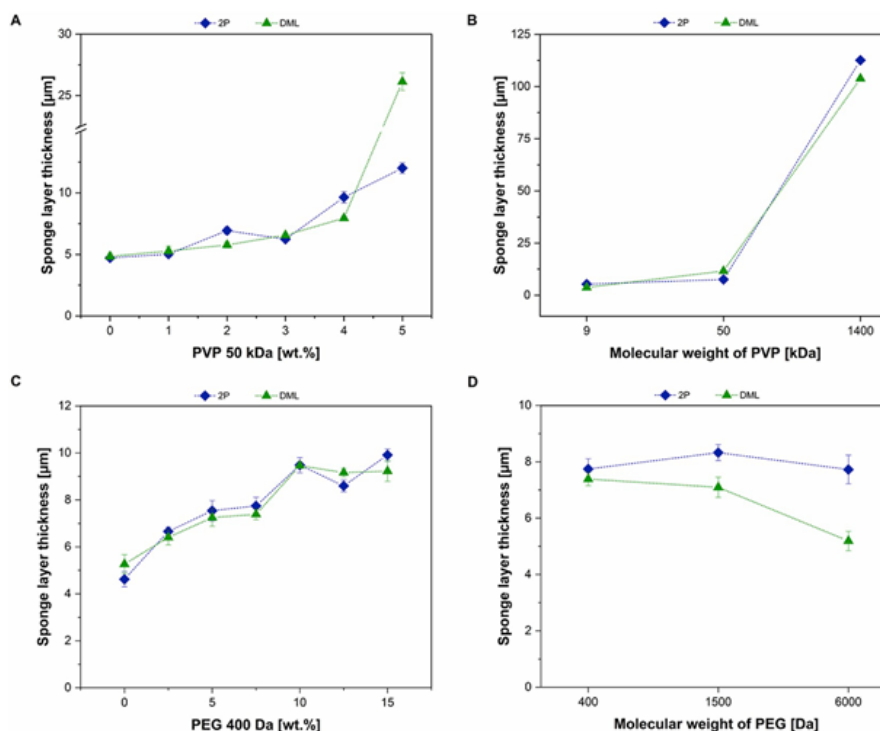


Fig. 3. Average sponge layer thickness  $\pm$  standard deviation ( $n = 5$ ) in dependence of the PVP 50 kDa concentration (A), the PVP molecular weight (B), the concentration of PEG 400 Da (C), and the PEG molecular weight (D) of membrane prototypes prepared by immersion precipitation using 2P and DML as solvents.

that if low-viscosity solvents were used for the membrane production, the comparatively thin retentive skin layer is directly followed by a porous sublayer. This sublayer is dominated by a finger-like morphology, which is characterized by narrow, but vertically elongated cavities. Below this layer so-called macrovoids are predominant, which in this case are large and oval-shaped cavities surrounded by sponge-like areas. In contrast to the upper sponge-like layer, this sponge-like morphology can be distinguished by a rather cellular and closed pore structure. In contrast, membranes prepared with solvents having a higher viscosity exhibited a significantly thicker sponge structure on the skin side. In turn, the finger-like structure begins deeper within the membrane cross-section. In addition, contrarily to the case of NMP and DMAc, the voids are smaller in size than the ones which can be found in membranes prepared with conventional solvents. Merely the lower third of the DML cross-section is crossed by a horizontally extended, large cavity. Below this cavity and below the macrovoids in the 2P membrane a sponge-like structure follows, which in comparison to the NMP and DMAc structure is relatively narrow. A reason for this could be that the coalescence of the pore-forming nuclei and the diffusive exchange of solvent and non-solvent are suppressed by the higher dope solution viscosity in case of 2P and DML. As a consequence the growth of the pore-forming domains is slowed down, which consequently results in smaller pore sizes [97]. The results fit those of the performance experiments which are addressed later. It confirms the assumed mechanisms and points out that structure and performance of the membrane are closely related to each other.

As indicated, nucleation and growth is also influenced by the viscosity. The growth of the developing nuclei is dependent on the diffusion rate of the solvent into the nucleus, where higher diffusion allows the formation of larger macrovoids [92,94]. In turn, this causes that the

macrovoids remain smaller at higher viscosities. On top of that, the choice of the solvent is crucial for the demixing speed of the solution, which is known to be a critical influencing factor for the nucleation and growth mechanism. The demixing speed is not only dependent on the diffusion rate but also on the location of the miscibility gap in relation to the location of the solution composition within the phase diagram. In this case it is similar for NMP and DMAc, as well as for 2P and DML, however, both solvent groups differ from each other.

The right part of Fig. 4 representatively expresses the effect of PVP 50 kDa on the morphology when it is added to the casting solution using the highest PVP concentration as example. It was found that the structure in all four solvent systems changed in the presence of PVP, although the behavior again differed between membranes prepared from conventional and alternative solvents. The PVP content in the casting solution strongly affects the thickness of the sponge-like layer. Figs. 2 and 3 show that the layer thickness increased from twofold up to fivefold, depending on the solvent which was used. On one hand this can be attributed to changes in the solution viscosity, which in turn slow down the diffusive processes. On the other hand it can also be attributed to the altered thermodynamics of the system caused by the addition of PVP. The change of the skin thickness can be one reason for a decreasing permeability, which is addressed later. The sponge-like layer significantly contributes to the flow resistance. If the thickness of this layer is considerably increased, it effects the permeability as a consequence of the raise in flux resistance.

In the substructure an increase of the PVP concentration caused an enlargement of the voids, however, at the same time the number of the voids in the substructure decreased. A possible reason for this could be that PVP has a dual effect on the membrane morphology [60]. On one hand it affects the thermodynamic stability of the casting solution,

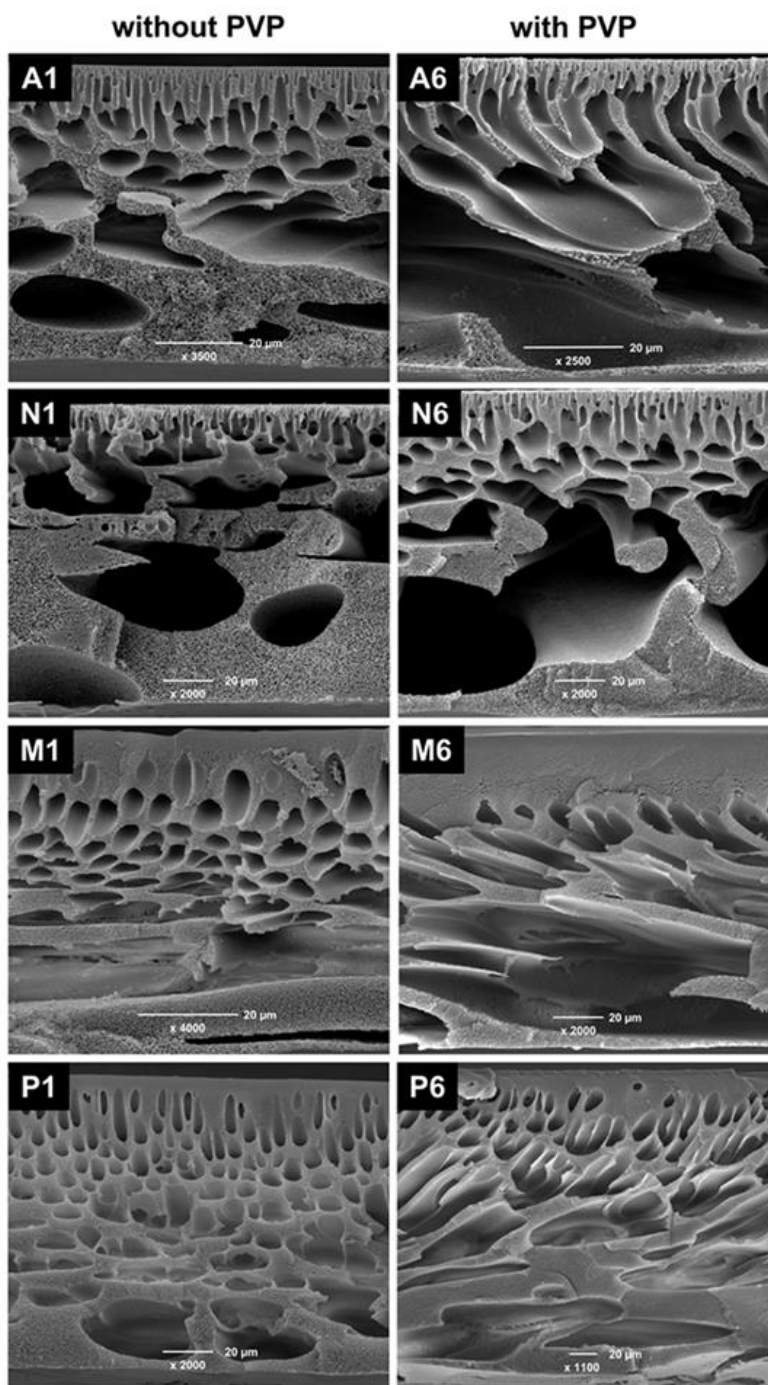


Fig. 4. Scanning electron microscopy cross-section images of membrane prototypes prepared by immersion precipitation with different solvents and without any PVP or with PVP 50 kDa added to the casting solution (image recording potential of 12.5 kV).

which leads to a change in demixing time. On top of that it affects the affinity between the solvent and the forming nuclei, which is responsible for the formation of macrovoids. Therefore, the uptake rate of the solvent by the nuclei is changed. As a consequence the size of the developing macrovoid is altered, since the size of the macrovoid is dependent on the ability of the nuclei to take up the solvent from its surroundings [60,96]. On the other hand the addition of PVP hinders the diffusion speed of the solvent and the non-solvent so that the uptake into the forming nuclei is slowed down. Hence, the resulting macrovoids should be smaller. However, in this case the first effect seems to superimpose so that larger macrovoids were able to form. Yet another reason for the larger sizes of the macrovoids could be that the sponge-like layer acts as a diffusion barrier for the non-solvent to diffuse into the casting film. Therefore, the time which the demixing solution needs to reach the solidification of the structure is prolonged. It has been previously reported that the size of the macrovoids is dependent on vitrification [98]. Therefore, the growth of the nuclei and their coalescence can proceed longer, which finally would lead to larger voids in the membrane substructure.

The membrane morphology is not only influenced by the presence of PVP, but also by the molecular weight of the added PVP. Both, the sponge-layer thickness and the morphology of the substructure are strongly influenced by the PVP molecular weight (Fig. 5).

If the added PVP has a low molecular weight, the sponge-like layer is rather thin. However, the thickness again differed in dependence on the viscosity of the used solvent. With an increase in the PVP molecular weight, the sponge-layer thickness visibly increased. Especially in case of the high viscous solvent systems the sponge-like morphologies occupies almost the complete cross-section of the membrane. This can be explained by the large effect of the PVP molecular weight on the viscosity as shown in Fig. 1. The viscosity raises above a point where the viscosity effect, which hinders the diffusion of solvent into the polymer-lean phase, overcomes the effect of PVP on the thermodynamics of the casting solution. Therefore, the growth of the nuclei is prevented and a sponge-like morphology is formed. In contrast, with respect to the proportions of sponge-like and finger-like morphology across the complete cross-section for DMAc and NMP membranes with PVP of 1400 kDa (Fig. 5), a similar structure was observed as for the membranes with PVP of 50 kDa (Fig. 4). The reason for the morphology in the substructure of the membrane with high molecular weight PVP, which is dominated by vertically elongated macrovoids, could be that the point at which the viscosity effect overcomes the effect on the thermodynamic stability of the casting solution has not been reached. Consequently, the difference between conventional and alternative solvent membranes when using high molecular weight PVP is likely due to the different viscosities in dependence of the solvent, which determine the effect that superimposes.

In contrast to the apparent effect of PVP on the membrane morphology, PEG 400 Da has a lower influence on the membrane structure. However, similar to the results found for PVP, the increase of the PEG concentration in the casting solution increased the thickness of the sponge-layer in membranes prepared with NMP, 2P and DML (Figs. 2 and 3). Comparable to the PVP results, the addition of PEG has an effect on the viscosity, however, it is less pronounced than in case of PVP. As the viscosity influences the formation of a sponge-like morphology [98], an increase in the sponge-layer thickness is caused. However, this effect is less obvious than in case of PVP, which can be explained by the comparatively lower increase of the viscosity. Furthermore, PEG slightly influences the thermodynamic stability of the system, which also contributes to the formation of a sponge-like morphology [99,100]. In contrast to the other three solvents, the trend for the concentration row in DMAc was found to be different. Although the skin thickness increased up to a concentration of 5 wt% PEG, with a further elevation of the PEG concentration the sponge layer thickness started to decrease again (Fig. 2). This observation might have several reasons. One explanation could be that the influence of the viscosity in DMAc is

relatively low, especially in contrast to 2P and DML, so that other effects are dominating. Another reason could be that the change in the thermodynamic stability of the solution is different than in the other solution systems. Yet another possible reason for the divergent trend might be the difference in the affinity of the various solvents to PEG. Regarding to the HSP values DMAc has the lowest affinity to PEG, which could be the reason for causing the different behavior in contrast to the other solvents.

Although it has been reported in literature that an increase of the PEG concentration can suppress the formation of macrovoids [100], this could not be confirmed in this study. If comparing the SEM images of membranes without PEG to those made with PEG, no obvious differences in the substructure can be observed (Fig. 6). A reason could be that the influence of the PEG content on the casting solution viscosity is rather low, so that the viscosity effect is not large enough to cause structural changes in the sublayer. Furthermore, the influence of PEG on the thermodynamic stability is in comparison lower than the influence of PVP on the solution thermodynamics, so that the increase of PEG is not sufficient to visibly affect the morphology of the substructure. However, there might be a PEG concentration above the tested 15 wt% at which the effects of the viscosity and the influence on the thermodynamics are high enough to cause any structural changes in the membrane substructure.

Although an increase of the PEG molecular weight affected the thickness of the sponge-layer, no significant changes could be observed in the substructure of the membrane (Fig. 7).

In case of DMAc, 2P and DML membranes the thickness of the sponge-like layer was found to decrease with an increase in the molecular weight of PEG. In contrast, the sponge layer thickness of NMP membranes remained constant when the PEG molecular weight was raised from 400 Da to 1500 Da. However, a further increase of the molecular weight to 6000 Da resulted in an increase of the sponge layer thickness by a factor of about three. The same trend has been previously reported for a system of PSf, PEG and NMP and was explained by the change in the thermodynamic stability of the solution [64]. Furthermore, the use of high molecular weight additives induces an increase in the solution viscosity. This in turn can promote the formation of a sponge-like morphology.

In contrast to the trend observed for NMP membranes, it has been previously reported that the dissolving of PES in DMF or DMAc results in membranes which exhibit an opposite behavior. It has been shown previously that the thickness of the sponge-like structure decreases with a rising PEG molecular weight [14,57], which is similar to the results found in this study for DMAc, 2P and DML membranes. Therefore, the opposing trends seem to be solvent-dependent. One explanation could be that the solvents have different affinities for both, the additives and the non-solvent. Since the affinity between the components contributes to the rate of phase separation, because they influence the thermodynamic stability as well as the exchange rate of solvent and non-solvent, this may be the reason for the observed differences. If the distance values of the HSPs of PEG and the different solvents are compared to each other, the distance value of NMP and PEG is lower in comparison to the distance between PEG and the other three solvents. Furthermore, it has been previously shown that the use of higher molecular weight PEG can shift the phase boundary, which in turn influences the resulting membrane morphology and in particular the formation of a sponge-like morphology [20,99]. Although the PEG molecular weight affected the structure on the skin-side of the membrane, no obvious differences could be observed for the morphology of the substructure. A reason could be that the parameters which influence the sponge layer thickness were not large enough to cause structural changes in the sublayer. Again, the influence of PEG on the thermodynamic stability is rather low in comparison to PVP so that higher molecular weights of PEG might not cause a visible change in the morphology of the substructure.

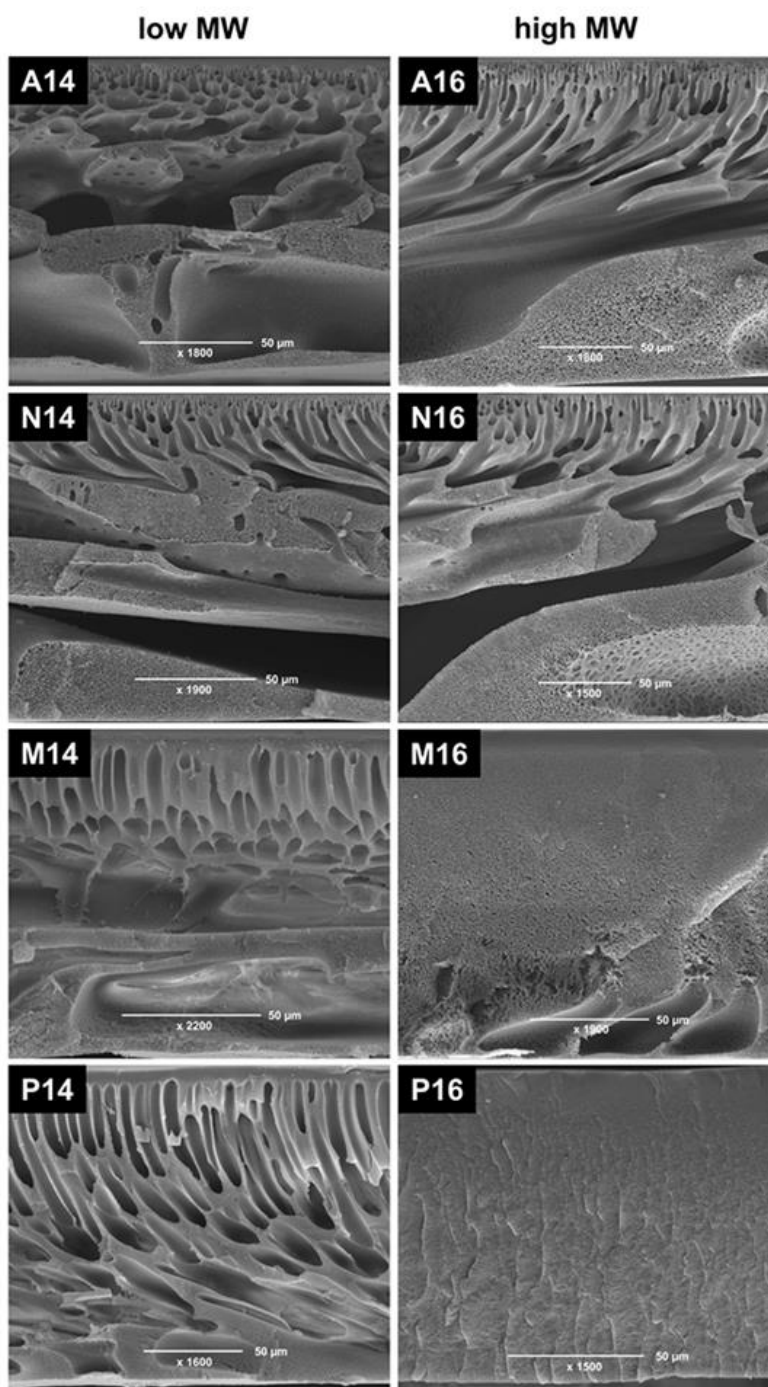


**Fig. 5.** Scanning electron microscopy cross-section images of membrane prototypes prepared by immersion precipitation with different solvents and PVP of different molecular weights (9 kDa or 1400 kDa) as additives (image recording potential of 12.5 kV).

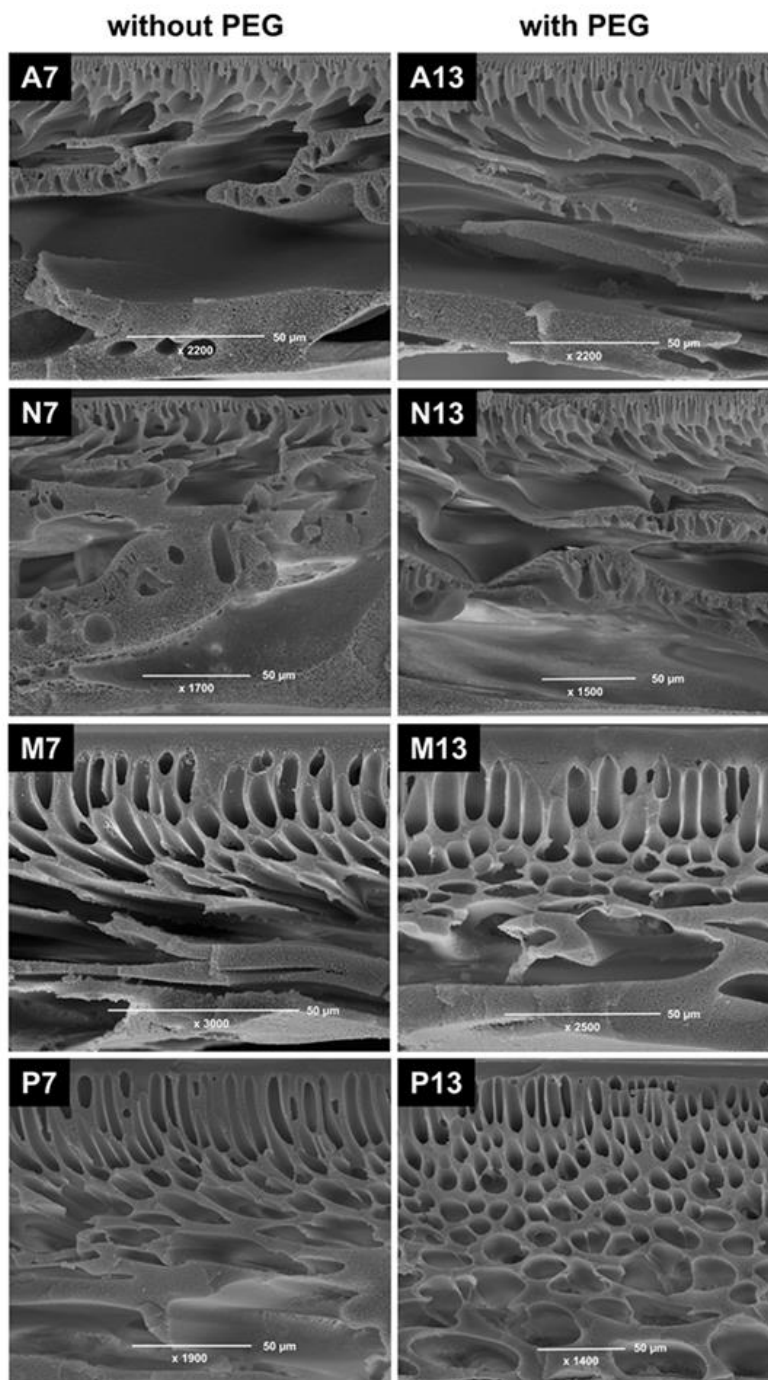


**Fig. 6.** Scanning electron microscopy cross-section images of membrane prototypes prepared by immersion precipitation with different solvents and without any PEG or with PEG 400 Da added to the casting solution (image recording potential of 12.5 kV).

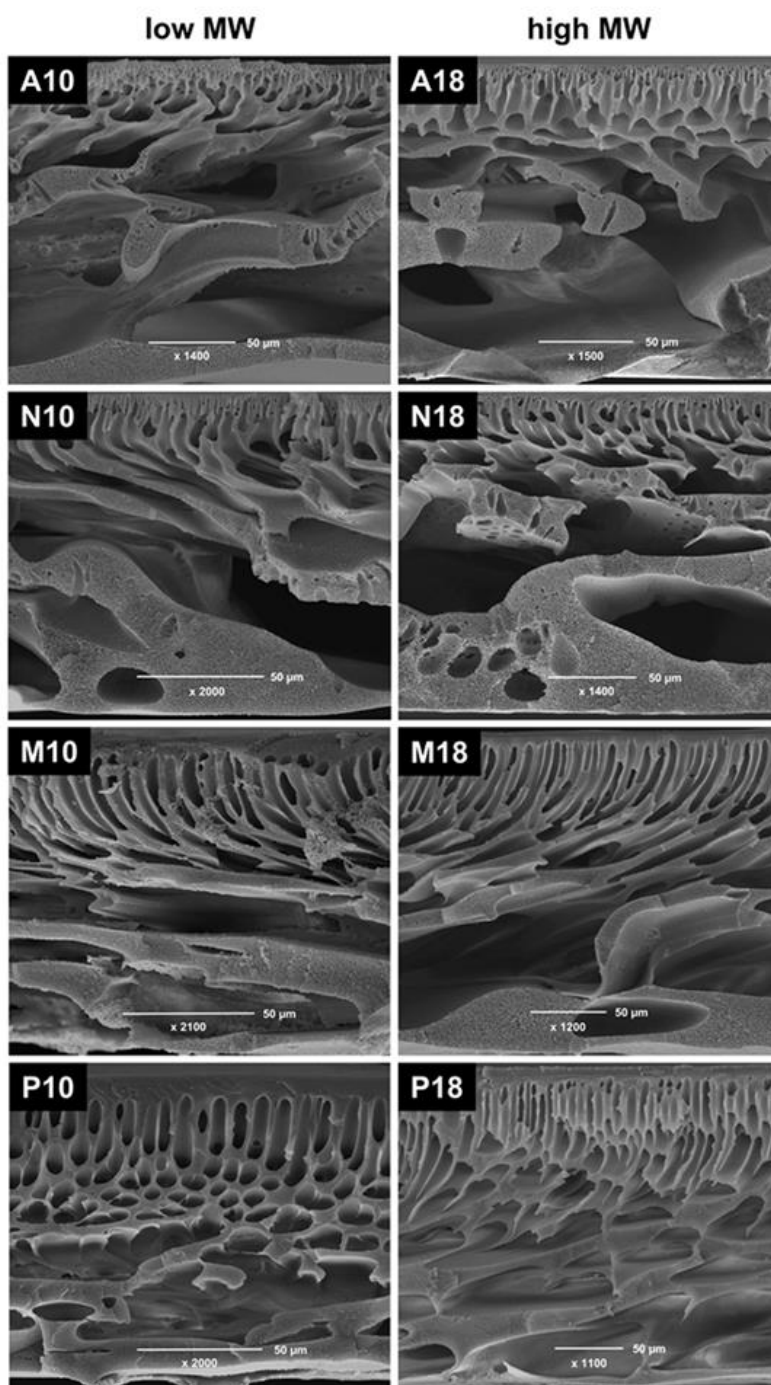


**Fig. 7.** Scanning electron microscopy cross-section images of membrane prototypes prepared by immersion precipitation with DMA or DML as solvent and PEG of different molecular weights (400 Da or 6000 Da) as additives (image recording potential of 12.5 kV).

### 3.4. Membrane permeability

It was found that the addition of PVP or PEG to the casting solution had an influence on the membrane permeability and that the observed effect is dependent on the concentration and molecular weight of the additive (Fig. 8).

For varying PVP 50 kDa concentrations in the casting solution the permeability of the manufactured membrane prototypes exhibited two different behaviors in dependence of the applied solvent. If the solvents 2P or DML were used for the preparation of the membrane samples, an increase of the PVP concentration lead to a decrease of the membrane permeability. In contrast, for DMAc and NMP membranes an increase of the PVP content in the casting solution resulted in an increase in the membrane permeability, until a certain concentration was reached. However, as it was also the case for 2P and DML membranes, a further addition of PVP to the solution lead to a reduction of the permeability. This behavior has already been reported in literature [55,60,62]. Anyhow it has been shown that the observed turning point can vary in dependence of the type and the concentration of the membrane-forming polymer which is applied. This is why the reported PVP concentration considerably varies, at which the permeability has its maximum in systems with NMP or DMAc.

The observation of a permeability maximum can be explained by two contrary effects. On one hand PVP acts as a pore-forming agent and can thus lead to an increase in permeability if its concentration is raised. On the other hand the addition of PVP to the solution results in a significant enlargement of the solution viscosity, which has an influence on the formation of the pore structure. During phase separation the pore network develops from the polymer-poor phase. When the solution composition during the NIPS process reaches a composition within the

miscibility gap, the solution separates into areas of polymer-rich phase and droplets of polymer-poor phase. Until the solidification sets in, the liquid polymer-poor phase is able to coalesce so that smaller droplets of this phase converge to larger droplets [101,102]. As a consequence the pores which are formed through these droplets increase in size. Therefore, the faster and the longer the coalescence can take place, the larger the pores will get during the phase separation process. Due to an increasing viscosity e.g. caused by the addition of higher PVP amounts, the coalescence is hindered and the developing pores remain smaller compared to solutions which exhibit a lower viscosity. As the pore size correlates with the membrane permeability, this is also the reason why the viscosity of the casting solution can impact the permeability. If this would be the reason why the permeability decreases, the protein retention should in turn increase due to the smaller pores. However, as this effect could not be observed, it is more likely that the flux decline can be attributed to the formation of a thicker sponge-like layer, which is also promoted by a higher viscosity. As the sponge-like structure contributes more to the flow resistance than a finger-like structure, this would explain why the previously discussed increase in the sponge layer thickness causes a decrease in permeability.

As mentioned, the two described effects of PVP act against each other. At low viscosities, the pore-forming properties of PVP dominate, which is why membranes prepared with DMAc or NMP show an increase in permeability when the concentration of PVP in the casting solution is raised. However, when a critical viscosity range is reached, the effect of PVP on the viscosity and thus on the coalescence overcomes the pore-forming effect. This is why the permeability reaches a maximum before it starts decreasing again. When 2P or DML are used as solvents, the viscosities of the casting solution are above the described critical viscosity, even without additional PVP in the polymer solution. In turn,

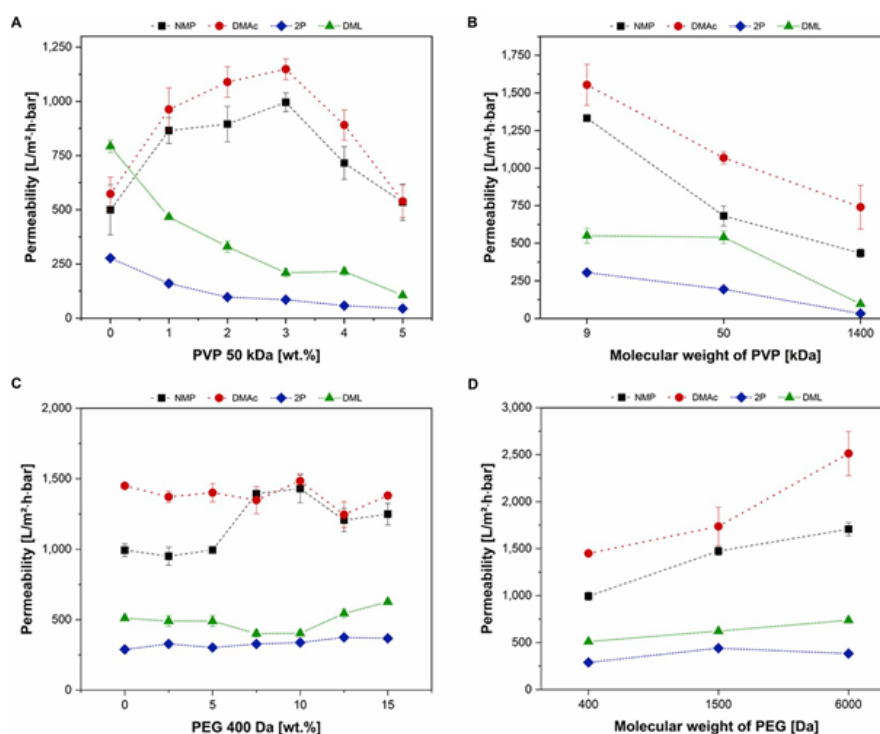


Fig. 8. Average permeability  $\pm$  standard deviation ( $n = 3$ ) of a 0.9 wt% sodium chloride solution in dependence of the PVP 50 kDa concentration (A), the PVP molecular weight (B), the concentration of PEG 400 Da (C), and the PEG molecular weight (D) of membrane prototypes prepared in four different solvent systems.

an addition of PVP immediately reduces the permeability of the membrane, since the effect on the coalescence is outweighing the pore-forming impact of PVP immediately.

Apart from the viscosity effects, other influences such as the distribution of the PVP molecules within the polymer-poor and the polymer-rich phase can impact the pore development during phase inversion. It can influence the nucleation and growth mechanism, which has been described as one of the key mechanisms for the formation of polymeric membranes [23,103]. As the distribution is dependent on the location of the miscibility gap, which in turn is strongly influenced by the applied solvent, this could also be a reason for the contrasting behaviors observed for the different solution systems. According to the HSP distance values, which are quite similar for DMAc and NMP, these two substances are better solvents for PES than 2P and DML, which are with respect to the HSPs likewise similar (Table 4). As a consequence, the miscibility gaps of NMP and DMAc are smaller than the ones of 2P and DML [59,90]. This could be confirmed by the cloud point experiments in this study (Table 5). In turn, together with the influence of the differences in viscosity between the two solvents groups, these properties influence the composition of the two phases and therefore the PVP concentration within them.

In contrast to the different trends found in case of varying PVP concentrations, the observed behavior for variations in the PVP molecular weight was the same for all four solvent systems. It was found that the higher the molecular weight of PVP which is added to the casting solution, the lower is the permeability. This can be explained by the impact of the chain length on the viscosity, which strongly affects the formation of macrovoids and the development of a sponge layer, respectively [89,98]. An increase of the chain length of PVP results in an increase of the casting solution viscosity. As a result, the coalescence of the polymer-lean droplets during the membrane formation process is suppressed due to the higher flow resistance in the polymer solution, and the nucleation and growth mechanism is influenced. Consequently the formation of macrovoids is hindered, and in comparison to solutions containing PVP of lower molecular weight thicker sponge-like areas are formed by adding PVP with higher molecular weight, which strongly contribute to the membrane's flow resistance.

In addition to the effects on the solution viscosity, the type of PVP also influences the thermodynamics of the polymeric system. It has previously been shown that the phase diagram and therefore the demixing time can be altered by changing the molecular weight of PVP [89, 104]. Furthermore, the composition of the developing phases can be influenced by the PVP molecular weight. For the membrane-forming polymer the low molecular weight polymeric contents primarily tend to remain in the polymer-poor phase, while the higher molecular weight contents primarily stay in the polymer-rich phase and therefore form the matrix of the membrane [105]. Likely, PVP will behave similarly, so that PVP with a higher molecular weight will increase the polymer content in the membrane matrix. This will in turn result in a tighter membrane structure. In contrast, PVP with lower molecular weight is predominantly accumulated in the polymer-poor phase and therefore washed out, so that the membrane matrix in comparison has a lower polymer content. This hypothesis could be confirmed by Matsuyama et al. who showed that the PVP retention factor increases with higher molecular weight [89]. Furthermore, the leaching of short-chained PVP from the membrane matrix is generally higher than the leaching of long-chained PVP [20].

For effects caused by variations of the PEG concentration, a dependence on the applied solvent could be observed. Similarly to the results of the PVP concentration row two different behaviors were found. In case of the low viscosity solvents DMAc and NMP, at low concentrations of PEG within the casting solution the permeability was not significantly influenced compared to membranes prepared without any PEG. However, a maximum for both systems was found in the middle concentration range, after which the permeability started to decrease again when even higher PEG concentrations were applied. A possible explanation for

the observed trend could be an interference of two opposite effects. In the literature, PEG 400 Da is described as a pore-forming agent [106]. The incorporation of PEG into the membrane matrix can lead to higher porosities and larger pores when it subsequently leaches out of the forming structure during the course of the immersion precipitation. This effect will account for the rising permeability at higher PEG concentrations, however a critical concentration is needed to create a visible effect. On the other hand, the addition of PEG increases the casting solution viscosity. Since a higher viscosity leads to a reduction in coalescence of the polymer-poor phase, it ultimately favors the formation of thicker sponge-like layer. Therefore, this effect will account for the decrease in permeability when a certain viscosity is reached, so that the pore-forming characteristics of PEG are compensated. The experimental results indicate that this critical viscosity lies at a value of around 1 Pa·s. For the solvents 2P and DML no visible effect on the permeability could be observed. This can be explained by the higher viscosities of the resulting casting solutions. As described before, the pore-forming characteristics of PEG might be compensated or superimposed by the hindrance of the coalescence at a viscosity of 1 Pa·s or above. When the pore-forming properties that lead to an increase of the permeability are compensated, the rise in flux is missing and the permeability stays at the same level or even decreases. As the use of 2P and DML results in casting solutions exhibiting viscosities already higher than 1 Pa·s, no flux increase could be achieved through a rising PEG concentration.

In contrast to the concentration variations of PEG, changes of the PEG molecular weight caused similar effects in all four solvent systems. It was observed that an increase in the PEG molecular weight induced a raise in permeability. This can be explained by the pore-forming properties of PEG. The concentration for the experiments with different molecular weights was set to 7.5 wt% PEG. Referring to the results of the concentration row, at this concentration the permeability results indicate a pore-forming effect of PEG in NMP and DMAc systems. The higher the molecular weight of the PEG molecule which is applied, the larger is its hydrodynamic diameter. During membrane formation the PEG molecules initially are embedded into the membrane matrix. However, in the course of the process PEG is washed out into the precipitation bath so that pores form at the positions where the PEG molecules were located [20]. Therefore, the larger the molecules are, the bigger will be the pores which result from their leaching.

While the effect for membranes prepared with NMP and DMAc is clearly visible, the effect for membranes produced with 2P or DML is much less pronounced. As indicated before, a reason for this could be the influence of the viscosity, since it counteracts the pore-forming effect of PEG. As the viscosity of casting solutions prepared with 2P or DML is much higher than the ones prepared with DMAc or NMP, the contrary effect of the viscosity is compensating the pore forming impact of PEG and the permeability is only slightly influenced.

Another reason for the observed trend could be that the use of larger polymeric molecules shifts the position of the casting solution within the phase diagram towards the miscibility gap, as well as the location of the miscibility gap itself [20]. As a result, the path the solution composition follows to reach the heterogeneous two phase region is modified, and consequently the compositions of the developing phases are altered. Since the path into the miscibility gap and the thereof resulting compositions of the two developing phases are crucial for the resulting membrane structure, this in turn can influence the permeability of the resulting membrane.

### 3.5. Protein retention

The effect of the applied additive variations on the retention of the model protein lysozyme is shown in Fig. 9.

In case of size exclusion based filtration, usually a correlation between the membrane permeability and its retention capacity of the target molecule can be observed. This is based on the dependence of both membrane properties on the pore size distribution of the



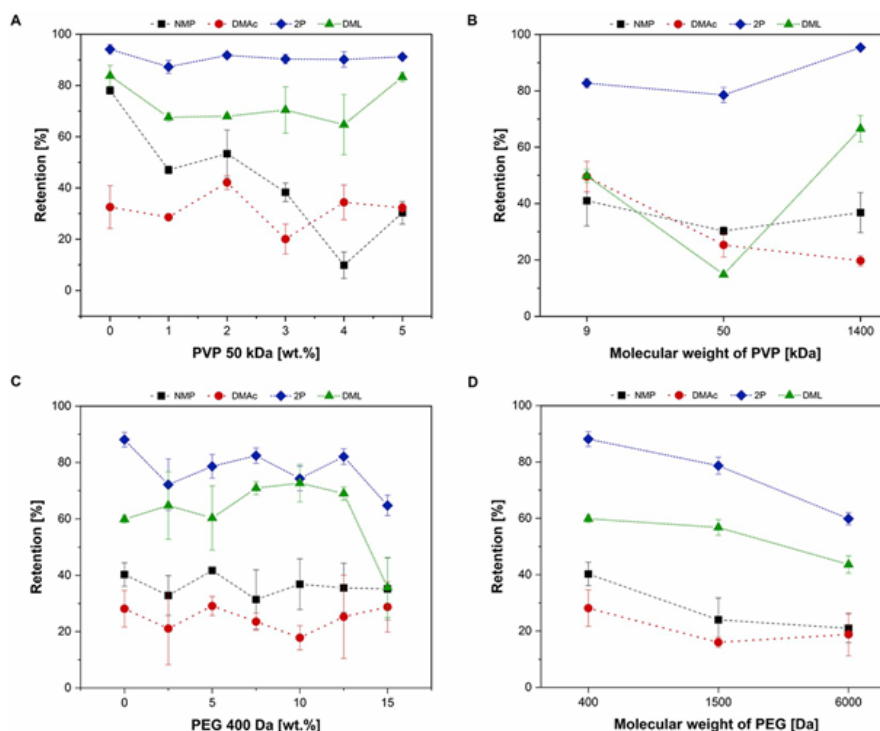


Fig. 9. Average lysozyme retention  $\pm$  standard deviation ( $n = 3$ ) in dependence of the PVP 50 kDa concentration (A), the PVP molecular weight (B), the concentration of PEG 400 Da (C), and the PEG molecular weight (D) of membrane prototypes prepared in four different solvent systems, measured with a filtration medium consisting of 1 g/L protein in 20 mM phosphate buffer (pH 7.0).

membrane, its porosity and especially of the pore sizes within the retentive layer [25]. Nevertheless, this correlation can be superimposed by absorptive effects during filtration as well as by influences of the membrane substructure. In case of NMP membranes the correlation between permeability and retention of lysozyme could be observed to some extent. A rising PVP 50 kDa content in the casting solution decreased the retention, while a simultaneous increase in the permeability could be observed. However, at higher PVP concentrations the results deviate from the expected correlation. A reason for this could be that the increase of the hydrophilic PVP molecules in the casting solution, and therefore in the membrane matrix, can reduce the adsorption of lysozyme to the membrane surface. Although the main retention mechanism is size exclusion, the adsorption of molecules can significantly contribute to the protein rejection of the filter as the adsorption to the pore walls leads to a net decrease in size of the pore. For DMAc membranes no correlation between permeability and retention could be observed. The lysozyme rejection fluctuated between 20% and 40% with no visible trends in dependence of changes in the PVP concentration. The same could be observed for 2P and DML. Although the permeability decreased with increasing PVP concentration in both cases, the retention was barely influenced. This indicates that the flow resistance of the membrane changes due to structural modifications, whereas the retention is not affected. However, it sticks out that the retention for both used solvent systems, and additionally also in the case of NMP, the retention is slightly higher in the absence of PVP than in its presence. This can be attributed to adsorptive effects. Since PVP should hydrophilize the membrane surface, fewer protein molecules can adhere to the surface through hydrophobic or unspecific interactions. As a result of this the retention tends to decrease. An explanation for the absence of

this influence in the DMAc system could be that the added PVP hardly remains in the membrane structure, but instead is washed out during the precipitation process.

Another sample which stands out is the DML membrane with the highest PVP concentration. At a concentration of 5 wt% PVP 50 kDa the retention increased, which correlates to the decrease in permeability. In this case, the cause could be a saturation of the membrane surface with PVP. As a consequence of this saturation, the retention does not decrease further due to a reduction of the protein adsorption to the membrane. In this case size exclusion is almost solely responsible for the particle retention. Since the flux is decreasing as well, this observation is in agreement with the assumption that flux and retention are correlating.

A slight decrease of the lysozyme retention was observed for NMP and DMAc membranes when the molecular weight of PVP was increased. The longer the chains of the PVP molecule, the lower is the leaching of the molecules from the membrane structure during the formation process. If more PVP remains in the membrane structure, and in particular on the surface, the membrane hydrophilicity increases. This results in a decrease of the protein adsorption and since adsorption contributes to the retention, the lysozyme rejection thus decreases.

The effect should also be visible for membranes prepared with more viscous solvents. As expected, initially an increase in the molecular weight from 9 kDa to 50 kDa resulted in a decreased retention. However, when the molecular weight was further raised, the retention significantly increased, which can be attributed to a viscosity effect. If longer PVP chains are applied, the casting solution becomes more viscous. In particular, the addition of PVP 1400 kDa to casting solutions with 2P or DML resulted in a significant increase in viscosity (Fig. 1). As a result the coalescence of the polymer-poor phase is hindered, the pore sizes in the

retentive layer remain smaller and thus the retention is increasing. In comparison, even in the presence of PVP 1400 kDa the viscosity of NMP and DMAc solutions is significantly lower than the one of 2P and DML so that the coalescence is not considerably effected. In turn, the effect of reduced adsorption superimposes the viscosity effect and the retention does not raise.

For the influence of PEG 400 Da concentration variations on the protein retention no obvious trends could be observed for all four solvent systems. These results agree with the outcomes of the permeability measurements. Although PEG in the literature is described as a hydrophilizing agent [14], no significant effect on the surface hydrophilicity could be observed. If the membrane surface gets more hydrophilic, it is expected that the retention decreases due to reduced adsorption, which in turn contributes to the protein rejection. A reason for the lack of this effect could be that most of the PEG is washed out during the formation process so that the membrane surface is not significantly hydrophilized. Yet, one conspicuous result was found for the highest PEG concentration in 2P and DML. In both cases the retention visibly decreased in comparison to the other applied PEG concentrations. A reason for this could be the reaching of a critical PEG concentration which is necessary to achieve that enough PEG will remain within the membrane matrix to hydrophilize the membrane surface. This could be caused by the increase of the viscosity. If a viscosity is reached that significantly prevents the leaching of PEG from the forming structure, the enrichment of the hydrophilic molecules on the membrane surface could reduce the adsorption of lysozyme molecules to the membrane surface during filtration and thus result in a decreased retention of these molecules.

In contrast, the molecular weight variations showed, that regardless of the solvent system which was applied, an increase of the PEG molecular weight causes a decrease in the retention of lysozyme. These results correlate to the permeability measurements, which showed a permeability increase when the added PEG molecules had higher molecular weights. As described before, the effect on the permeability and thus on the retention capacity can be explained by the removal of the PEG molecules from the membrane matrix during immersion precipitation. This leaching of larger PEG molecules results in the formation of larger pores in comparison to the leaching of smaller PEG chains. On the other hand the effect can result from a shift of the casting solution composition within the phase diagram [20].

### 3.6. Mechanical stability

In order to gain information about the mechanical stability of the membrane prototypes the bursting pressure was determined. The results of selected membrane samples are summarized in Table 6.

It was found that the PVP 50 kDa concentration has an effect on the mechanical stability. A decrease was observed for the conventional solvents, while membranes prepared with the alternative solvents exhibited higher bursting pressures when the PVP concentration was raised. The different behaviors can be explained by two opposing effects. On one hand the increase of the PVP concentration leads to a higher porosity, which in turn leads to a decrease of the mechanical stability [15]. On the other hand it was found that a higher PVP concentration leads to a thicker sponge-layer, which exhibits a higher mechanical stability than structures containing macrovoids [55]. While the effect on the porosity seems to be superimpose in case of NMP and DMAc membranes, the effect on the sponge-layer thickness seems to dominate in case of 2P and DML membranes. This is why different solvent-dependent trends were found.

In contrast, variations in PVP molecular weight, PEG 400 Da concentration and PEG molecular weight did not cause any significant changes in the mechanical strength. The slight differences can rather be attributed to the experimental error than to an actual effect of the variations.

**Table 6**

Bursting pressure, water contact angle, unspecific protein binding determined with lysozyme and specific surface area of selected membrane prototypes prepared in DMAc, NMP, DML or 2P and with variations in additive concentrations and molecular weights.

Sample	Bursting pressure [bar]		Water contact angle [°]		Unspecific protein binding [ $\mu\text{g}/\text{cm}^2$ ]		Surface area [ $\text{m}^2/\text{g}$ ]
	Average (n = 3)	$\pm$	Average (n = 3)	$\pm$	Average (n = 4)	$\pm$	
A1	0.32	0.005	67.5	2.9	14.2	0.8	19.6
A6	0.18	0.008	60	1.0	16.2	1.1	20.8
N1	0.32	0.050	76.2	1.8	76.2	1.8	19.5
N6	0.18	0.005	63	1.9	63.0	1.9	21.0
M1	0.22	0.031	74.5	0.7	54.3	2.8	39.5
M6	0.39	0.017	63.6	1.2	29.5	2.1	33.0
P1	0.37	0.031	66.8	1.7	53.6	3.6	50.6
P6	0.44	0.024	54.9	6.0	29.2	1.3	44.8
A14	0.28	0.042	62.1	2.3	24.1	1.6	19.4
A16	0.25	0.012	56.2	3.7	21.7	0.8	25.3
N14	0.38	0.033	67	3.4	20.2	1.7	24.4
N16	0.39	0.021	56	1.4	23.2	1.6	21.1
M14	0.26	0.045	54.7	1.7	35.0	2.0	39.5
M16	0.27	0.026	45.4	1.4	30.5	1.6	42.0
P14	0.28	0.009	68.6	1.9	43.9	1.5	49.4
P16	0.37	0.004	47.5	4.8	29.9	2.5	45.2
A7	0.17	0.029	64.6	2.9	19.5	1.2	20.8
A13	0.15	0.033	62.8	3.6	20.0	1.3	28.0
N7	0.20	0.012	57.9	3.5	22.8	1.5	22.2
N13	0.22	0.005	56.3	3.2	28.2	4.6	24.5
M7	0.22	0.012	65.5	4.2	31.5	2.0	58.5
M13	0.22	0.028	66.7	2.3	34.3	0.7	44.1
P7	0.29	0.012	60.9	1.5	43.8	3.5	41.6
P13	0.29	0.017	50	2.9	53.3	1.6	47.8
A10	0.25	0.039	57.2	4.1	22.4	2.1	24.5
A18	0.19	0.034	59.3	1.5	32.9	1.2	15.8
N10	0.25	0.045	60.3	2.5	27.3	4.4	24.7
N18	0.21	0.052	68	1.8	30.9	5.1	22.6
M10	0.25	0.031	61.2	4.5	32.6	2.6	42.1
M18	0.23	0.017	64.8	1.2	47.5	2.0	22.8
P10	0.24	0.012	66.2	2.3	45.5	2.5	52.2
P18	0.29	0.012	63.9	2.1	58.7	0.5	29.9

### 3.7. Surface characteristics

The surface characteristics were evaluated by measurements of the contact angle, the unspecific protein binding capacity using lysozyme as model protein, and the specific surface area. The results for selected membrane samples are summarized in Table 6.

The higher the hydrophilicity, the lower should be the protein binding to the membrane surface. However, the protein binding is not only influenced by the surface hydrophilicity but also by the surface area of the membrane [107]. This is why both properties were determined, so that all three surface characteristics can be interpreted in dependence of each other.

In general, if comparing the membranes prepared from the different solvents among each other without considering the additive effects, it can be seen that the contact angles lie in the same order of magnitude. However, a difference can be observed in case of protein binding and specific surface area, which correlate with each other, however. In most cases the surface area and therefore the protein binding is lower for membranes prepared with conventional solvents than for those prepared with the alternative ones. The reason for this could be that different structure-forming mechanisms take place in dependence of the applied solvent [5]. The different mechanisms can either result in a closed pore structure with a lower surface area, as observed for NMP and DMAc membranes, or a bicontinuous structure with a higher surface area, as observed for 2P and DML membranes [102].

However, not only the solvent has an impact on the surface characteristics, but also the applied additives. It was found that both, an increase of the PVP 50 kDa concentration and the use of PVP with a higher

molecular weight, lead to a slight decrease of the water contact angle. This increase of the surface hydrophilicity can be explained by the hydrophilic nature of PVP [55]. The more of the hydrophilic additive is used, the more hydrophilic will be the originally hydrophobic surface caused by the hydrophobic nature of PES. The increase of the surface hydrophilicity could not only be confirmed through the water contact angle, but also through the determination of the unspecific protein binding. It was found that an increase of the PVP concentration decreased the lysozyme binding to NMP, DML and 2P membranes. In case of NMP this can mainly be attributed to the hydrophilicity, since the protein binding decreased although the surface area slightly increased. In case of 2P and DML the decreased protein binding is not solely caused by the surface hydrophilicity, but also by the decrease of the surface area. In case of DMAc neither the surface area nor the protein binding was found to change.

When the PVP molecular weight was increased the specific surface was found to increase as well. In turn, more surface is available to which protein molecules can bind. However, the protein binding was found to remain constant when the PVP molecular weight was changed, or it even decreased when PVP 1400 kDa was used. Therefore, these results confirm that a higher molecular weight of PVP results in an increased surface hydrophilicity.

For changes in the PEG 400 Da concentration the effects on the surface characteristics are not straightforward. For membranes prepared with the conventional solvents the surface area slightly increased with raised PEG concentration. A similar effect was observed for 2P membranes. However, in case of DML membranes an opposite behavior was seen. Although PEG is frequently used to increase the membrane surface hydrophilicity [108], it was found that both, the water contact angle and the protein binding, are not significantly affected by a raise in the PEG concentration. The only exception was observed for 2P membranes, where a decrease of the contact angle and a simultaneous increase of the protein binding was observed.

In contrast, an increase of the PEG molecular weight resulted in more definable effects. It was found that the surface area in case of DMAc, DML and 2P membranes is decreasing with increasing PEG molecular weight, whereas the unspecific protein binding was increasing at the same time. This indicates that the surface hydrophobicity is raising when using high molecular weight PEG. A reason for this could be that the share of the hydrophilic part of the PEG molecule in relation to the hydrophobic part of the PEG molecule is changed when the chain length increases.

#### 4. Conclusion

A comparative study was conducted to prove that it is possible to substitute the hazardous solvents NMP and DMAc through the sustainable alternatives 2P and DML. Furthermore this study improves the understanding of polymeric membrane formation by creating a holistic picture of different influencing variables. The impact of the two commonly applied additives PVP and PEG was studied in dependence of the solvent used for the preparation of different PES membranes. In this context, concentrations and molecular weights of the two chosen additives in each of the investigated solvents was varied systematically.

It was found that the viscosity is strongly dependent on the choice of the additive conditions and on the applied solvent. Since the viscosity strongly impacts the demixing process, it determines the properties of the forming membrane. This is why concentration and molecular weight variations of PVP and variations of the PEG molecular weight considerably influenced the water permeability. In contrast, changes in PEG concentration did not exhibit clear effects on the permeability, since the influence of the PEG concentration on the viscosity was found to be smaller. The effects of the variations on the lysozyme retention largely correlated with the influences they had on the permeability. These correlations can be attributed to structural changes. The determination of the sponge layer thickness on the skin-side confirmed this assumption,

as it was influenced by all varied parameters. Since the results regarding the morphology particularly showed correlations to the trends found for the permeabilities, the observed effects on the membrane permeability can be attributed to structural changes of the membrane, which are caused by additives and solvent choice. However, not only membrane morphology and performance are influenced by variations in additives and solvents, but also the mechanical stability as well as the surface characteristics.

The results show that the influences of the additives strongly depend on the applied solvent. The effects of additive variations on polymer solution and membrane characteristics were found for all four solvents systems, however, in general they were more pronounced for 2P and DML membranes. The observed differences can be explained by the respective solvent properties, since mainly the solubility criteria of the solvent and the solution viscosity play an important role.

Thus, 2P and DML are suitable sustainable alternatives for replacing hazardous solvent for PES membrane production. However, the influencing parameters have to be well-controlled to obtain membranes with similar characteristics. This study proved that the use of the appropriate solvent in combination with a suitable choice of the additives enables the production of membranes with desired properties. All in all, this study creates a holistic picture on the membrane formation process which can be applied to create new membrane casting solutions with new sustainable solvents.

#### Credit author statement

Catharina Kahrs: Conceptualization, Investigation, Methodology, Project administration, Visualization, Writing - original draft. Jan Schwollenbach: Supervision, Writing - review & editing.

#### Funding

This research did not receive any specific grant from funding agencies in the public, commercial, or not-for-profit sectors.

#### Declaration of competing interest

The authors declare that they have no known competing financial interests or personal relationships that could have appeared to influence the work reported in this paper.

#### Acknowledgement

The authors would like to thank Wulf Linke from the Sartorius membrane development team for the recording of the SEM cross-section images, as well as Chiara Knoblich, Sarah Therre and Lasse Tjark Gericke for their assistance in performing the experiments.

#### Appendix A. Supplementary data

Supplementary data to this article can be found online at <https://doi.org/10.1016/j.polymer.2019.122071>.

#### References

- [1] H. Strathmann, The use of membranes in downstream processing, *Food Biotechnol.* 4 (1990) 253–272.
- [2] R. van Reis, A. Zydney, Membrane separations in biotechnology, *Curr. Opin. Biotechnol.* 12 (2001) 208–211.
- [3] R. van Reis, A. Zydney, Bioprocess membrane technology, *J. Membr. Sci.* 297 (2007) 16–50.
- [4] T. Matsuura, *Synthetic Membranes and Membrane Separation Processes*, CRC Press, 1993.
- [5] M. Mulder, *Basic Principles of Membrane Technology*, Kluwer Academic Publishers, Dordrecht, Boston, London, 1996.
- [6] P.A. Marichal-Gallardo, M.M. Alvarez, State-of-the-art in downstream processing of monoclonal antibodies: process trends in design and validation, *Biotechnol. Prog.* 28 (2012) 899–916.

- [7] E. Eren, A. Sarihan, B. Eren, H. Gumus, F.O. Kocak, Preparation, characterization and performance enhancement of polysulfone ultrafiltration membrane using PBI as hydrophilic modifier, *J. Membr. Sci.* 475 (2015) 1–8.
- [8] G.R. Guillen, Y. Pan, M. Li, E.M.V. Hoek, Preparation and characterization of membranes formed by nonsolvent induced phase separation: a review, *Ind. Eng. Chem. Res.* 50 (2011) 3798–3817.
- [9] R. Bernstein, Y. Kaufman, V. Freger, E.M.V. Hoek, V.V. Tarabara, Membrane characterization, in: J. Dong, C.-C. Ho (Eds.), *Encyclopedia of Membrane Science and Technology*, John Wiley & Sons, Inc, 2013.
- [10] A. Akbari, R. Yegani, Study on the impact of polymer concentration and coagulation bath temperature on the porosity of polyethylene membranes fabricated via TIPS method, *J. Membr. Sep. Technol.* 1 (2012) 100–107.
- [11] P. Gronemeyer, R. Ditz, J. Strube, Trends in upstream and downstream process development for antibody manufacturing, *Bioengineering* 1 (2014) 188–212.
- [12] H. Fröhlich, L. Villian, D. Melzner, J. Strube, Membrane technology in bioprocess science, *Chem. Ing. Tech.* 84 (2012) 905–917.
- [13] A.S. Rathore, A. Shirke, Recent developments in membrane-based separations in biotechnology processes: Review, *Prep. Biochem. Biotechnol.* 41 (2011) 398–421.
- [14] A. Idris, N. Mat Zain, M.Y. Noordin, Synthesis, characterization and performance of asymmetric polyethersulfone (PES) ultrafiltration membranes with polyethylene glycol of different molecular weights as additives, *Desalination* 207 (2007) 324–339.
- [15] J.T. Jung, J.F. Kim, H.H. Wang, E. Di Nicolò, E. Drioli, Y.M. Lee, Understanding the non-solvent induced phase separation (NIPS) effect during the fabrication of microporous PVDF membranes via thermally induced phase separation (TIPS), *J. Membr. Sci.* 514 (2016) 250–263.
- [16] S. Mazinani, S. Darvishmanesh, A. Ehsanzadeh, B. van der Bruggen, Phase separation analysis of Extrem/solvent/non-solvent systems and relation with membrane morphology, *J. Membr. Sci.* 526 (2017) 301–314.
- [17] D.-M. Wang, J.-Y. Lai, Recent advances in preparation and morphology control of polymeric membranes formed by nonsolvent induced phase separation, *Curr. Opin. Chem. Eng.* 2 (2013) 229–237.
- [18] R.W. Baker, *Membrane Technology and Applications*, third ed., John Wiley & Sons, Ltd, 2012.
- [19] A. Figoli, T. Marino, S. Simone, E. Di Nicolò, X.-M. Li, T. He, S. Tornaghi, E. Drioli, Towards non-toxic solvents for membrane preparation: a review, *Green Chem.* 16 (2014) 4034–4059.
- [20] M. Sadrzadeh, S. Bhattacharjee, Rational design of phase inversion membranes by tailoring thermodynamics and kinetics of casting solution using polymer additives, *J. Membr. Sci.* 441 (2013) 31–44.
- [21] S.S. Madaeni, L. Bakhtiari, Thermodynamic-based predictions of membrane morphology in water/dimethylsulfoxide/polyethersulfone systems, *Polymer* 53 (2012) 4481–4488.
- [22] Y. Liu, G.H. Koops, H. Strathmann, Characterization of morphology controlled polyethersulfone hollow fiber membranes by the addition of polyethylene glycol to the dope and bore liquid solution, *J. Membr. Sci.* 223 (2003) 187–199.
- [23] C.A. Smolders, A.J. Reuvers, R.M. Boom, I.M. Wienk, Microstructures in phase-inversion membranes. Part 1. Formation of macrovoids, *J. Membr. Sci.* 73 (1992) 259–275.
- [24] T.-H. Young, L.-W. Chen, Pore formation mechanism of membranes from phase inversion process, *Desalination* 103 (1995) 233–247.
- [25] B.S. Lalia, V. Kochkodan, R. Hashaikeh, N. Hilal, A review on membrane fabrication: structure, properties and performance relationship, *Desalination* 326 (2013) 77–95.
- [26] A.K. Holda, L.F.J. Vankelecom, Understanding and guiding the phase inversion process for synthesis of solvent resistant nanofiltration membranes, *J. Appl. Polym. Sci.* 132 (2015).
- [27] G. Arthanareeswaran, S. Ananda Kumar, Effect of additives concentration on performance of cellulose acetate and polyethersulfone blend membranes, *J. Porous Mater.* 17 (2010) 515–522.
- [28] J. Barzin, S.S. Madaeni, H. Mirzadeh, M. Mehrabzadeh, Effect of polyvinylpyrrolidone on morphology and performance of hemodialysis membranes prepared from polyether sulfone, *J. Appl. Polym. Sci.* 92 (2004) 3804–3813.
- [29] J.H. Jhaveri, Z.V.P. Murthy, A comprehensive review on anti-fouling nanocomposite membranes for pressure driven membrane separation processes, *Desalination* 379 (2016) 137–154.
- [30] N.A. Alenazi, M.A. Hussein, K.A. Alamry, A.M. Asiri, Modified polyether-sulfone membrane: a mini review, *Des. Monomers Polym.* 20 (2017) 532–546.
- [31] G. Arthanareeswaran, V.M. Starov, Effect of solvents on performance of polyethersulfone ultrafiltration membranes: investigation of metal ion separations, *Desalination* 267 (2011) 57–63.
- [32] K.-J. Baik, J.Y. Kim, H.K. Lee, S.C. Kim, Liquid–liquid phase separation in polysulfone/polyethersulfone/N-methyl-2-pyrrolidone/water quaternary system, *J. Appl. Polym. Sci.* 74 (1999) 2113–2123.
- [33] X. Dong, A. Al-Jumaily, I.C. Escobar, Investigation of the use of a bio-derived solvent for non-solvent-induced phase separation (NIPS) fabrication of polysulfone membranes, *Membranes* 8 (2018) 23.
- [34] A. Figoli, A. Criscuoli, *Sustainable Membrane Technology for Water and Wastewater Treatment*, first ed., Springer, 2017.
- [35] M.A. Rasool, L.F.J. Vankelecom, Use of  $\gamma$ -valerolactone and glycerol derivatives as bio-based renewable solvents for membrane preparation, *Green Chem.* 21 (2019) 1054–1064.
- [36] A. Amelio, G. Genduso, S. Vreysen, P. Luis, B. van der Bruggen, Guidelines based on life cycle assessment for solvent selection during the process design and evaluation of treatment alternatives, *Green Chem.* 16 (2014) 3045–3063.
- [37] C. Capello, U. Fischer, K. Hungerbühler, What is a green solvent? A comprehensive framework for the environmental assessment of solvents, *Green Chem.* 9 (2007) 927–934.
- [38] A. Mohammad, *Green Solvents I: Properties and Applications in Chemistry*, first ed., Springer Science & Business Media, 2012.
- [39] D.Y. Xing, W.Y. Dong, T.-S. Chung, Effects of different ionic liquids as green solvents on the formation and ultrafiltration performance of CA hollow fiber membranes, *Ind. Eng. Chem. Res.* 55 (2016) 7505–7513.
- [40] H.H. Wang, J.T. Jung, J.F. Kim, S. Kim, E. Drioli, Y.M. Lee, A novel green solvent alternative for polymeric membrane preparation via nonsolvent-induced phase separation (NIPS), *J. Membr. Sci.* 574 (2019) 44–54.
- [41] T. Marino, F. Galiano, A. Molino, A. Figoli, New frontiers in sustainable membrane preparation: Cyrene™ as green bioderived solvent, *J. Membr. Sci.* 580 (2019) 224–234.
- [42] X. Dong, H.D. Shannon, I.C. Escobar, Investigation of PolarClean and gamma-valerolactone as solvents for polysulfone membrane fabrication, in: *Green Polymer Chemistry: New Products, Processes, and Applications*, American Chemical Society, 2018, pp. 385–403.
- [43] P.T. Anastas, J.C. Warner, *Green Chemistry: Theory and Practice*, Oxford University Press, New York, 1998.
- [44] A. Ivanković, A. Dronjić, A.M. Bevanda, S. Talić, Review of 12 principles of green chemistry in practice, *Int. J. Sustain. Green Energy* 6 (2017) 39–48.
- [45] K. Hackl, W. Kunz, Some aspects of green solvents, *Compt. Rendus Chem.* 21 (2018) 572–580.
- [46] H.N. Cheng, R.A. Gross, P.B. Smith, *Green Polymer Chemistry: Biobased Materials and Biocatalysis*, ACS Publications, Washington DC, 2015.
- [47] F. Pena-Pereira, M. Tobiszewski (Eds.), *The Application of Green Solvents in Separation Processes*, Elsevier, 2017.
- [48] A. Randová, L. Bartovská, P. Morávek, P. Matejka, M. Novotná, S. Matejková, E. Drioli, A. Figoli, M. Lanč, K. Friess, A fundamental study of the physicochemical properties of Rhodiasolv®Polarclean: a promising alternative to common and hazardous solvents, *J. Mol. Liq.* 224 (2016) 1163–1171.
- [49] N.T. Hassankiadeh, Z. Cui, J.H. Kim, D.W. Shin, S.Y. Lee, A. Sanguineti, V. Arcella, Y.M. Lee, E. Drioli, Microporous poly(vinylidene fluoride) hollow fiber membranes fabricated with PolarClean as water-soluble green diluent and additives, *J. Membr. Sci.* 479 (2015) 204–212.
- [50] T. Marino, E. Blasi, S. Tornaghi, E. Di Nicolò, A. Figoli, Polyethersulfone membranes prepared with Rhodiasolv®Polarclean as water soluble green solvent, *J. Membr. Sci.* 549 (2018) 192–204.
- [51] N. Evenepoel, S. Wen, M. Tilahun Tsehaye, B. van der Bruggen, Potential of DMSO as greener solvent for PES ultra- and nanofiltration membrane preparation, *J. Appl. Polym. Sci.* 135 (2018) 46494.
- [52] A. Akbari, R. Yegani, Study on the impact of polymer concentration and coagulation bath temperature on the porosity of polyethylene membranes fabricated via TIPS method, *J. Membr. Sep. Technol.* 1 (2012) 100–107.
- [53] B. Chakrabarty, A.K. Ghoshal, M.K. Purkait, Effect of molecular weight of PEG on membrane morphology and transport properties, *J. Membr. Sci.* 309 (2008) 209–221.
- [54] B. Chakrabarty, A.K. Ghoshal, M.K. Purkait, Preparation, characterization and performance studies of polysulfone membranes using PVP as an additive, *J. Membr. Sci.* 315 (2008) 36–47.
- [55] S.A. Al Malek, M.N. Abu Seman, D. Johnson, N. Hilal, Formation and characterization of polyethersulfone membranes using different concentrations of polyvinylpyrrolidone, *Desalination* 288 (2012) 31–39.
- [56] K.A. Gebru, C. Das, Effects of solubility parameter differences among PEG, PVP and CA on the preparation of ultrafiltration membranes: impacts of solvents and additives on morphology, permeability and fouling performances, *Chin. J. Chem. Eng.* 25 (2017) 911–923.
- [57] J.-F. Li, Z.-L. Xu, H. Yang, C.-P. Feng, J.-H. Shi, Hydrophilic microporous PES membranes prepared by PES/PEG/DMAc casting solutions, *J. Appl. Polym. Sci.* 107 (2008) 4100–4108.
- [58] H. Susanto, M. Ulbricht, Characteristics, performance and stability of polyethersulfone ultrafiltration membranes prepared by phase separation method using different macromolecular additives, *J. Membr. Sci.* 327 (2009) 125–135.
- [59] S.M. Mousavi, A. Zadhoush, Investigation of the relation between viscoelastic properties of polysulfone solutions, phase inversion process and membrane morphology: the effect of solvent power, *J. Membr. Sci.* 532 (2017) 47–57.
- [60] M. Amirilargani, E. Saljoughi, T. Mohammadi, M.R. Moghbeli, Effects of coagulation bath temperature and polyvinylpyrrolidone content on flat sheet asymmetric polyethersulfone membranes, *Polym. Eng. Sci.* 50 (2010) 885–893.
- [61] M. Amirilargani, T. Mohammadi, Synthesis and characterization of asymmetric polyethersulfone membranes: effects of concentration and polarity of nonsolvent additives on morphology and performance of the membranes, *Polym. Adv. Technol.* 22 (2011) 962–972.
- [62] M.-J. Han, S.-T. Nam, Thermodynamic and rheological variation in polysulfone solution by PVP and its effect in the preparation of phase inversion membrane, *J. Membr. Sci.* 202 (2002) 55–61.
- [63] A.F. Ismail, A.R. Hassan, Effect of additive contents on the performances and structural properties of asymmetric polyethersulfone (PES) nanofiltration membranes, *Separ. Purif. Technol.* 55 (2007) 98–109.
- [64] J.-H. Kim, K.-H. Lee, Effect of PEG additive on membrane formation by phase inversion, *J. Membr. Sci.* 138 (1998) 153–163.
- [65] E. Saljoughi, M. Amirilargani, T. Mohammadi, Effect of poly(vinyl pyrrolidone) concentration and coagulation bath temperature on the morphology, permeability, and thermal stability of asymmetric cellulose acetate membranes, *J. Appl. Polym. Sci.* 111 (2009) 2537–2544.

- [66] E. Saljoughi, M. Amirilargani, T. Mohammadi, Effect of PEG additive and coagulation bath temperature on the morphology, permeability and thermal/chemical stability of asymmetric CA membranes, *Desalination* 262 (2010) 72–78.
- [67] J. Peng, Y. Su, W. Chen, Q. Shi, Z. Jiang, Effects of coagulation bath temperature on the separation performance and antifouling property of poly(ether sulfone) ultrafiltration membranes, *Ind. Eng. Chem. Res.* 49 (2010) 4858–4864.
- [68] F.W. Altna, Phase Separation Phenomena in Cellulose Acetate Solutions in Relation to Asymmetric Membrane Formation, 1982.
- [69] M. Liu, Y.-M. Wei, Z.-L. Xu, R.-Q. Guo, L.-B. Zhao, Preparation and characterization of polyethersulfone microporous membrane via thermally induced phase separation with low critical solution temperature system, *J. Membr. Sci.* 437 (2013) 169–178.
- [70] P. van de Witte, P.J. Dijkstra, J.W.A. van den Berg, J. Feijen, Phase behavior of poly(lactides) in solvent-nonsolvent mixtures, *J. Polym. Sci. B Polym. Phys.* 34 (1996) 2553–2568.
- [71] K.-W. Lee, B.-K. Seo, S.-T. Nam, M.-J. Han, Trade-off between thermodynamic enhancement and kinetic hindrance during phase inversion in the preparation of polysulfone membranes, *Desalination* 159 (2003) 289–296.
- [72] S.H. Yoo, J.H. Kim, J.Y. Jho, J. Won, Y.S. Kang, Influence of the addition of PVP on the morphology of asymmetric polyimide phase inversion membranes: effect of PVP molecular weight, *J. Membr. Sci.* 236 (2004) 203–207.
- [73] S. Vidya, A. Vijayalakshmi, A. Nagendran, D. Mohan, Effect of additive concentration on cellulose acetate blend membranes-preparation, characterization and application studies, *Separ. Sci. Technol.* 43 (2008) 1933–1954.
- [74] E. Saljoughi, M. Sadrzadeh, T. Mohammadi, Effect of preparation variables on morphology and pure water permeation flux through asymmetric cellulose acetate membranes, *J. Membr. Sci.* 326 (2009) 627–634.
- [75] Merck, 2-Pyrrolidone safety data sheet. [http://www.merckmillipore.com/DE/de/product/msds/MDA\\_CHEM-807041?ReferrerURL=https%3A%2F%2Fwww.google.com%2F](http://www.merckmillipore.com/DE/de/product/msds/MDA_CHEM-807041?ReferrerURL=https%3A%2F%2Fwww.google.com%2F) accessed 10 November 2019.
- [76] Chemira GmbH, Agnique® AMD 3L. <https://blog.chemira.ch/agnique-amd-3l>, 2017 accessed 6 June 2019.
- [77] A.L. Harreus, R. Backes, J.-O. Eichler, R. Feuerhake, C. Jäkel, U. Mahn, R. Pinkos, R. Vogelsang, 2-Pyrrolidone, Wiley-VCH Verlag GmbH & Co. KGaA, Weinheim, 2005.
- [78] X. Tian, Z. Wang, S. Zhao, S. Li, J. Wang, S. Wang, The influence of the nonsolvent intrusion through the casting film bottom surface on the macrovoid formation, *J. Membr. Sci.* 464 (2014) 8–19.
- [79] O. Bertrand, P. Wilson, J.A. Burns, G.A. Bell, D.M. Haddleton, Cu(0)-mediated living radical polymerisation in dimethyl lactamide (DML); an unusual green solvent with limited environmental impact, *Polym. Chem.* 6 (2015) 8319–8324.
- [80] R.-C. Ruaan, T. Chang, D.-M. Wang, Selection criteria for solvent and coagulation medium in view of macrovoid formation in the wet phase inversion process, *J. Polym. Sci. B Polym. Phys.* 37 (1999) 1495–1502.
- [81] A. Ley, P. Altschuh, V. Thom, M. Selzer, B. Nestler, P. Vana, Characterization of a macro porous polymer membrane at micron-scale by Confocal-Laser-Scanning Microscopy and 3D image analysis, *Int. Symp. Prog. Membr. Sci. Technol.* 564 (2018) 543–551.
- [82] S. Budavari, The Merck Index an Encyclopedia of Chemicals, Drugs, and Biologicals, twelfth ed., Merck & Co. Inc., Whitehouse Station, 1996.
- [83] A. Piennig, in: fourth ed., in: M. Howe-Grant (Ed.), Kirk-Othmer Encyclopedia of Chemical Technology, vol. 10, John Wiley & Sons, New York, 1993, pp. 352–353. *Chemie Ingenieur Technik* (1995) vol. 67.
- [84] C.M. Hansen, Hansen Solubility Parameters: A User's Handbook, second ed., CRC Press, Boca Raton, 2007.
- [85] Thomas Schroeder, *Rheologie der Kunststoffe, Theorie und Praxis*, Carl Hanser Verlag GmbH & Co. KG, München, 2018.
- [86] L.J. Fetters, D.J. Lohse, D. Richter, T.A. Witten, A. Zirkel, Connection between polymer molecular weight, density, chain dimensions, and melt viscoelastic properties, *Macromolecules* 27 (1994) 4639–4647.
- [87] T. Osswald, N. Rudolph (Eds.), *Polymer Rheology*, first ed., Hanser, München, 2014.
- [88] G.C. Berry, T.G. Fox, *Adv. Polym. Sci.* 261–357.
- [89] H. Matsuyama, T. Maki, M. Teramoto, K. Kobayashi, Effect of PVP additive on porous polysulfone membrane formation by immersion precipitation method, *Separ. Sci. Technol.* 38 (2003) 3449–3458.
- [90] J. Barzin, B. Sadatnia, Theoretical phase diagram calculation and membrane morphology evaluation for water/solvent/polyethersulfone systems, *Polymer* 48 (2007) 1620–1631.
- [91] W.W.Y. Lau, M.D. Guiver, T. Matsuura, Phase separation in polysulfone/solvent/water and polyethersulfone/solvent/water systems, *J. Membr. Sci.* 59 (1991) 219–227.
- [92] G.R. Guillen, G.Z. Ramon, H.P. Kavehpour, R.B. Kaner, E.M.V. Hoek, Direct microscopic observation of membrane formation by nonsolvent induced phase separation, *J. Membr. Sci.* 431 (2013) 212–220.
- [93] C. Barth, M.C. Gonçalves, A.T.N. Pires, J. Roeder, B.A. Wolf, Asymmetric polysulfone and polyethersulfone membranes: effects of thermodynamic conditions during formation on their performance, *J. Membr. Sci.* 169 (2000) 287–299.
- [94] W.-L. Hung, D.-M. Wang, J.-Y. Lai, S.-C. Chou, On the initiation of macrovoids in polymeric membranes—effect of polymer chain entanglement, *J. Membr. Sci.* 505 (2016) 70–81.
- [95] V. Kaiser, C. Stropnik, Membranes from polysulfone/N, N-dimethylacetamide/water system; structure and water flux, *Acta Chim. Slov.* 47 (2000) 205–214.
- [96] D.-M. Wang, F.-C. Lin, T.-T. Wu, J.-Y. Lai, Formation mechanism of the macrovoids induced by surfactant additives, *J. Membr. Sci.* 142 (1998) 191–204.
- [97] Y. Zhou, D.-L. Xi, Effect of PVP additive on PVDF/TPU blend hollow membrane by phase inversion, *Iran. Polym. J. (Engl. Ed.)* (2007) 16. English Edition.
- [98] J. Barzin, B. Sadatnia, Correlation between macrovoid formation and the ternary phase diagram for polyethersulfone membranes prepared from two nearly similar solvents, *J. Membr. Sci.* 325 (2008) 92–97.
- [99] Y. Ma, F. Shi, J. Ma, M. Wu, J. Zhang, C. Gao, Effect of PEG additive on the morphology and performance of polysulfone ultrafiltration membranes, *Desalination* 272 (2011) 51–58.
- [100] Q.-Z. Zheng, P. Wang, Y.-N. Yang, Rheological and thermodynamic variation in polysulfone solution by PEG introduction and its effect on kinetics of membrane formation via phase-inversion process, *J. Membr. Sci.* 279 (2006) 230–237.
- [101] H. Matsuyama, M. Teramoto, T. Uesaka, M. Goto, F. Nakashio, Kinetics of droplet growth in the metastable region in cellulose acetate/acetone/nonsolvent system, *J. Membr. Sci.* 152 (1999) 227–234.
- [102] J.T. Tsai, Y.S. Su, D.M. Wang, J.L. Kuo, J.Y. Lai, A. Deratani, Retainment of pore connectivity in membranes prepared with vapor-induced phase separation, *J. Membr. Sci.* 362 (2010) 360–373.
- [103] H. Strathmann, K. Kock, P. Amar, R.W. Baker, The formation mechanism of asymmetric membranes, *Desalination* 16 (1975) 179–203.
- [104] J.S. Kang, Y.M. Lee, Effects of molecular weight of polyvinylpyrrolidone on precipitation kinetics during the formation of asymmetric polyacrylonitrile membrane, *J. Appl. Polym. Sci.* 85 (2002) 57–68.
- [105] C. Kahrs, M. Metzke, C. Fricke, J. Schwollenbach, Thermodynamic analysis of polymer solutions for the production of polymeric membranes, *J. Mol. Liq.* 291 (2019) 111351.
- [106] D.-y. Zuo, Y.-Y. Xu, W.-l. Xu, H.-t. Zou, The influence of PEG molecular weight on morphologies and properties of PVDF asymmetric membranes, *Chin. J. Polym. Sci.* 26 (2008) 405–414.
- [107] K.M. Persson, G. Capannelli, A. Bottino, G. Träg-dh, Porosity and protein adsorption of four polymeric microfiltration membranes, *Int. Symp. Prog. Membr. Sci. Technol.* 76 (1993) 61–71.
- [108] G. Yilmaz, H. Toiserkani, D.O. Demirkol, S. Sakarya, S. Timur, L. Torun, Y. Yagci, Polysulfone based amphiphilic graft copolymers by click chemistry as bioinert membranes, *Mater. Sci. Eng. C* 31 (2011) 1091–1097.

## Supplementary material

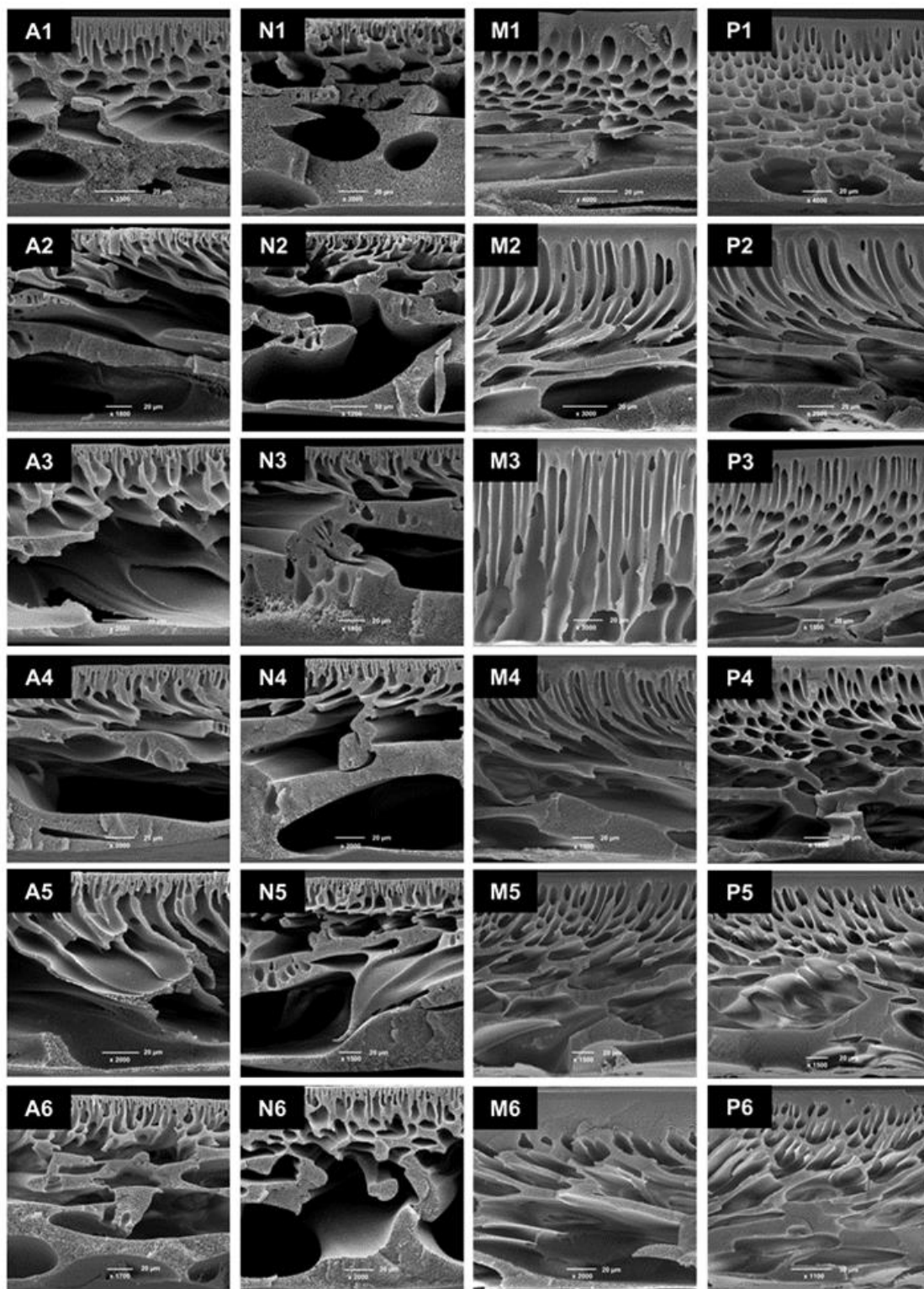
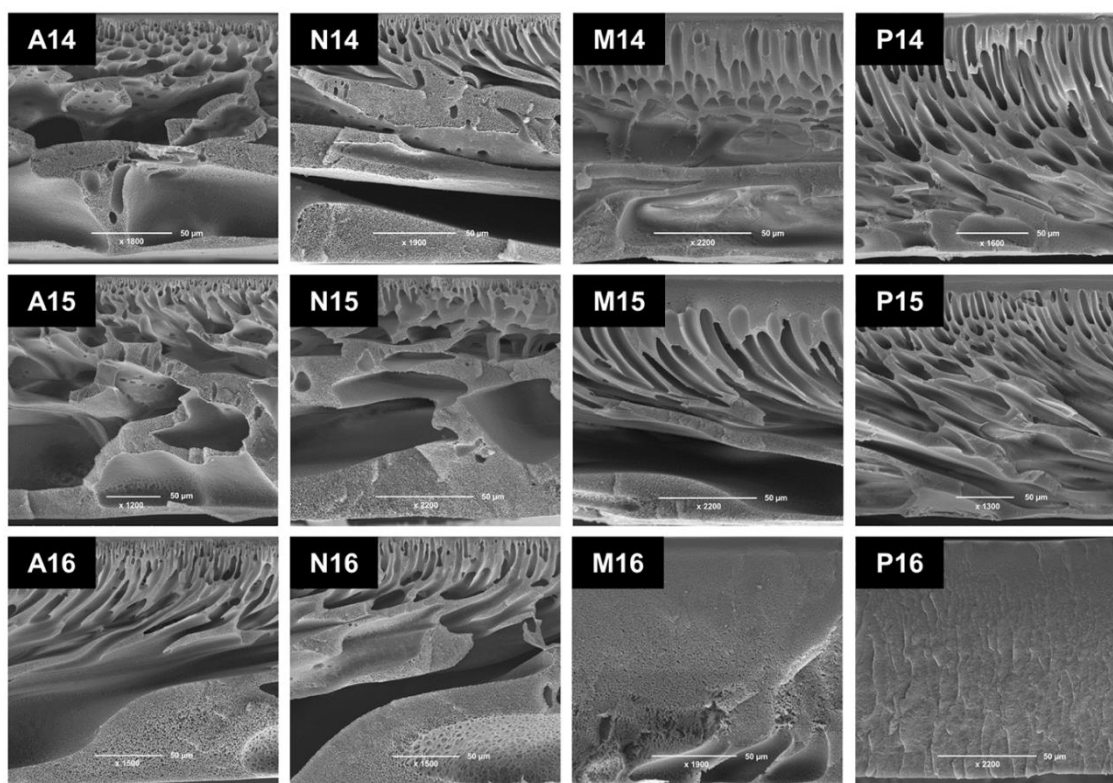


Figure S1 Scanning electron microscopy cross-section images of membrane prototypes prepared by immersion precipitation with different solvents and with different concentrations of PVP 50 kDa added to the casting solution (image recording potential of 12.5 kV).



**Figure S2** Scanning electron microscopy cross-section images of membrane prototypes prepared by immersion precipitation with different solvents and PVP of different molecular weights as additives (image recording potential of 12.5 kV).

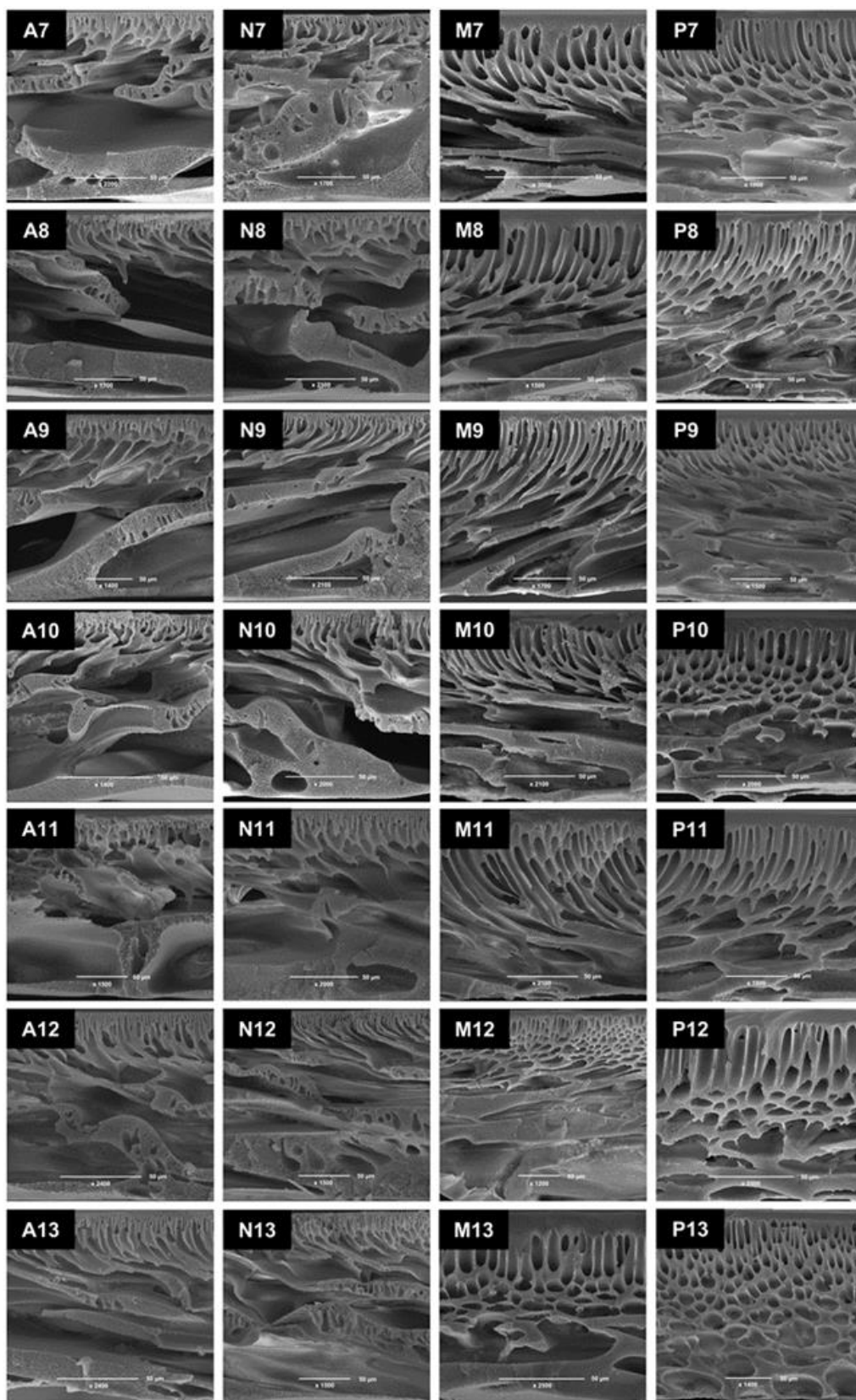
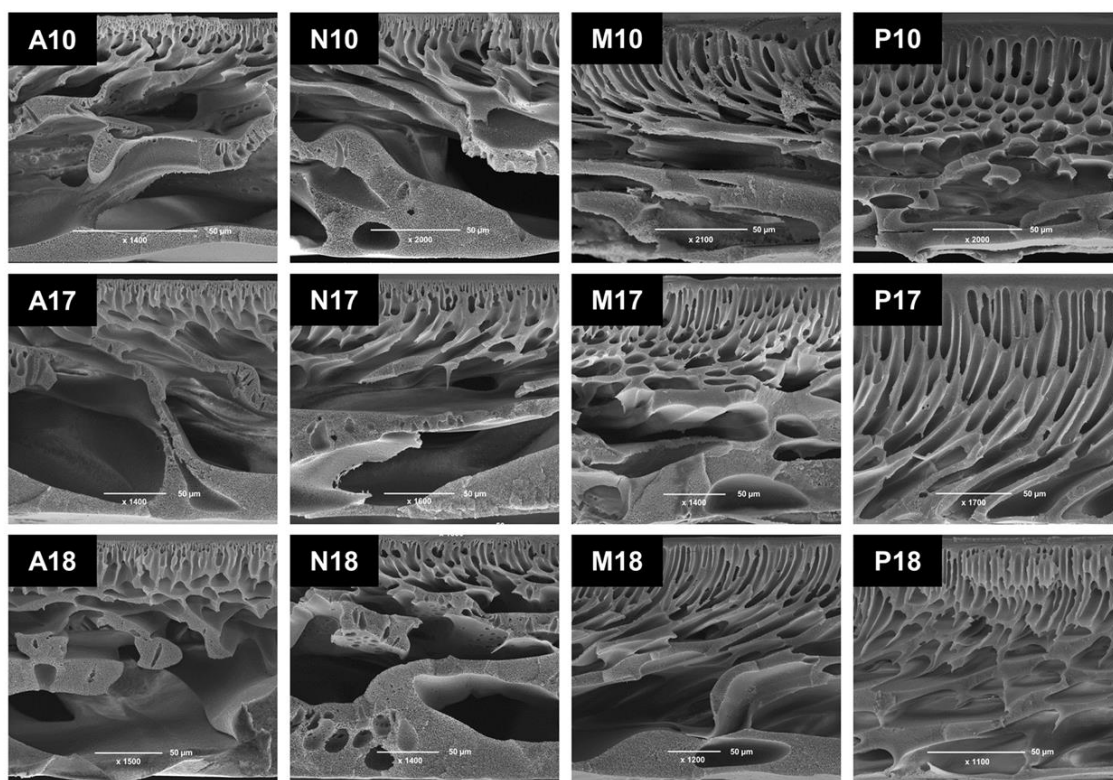


Figure S3 Scanning electron microscopy cross-section images of membrane prototypes prepared by immersion precipitation with different solvents and with different concentrations of PEG 400 Da added to the casting solution (image recording potential of 12.5 kV).





**Figure S4** Scanning electron microscopy cross-section images of membrane prototypes prepared by immersion precipitation with different solvents and PEG of different molecular weights as additives (image recording potential of 12.5 kV).

### 4.3 Influences of casting solution composition and precipitation conditions

#### Membrane fabrication variables

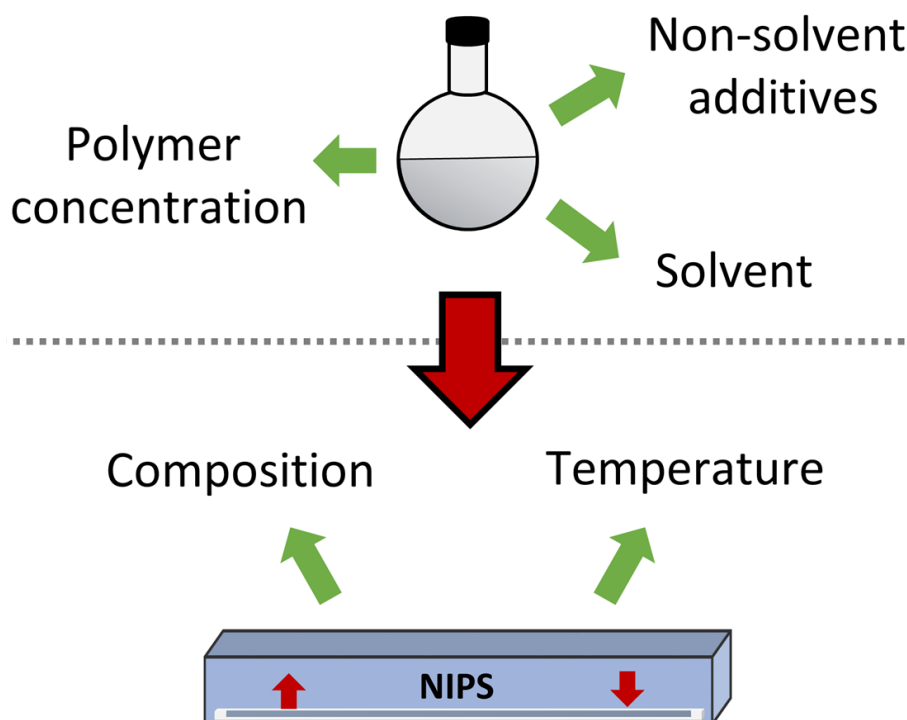


Figure 15 Graphical abstract of the publication "Influences of different preparation variables on membrane formation via non-solvent induced phase separation in dependence of the applied solvent system" [167].

As one aspect, the thermodynamic characterization of polymer solution systems was focused in this work. As another aspect, the influences of polymeric additive variations in different solvent systems on the resulting membrane characteristics was studied. However, the thermodynamics and kinetics cannot only be impacted by polymeric additives, but also by other components of the polymer solution system [31]. Furthermore, the precipitation conditions play a crucial role for membrane formation, since they can modify the kinetics of the membrane formation process and therefore the resulting membrane characteristics [164]. Since previous studies on these aspects only focused on conventional solvent systems like NMP and DMAc, this part of the thesis presents a comparative investigation of the effects of the known controlling factors, which have not already been focused in the previous section. These parameters include the polymer concentration and the addition of differently concentrated additives to the membrane dope solution, as well as the precipitation conditions in terms of the temperature and the composition of the non-solvent bath.

As already emphasized, the substitution of toxic solvents like NMP is highly desirable. However, as it has already been shown in the previous section, the impacts of variations in the preparation parameters during NIPS are not straightforward. It was found that the effects of the polymeric additive variations partially differed between conventional solvents and less harmful alternative solvents. This is why this part of the work demonstrates a comparative study between NMP as conventional solvent and 2P as ecologically more harmless alternative, each solvent representatively for the group of hazardous and alternative solvents.

Similar as in case of the study on the polymeric additives, systematic variations of the focused parameters were performed during membrane fabrication via NIPS. The dope solutions, which were prepared with variations in their composition, were characterized in terms of their viscosity for each of the two solvent systems. Furthermore, the miscibility gap of both systems was compared to each other. The subsequently prepared membrane prototypes were characterized in terms of structure and performance. Therefore, cross-section images of the membrane structures were recorded and analyzed. Furthermore, permeability and lysozyme retention measurements were performed and the results were compared among each other in dependence of the focused variables.

It was found that the general structure differs between the two solvent systems. While the NMP membranes exhibited a closed-cellular structure, 2P membranes featured a bicontinuous morphology. With respect to the location of the miscibility gap, this can be explained by different entry points into the heterogeneous region, which differ in dependence of the applied solvent and therefore cause dissimilar decomposition mechanisms. Furthermore, it could be shown that independently of the used solvent the presence of macrovoids can be controlled by the addition of either water, glycerol or acetic acid as non-solvents to the solution, by the application of lower precipitation temperatures, or by the addition of a weaker non-solvent to the precipitation bath.

In contrast to their similar effect on the structure, the performance data in this part reveal that the impact of the non-solvent concentration in the dope solution and the impact of the varying precipitation conditions differ between the two studied solvent systems. In this case, the only exception is the polymer concentration, which in both solvent systems caused a decline of the permeability and a simultaneous increase of the protein retention, when it was raised.

To conclude, this part of the thesis again proves that 2P is a suitable less harmful alternative for hazardous solvents like NMP. Furthermore, the effects of the missing relevant process parameters were identified to complement the impact of the variables studied in the previous section of this thesis. It could be shown that all studied variables in this section are suitable control parameters for modifying the properties of the resulting membranes. Therefore, this part presents a valuable contribution to the holistic picture, which should be created through this doctoral thesis.

## Influences of different preparation variables on polymeric membrane formation via nonsolvent induced phase separation

Catharina Kahrs <sup>1,2</sup> Thorben Gühlstorf,<sup>1,3</sup> Jan Schwellenbach<sup>1</sup>

<sup>1</sup>Sartorius Stedim Biotech GmbH, 37079, Goettingen, Germany

<sup>2</sup>Institute for Technical Chemistry, Leibniz University Hannover, 30167, Hannover, Germany

<sup>3</sup>Faculty of Computer Science and Engineering, Frankfurt University of Applied Sciences, 60318, Frankfurt/Main, Germany

Correspondence to: C. Kahrs (E-mail: catharina.kahrs@sartorius.com)

**ABSTRACT:** This work presents a comparative study on the formation of polyethersulfone ultrafiltration membranes via nonsolvent-induced phase separation (NIPS) in two different solvent systems. *N*-methyl-2-pyrrolidone was chosen as conventional solvent and 2-pyrrolidone as a greener alternative. The overall objective was to obtain a mechanistic clarification of the membrane formation process in dependence of the most important controlling parameters. By performing different series of experiments, it was possible to determine the differences between the two solvents regarding the effects of variations in nonsolvent additives, polymer concentration, and precipitation conditions. It was found that a raising concentration of several nonsolvents, the increase of the polymer concentration and changes in the precipitation conditions can suppress the formation of macrovoids, regardless of the applied solvent. In contrast, differences were observed with regard to the performance of the membrane prototypes. This study improves the understanding of membrane formation via NIPS and identifies the effects of different variables. It shows that the choice of the solvent is essential for the dominating formation mechanisms and therefore for the resulting membrane features. It also proves that green solvents can substitute hazardous solvents if the influencing variables are well-understood in order to control them for obtaining desired membrane properties. © 2019 Wiley Periodicals, Inc. *J. Appl. Polym. Sci.* **2019**, *137*, 48852.

**KEYWORDS:** membranes; microscopy; separation techniques

Received 12 September 2019; accepted 9 December 2019

DOI: 10.1002/app.48852

### INTRODUCTION

Nowadays, filtration with polymeric membranes is an important operation unit for various separation processes in different application fields.<sup>1–5</sup> Depending on the purpose of the filtration process as well as on the correspondingly valid regulations, the membranes have to fulfill a large variety of different demands.<sup>6–8</sup> However, in order to enable the control of the resulting membrane features for the obtainment of desired product properties, it is necessary to well understand the mechanisms of membrane formation and their influencing variables.<sup>9–11</sup>

One of the most frequently used materials for the production of polymeric membranes is polyethersulfone (PES).<sup>12,13</sup> In contrast to other commonly applied polymers such as polysulfone (PSf), cellulose acetate (CA), polyvinylidene fluoride (PVDF), or polyamide (PA), it stands out due to particular characteristics. The favoring properties of PES include a high glass transition temperature of 225 °C, a large chemical, mechanical, and thermal resistance, an excellent biocompatibility, as well as the potential application within a large pH

range.<sup>14–17</sup> Furthermore, the use of PES enables an easy fabrication of membranes with a large range of different pore sizes, which can be applied in several different modules and configurations.<sup>10</sup> This is the reason why PES membranes are used in several different fields such as gas separation, water processing, medical treatments, and biotechnology.<sup>17–19</sup> Specific applications include the sterilization of drinking water, the concentration of juices, hemodialysis, drug delivery, as well as the purification and concentration of biopharmaceutical drugs with a biological source.<sup>20–22</sup> In dependence of the respective application, a PES membrane has to possess certain features with respect to pore size, structure, and performance. In order to gain the desired membrane characteristics the production process of PES membranes has to be strictly controlled. The main controlling factors include the composition of the membrane dope solution on one hand, and the process parameters on the other hand.<sup>19</sup>

Nonsolvent induced phase separation (NIPS) is one of the most frequently applied approaches for PES membrane fabrication.<sup>23–25</sup> It enables the production of asymmetric structures with a large

Additional Supporting Information may be found in the online version of this article.

© 2019 Wiley Periodicals, Inc.

range of different characteristics, since the resulting membrane properties can be largely controlled if the formation process is well understood.<sup>26–29</sup> During NIPS a homogenous PES solution is immersed into a nonsolvent bath.<sup>11</sup> The diffusive exchange between the solvent from the polymer film and the nonsolvent from the precipitation bath changes the composition within the polymer film, till phase separation occurs.<sup>16,30,31</sup> Until solidification sets in different structure forming mechanisms occur, which result in different morphologies.<sup>16,32,33</sup> Apart from the composition path through the phase diagram, the occurring mechanism is ultimately dependent on the entry point into the miscibility gap.<sup>34,35</sup> When the system directly enters the metastable region binodal decomposition occurs, which induces the formation of a closed-cellular, an open-cellular or a nodular morphology. In contrast, spinodal decomposition occurs if the entry into the miscibility gap occurs directly through the critical point into the unstable region, leading to a bicontinuous structure.<sup>34,36,37</sup> If the structure is fixed immediately after the phase separation has occurred, one of the characteristic membrane morphologies can be observed (Figure 1).

In this special case, the actual membrane morphology is ultimately determined by the point of entry into the miscibility gap.<sup>36</sup> However, in most cases, different coarsening mechanisms take place after the solution has reached the two-phase region, so that an unambiguous conclusion from the final structure to the original decomposition mechanism is almost impossible.<sup>24,38</sup> Especially the formation of larger voids is caused by different coarsening effects.<sup>39–42</sup> In this context, the speed and duration of the diffusional solvent replacement from the polymer film determines if the membrane morphology is either sponge-like, finger-like, or a distinct mixture of both.<sup>43–45</sup> Consequently, the nascent structure formed after the onset of phase separation should not be regarded as static, since structure-forming effects can result from a steady mass transfer until solidification is reached.<sup>46</sup> If a critical viscosity is reached, the polymer solution turns into a gel state and solidifies, as coalescence and other coarsening mechanisms are no longer possible.<sup>47–50</sup>

Apart from the thermodynamics of the system, the phase separation process is dependent on the kinetics.<sup>51–53</sup> Especially the diffusion rate, which determines the exchange speed between solvent and nonsolvent, plays a critical role for the change of the solution composition and for the promotion of certain mechanisms such as

coalescence, consequently resulting in different morphologies.<sup>14,54–56</sup> This is why the formation of the final membrane structure can be manipulated by alterations in the temperature, which affects both, kinetics and thermodynamics of the system.<sup>57–60</sup> Furthermore, it can be influenced by variances in the viscosity through compositional changes, as the viscosity has a high impact on the diffusion rate.<sup>61,62</sup> Another important influencing factor is the choice of the solvent. Depending on the affinity between the solvent and the chosen nonsolvent, the diffusional exchange can be regulated.<sup>14,63,64</sup> Additionally, the solubility of the polymer in the solvent is a relevant factor. On one hand, it has been shown that the choice of the solvent strongly impacts the viscoelastic properties of the polymer solution, which consequently alters the diffusional processes during membrane formation.<sup>29,65</sup> On the other hand, the miscibility gap is strongly dependent on the solvent.<sup>17,29,65</sup> Therefore, the thermodynamic basis for the phase separation can be tuned by applying different solvents.

Currently, an emerging topic is the substitution of potentially hazardous solvents such as *N*-methyl-2-pyrrolidone (NMP) through greener alternatives.<sup>66–70</sup> The aim of this substitution is the minimization of the environmental impact and the simultaneous maximization of the membrane fabrication sustainability, in order to meet the criteria of green chemistry.<sup>71–74</sup> However, for the replacement of potentially harmful solvents, a profound understanding of the solvent impact is crucial. This is why a comparative investigation of several controlling variables was conducted by performing all experiments in a hazardous solvent and a potential greener alternative.

The listed mechanisms contributing to the structure formation of the membrane are part of controversial discussions.<sup>8,24,53,75</sup> Individual physicochemical phenomena can be described in isolation, however, quantitatively and qualitatively predictions of the final membrane structure are hardly possible due to the large number of factors and dependencies of the formation mechanisms.<sup>8,24,42,53,75,76</sup> Although qualitative correlations have been published in the literature, they are yet predominantly discussed on the basis of investigations limited to individual casting solution systems. This is why an empirical approach was chosen to qualitatively identify the influencing factors and their effects on membrane morphology and performance in order to obtain the currently missing holistic picture on membrane formation via NIPS. Through targeted variations of the casting solution

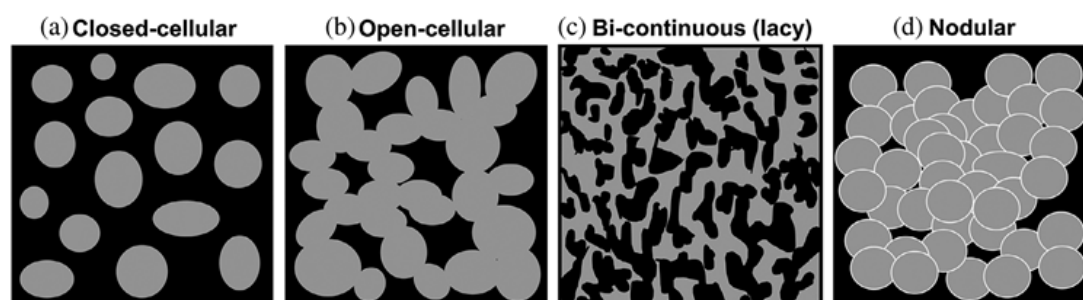


Figure 1. Schematic depiction of the four most common membrane morphologies developing during the phase separation of polymeric solutions.

composition and the manufacturing conditions, a broad database should be created by applying selected characterization methods to identify the physicochemical relationships of membrane formation. In this case, the polymer concentration, the concentration of three different nonsolvents, the precipitation bath composition and the precipitation temperature were varied to affect the thermodynamic and kinetic properties of the membrane formation process. Furthermore, NMP was applied as a good but hazardous solvent, whereas 2-pyrrolidone (2P) was used as a greener alternative with a poorer dissolving power for PES. All variations were conducted comparatively in both solvent systems. By doing so, a comprehensive picture should be established in order to broaden the understanding of the interplay between different factors, which affect the kinetics and the thermodynamics of the phase separation process. Consequently, this study shall enable an improved morphological control of the membrane structure. Furthermore, since the membrane performance is strongly related to the membrane morphology, this enhanced understanding of the membrane formation process shall facilitate to fulfill the requirements of regulators and users of membranes.

## EXPERIMENTAL

### Materials

The membrane-forming polymer PES was obtained from BASF (Ludwigshafen, Germany). In order to dissolve the polymer, NMP and 2P were purchased from Carl Roth (Karlsruhe, Germany). Polyvinylpyrrolidone (PVP) with a molecular weight of 1400 kDa was purchased from BASF (Ludwigshafen, Germany) and added to the casting solutions as a hydrophilic additive. Furthermore, reverse-osmosis (RO) water from Sartorius Stedim Biotech (Goettingen, Germany) was applied as a nonsolvent additive within the casting solution, as well as the phase separation inducing agent in the precipitation bath. Further applied nonsolvent additives were glycerol and acetic acid, both acquired from CG Chemicals (Laatzen, Germany). For membrane permeability and

retention measurements, a 20 mM potassium phosphate buffer (pH 7.0) was used. This buffer was prepared from stock solutions of di-potassium hydrogen phosphate and potassium dihydrogen phosphate, both acquired from Carl Roth (Karlsruhe, Germany). The alternative precipitating agent isopropanol was acquired from CG Chemicals (Laatzen, Germany).

### Preparation of Membrane Dope Solutions

Membrane dope solutions with varying solution compositions were prepared. Every single composition was fabricated twice, where the replicating formulations only differed in the type of the applied solvent. In addition to the impact of PES concentration variations from 15 to 20 wt%, the influence of different amounts of water, glycerol, and acetic acid as nonsolvent additives was investigated. In both solvents, the amount of glycerol was varied from 0 to 5 wt%, whereas the share of acetic acid ranged from 0 to 7.5 wt%. In contrast, the corresponding amounts of water within the casting solution were adapted to the solvent-dependent location of the miscibility gap. In case of NMP, the water concentration was varied between 7 and 9.25 wt %, whereas in case of 2P, the concentration ranged between 3.5 and 5.75 wt% water. The applied membrane preparation conditions are summarized in Table I. For a list with the exact compositions of each polymer solution refer to the supporting information (refer to Table S1 to Table S4).

For dope solution preparation, the water content of each raw material was determined. In case of the solid components PES and PVP, the determination was carried out with a moisture analyzer, while the water content of the liquids was analyzed via Karl-Fisher titration (KF Ti-Touch, Metrohm GmbH & Co. KG, Filderstadt, Germany). Under consideration of the water amount, which is introduced through the raw materials, the remaining volume of needed RO-water as well as the proportion of the respective solvent was poured into a 500 mL twin-neck flask (Carl Roth, Karlsruhe, Germany) and then preheated to 60 °C in a

**Table I.** Casting Solution Compositions for the Preparation of PES Membrane Prototypes With Variations in the Concentration of Acetic Acid Using NMP and 2P as Solvents for the Preparation of the Dope Solutions

Samples (N: NMP / P: 2P)	Variable		Fixed parameter [wt%]	Precipitation bath	Precipitation temperature
N1-N5 P1-P5	Water [wt%]	7.5, 8.0, 8.5, 9.0, 9.25 (N) 3.5, 4.0, 4.5, 5.0, 5.75 (P)	PES: 16.88 PVP: 0.84	Water	20 °C
N6-N8 P6-P8	PES [wt%]	15, 18, 20	PVP: 0.84 Water: 9.0 (N) Water: 5.0 (P)	Water	20 °C
N9-N11 P9-P11	Glycerol [wt%]	0.0, 2.5, 5.0, 7.5	PVP: 0.84 Water: 7.5 (N) Water: 3.5 (P)	Water	20 °C
N12-N15 P12-P15	Acetic acid [wt%]	0.0, 2.5, 5.0, 7.5	PVP: 0.84 Water: 7.5 (N) Water: 3.5 (P)	Water	20 °C
N1 P1	Precipitation conditions	water 20 °C, water 40 °C, IPA-water 20 °C	PES: 16.88 PVP: 0.84 Water: 7.5 (N) Water: 3.5 (P)	Water or IPA-water	20 °C or 40 °C

tempered oil bath. Subsequently, the solid components were added under constant stirring at 250 rpm using a RW20 overhead stirrer (IKA, Staufen, Germany). In all cases, PVP was added first and PES was added last. The dope solutions were stirred overnight to guarantee a homogenous mixing. Finally the polymer solutions were degassed in an oven for 2 h at 50 °C. For membrane preparation, the polymer solutions were cooled down to room temperature.

#### Cloud Point Experiments

Cloud point experiments were performed for both solvent systems with water as nonsolvent. The prepared polymer solutions were filled into a reactor (HWS, Mainz, Germany) and tempered to 20 °C. By application of an automatic titration system (Metrohm 900 Touch Control, Metrohm 846 Dosing Interface, Metrohm 807 Dosing Unit and Metrohm 800 Dosino, Metrohm GmbH and Co. KG, Filderstadt, Germany), 0.03 mL/min of water was added to the tempered solution under constant stirring at 300 rpm (IKA overhead stirrer RW20, IKA, Staufen, Germany). During this procedure, the transmitted light was measured as a function of time by a photometric sensor (Metrohm 662 Photometer, Metrohm GmbH and Co. KG, Filderstadt, Germany). The measurement was stopped when the light transmitted dropped below a value of 5%. Afterward the composition at the inflection point of the titration data was determined using Origin 2018b (Northampton, MA), since this point represents the cloud point of the solution. For each system solutions with different polymer concentrations were analyzed and used to extrapolate a binodal curve as described by Smolder *et al.*<sup>77</sup>:

$$\ln \frac{\phi_{NS}}{\phi_P} = b \cdot \ln \frac{\phi_S}{\phi_P} + a \quad (1)$$

where  $\phi_{NS}$  is the weight fraction of the nonsolvent,  $\phi_P$  is the weight fraction of the polymer,  $\phi_S$  is the weight fraction of the solvent, and  $a$  and  $b$  are the constants resulting from the equation of the linear regression from the experimentally determined cloud point data.

#### Dynamic Casting Solution Viscosity

By using a HAAKE falling ball viscometer (ThermoFisher Scientific, Waltham, MA), the dynamic viscosity of each dope solution was measured at 25 °C. The casting solution and an appropriate nickel-steel ball, with respect to the expected viscosity range, were filled into the inner pipe of the double-walled viscometer. The solution was tempered to 25 °C for at least 15 min by pumping preheated water through the outer casing of the viscometer using a thermostat (Lauda, Lauda-Koenigshofen, Germany). The actual measurement was conducted by stopping the falling time of the ball for a certain distance in a fivefold replication. Finally, the dynamic viscosity was calculated:

$$\eta = \frac{t_m \cdot (\rho_B - \rho_S) \cdot K}{1000} \quad (2)$$

where  $\eta$  is the dynamic viscosity (Pa·s),  $t_m$  is the average falling time of the ball (sec),  $\rho_B$  is the density of the ball ( $\text{g}/\text{cm}^3$ ),  $\rho_S$  is the density of the dope solution ( $\text{g}/\text{cm}^3$ ), and  $K$  is the ball constant ( $\text{mPa}\cdot\text{cm}^3\cdot\text{g}^{-1}$ ), which was determined during the calibration of the ball.

#### Preparation of Membrane Prototypes

The prepared dope solutions were used to fabricate different membrane prototypes. Using a casting rake with a defined thickness of 250  $\mu\text{m}$ , the polymer solutions were equally coated onto a glass support at room temperature. After coating, the casting film was immediately precipitated by immersing the support plate with the polymer film into a precipitation bath consisting of nonsolvent either tempered to 20 or 40 °C. The nonsolvent in the precipitation bath was either RO-water or isopropanol. The samples remained in the nonsolvent bath for five minutes to ensure a complete exchange of solvent and nonsolvent, resulting in a self-initiated detaching of the membrane from the glass support. Following this, the prototypes were soaked with RO-water containing 40 wt% glycerol in order to prevent a collapse of the pore network during storage. Subsequently, the membranes were placed into an oven for 10 min at 50 °C and finally stored in airtight sealed bags until further used.

#### Scanning Electron Microscopy

In preparation for scanning electron microscopy, a piece of the respective membrane prototype was cut and rinsed with RO-water for 15 min to extract the remaining glycerol from the membrane structure. In order to prepare membrane cross-sections, the wetted samples were immersed into liquid nitrogen and smoothly broken using a razor blade. The prepared cross-sections were placed into a sample holder, fixed with conductive silver and sputter coated with argon. Finally, the cross-section images were recorded at high vacuum and a voltage of 12.5 kV by using a FEI Quanta 200 ESEM (ThermoFisher Scientific).

#### Mechanical Stability

The bursting pressure is defined as the pressure, which is needed to rupture the membrane. It provides information about the mechanical stability of a sample. Since the bursting pressure strongly depends on the membrane thickness, it was normalized to the thickness of the respective sample. This is why the thickness of each sample was measured previous to the actual bursting pressure determination. Since both measurements were run in triplicates, three membrane samples with a diameter of 47 mm were cut from different locations distributed across the whole membrane sheet. Afterward, the thickness of the dry membrane blanks was measured by means of a thickness gauge (Hahn + Kolbe Group, Ludwigsburg, Germany). Following that, the same membrane samples were wetted with water and placed with the skin-side down into the bursting pressure device. The measurement was started by moving the plunger with the pressure supply directly onto the membrane blank. Subsequently, the pressure was continuously increased until the membrane cracked with an audible bang. The pressure gauge remained at the highest achieved pressure so that the bursting pressure could be read from the meter of the device.

#### Membrane Permeability

The membrane samples were tested in terms of their permeability. Therefore, a 20 mM phosphate buffer (pH 7.0) was prepared in RO-water. A sample of the respective membrane was cut out of the prepared membrane sheet with a diameter of 26 mm. Together with a fibrous support, it was then integrated into a 10 mL of stirring cell (Sartorius Stedim Biotech GmbH,

Goettingen, Germany). The cell was filled with the prepared buffer and was closed with a lid having a connection to the pressure supply. Subsequently, the filtration was started by applying a pressure of 1 bar to the stirring cell. After collecting 10 mL of the filtrate, which was filtered over the effective filter area of 3.8 cm<sup>2</sup> at a stirring speed of 1100 rpm (IKA color quid, IKA, Staufen, Germany), the pressure supply was switched off and the filtration time was recorded. Finally, the filtration time and the operation conditions were used to calculate the permeability:

$$J = \frac{V_F}{A_M \cdot t \cdot p} \quad (3)$$

where  $J$  is the membrane permeability (L·m<sup>-2</sup>·h<sup>-1</sup>·bar<sup>-1</sup>),  $V_F$  is the filtration volume (L),  $A_M$  is the effective filtration area of the membrane (m<sup>2</sup>),  $t$  is the filtration time (h), and  $p$  is the applied pressure (bar).

#### Protein Retention Capacity

Lysozyme (Lot. 235 225 855, Carl Roth, Karlsruhe, Germany) was applied as model protein for determining the protein retention capacity of the prepared membrane prototypes. Using the 20 mM potassium phosphate buffer (pH 7.0) as diluent, a 0.2 g/L protein suspension was prepared and homogenized on a magnetic stirrer (IKA color squid, IKA, Staufen, Germany) at 250 rpm, until the protein was completely dissolved. The stirring cells from the permeability determination were used again to test the protein retention on the same membrane samples. The remaining solution from the previous measurement was completely removed from the cell, and it was then filled again with 10 mL of the protein solution. The cells were closed and a pressure of 1 bar was applied to start the filtration, which was carried out on a magnetic stirrer (IKA color squid, IKA, Staufen, Germany) at a stirring rate of 1100 rpm in order to simulate

cross flow conditions. After collecting 5 mL of the filtrate in a designated test tube, the filtration was stopped and the filtration time was recorded. Before the cell was filled again with 5 mL of the pure buffer, it was rinsed twice with buffer to remove protein residues from the measuring module. In order to collect the protein solution remaining downstream of the membrane sample within the tubing of the measuring module, the filtration was continued at 1 bar and 1100 rpm until a final filtrate volume of 7.5 mL was reached. Ultimately, the protein concentrations in the initial solution and the collected filtrates were determined by UV spectrometry (Infinite<sup>®</sup> 200 PRO, Tecan, Maennedorf, Switzerland) at a wavelength of 280 nm. Based on the proportionality between the UV absorption of the protein and its concentration, the lysozyme retention was calculated by comparing the concentration in the initial solution to those of the respective filtrate:

$$R = 1 - \frac{c_P}{c_I} \cdot 100 \quad (4)$$

where  $R$  is the protein retention (%),  $c_P$  is the protein concentration in the filtrate (g/L), and  $c_I$  is the protein concentration in the initial solution (g/L).

## RESULTS AND DISCUSSION

### Location of the Miscibility Gap

Cloud point titrations have frequently been used to determine the miscibility gap of ternary polymeric systems.<sup>16,30,78</sup> It has previously been shown that the location of a system's heterogeneous region is dependent on the combination of polymer, solvent, and nonsolvent.<sup>23,79</sup> In order to gain information on the thermodynamic fundamentals of the PES/NMP/water and PES/2P/water systems applied in this study, cloud point experiments were performed for both systems and used to extrapolate the border between homogeneous and heterogeneous region. The experimental determined cloud points as well as the extrapolated binodal curve for each of the two systems are shown in the phase diagram depicted in Figure 2.

The system consisting of PES/NMP/water has been frequently studied in the past,<sup>17,48,80,81</sup> whereas the phase diagram for PES/2P/water has not been reported before. The experimentally determined phase boundaries for the NMP system in this study agree with the results, which have been previously reported in the referred literature. In comparison to the NMP system, the system with 2P has a larger miscibility gap. This indicates that the thermodynamic stability of 2P solutions is lower than the one of NMP solutions. Therefore, less water is needed to induce the liquid–liquid demixing in the 2P system, so that in contrast to PES solutions prepared with NMP the phase inversion occurs earlier. It was found that the amount of water, which can be added before phase separation occurs significantly differs between the two studied solvent systems. Based on the extrapolated cloud point data, the water amount, which is needed to induce phase separation in the NMP system lies between 10 and 20 wt%, where the exact amount depends on the polymer concentration. In contrast, for 2P the range lies between 3 and 8 wt%. As a consequence of the different thermodynamic stabilities, it can be expected that the resulting membrane structures differ in dependence of the solvent which is used.

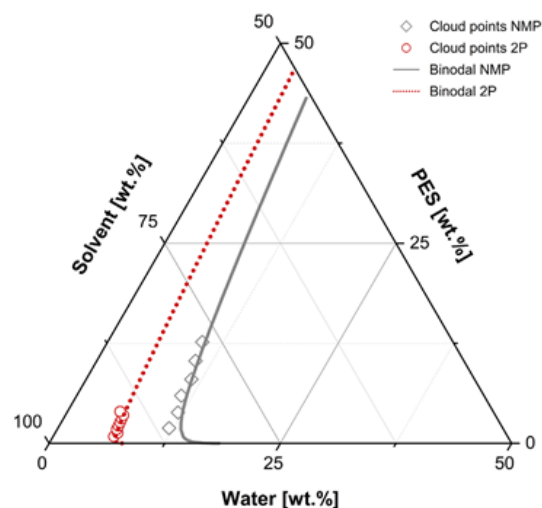


**Figure 2.** Experimental cloud point data and the thereof extrapolated binodal curves for PES/NMP/water and PES/2P/water at 20 °C. [Color figure can be viewed at wileyonlinelibrary.com]



### Control of the Morphological Structure by Nonsolvent Additives

It is reported in the literature that the addition of nonsolvent additives to the polymeric dope solution can suppress the formation of finger-like structures.<sup>10,35</sup> However, the knowledge of the impact of nonsolvent additives is limited. This is why in this study the influences of three selected nonsolvents with varying concentrations were investigated comparatively in two different solvent systems. More precisely, changing ratios of water, glycerol, and acetic acid were added to the membrane dope solutions prepared with NMP or 2P, respectively, and consequently their effects were examined with regard to the morphology of the resulting membrane prototypes. In order to study the morphology of the membranes, scanning electron microscopy was applied. Aiming to gain insights into the morphology of both, retentive layer and support layer, cross-section images of each membrane type were recorded.

Figure 3 shows the cross-sections of membranes, which were prepared with NMP as solvent and with different water concentrations in the dope solutions varying from 7.5 to 9.25 wt%. It could be observed that the increase of the water content within the polymer solution lead to a suppression of the finger-like structure, and thus conversely promoted the formation of a sponge-like structure. The more water was added, the more the number of finger-like cavities and macrovoids decreased. Furthermore, the appearance of the cavities within the membrane cross-section moved toward the bottom of the membrane when the water concentration was raised. At the same time, the size of the macrovoids was visibly reduced. This can be explained by the impacts of the water content on the thermodynamic and kinetic aspects of phase separation. In general, the addition of water to the polymer solution moves the starting point of the solution closer to the miscibility gap. If the position of the starting composition is already located close to the miscibility gap, only small amounts of the entering nonsolvent are required to initiate the phase separation across the entire casting solution profile. Therefore, the proportion of the polymer film, which remains stable, since its composition stays within the homogenous region after immersion into the precipitation bath, decreases when the distance to the miscibility gap is reduced. Furthermore, an increase of the nonsolvent concentration within the casting solution will not only reduce the proportion of the film, which remains stable, but also the residence time of the film composition within the homogenous region. As a consequence, the time until phase separation sets in is generally reduced.<sup>42</sup> This in turn suppresses locally delayed phase separation events and thus the formation of finger-like cavities or macrovoids toward the support-facing side of the membrane. This results from an immediate segregation followed by an earlier solidification of the structure across the whole cross-section of the polymer film. As a result, the occurrence of coarsening mechanisms, which lead to the formation of larger voids, is prevented.<sup>42</sup>

When glycerol or acetic acid were added as nonsolvent additives to the casting solution instead of water, similar effects on the morphology could be observed (Figure S1 in the Supporting Information). Although glycerol and acetic acid are in comparison to water less strong nonsolvents, the formation of voids was

prevented at similar concentration levels than in case of water. This can be explained by the fact that the use of nonsolvents other than water can lead to a larger heterogeneous region, as it has been observed for other ternary systems.<sup>58,82</sup> As a result, the distance between miscibility gap and composition of the starting solution decreases and less nonsolvent is needed to induce phase separation.<sup>83</sup>

The results, which could be found for the system with NMP were also observed for solutions with 2P as solvent (Figure 4). Similar to the previous case, the formation of macrovoids was suppressed when the amount of nonsolvent within the dope solution was increased. However, there are two main differences between the two solvent systems. On one hand, more water can be added to casting solutions prepared with NMP until the starting composition is close enough to the miscibility gap to cause a suppression of the finger-like morphology. This results from the fact that the miscibility gap for the 2P system is significantly larger than the one of NMP since NMP is a good solvent for PES, whereas 2P is a rather poor solvent.<sup>29</sup> On the other hand, it is striking that the morphology of the sponge-like structure in between the cavities is basically different if comparing the two solvent systems. In particular at high water concentrations, the morphology of the NMP membranes as shown in Figure 2 can rather be regarded as a closed-pore structure. In turn, this can be an indication for a binodal segregation. In contrast, Figure 3 reveals that 2P membranes rather have a lacy structure, which in turn indicates a spinodal segregation followed by a coarsening of the structure. The occurrence of spinodal decomposition in case of 2P can result from a combination of the reduced diffusional exchange and the relatively large overlap of the binodal and the spinodal at low polymer concentrations as it has been shown by Tsai *et al.* for a system with PSf dissolved in 2P.<sup>65</sup> Although the overlap of binodal and spinodal for PSf dissolved in NMP is also relatively large at lower polymer concentrations,<sup>17</sup> the higher diffusional exchange rate may result in a different precipitation path leading to a binodal decomposition.

The differences in the diffusional exchange rates at same solution compositions result from the different dynamic viscosities, which can be observed for the two different solvents. Furthermore, in case of both solvents, the viscosity of the casting solution increased with a rising water concentration (Figure 5).

This can be explained by an increased interaction between the solution components, which are caused by the formation of hydrogen bonds between the molecules.<sup>84,85</sup> The rising viscosity induces a slowdown of the diffusional exchange between solvent and nonsolvent. As a result, the nuclei of the polymer-poor phase grow with a reduced rate and the formation of macrovoids is suppressed. Ultimately, this effect results in the formation of tighter pore structures.<sup>27,50</sup> Furthermore, the results indicate that the viscosity of the solutions prepared with 2P are about ten times higher than the ones prepared with NMP. On one hand, this can result from the different abilities of the solvents to dissolve PES. It has been previously discussed in the literature that the solvent power has an impact on the viscoelasticity of the resulting solution.<sup>29</sup> On the other hand, 2P has a higher polarity in comparison to NMP.<sup>29</sup> Since the polarity of the solvent can

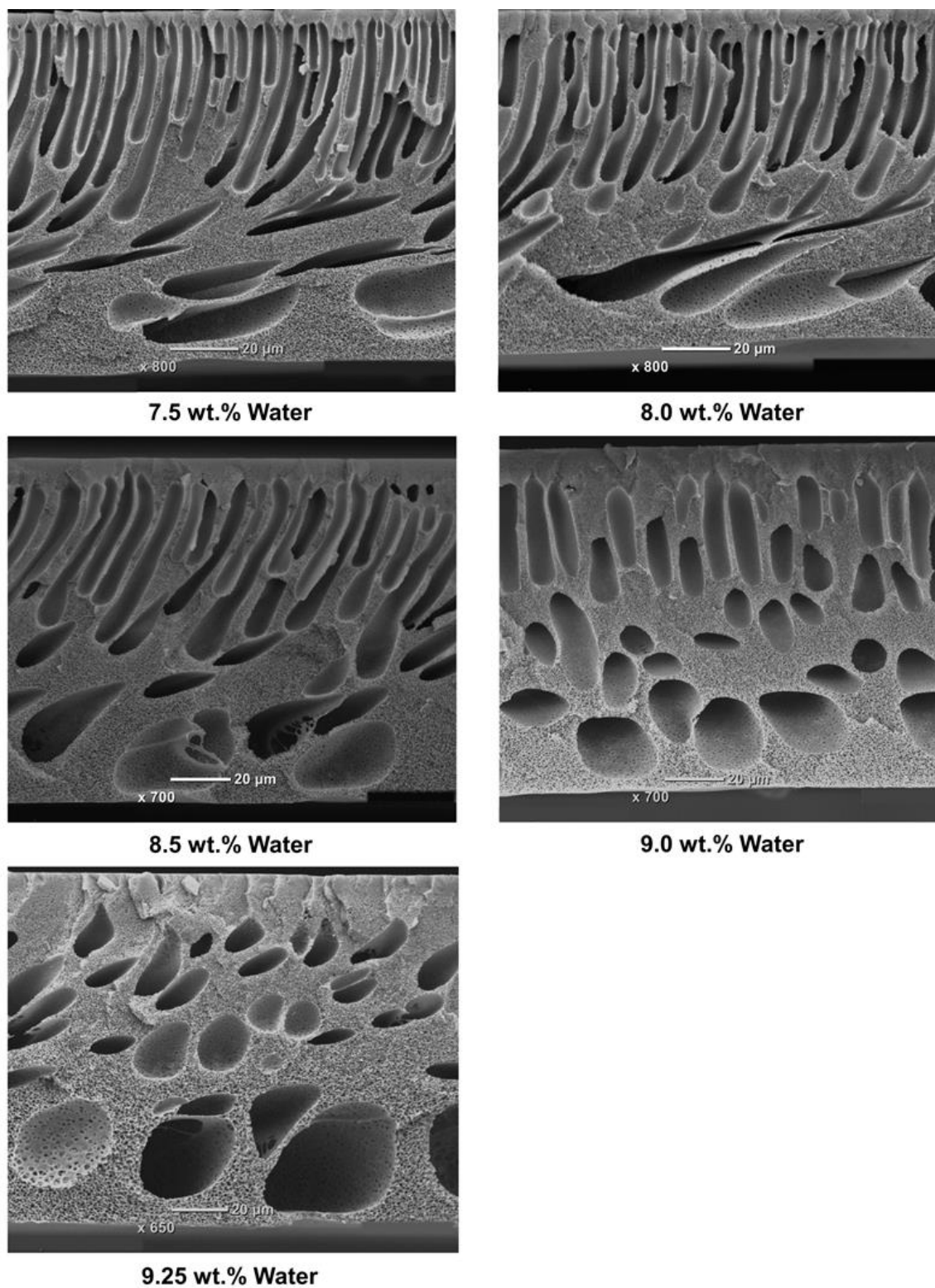


**Figure 3.** Scanning electron microscopy cross-section images of PES membranes prepared by immersion precipitation with water tempered to 20 °C as non-solvent, where the polymer dope solutions were prepared with 16.88 wt% PES, 0.84 wt% PVP, NMP as solvent and water concentrations varying from 7.5 to 9.25 wt% (image recording potential of 12.5 kV).

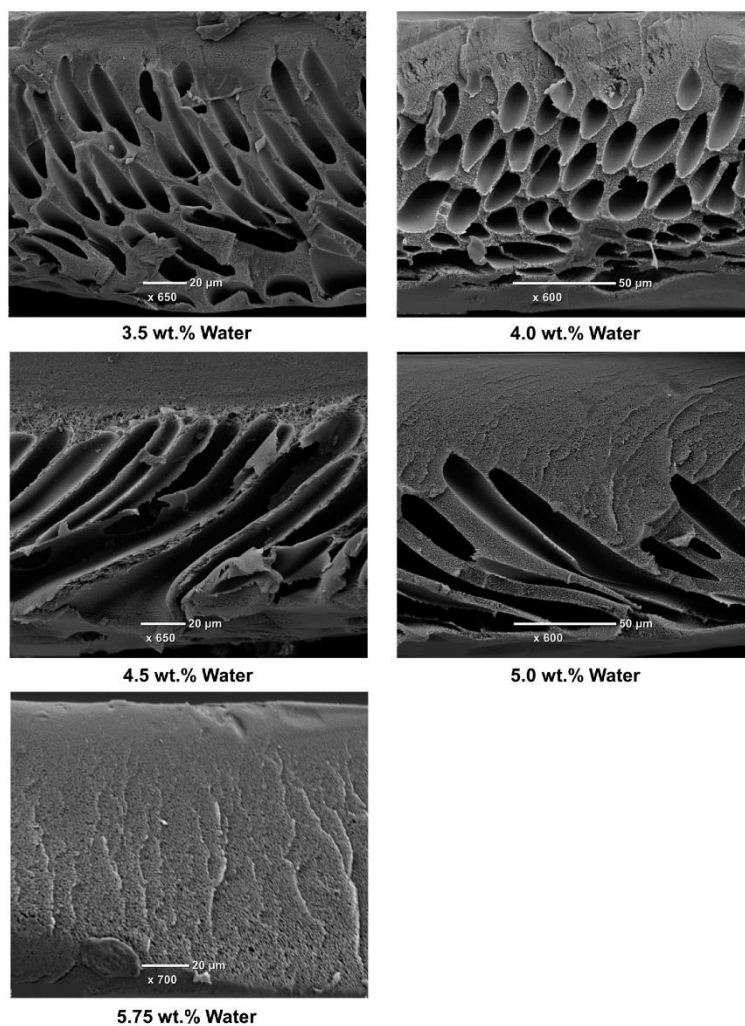


**Figure 4.** Scanning electron microscopy cross-section images of PES membranes prepared by immersion precipitation with water tempered to 20 °C as nonsolvent, where the polymer dope solutions were prepared with 16.88 wt% PES, 0.84 wt% PVP, 2P as a solvent and water concentrations varying from 3.5 to 5.75 wt% (image recording potential of 12.5 kV).

induces a slowdown of the diffusional exchange between solvent and nonsolvent. As a result, the nuclei of the polymer-poor phase grow with a reduced rate and the formation of macrovoids is suppressed. Ultimately, this effect results in the formation of tighter pore structures.<sup>27,50</sup> Furthermore, the results indicate that the viscosity of the solutions prepared with 2P are about ten times higher than the ones prepared with NMP. On one hand, this can result from the different abilities of the solvents to dissolve PES. It has been previously discussed in the literature that the solvent power has an impact on the viscoelasticity of the resulting solution.<sup>29</sup> On the other hand, 2P has a higher polarity in comparison to NMP.<sup>29</sup> Since the polarity of the solvent can

affect the conformation of the polymer, the polarity has an impact on the solution viscosity.<sup>86</sup> Furthermore, the large differences in the solution viscosity would explain why a complete suppression of the finger-like cavities can be achieved when using 2P as solvent. It can be observed in Figure 4 that at water concentrations close to the two phase region a complete sponge-like morphology was obtained in case of membranes prepared with 2P. In contrast, with NMP no complete suppression of macrovoids could be achieved, even if the composition was close to the two phase region (Figure 3). The presence of the finger-like morphology at even higher nonsolvent concentrations can result from the lower viscosity of the polymer solutions, which is not high

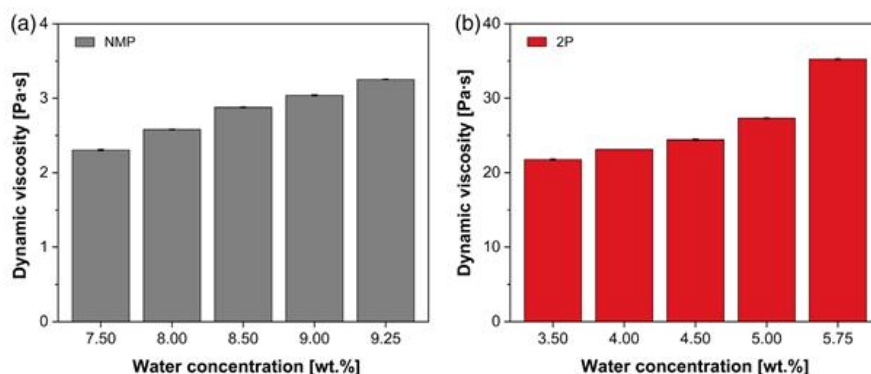


**Figure 5.** Average dynamic viscosity  $\pm$  standard deviation ( $n = 5$ ) in dependence of the water concentration for casting solutions containing 16.88 wt% PES, 0.84 wt% PVP and either NMP (a) or 2P (b) as solvent, determined at 25 °C with a falling ball viscometer. [Color figure can be viewed at wileyonlinelibrary.com]

side of the polymer film. As a result, the entry of nonsolvent into the polymer film is slowed down, which in turn extends the time between the onset of phase separation and solidification. In turn, the time for growth and coalescence of the polymer-poor nuclei is prolonged, which ultimately leads to the formation of coarser membrane structures.<sup>25</sup> However, when 2P was used as solvent, the pore size became progressively tighter in the area in which macrovoids are prevalent. This area is indicated by the red arrows in Figure 6. The observation confirms the theory that the growth of the voids is caused by diffusion of the solvent from the surrounding homogenous solution into a nucleus of the polymer-poor phase. As a result of this process, the polymer concentration in the surrounding polymer solution increases. Consequently, this leads to the formation of narrow pores around the voids since the time between onset of phase separation and solidification is reduced by the high polymer concentration. Overall, these results can be attributed to the macrovoid formation mechanism of Smolder and Reuvers, which describes the growth of the voids by solvent diffusion.<sup>42</sup>

Although this phenomenon is not visible for membranes prepared with NMP (Figure 6), it can be assumed that the same mechanism occurs during the structure formation of NMP membranes. However, the effect is not obvious such as in case of 2P due to the open-cellular structure.

#### Control of the Morphological Structure by Polymer Concentration

Another factor, which leads to a structural transition is the concentration of the membrane-forming polymer within the casting solution. In case of both solvents, a reduction of the macrovoids could be observed when the PES concentration was increased (Figure 7).

In case of NMP, the number and the size of macrovoids visibly decreased when the polymer concentration was raised from 15 to 20 wt%. A similar trend has previously been described for a system with dimethylacetamide (DMAc) and PSf. However, within the same study the investigation of PSf concentration variations with NMP as solvent did not show a clear effect, which is

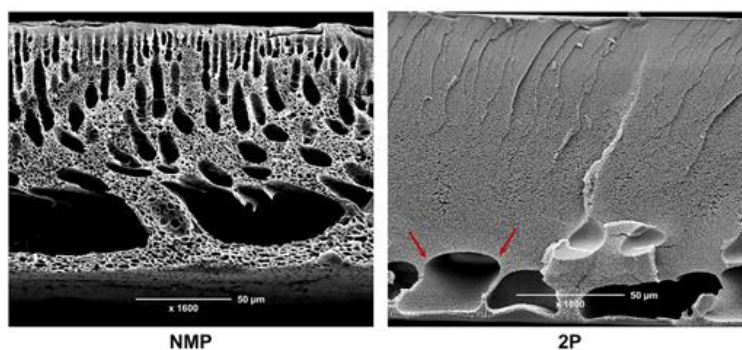


**Figure 6.** Scanning electron microscopy cross-section images focusing the pore size morphology around the macrovoids of PES membranes prepared by immersion precipitation with water tempered to 40 °C, where the dope solutions were prepared with 16.88 wt% PES, 0.84 wt% PVP, 2.5 wt% glycerol, and either 7.5 wt% water for NMP or 3.5 wt% water for 2P as solvent (image recording potential of 12.5 kV; the red arrows indicate a solvent diffusion-based pore size gradient in case of 2P). [Color figure can be viewed at wileyonlinelibrary.com]

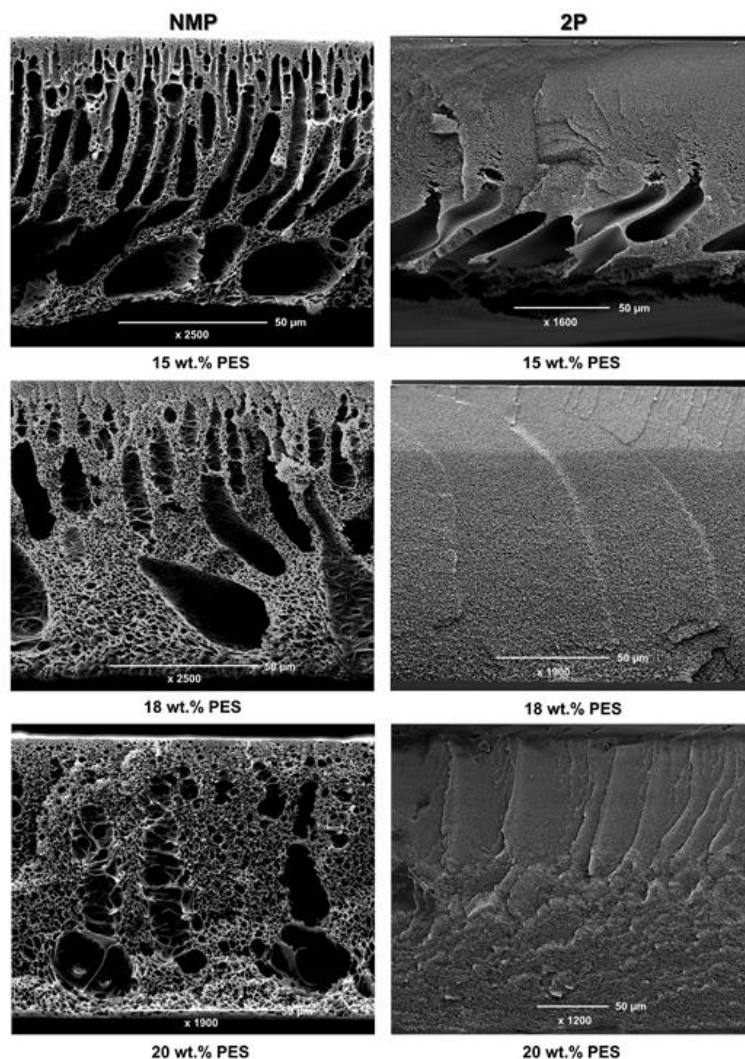


**Figure 7.** Scanning electron microscopy cross-section images of PES membranes prepared by immersion precipitation with water tempered to 20 °C as non-solvent, where the polymer dope solutions were prepared with PES concentrations varying from 15 to 20 wt%, 0.84 wt% PVP and either 9.0 wt% water in case of NMP or 5.0 wt% water in case of 2P as solvent (image recording potential of 12.5 kV).

contradictory to the observations made in this study.<sup>23</sup> In contrast, a complete sponge-like morphology could already be obtained at a medium PES concentration when 2P was applied as the solvent. If the PES concentration was further increased to 20 wt%, the sponge-like pore structure became even denser in comparison to the structure obtained with an intermediate concentration. Similar results for both, NMP and 2P, have been published for a system with PSf as the membrane-forming polymer.<sup>40</sup> The effects on the membrane morphology can be explained by the significant increase of the viscosity has been found for both solvent systems when the PES concentration was raised (Figure 8).

As a result of the enhanced viscosity, the growth of the nuclei, which are responsible for the development of the macrovoids, is hindered. This is caused by the slowdown of the diffusional exchange of solvent and nonsolvent as well as by the general decrease of the mass transfer processes during structure formation.<sup>39</sup>

Apart from the significant effect on the viscosity, it was found that an elevation of the polymer concentration increases the volume fraction of the polymer matrix. This can be derived from the results of the mechanical stability, which was determined by measurements of the bursting pressure. It was found that the

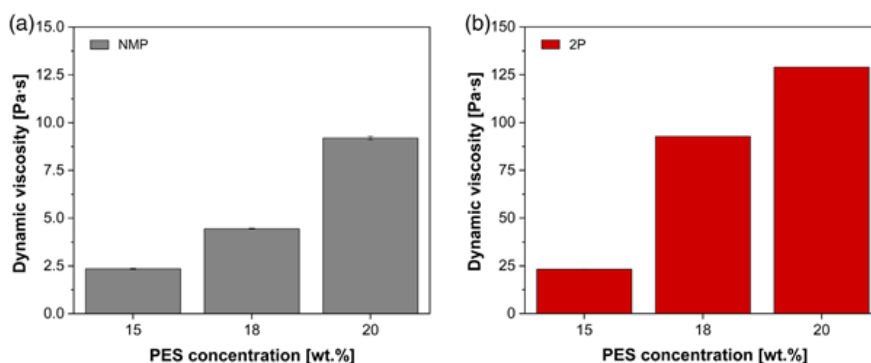


**Figure 8.** Average dynamic viscosity  $\pm$  standard deviation ( $n = 5$ ) in dependence of the PES concentration for casting solutions containing 0.84 wt% PVP and either 9.0 wt% water in case of NMP (a) or 5.0 wt% water in case of 2P (b) as solvent, determined at 25 °C with a falling ball viscometer. [Color figure can be viewed at [wileyonlinelibrary.com](http://wileyonlinelibrary.com)]

stability of the membranes increased when more PES was added to the membrane casting solution (Figure 9).

Based on the model concept described by Smolders and Reuvers, the observed results can be explained by two opposing effects, which are mainly responsible for the formation of the membrane morphology.<sup>42</sup> On one hand, the increasing polymer concentration at the interface between the polymer film and the precipitation bath provokes the formation of a dense skin layer, which is responsible for the selective separation of molecules. Consequently, this layer acts as an increased diffusion barrier at the air-facing side of the membrane. In turn, this increases the probability that the polymer solution in the lower part of the film remains stable after immersion into the precipitation bath. Therefore, the time until solidification is achieved is prolonged and the formation of finger-like structures is promoted. On the other hand, the phase diagrams of the two systems indicate that with an increase of polymer concentration within the casting solution a smaller amount of water is sufficient to induce phase separation

(Figure 2).<sup>29,88</sup> Therefore, it can be assumed that the precipitation process is proceeding quickly so that a locally delayed segregation and solidification is suppressed, resulting in a uniform sponge-like morphology. As it was found that the sponge-like morphology predominates when the polymer concentration is raised, it can be concluded that the second effect overcomes the first one when a certain polymer concentration is reached. A similar relationship between the precipitation rate and the resulting membrane morphology were reported by Smolder and Reuvers.<sup>42</sup> Their investigation of the precipitation rate in a CA/dioxane/water system showed that at a higher polymer content in the casting solution a higher amount of solvent in the precipitation is needed to induce the formation of finger-like structures. Since the share of solvent in the casting solution is reduced with an increase in the polymer concentration, less solvent can diffuse into the precipitation bath. Consequently, a macrovoid-free structure is favored when the polymer concentration is raised. The presence of less solvent in the precipitation bath is additionally enhanced through the decelerated diffusion rate resulting from

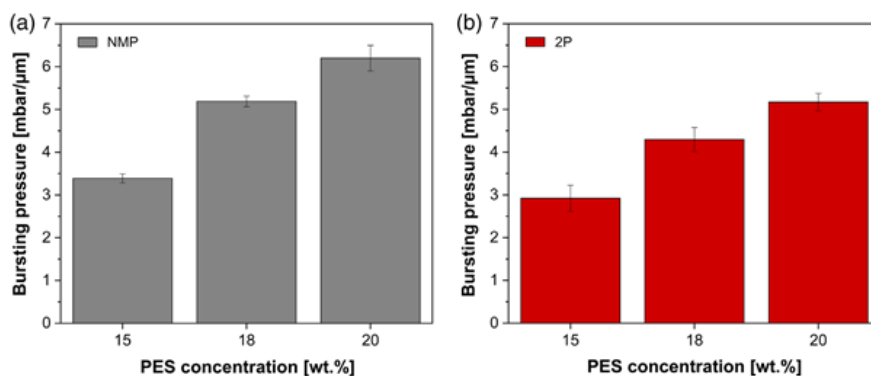


**Figure 9.** Average bursting pressure normalized to the membrane thickness  $\pm$  standard deviation ( $n = 3$ ) in dependence of the PES concentration for membrane prototypes prepared from casting solutions containing 0.84 wt% PVP and either 9.0 wt% water in case of NMP (a) or 5.0 wt% water in case of 2P (b) as solvent. [Color figure can be viewed at [wileyonlinelibrary.com](http://wileyonlinelibrary.com)]

an increase in viscosity at raised polymer amounts in the casting film. As the result, which were found by Smolders and Reuvers are similar to the observations of this study, the mechanisms caused by an increase of the polymer concentration seem to be independent of the polymer and solvent, which are used for membrane preparation.

#### Control of the Morphological Structure by Precipitation Conditions

Another possibility to control the membrane structure is the choice of the precipitation medium and the precipitation bath temperature, since both factors influence the mass transfer during the membrane formation process. In general, precipitants with a high affinity toward the solvent promote a fast phase separation process. In contrast, precipitants with a low affinity toward the solvent retard the time between onset of phase separation and solidification of the structure. In order to control the precipitation rate, alcohols have previously been used instead of pure water for ternary systems involving other solvents and membrane-forming polymers than those used in this study.<sup>56,58</sup> Furthermore, it has previously been shown that the precipitation temperature has an impact on the membrane properties due to its effects on both, the rate of diffusion and the viscosity of the casting film within the precipitation bath.<sup>10,26,57,59</sup> However, all these studies only focus on one distinct solvent system. Therefore, until now no comparative study has been conducted, which investigates the effect of the coagulation bath temperature in dependence of the applied solvents including distinct solvent affinities toward the polymer.

This is why the influence of the precipitation conditions on the membrane structure was investigated by comparing the temperature of pure RO-water as precipitant between 20 and 40 °C for membranes prepared with both, NMP and 2P. Additionally, isopropanol was used as an alternative precipitating agent for membrane preparation with both solvents, which exhibit different affinities toward the polymer and the nonsolvent, respectively. The structural results for each precipitation condition and each solvent, respectively, are depicted in Figure 10.

The cross-section images show that the membrane morphology is dependent on the precipitation temperature. When the temperature was set to 20 °C, the morphology was found to consist of a mixture of finger-like and sponge-like structures. While the region of finger-like structures dominated in case of NMP membranes, the sponge-like morphology was found to be prevalent when 2P was applied as a solvent. When the precipitation temperature was raised to 40 °C, however, it could be observed for both solvents that the number of the voids increased. This can be explained by the effect of the temperature on the viscosity of the polymer film. When the temperature of the precipitation bath is increased, the viscosity of the casting film decreases and at the same time the diffusion rate of solvent and nonsolvent increases.<sup>57</sup> As a consequence of the increased diffusion speed, the solvent uptake is enhanced, which results in an increased growth of the polymer-poor nuclei. This in turn promotes the development of voids and the formation of open pore structures.<sup>33</sup> In contrast, at low precipitation temperatures, the growth of the nuclei is inhibited. Consequently, new nuclei can form

below the already existing ones so that the formation of the macrovoids is suppressed. A similar effect has been reported for a system consisting of cellulose acetate in NMP.<sup>89</sup> Furthermore, it would be expected that the temperature has an effect on the thermodynamics of the system and therefore affects the resulting membrane structure. However, it has been previously shown, that the location of the miscibility gap for the systems examined in this study is not affected by the temperature at which phase separation takes place.<sup>88</sup> Therefore, the effect of the temperature on the thermodynamics and its influence on the membrane structure is negligible.

When isopropanol was used instead of water as the precipitating agent, it could be clearly observed that the turbidity of the polymer film increased significantly slower in case of isopropanol during the precipitation process. This results from the lower precipitation rate when using isopropanol, which consequently causes a delayed precipitation of the film.<sup>90</sup> Since the exchange of solvent and nonsolvent proceeds more equally across the entire polymer solution profile, the formation of nuclei occurs almost simultaneously at every position within the film. In turn, this reduces the probability for the development of finger-like structures. Although in case of both solvents, a few voids were still present in the substructure of the membrane cross-section, in comparison to the precipitation at the same temperature with water, the number and size of the voids visibly decreased for membranes prepared with isopropanol as nonsolvent.

#### Control of the Membrane Performance by Non-Solvent Additives

The addition of nonsolvent additives to the casting solution does not only influence the morphology of the membrane but it has also an impact on the membrane permeability and its retention capacity. In dependence of the applied solvent, two different behaviors could be observed if water was added to the polymer solution (Figure 11). When NMP was applied for the preparation of the casting solutions, the permeability increased with a raising amount of water within the solution. At a concentration of 8.5 wt % water, however, the permeability reached a maximum and started to decrease with a further addition of water to the casting solution. At the same time, the retention of lysozyme exhibited an inversely proportional behavior. It declined with raising water concentrations in the casting solution until an amount of 8.5 wt % water was reached, and started to increase again when the water share within the polymer solution was further increased. However, the changes in lysozyme retention are rather small. In contrast, the permeability of 2P membranes did not show a clear trend in dependence on the water concentration. It rather fluctuated around a value of 200 L/m<sup>2</sup>·h·bar. Nonetheless, a clear trend could be observed for the lysozyme retention as it continuously decreased when the water concentration was raised.

Similar trends for permeability and lysozyme retention were found when glycerol was applied as nonsolvent instead of water (Figure 12). In case of NMP, the permeability raised and exhibited a maximum at 2.5 wt% glycerol whereas it decreased when the concentration was further raised to 5 wt%. In contrast to the water variation, the retention slightly increased with an addition of 2.5 wt% glycerol and stayed at the same level when

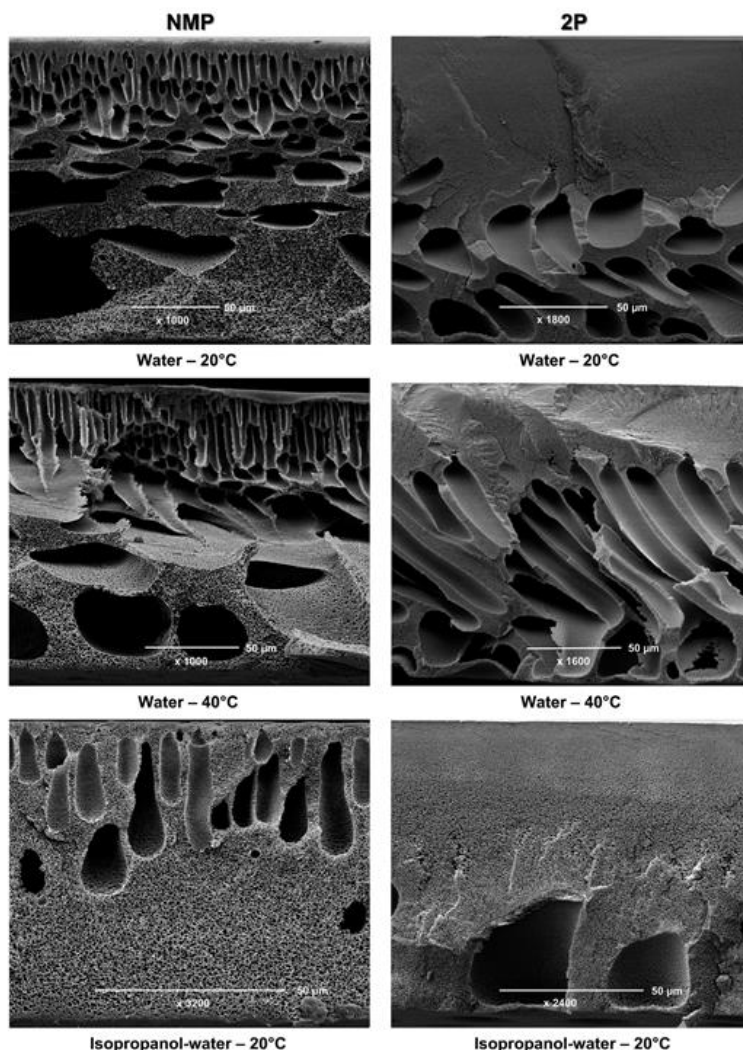


**Figure 10.** Scanning electron microscopy cross-section images of PES membranes prepared by immersion precipitation at different precipitation temperatures and with different precipitating agents, where the polymer dope solutions were prepared with 16.88 wt% PES, 0.84 wt% PVP, and either 7.5 wt% water in case of NMP or 3.5 wt% water in case of 2P as solvent (image recording potential of 12.5 kV).

the concentration was further increased 5 wt%. However, the effect on the retention again was rather small. In contrast, the permeability constantly raised with an increase of glycerol in the dope solution, if 2P was applied as solvent. At the same time, the lysozyme retention exhibited an inversely proportional behavior and declined with raising glycerol concentrations.

When 2P was applied as a solvent and acetic acid was added as nonsolvent to the polymer solution, the same observations were made as in case of the glycerol variations (Figure 12). While the permeability constantly increased with a raise in the acetic acid concentration, the lysozyme retention decreased inversely

proportional. In contrast, the behavior for NMP membranes was slightly different. The permeability continuously increased with a raising acetic acid concentration. However, the lysozyme retention was not significantly influenced by changes in the acetic acid amount since it constantly fluctuates around 20%.

The increase of the permeability, which was partially observed for the different variation series, has also been reported for other ternary systems. Chaturvedi *et al.* for instance varied the proportions of maleic acid (nonsolvent) and dimethylformamide (solvent), while the PES concentration was at the same time held at a constant level. They found that an increase of the maleic acid



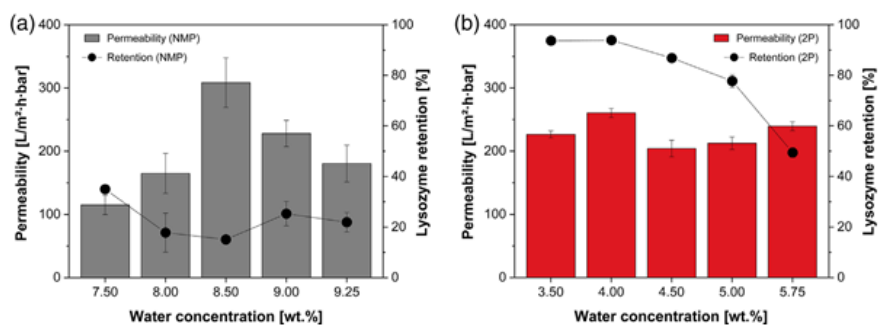


**Figure 11.** Average membrane permeability and respective lysozyme retention  $\pm$  standard deviation ( $n = 3$ ) in dependence of the water concentration for membrane prototypes prepared with water tempered to 20 °C from casting solutions containing 16.88 wt% PES, 0.84 wt% PVP and either NMP (a) or 2P (b) as solvent. [Color figure can be viewed at [wileyonlinelibrary.com](http://wileyonlinelibrary.com)]

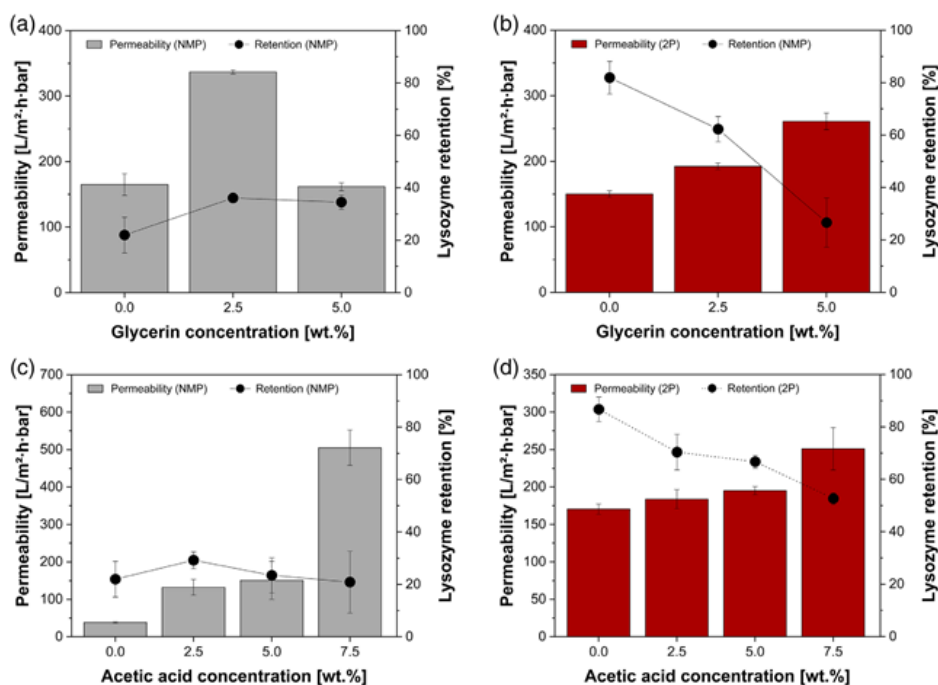


**Figure 12.** Average membrane permeability and the respective lysozyme retention  $\pm$  standard deviation ( $n = 3$ ) in dependence of the glycerol concentration for membrane prototypes prepared with water tempered to 20 °C from casting solutions containing 16.88 wt% PES, 0.84 wt% PVP, and either 7.5 wt% water in case of NMP (a) or 3.5 wt% water in case of 2P (b) as solvent, as well as in dependence of the acetic acid concentration for membrane prototypes prepared from casting solutions containing 16.88 wt% PES, 0.84 wt% PVP, and either 7.5 wt% water in case of NMP (c) or 3.5 wt% in case of 2P (d) as solvent. [Color figure can be viewed at [wileyonlinelibrary.com](http://wileyonlinelibrary.com)]

concentration results in an linearly raising water permeability.<sup>91</sup> On one hand, the morphology results indicate that the thickness of the sponge-like layer is strongly influenced by the content of nonsolvent within the casting solution (Figures 3 and 4). Since the sponge-like proportions significantly contribute to the flow resistance of the membrane, it also has an impact on the

permeability of the membrane. On the other hand, the impact of nonsolvents on the membrane performance can be explained by two contrary effects, which influence the position of the dope solution composition within the phase diagram, and therefore the entry point into the miscibility gap. The effects have been explained by Wijmans.<sup>92</sup> In general, the original position of the

dope solution is shifted toward the miscibility gap when the nonsolvent concentration is raised, while the polymer concentration at the same time remains constant. Consequently, the starting phase separation leads to lower polymer concentrations in the polymer-rich phase so that more open pore structures result from an increasing nonsolvent concentration in the dope solution. On the other hand, the exchange ratio of solvent and nonsolvent cannot be considered to remain constant. As the content of nonsolvent increases, the ratio between the inflow of nonsolvent and the export of solvent from the casting film declines, because with respect to the nonsolvent the chemical potential between the casting film and the precipitation bath is reduced. In comparison, a higher level of nonsolvent leads to an increased export of solvent from the casting film, which causes a steeper entry into the miscibility (refer to Figure S2 in the supporting information). This in turn would lead to an open pore structure since the entry into the heterogeneous region shifts toward lower polymer concentrations with a raising amount of nonsolvent.

Therefore, an overall prediction of the effect on the pore sizes caused by an increasing nonsolvent amount in the dope solution is not possible. However, for the 2P system the shift of the initial dope solution composition toward the miscibility gap seems to superimpose the influence on the mass transfer ratio. Similarly, the effect caused by the location of the initial composition also seems to superimpose the second effect in case of NMP, until a concentration of 8.5 wt% is reached. When the amount of nonsolvent is further increased, however, this effect is exceeded by the change in the mass transfer ratio. As a consequence, the permeability starts to decrease with a further raise of the nonsolvent amount in the dope solution. An exception for this behavior could be observed for the acetic acid variations in NMP. In this case, a continuous increase of the permeability was found when the acetic acid concentration was raised. As in case of 2P, this can be explained by the effect caused through the shift of the initial solution composition toward the miscibility gap, which overweighs the effect on the mass transfer ratio over the entire investigated concentration range. The different behavior in contrast to water and glycerol variations in NMP can be related to the strength of the nonsolvent. While water is a very strong nonsolvent for PES, acetic acid is a rather weak nonsolvent for this polymer. Therefore, the balance of both effects shifts in

dependence of the nonsolvent strength, which would explain the different trends.

#### Control of the Membrane Performance by Polymer Concentration

Apart from the mechanical stability of the membrane, the concentration of the membrane-forming polymer generally influences the overall porosity and the pore sizes of the membrane.<sup>7</sup> Therefore both, permeability and protein retention, are affected by changes in the polymer concentration. Independent of the solvent, which was applied, a decline of the permeability could be observed when the PES concentration was raised. Inversely proportional to the permeability, the lysozyme retention increased with a raising PES concentration (Figure 13).

A similar tendency has already been reported for polysulfone dissolved in a mixture of NMP and tetrahydrofuran,<sup>24</sup> which confirms that the influence of the polymer concentration is completely independent of the applied solvent. The impact of the polymer concentration on the membrane features can be explained on the basis of the phase diagram. If it is assumed that the influence of the polymer concentration on the mass transfer ratio of nonsolvent and solvent is negligible, the slope of the entry path into the heterogeneous region remains identical, regardless of the polymer concentration in the dope solution.<sup>92</sup> Therefore, the composition at the entry point into the miscibility gap is strongly influenced by the initial polymer concentration (refer to Figure S3 of the supporting information). If the initial composition is located at a higher polymer concentration, the proportion of solvent within the polymer-poor phase is reduced after onset of the phase separation. In turn, the nascent pore size after phase separation is significantly influenced. Due to the thermodynamic equilibrium between the two forming phases, the polymer-rich phase consequently consists of a higher polymer content. This in turn results in a higher amount of polymer within the membrane matrix and therefore in a decreased permeability on one hand, and an increased protein retention on the other hand.

#### Control of the Membrane Performance by Precipitation Conditions

It has been shown earlier that the membrane structure is visibly influenced by the precipitation conditions. Since membrane performance and structure are closely related to each other, the

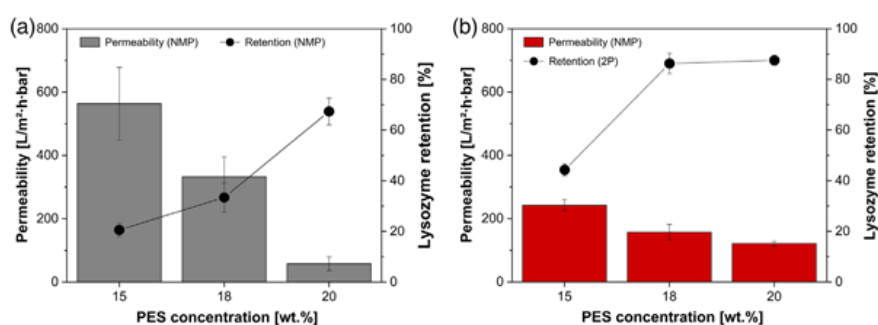


**Figure 13.** Average membrane permeability and the respective lysozyme retention  $\pm$  standard deviation ( $n = 3$ ) in dependence of the PES concentration for membrane prototypes prepared with water tempered to 20 °C from casting solutions additionally containing 0.84 wt% PVP and 9.0 wt% water in case of NMP (a) or 5.0 wt% water in case of 2P (b) as solvent. [Color figure can be viewed at [wileyonlinelibrary.com](http://wileyonlinelibrary.com)]

membrane performance was also found to be influenced by a change of the conditions within the precipitation bath. It could be observed that an increase of the water temperature in the precipitation bath resulted in a decreased permeability for membranes prepared with NMP, whereas the permeability of 2P membranes was significantly increased (Figure 14). When the water in the precipitation bath was displaced by isopropanol as a weaker nonsolvent for PES, the permeability increased independently of the solvent, which was applied. In all cases, the observed changes in the lysozyme retention were inversely proportional to the changes in the permeability.

In case of 2P, the observed permeability increase at a higher precipitation temperature can be explained by two effects. On one hand, the increasing temperature accelerates the diffusive exchange between nonsolvent and solvent. On the other hand, the viscosity of the casting solution film is reduced when the temperature is raised, which in turn also accelerates the mass transfer between casting film and precipitation bath.<sup>58</sup> Consequently, the nuclei of the polymer-poor phase can grow more quickly so that larger pores are formed. This in turn causes an increase in permeability and a simultaneous decrease in the lysozyme retention.

In case of NMP a similar effect would be expected, since due to the two described effects the pore structure is expected to become more open, which in turn increases the permeability. However, against the expectations it was found that the permeability slightly decreased when the precipitation temperature was raised, whereas the retention in contrast slightly increased. Although this increase cannot be regarded to be significant, the observed differences between the two solvent systems can be explained by the different formation mechanisms, which dominate depending on the respective solvent type. While the lacy structures of the 2P membranes indicate that these membranes were formed through a spinodal decomposition, which is followed by a subsequent coarsening of the structures, the structure of the NMP membranes can be described as a closed-cellular structure. On one hand, the combination of the increased water content and the higher precipitation temperature results in an instantaneous entry into the two-phase region when the casting film is immersed into

the precipitation bath. On the other hand, the enhanced diffusion rate caused by the temperature increase leads to a higher rate of coalescence with respect to the polymer-poor phase. Although this should lead to the formation of coarser structures, the overall number of pores decreases in case of NMP membranes due to the formation of a closed-cellular structure. As a result, the reduction of the pore quantity and the thereby caused decrease in permeable pores finally leads to a decline in permeability. Since the closed-cellular structure of the NMP membranes in comparison to the lacy structure of the 2P membranes affects the flow-retention ratio in an undesired manner, there was found hardly any difference between the lysozyme retention for NMP membranes prepared at 20 or 40 °C.

When isopropanol was used for membrane fabrication at a constant precipitation temperature of 20 °C instead of water, the permeability increased and the lysozyme retention decreased independent of the solvent which was used. As already mentioned, the addition of isopropanol leads to a reduction of the precipitation rate, which in turn prolongs the duration between the onset of phase separation and the solidification of the structure.<sup>90</sup> Consequently, this enables a coarsening of the pore structure through growth and coalescence, which in turn results in an increase in membrane permeability. The opposite effect of isopropanol precipitation in comparison to a change in the water bath temperature can be explained by the phase diagram of the respective system. It has been previously shown for a system of NMP, PES, and water that the temperature has no visible influence on the location of the two-phase region.<sup>88</sup> However, the addition of isopropanol results in a shift of the miscibility gap, as its addition expands the ternary system consisting of water, solvent and PES to a four component system consisting of water, isopropanol, the solvent, and PES. Since isopropanol is a weaker solvent than water, the size of the miscibility gap decreases, which has been shown for other systems such as for PES in DMSO.<sup>66,93</sup> As a result, the phase separation in isopropanol is introduced at a later point of time in comparison to a precipitation in pure water. Furthermore, the ratio of polymer, solvent and nonsolvent in the developing phases is affected, which can

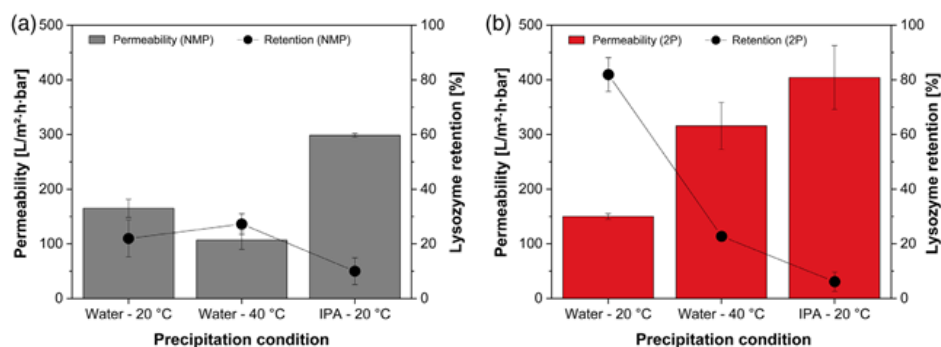


**Figure 14.** Average membrane permeability and the respective lysozyme retention  $\pm$  standard deviation ( $n = 3$ ) in dependence of the precipitation bath conditions for the fabrication of membrane prototypes prepared with different nonsolvents at different temperatures from casting solutions containing 16.88 wt % PES, 0.84 wt % PVP, and either 7.5 wt % water in case of NMP (a) or 3.5 wt % water in case of 2P (b) as solvent. [Color figure can be viewed at wileyonlinelibrary.com]

NMP, PES, and water that the temperature has no visible influence on the location of the two-phase region.<sup>88</sup> However, the addition of isopropanol results in a shift of the miscibility gap, as its addition expands the ternary system consisting of water, solvent and PES to a four component system consisting of water, isopropanol, the solvent, and PES. Since isopropanol is a weaker solvent than water, the size of the miscibility gap decreases, which has been shown for other systems such as for PES in DMSO.<sup>66,93</sup> As a result, the phase separation in isopropanol is introduced at a later point of time in comparison to a precipitation in pure water. Furthermore, the ratio of polymer, solvent and nonsolvent in the developing phases is affected, which can also contribute to the observed increase in permeability and the slight decrease in retention.

### CONCLUSIONS

This work presents a comparative study of PES membrane formation via nonsolvent induced phase separation between two different polymeric systems using NMP as conventional solvent and 2P as a greener alternative for the preparation of the dope solutions. In this context, a comprehensive investigation on the effects of the polymer concentration, the choice of the nonsolvent additives, and the precipitation conditions was performed in both solvent systems, NMP and 2P, respectively. The effects of the variables were studied with regard to the formation of the structure on one hand, and regarding the performance of the resulting membrane prototypes on the other hand. It was found that the general structure differs between the two solvent systems. NMP membranes exhibited a closed-cellular structure, while the membranes prepared with 2P exhibited a lacy structure. It was found that the addition of different nonsolvents to the dope solutions, the application of lower precipitation temperatures and weaker nonsolvents in the precipitation bath as well as the increase of the polymer concentration suppressed the formation of finger-like structures and macrovoids. The effects on the morphological cross-section features were observed for all systems, regardless of the solvent, which was applied for dope solution preparation. In contrast, the effects on the performance of the membranes partially differed in dependence on the applied solvent system. While an increasing polymer concentration in both solution systems resulted in a decrease in permeability and a simultaneous increase in retention, the influences of nonsolvent addition and precipitation conditions on membrane performance in certain cases differed in dependence of the applied solvent. It could be shown that the addition of nonsolvent to 2P dope solutions results in an increase in permeability and an inversely correlating decrease in the lysozyme retention. In contrast to these findings, with an exception of acetic acid variations, the prototypes produced with NMP exhibited a maximum at a certain nonsolvent concentration in the solution. When the concentration was further raised, the permeability started decreasing again. However, the lysozyme retention was also in all cases negatively proportional to the permeability, although the effects on the retention were less pronounced than in case of 2P membranes. Furthermore, the increase of the precipitation temperature resulted in an increased permeability and a decreased retention for 2P membranes, whereas the permeability declined and the retention increased when the same precipitation conditions were applied for membrane fabrication using NMP. The results can be explained by

the different thermodynamic and kinetic features of the formation process, which are strongly related to the applied solvent system. While the dominating formation mechanism in case of NMP is assumed to be a binodal decomposition, 2P membranes result from a spinodal decomposition. Both formation mechanisms are differently influenced by the tested variables and therefore result in different outcomes on structure and performance in dependence of the applied solvent.

### ACKNOWLEDGMENTS

The authors would like to thank Heike Hepprich from the Sartorius membrane development team for the recording of the SEM crosssection images, as well as Pascal Kircher for his assistance in performing the experiments.

### REFERENCES

- Baker, R. W. *Membrane Technology and Applications*; John Wiley & Sons, Ltd.: Chichester, UK, **2012**.
- Wickramasinghe, S. R.; Stump, E. D.; Grzenia, D. L.; Husson, S. M.; Pellegrino, J. J. *J. Membr. Sci.* **2010**, *365*, 160.
- Fang, X.; Li, J.; Li, X.; Sun, X.; Shen, J.; Han, W.; Wang, L. *J. Membr. Sci.* **2015**, *476*, 216.
- Eren, E.; Sarihan, A.; Eren, B.; Gumus, H.; Kocak, F. O. *J. Membr. Sci.* **2015**, *475*, 1.
- Tylkowski, B.; Tsibranska, I. J. *Chem. Technol. Metallur.* **2015**, *50*, 3.
- Strathmann, H. *Food Biotechnol.* **1990**, *4*, 253.
- Akbari, A.; Yegani, R. *J. Membrane Separation Technol.* **2012**, *1*, 100.
- Guillen, G. R.; Pan, Y.; Li, M.; Hoek, E. M. V. *Indus. Eng. Chem. Res.* **2011**, *50*, 3798.
- Strathmann, H.; Kock, K. *Desalination.* **1977**, *21*, 241.
- Li, J.-F.; Xu, Z.-L.; Yang, H. *Polym. Adv. Technol.* **2008**, *19*, 251.
- Wang, D.; Li, K.; Sourirajan, S.; Teo, W. K. *J. Appl. Polym. Sci.* **1993**, *50*, 1693.
- Barzin, J.; Madaeni, S. S.; Mirzadeh, H.; Mehrabzadeh, M. *J. Appl. Polym. Sci.* **2004**, *92*, 3804.
- Rahimpour, A.; Madaeni, S. S. *J. Membr. Sci.* **2007**, *305*, 299.
- Arthanareeswaran, G.; Starov, V. M. *Desalination.* **2011**, *267*, 57.
- Alenazi, N. A.; Hussein, M. A.; Alamry, K. A.; Asiri, A. M. *Desig. Monomers Polym.* **2017**, *20*, 532.
- Baik, K.-J.; Kim, J. Y.; Lee, H. K.; Kim, S. C. *J. Appl. Polym. Sci.* **1999**, *74*, 2113.
- Barzin, J.; Sadatnia, B. *Polymer.* **2007**, *48*, 1620.
- Yi, Z.; Zhu, L.-P.; Xu, Y.-Y.; Zhao, Y.-F.; Ma, X.-T.; Zhu, B.-K. *J. Membr. Sci.* **2010**, *365*, 25.
- Zhou, C.; Hou, Z.; Lu, X.; Liu, Z.; Bian, X.; Shi, L.; Li, L. *Indus. Eng. Chem. Res.* **2010**, *49*, 9988.
- Irfan, M.; Idris, A. *Mater. Sci. Eng. C.* **2015**, *56*, 574.

27. Saljoughi, E.; Sadrzadeh, M.; Mohammadi, T. *J. Membr. Sci.* **2009**, *326*, 627.
28. Barth, C.; Wolf, B. A. *Macromol. Chem. Phys.* **2000**, *201*, 365.
29. Mousavi, S. M.; Zadhoush, A. *J. Membr. Sci.* **2017**, *532*, 47.
30. Idris, A.; Man, Z.; Maulud, A. S.; Khan, M. S.; Suetsugu, S. *Membranes*. **2017**, *7*, 21.
31. Yu, L.; Yang, F.; Xiang, M. *RSC Adv.* **2014**, *4*, 42391.
32. Chakrabarty, B.; Ghoshal, A. K.; Purkait, M. K. *J. Membr. Sci.* **2008**, *315*, 36.
33. Xu, J.; Tang, Y.; Wang, Y.; Shan, B.; Yu, L.; Gao, C. *J. Membr. Sci.* **2014**, *455*, 121.
34. Ohlrogge, K.; Ebert, K., Eds. *Membranen: Grundlagen, Verfahren und industrielle Anwendungen*; Wiley-VCH Verlag GmbH & Co. KGaA: Weinheim, Germany, **2006**.
35. Xu, Z.-L.; Alsally Qusay, F. *J. Membr. Sci.* **2004**, *233*, 101.
36. Zeman, L. J.; Zydney, A. L. *Microfiltration and Ultrafiltration: Principles and Applications*; CRC Press: Boca Raton, FL, **1996**.
37. Drioli, E.; Giorno, L.; Fontananova, E., Eds. *Comprehensive Membrane Science and Engineering*. 2nd ed.; Oxford: Elsevier, **2017**.
38. Feng, Y.; Han, G.; Zhang, L.; Chen, S.-B.; Chung, T.-S.; Weber, M.; Staudt, C.; Maletzko, C. *Polymer*. **2016**, *99*, 72.
39. Guillen, G. R.; Ramon, G. Z.; Kavehpour, H. P.; Kaner, R. B.; Hoek, E. M. V. *J. Membr. Sci.* **2013**, *431*, 212.
40. Hung, W.-L.; Wang, D.-M.; Lai, J.-Y.; Chou, S.-C. *J. Membr. Sci.* **2016**, *505*, 70.
41. Strathmann, H.; Kock, K.; Amar, P.; Baker, R. W. *Desalination*. **1975**, *16*, 179.
42. Smolders, C. A.; Reuvers, A. J.; Boom, R. M.; Wienk, I. M. *J. Membr. Sci.* **1992**, *73*, 259.
43. Prakash, S. S.; Francis, L. F.; Scriven, L. E. *J. Membr. Sci.* **2006**, *283*, 328.
44. Wang, B.; Lai, Z. *J. Membr. Sci.* **2012**, *405-406*, 275.
45. Wang, D.-M.; Lin, F.-C.; Wu, T.-T.; Lai, J.-Y. *J. Membr. Sci.* **1998**, *142*, 191.
46. Kaiser, V.; Stropnik, C. *Acta Chimica Slovenica*. **2000**, *47*, 205.
47. Kim, J. Y.; Kim, Y. D.; Kanamori, T.; Lee, H. K.; Baik, K.-J.; Kim, S. C. *J. Appl. Polym. Sci.* **1999**, *71*, 431.
48. Li, S.-G.; van den Boomgaard, T.; Smolders, C. A.; Strathmann, H. *Macromolecules*. **1996**, *29*, 2053.
49. Wijmans, J. G.; Kant, J.; Mulder, M. H. V.; Smolders, C. A. *Polymer*. **1985**, *26*, 1539.
50. van de Witte, P.; Dijkstra, P. J.; van den Berg, J. W. A.; Feijen, J. *J. Membr. Sci.* **1996**, *117*, 1.
51. Lee, K.-W.; Seo, B.-K.; Nam, S.-T.; Han, M.-J. *Desalination*. **2003**, *159*, 289.
52. Wienk, I. M.; Boom, R. M.; Beerlage, M. A. M.; Bulte, A. M. W.; Smolders, C. A.; Strathmann, H. *J. Membr. Sci.* **1996**, *113*, 361.
53. Sadrzadeh, M.; Bhattacharjee, S. *J. Membr. Sci.* **2013**, *441*, 31.
54. Barton, B. F.; Reeve, J. L.; McHugh, A. J. *J. Polym. Sci. B.* **1997**, *35*, 569.
55. Kim, H. J.; Tyagi, R. K.; Fouda, A. E.; Jonasson, K. *J. Appl. Polym. Sci.* **1996**, *62*, 621.
56. Yong, S. K.; Hyo, J. K.; Un, Y. K. *J. Membr. Sci.* **1991**, *60*, 219.
57. Zheng, Q.-Z.; Wang, P.; Yang, Y.-N. *J. Membr. Sci.* **2006**, *279*, 230.
58. Mazinani, S.; Darvishmanesh, S.; Ehsanzadeh, A.; van der Bruggen, B. *J. Membr. Sci.* **2017**, *526*, 301.
59. Peng, J.; Su, Y.; Chen, W.; Shi, Q.; Jiang, Z. *Indus. Eng. Chem. Res.* **2010**, *49*, 4858.
60. Saljoughi, E.; Amirilargani, M.; Mohammadi, T. *J. Appl. Polym. Sci.* **2009**, *111*, 2537.
61. Zhang, Z.; An, Q.; Ji, Y.; Qian, J.; Gao, C. *Desalination*. **2010**, *260*, 43.
62. Kang, J. S.; Lee, Y. M. *J. Appl. Polym. Sci.* **2002**, *85*, 57.
63. Li, Z.; Ren, J.; Fane, A. G.; Li, D. F.; Wong, F.-S. *J. Membr. Sci.* **2006**, *279*, 601.
64. Ruaan, R.-C.; Chang, T.; Wang, D.-M. *J. Polym. Sci. B.* **1999**, *37*, 1495.
65. Tsai, J. T.; Su, Y. S.; Wang, D. M.; Kuo, J. L.; Lai, J. Y.; Deratani, A. *J. Membr. Sci.* **2010**, *362*, 360.
66. Evenepoel, N.; Wen, S.; Tilahun Tsehaye, M.; van der Bruggen, B. *J. Appl. Polym. Sci.* **2018**, *135*, 46494.
67. Wang, H. H.; Jung, J. T.; Kim, J. F.; Kim, S.; Drioli, E.; Lee, Y. M. *J. Membr. Sci.* **2019**, *574*, 44.
68. Dong, X.; Al-Jumaily, A.; Escobar, I. C. *Membranes*. **2018**, *8*, 23.
69. Figoli, A.; Marino, T.; Simone, S.; Di Nicolò, E.; Li, X.-M.; He, T.; Tornaghi, S.; Drioli, E. *Green Chem.* **2014**, *16*, 4034.
70. Marino, T.; Blasi, E.; Tornaghi, S.; Di Nicolò, E.; Figoli, A. *J. Membr. Sci.* **2018**, *549*, 192.
71. Rasool, M. A.; Vankelecom, I. F. J. *Green Chem.* **2019**, *21*, 1054.
72. Amelio, A.; Genduso, G.; Vreysen, S.; Luis, P.; van der Bruggen, B. *Green Chem.* **2014**, *16*, 3045.
73. Marino, T.; Galiano, F.; Molino, A.; Figoli, A. *J. Membr. Sci.* **2019**, *580*, 224.
74. Häckl, K.; Kunz, W. C. R. *Chim.* **2018**, *21*, 572.
75. Lalia, B. S.; Kochkodan, V.; Hashaikh, R.; Hilal, N. *Desalination*. **2013**, *326*, 77.
76. Young, T.-H.; Chen, L.-W. *Desalination*. **1995**, *103*, 233.
77. Boom, R. M.; van den Boomgaard, T.; van den Berg, J. W. A.; Smolders, C. A. *Polymer*. **1993**, *34*, 2348.
78. Xu, L.; Qiu, F. *Polymer*. **2014**, *55*, 6795.
79. Keshavarz, L.; Khansary, M. A.; Shirazian, S. *Polymer*. **2015**, *73*, 1.
80. Lau, W. W. Y.; Guiver, M. D.; Matsuura, T. *J. Membr. Sci.* **1991**, *59*, 219.
81. Zeman, L.; Tkacik, G. *J. Membr. Sci.* **1988**, *36*, 119.

82. Swinyard, B. T.; Barrie, J. A. *Br. Polym. J.* **1988**, *20*, 317.
83. Mansourizadeh, A.; Ismail, A. F. *J. Membr. Sci.* **2010**, *348*, 260.
84. Appaw, C.; Gilbert, R. D.; Khan, S. A.; Kadla, J. F. *Bio-macromolecules.* **2007**, *8*, 1541.
85. Lin, K.-Y.; Wang, D.-M.; Lai, J.-Y. *Macromolecules.* **2002**, *35*, 6697.
86. Xu, Z.; Tsai, H.; Wang, H.-L.; Cotlet, M. *J. Phys. Chem. B.* **2010**, *114*, 11746.
87. Wang, L. K.; Chen, J. P.; Hung, Y.-T.; Shamma, N. K., Eds. *Membrane and Desalination Technologies*; New York: Springer Science & Business Media, **2011**.
88. Kahrs, C.; Metze, M.; Fricke, C.; Schwellenbach, J. *J. Mol. Liq.* **2019**, *291*, 111351.
89. Saljoughi, E.; Amirilargani, M.; Mohammadi, T. *Desalination.* **2010**, *262*, 72.
90. Moradihamedani, P.; Ibrahim, N. A.; Yunus, W. M. Z. W.; Yusof, N. A. *Polym. Eng. Sci.* **2014**, *54*, 1686.
91. Chaturvedi, B. K.; Ghosh, A. K.; Ramachandran, V.; Trivedi, M. K.; Hanra, M. S.; Misra, B. M. *Desalination.* **2001**, *133*, 31.
92. Wijmans, H. *Synthetic Membranes: On the mechanisms of formation of membranes and the concentration polarization phenomenon in ultrafiltration*. Dissertation: Enschede, **1984**.
93. Lakshmi, D. S.; Figoli, A.; Buonomenna, M. G.; Golemme, G.; Drioli, E. *Adv. Polym. Technol.* **2012**, *31*, 231.

## SUPPORTING INFORMATION

### **Influences of different preparation variables on polymeric membrane formation via non-solvent induced phase separation**

Catharina Kahrs <sup>a,b</sup>, Thorben Gühlstorf <sup>a,c</sup>, Jan Schwellenbach <sup>a</sup>

<sup>a</sup> Sartorius Stedim Biotech GmbH, 37079 Goettingen, Germany

<sup>b</sup> Leibniz University Hannover, Institute for Technical Chemistry, 30167 Hannover, Germany

<sup>c</sup> Frankfurt University of Applied Sciences, Faculty of Computer Science and Engineering, 60318 Frankfurt/Main, Germany

Correspondence to: Catharina Kahrs (E-mail: [catharina.kahrs@sartorius.com](mailto:catharina.kahrs@sartorius.com))

**Table S1 Casting solution compositions for the preparation of PES membrane prototypes with variations in the concentration of water using NMP and 2P as solvents for the preparation of the dope solutions.**

Water variation	Components [wt.%]			
	PES	PVP (9 kDa)	Water	Solvent
<b>NMP</b>				
N1	16.88	0.84	7.5	74.78
N2	16.88	0.84	8.0	74.28
N3	16.88	0.84	8.5	73.78
N4	16.88	0.84	9.0	73.28
N5	16.88	0.84	9.25	72.53
<b>2P</b>				
P1	16.88	0.84	3.5	78.78
P2	16.88	0.84	4.0	78.28
P3	16.88	0.84	4.5	77.78
P4	16.88	0.84	5.0	77.28
P5	16.88	0.84	5.75	76.53

**Table S2 Casting solution compositions for the preparation of PES membrane prototypes with variations in the concentration of PES using NMP and 2P as solvents for the preparation of the dope solutions.**

PES variation	Components [wt.%]			
	PES	PVP (1400 kDa)	Water	Solvent
<b>NMP</b>				
N6	15	0.84	9.0	75.16
N7	18	0.84	9.0	72.16
N8	20	0.84	9.0	70.16
<b>2P</b>				
P6	15	0.84	5.0	79.16
P7	18	0.84	5.0	76.16
P8	20	0.84	5.0	74.16



**Table S3 Casting solution compositions for the preparation of PES membrane prototypes with variations in the concentration of glycerol using NMP and 2P as solvents for the preparation of the dope solutions.**

Glycerol variation	Components [wt.%]				
	PES	PVP (1400 kDa)	Glycerol	Water	Solvent
<b>NMP</b>					
N9	16.88	0.84	0.0	7.5	74.78
N10	16.88	0.84	2.5	7.5	72.28
N11	16.88	0.84	5.0	7.5	69.78
<b>2P</b>					
P9	16.88	0.84	0.0	3.5	78.78
P10	16.88	0.84	2.5	3.5	76.28
P11	16.88	0.84	5.0	3.5	73.78

**Table S4 Casting solution compositions for the preparation of PES membrane prototypes with variations in the concentration of acetic acid using NMP and 2P as solvents for the preparation of the dope solutions.**

Acetic acid variation	Components [wt.%]				
	PES	PVP (1400 kDa)	Acetic acid	Water	Solvent
<b>NMP</b>					
N12	16.88	0.84	0.0	7.5	74.78
N13	16.88	0.84	2.5	7.5	72.28
N14	16.88	0.84	5.0	7.5	69.78
N15	16.88	0.84	7.5	7.5	67.28
<b>2P</b>					
P12	16.88	0.84	0.0	3.5	78.78
P13	16.88	0.84	2.5	3.5	76.28
P14	16.88	0.84	5.0	3.5	73.78
P15	16.88	0.84	7.5	3.5	71.28

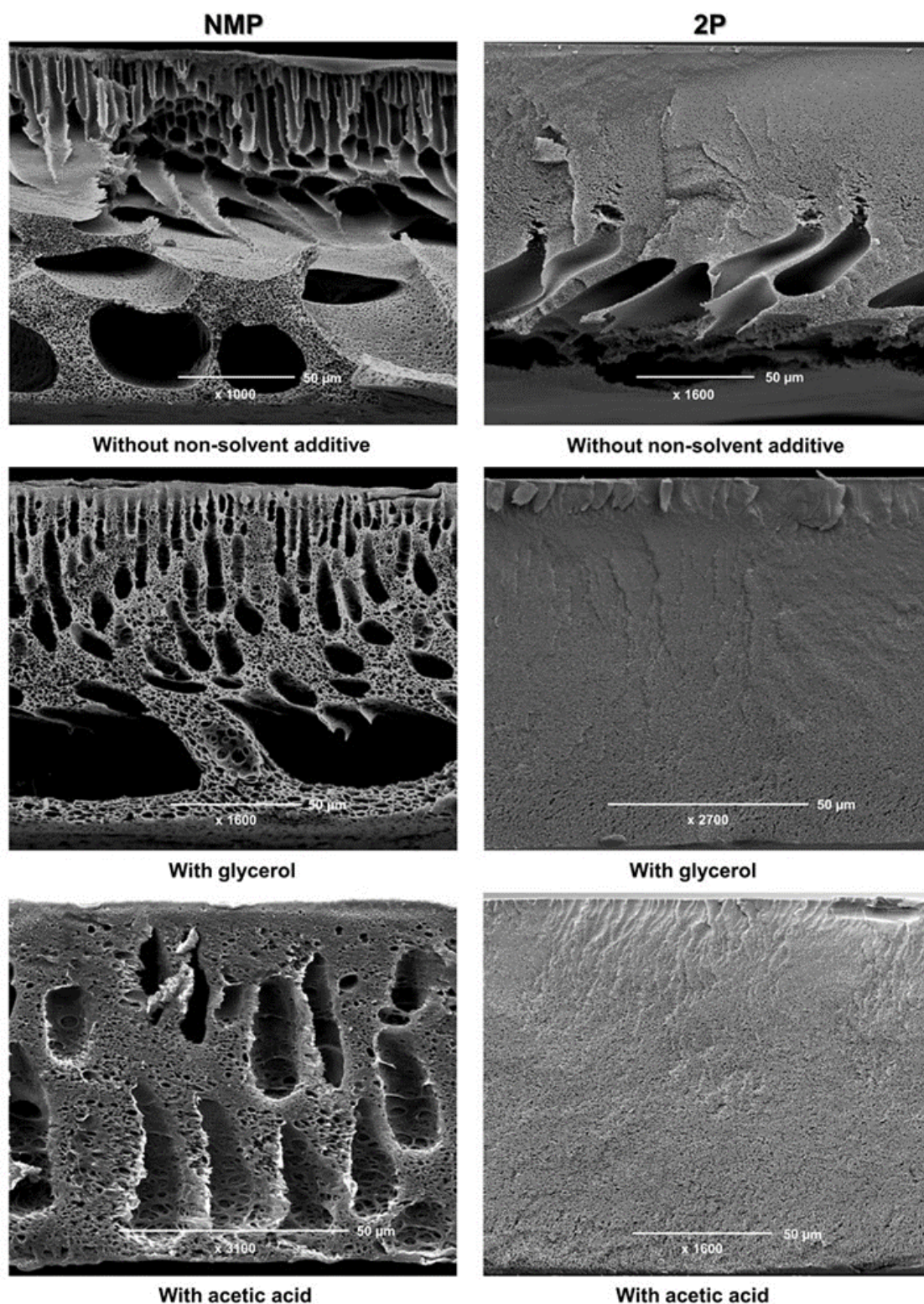


Figure S1 Scanning electron microscopy cross-section images of PES membranes prepared by immersion precipitation with water tempered to 20 °C as non-solvent, where the polymer dope solutions were prepared with 2.5 wt.% glycerol or 5.0 wt.% acetic acid as different non-solvent additives, as well as with 16.88 wt.% PES, 0.84 wt.% PVP and either 7.5 wt.% water in case of NMP (c) or 3.5 wt.% in case of 2P (d) as solvent (image recording potential of 12.5 kV).

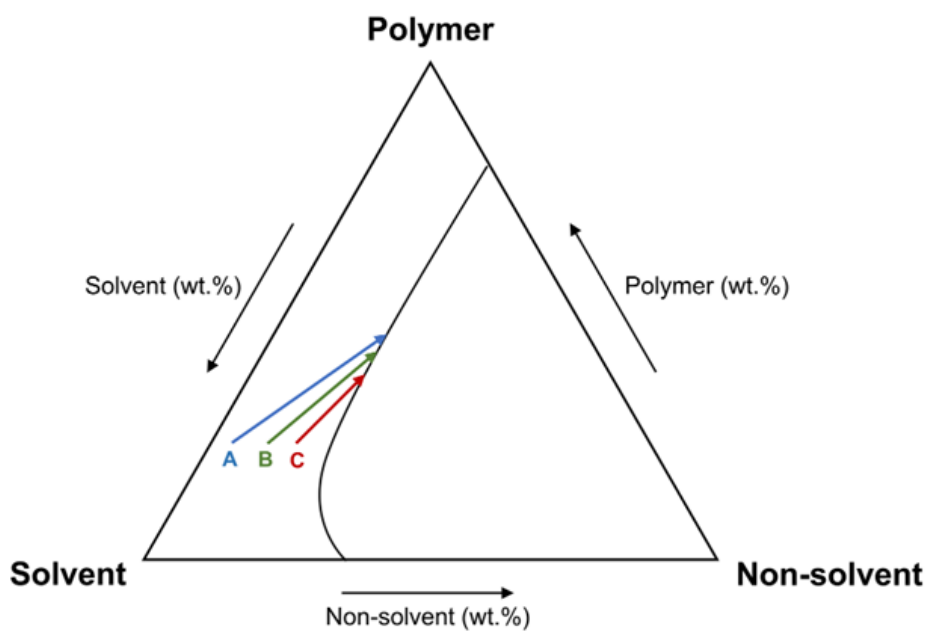


Figure S2 Schematic depiction of the influence of the non-solvent amount in the dope solution on the entry point into the miscibility gap with an increasing non-solvent amount from A to C.

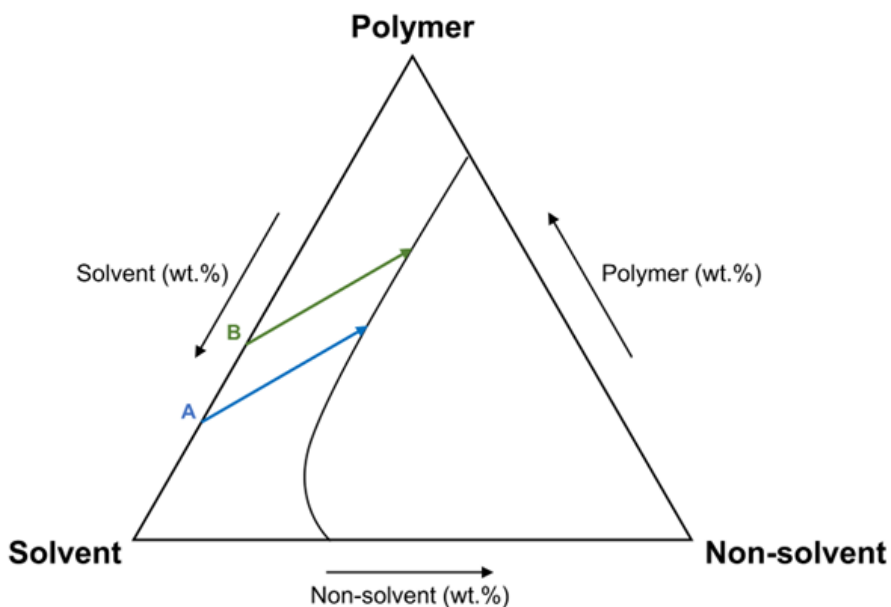


Figure S3 Schematic depiction of the influence of the polymer amount in the dope solution on the entry point into the miscibility gap with an increasing polymer amount from A to B.

## 5 Summary and Conclusion

Nowadays, polymeric membranes produced by immersion precipitation are widely applied in different areas of application. Depending on the ultimate field of operation, certain demands are placed onto the membranes. However, in order to enable the fabrication of membranes with desired features, the membrane formation process has to be well-understood. Although several studies have been conducted in the past on membrane formation via phase inversion, the results of different research groups are somewhat contradictory. Furthermore, the emerging topic of substituting hazardous solvents through less harmful alternatives requires continuing studies involving the potential alternative solvents and which therefore further increase the insight into the process fundamentals.

This is why the motivation of this work was to gain an improved understanding of the mechanisms, which impact membrane formation via non-solvent induced phase separation. Since the replacement of hazardous solvents is currently a critical topic, one of the main focuses was laid onto the comparison of the investigated membrane formation variables between conventional and alternative solvents.

To reach the formulated goal of this work, a holistic study of the influencing process control parameter was designed. Therefore, the work was divided up into three different parts, which focused on different key aspects. All together, these three parts should cover the two crucial process fundamentals, which include the thermodynamic aspects of the membrane formation process on one hand and the kinetic aspects of this process on the other hand.

As one main aspect, the characterization of the polymer solution thermodynamics was emphasized. Since the previously applied common methods bring along several disadvantages, a novel method for the determination of the polymer solution phase diagrams was developed. In the frame of a method validation it could be shown that the novel procedure provides reproducible and reliable results. Furthermore, an exemplary ternary system of PES/NMP/water was investigated and the outcomes between the state-of-the-art cloud point method and the novel procedure were compared. It could be shown that both methods result in a similar location of the miscibility gap. However, it was proven that the novel method provides more information about the polymer solution thermodynamics than the cloud point procedure. Apart from the location of the binodal curve, it was confirmed that the exact phase compositions can be determined by the novel method. On top of that, further information delivered by the developed procedure include an indication of the solidification boundary and an exact allocation of the polymer molecular weight distribution in the two phases. Therefore, the developed method contributes to an advanced understanding of the system of interest, which in turn can be used to improve the control of the membrane formation process. It is a valuable tool for characterizing new polymer solution systems, especially with respect to a solvent substitution, and therefore contributes to the development of new solutions for the fabrication of membranes via immersion precipitation.

Nonetheless, the thermodynamics of a system cannot be considered alone for the design of the respective membrane formation process. This is why another main focus was laid onto the different process parameters, which can be varied during membrane fabrication via NIPS. These variables does not only influence the thermodynamics, but also the kinetics of the membrane formation process.

It could be shown that both, the polymer solution composition as well as the precipitation conditions are suitable process parameters for controlling the resulting membranes features. The variables, which can be used to affect the formation process with respect to the dope solution composition, were found to involve the concentrations and molecular weights of the additives PVP and PEG, the concentration of the membrane-forming polymer, and the use of the non-solvents water, glycerol or acetic acid in different concentrations. While the effects observed for PEG additions were rather small, all other of these parameters were demonstrated to offer a powerful opportunity for controlling the membrane characteristics and therefore for obtaining membranes with any required features. On top of that, it could be proven that both, the precipitation temperature and the precipitation medium in the non-solvent bath, are two further powerful tools to adapt the kinetics of the NIPS mechanisms and therefore to control the properties of the resulting membranes. Apart from the already mentioned variables, however, it was shown that one of the most significant impact factors is the choice of the solvent used for the preparation of the membrane dope solutions. It was demonstrated that the exchange of the solvent, without adapting the rest of the solution composition, can change the fundamental mechanisms occurring during NIPS.

Since the substitution of hazardous solvents through non-carcinogenic alternatives is currently of high interest, the results gained from this work are of high relevance. Usually, the existing membrane products have to maintain their previous structures and performances, although one component of the dope solution they are prepared of is substituted by another one. Therefore, this work presents a valuable pool of different possibilities for controlling the changes caused by a solvent substitution, in order to maintain the demanded membrane features. On top of that, this thesis presents 2P and DML as two novel alternative solvents for the preparation of PES ultrafiltration membranes.

All in all, the findings of this work provide a broader mechanistic understanding of the membrane formation process via immersion precipitation and the underlying thermodynamic and kinetic processes. Therefore, the knowledge gained from this work, which was performed in a laboratory scale, can be transferred to the production of membranes in a pilot or production scale. This can on one hand be used in case of the substitution of a hazardous solvent through a less harmful alternative. However, the outcomes of these works can also be used to optimize the structure or performance of existing membranes, or to develop completely new membrane fabrication processes for the launching of advanced membrane products to the existing ultrafiltration market.

## 6 References

- [1] M. Mulder, *Basic Principles of Membrane Technology*, Kluwer Academic Publishers, Dordrecht, Boston, London, 1996.
- [2] L.K. Wang, J.P. Chen, Y.-T. Hung, N.K. Shamas (Eds.), *Membrane and Desalination Technologies*, Springer Science & Business Media, New York, 2011.
- [3] H. Watson, *Biological membranes*, *Essays Biochem* 59 (2015) 43–69.
- [4] R. van Reis, A. Zydney, *Bioprocess membrane technology*, *Journal of Membrane Science* 297 (2007) 16–50.
- [5] H. Strathmann, H. Chmiel, *Membranen in der Verfahrenstechnik*, *Chemie Ingenieur Technik* 57 (1985) 581–596.
- [6] K.K. Sirkar, *Separation of Molecules, Macromolecules and Particles: Principles, Phenomena and Processes*, Cambridge University Press, Cambridge, 2014.
- [7] X. Li, J. Li, *Fluxes and Driving Forces in Membrane Separation Processes*, in: E. Drioli, L. Giorno (Eds.), *Encyclopedia of Membranes*, Springer Berlin Heidelberg, Berlin, Heidelberg, 2015, pp. 1–3.
- [8] A. Figoli, A. Criscuoli, *Sustainable Membrane Technology for Water and Wastewater Treatment*, 1st ed., Springer, 2017.
- [9] T. Matsuura, *Synthetic membranes and membrane separation processes*, CRC Press, 1993.
- [10] B. Ladewig, M.N.Z. Al-Shaeli, *Fundamentals of Membrane Processes*, in: B. Ladewig, M.N.Z. Al-Shaeli (Eds.), *Fundamentals of Membrane Bioreactors: Materials, Systems and Membrane Fouling*, Springer Singapore, Singapore, 2017, pp. 13–37.
- [11] H. Verweij, *Inorganic membranes*, *Nanotechnology / Separation engineering* 1 (2012) 156–162.
- [12] B. Ladewig, M.N.Z. Al-Shaeli (Eds.), *Fundamentals of Membrane Bioreactors: Materials, Systems and Membrane Fouling*, Springer Singapore, Singapore, 2017.
- [13] H. Fröhlich, L. Villian, D. Melzner, J. Strube, *Membrane Technology in Bioprocess Science*, *Chemie Ingenieur Technik* 84 (2012) 905–917.
- [14] K.-V. Peinemann, S. Pereira Nunes, *Polymermembranen*, in: K. Ohlrogge, K. Ebert (Eds.), *Membranen: Grundlagen, Verfahren und industrielle Anwendungen*, Wiley-VCH Verlag GmbH & Co. KGaA, 2006, pp. 1–21.
- [15] K. Ohlrogge, K. Ebert (Eds.), *Membranen: Grundlagen, Verfahren und industrielle Anwendungen*, Wiley-VCH Verlag GmbH & Co. KGaA, 2006.
- [16] P. Abaticchio, A. Bottino, G.C. Roda, G. Capannelli, S. Munari, *Characterization of ultrafiltration polymeric membranes*, *Desalination* 78 (1990) 235–255.
- [17] C. Charcosset, *Membrane processes in biotechnology and pharmaceuticals*, Elsevier, Amsterdam, Heidelberg, London [u.a], 2012.
- [18] H.-W. Rösler, *Membrantechnologie in der Prozessindustrie – Polymere Membranwerkstoffe*, *Chemie Ingenieur Technik* 77 (2005) 487–503.
- [19] R.W. Baker, *Membrane technology and applications*, 3rd ed., John Wiley & Sons, Ltd, 2012.
- [20] H.K. Lonsdale, U. Merten, R.L. Riley, *Transport properties of cellulose acetate osmotic membranes*, *Journal of Applied Polymer Science* 9 (1965) 1341–1362.

- [21] C. Charcosset, Membrane processes in biotechnology: An overview, *Biotechnology Advances* 24 (2006) 482–492.
- [22] E. Walitza, N. Stroh, H. Brunner, Synthetische Membranen: Stofftransport, Herstellung, Verwendung 53 (2002) 208–216.
- [23] A. Mehta, A.L. Zydney, Effect of Membrane Charge on Flow and Protein Transport during Ultrafiltration, *Biotechnology Progress* 22 (2008) 484–492.
- [24] P. Kosiol, C. Kahrs, V. Thom, M. Ulbricht, B. Hansmann, Investigation of virus retention by size exclusion membranes under different flow regimes, *Biotechnology Progress* 35 (2019) e2747.
- [25] K.-V. Peinemann, S.P. Nunes (Eds.), *Membranes for the Life Sciences*, WILEY-VCH Verlag, Weinheim, 2008.
- [26] S.R. Wickramasinghe, E.D. Stump, D.L. Grzenia, S.M. Husson, J. Pellegrino, Understanding virus filtration membrane performance, *Journal of Membrane Science* 365 (2010) 160–169.
- [27] T. Melin, R. Rautenbach, *Membranverfahren: Grundlagen der Modul- und Anlagenauslegung*, 3rd ed., Springer Berlin Heidelberg, Berlin, Heidelberg, 2007.
- [28] C. Zhou, Z. Hou, X. Lu, Z. Liu, X. Bian, L. Shi, L. Li, Effect of Polyethersulfone Molecular Weight on Structure and Performance of Ultrafiltration Membranes, *Industrial & Engineering Chemistry Research* 49 (2010).
- [29] E.Y. Astakhov, S.F. Zhironkin, I.M. Kolganov, E.R. Klinshpont, P.G. Tsarin, Study of the formation of the porous structure of membranes during phase separation of a poly(ester sulfone) solution, *Polymer Science Series A* 53 (2011) 613–620.
- [30] F.P. Cuperus, C.A. Smolders, Characterization of UF membranes: Membrane characteristics and characterization techniques, *Advances in Colloid and Interface Science* 34 (1991) 135–173.
- [31] G.R. Guillen, Y. Pan, M. Li, E.M.V. Hoek, Preparation and Characterization of Membranes Formed by Nonsolvent Induced Phase Separation: A Review, *Industrial & Engineering Chemistry Research* 50 (2011) 3798–3817.
- [32] M. Liu, Y.-M. Wei, Z.-L. Xu, R.-Q. Guo, L.-B. Zhao, Preparation and characterization of polyethersulfone microporous membrane via thermally induced phase separation with low critical solution temperature system, *Journal of Membrane Science* 437 (2013) 169–178.
- [33] J. Barzin, B. Sadatnia, Correlation between macrovoid formation and the ternary phase diagram for polyethersulfone membranes prepared from two nearly similar solvents, *Journal of Membrane Science* 325 (2008) 92–97.
- [34] X. Tian, Z. Wang, S. Zhao, S. Li, J. Wang, S. Wang, The influence of the nonsolvent intrusion through the casting film bottom surface on the macrovoid formation, *Journal of Membrane Science* 464 (2014) 8–19.
- [35] S.S. Prakash, L.F. Francis, L.E. Scriven, Microstructure evolution in dry–wet cast polysulfone membranes by cryo-SEM: A hypothesis on macrovoid formation, *Journal of Membrane Science* 313 (2008) 135–157.
- [36] Muthusamy Sivakumar, Doraisamy Raju Mohan, Ramamoorthy Rangarajan, Yoshiharu Tsujita, Studies on cellulose acetate–polysulfone ultrafiltration membranes: I. Effect of polymer composition, *Polymer International* 54 (2005) 956–962.
- [37] R. van Reis, A. Zydney, Membrane separations in biotechnology, *Current Opinion in Biotechnology* 12 (2001) 208–211.

- [38] S. Vidya, A. Vijayalakshmi, A. Nagendran, D. Mohan, Effect of Additive Concentration on Cellulose Acetate Blend Membranes-Preparation, Characterization and Application Studies, *Separation Science and Technology* 43 (2008) 1933–1954.
- [39] H. Strathmann, The use of membranes in downstream processing, *Food Biotechnology* 4 (1990) 253–272.
- [40] A. Akbari, R. Yegani, Study on the Impact of Polymer Concentration and Coagulation Bath Temperature on the Porosity of Polyethylene Membranes Fabricated Via TIPS Method, *Journal of Membrane and Separation Technology* 1 (2012) 100–107.
- [41] H. Strathmann, K. Kock, The formation mechanism of phase inversion membranes, *Desalination* 21 (1977) 241–255.
- [42] B.S. Lalia, V. Kochkodan, R. Hashaiekh, N. Hilal, A review on membrane fabrication: Structure, properties and performance relationship, *Desalination* 326 (2013) 77–95.
- [43] Sadrzadeh M, Bhattacharjee S, Rational design of phase inversion membranes by tailoring thermodynamics and kinetics of casting solution using polymer additives, *Journal of Membrane Science* 441 (2013) 31–44.
- [44] H. Strathmann, *Introduction to Membrane Science and Technology*, Wiley, 2011.
- [45] W. Pusch, A. Walch, *Synthetische Membranen — Herstellung, Struktur und Anwendung*, *Angewandte Chemie* 94 (1982) 670–695.
- [46] J.T. Jung, J.F. Kim, H.H. Wang, E. Di Nicolo, E. Drioli, Y.M. Lee, Understanding the non-solvent induced phase separation (NIPS) effect during the fabrication of microporous PVDF membranes via thermally induced phase separation (TIPS), *Journal of Membrane Science* 514 (2016) 250–263.
- [47] A.K. Hořda, I.F.J. Vankelecom, Understanding and guiding the phase inversion process for synthesis of solvent resistant nanofiltration membranes, *Journal of Applied Polymer Science* 132 (2015).
- [48] R.M. Boom, T. van den Boomgaard, J.W.A. van den Berg, C.A. Smolders, Linearized cloudpoint curve correlation for ternary systems consisting of one polymer, one solvent and one non-solvent, *Polymer* 34 (1993) 2348–2356.
- [49] A. Figoli, T. Marino, S. Simone, E. Di Nicolo, X.-M. Li, T. He, S. Tornaghi, E. Drioli, Towards non-toxic solvents for membrane preparation: a review, *Green Chemistry* 16 (2014) 4034–4059.
- [50] S.S. Madaeni, L. Bakhtiari, Thermodynamic-based predictions of membrane morphology in water/dimethylsulfoxide/polyethersulfone systems, *Polymer* 53 (2012) 4481–4488.
- [51] Dongliang Wang, K. Li, S. Sourirajan, W. K. Teo, Phase separation phenomena of polysulfone/solvent/organic nonsolvent and polyethersulfone/solvent/organic nonsolvent systems, *Journal of Applied Polymer Science* 50 (1993) 1693–1700.
- [52] J.T. Tsai, Y.S. Su, D.M. Wang, J.L. Kuo, J.Y. Lai, A. Deratani, Retainment of pore connectivity in membranes prepared with vapor-induced phase separation, *Journal of Membrane Science* 362 (2010) 360–373.
- [53] V.P. Khare, A.R. Greenberg, W.B. Krantz, Vapor-induced phase separation—effect of the humid air exposure step on membrane morphology: Part I. Insights from mathematical modeling, *Journal of Membrane Science* 258 (2005) 140–156.
- [54] S.A. Altinkaya, B. Ozbas, Modeling of asymmetric membrane formation by dry-casting method, *Journal of Membrane Science* 230 (2004) 71–89.



- [55] T. Marino, E. Blasi, S. Tornaghi, E. Di Nicolò, A. Figoli, Polyethersulfone membranes prepared with Rhodiasolv®Polarclean as water soluble green solvent, *Journal of Membrane Science* 549 (2018) 192–204.
- [56] C. Barth, M.C. Gonçalves, A.T.N. Pires, J. Roeder, B.A. Wolf, Asymmetric polysulfone and polyethersulfone membranes: effects of thermodynamic conditions during formation on their performance, *Journal of Membrane Science* 169 (2000) 287–299.
- [57] M.B. Ghandashtani, F. Zokaei Ashtiani, M. Karimi, A. Fouladitajar, A novel approach to fabricate high performance nano-SiO<sub>2</sub> embedded PES membranes for microfiltration of oil-in-water emulsion, *Applied Surface Science* 349 (2015) 393–402.
- [58] Y. Yip, A.J. McHugh, Modeling and simulation of nonsolvent vapor-induced phase separation, *Journal of Membrane Science* 271 (2006) 163–176.
- [59] K.-J. Baik, J.Y. Kim, H.K. Lee, S.C. Kim, Liquid–liquid phase separation in polysulfone/polyethersulfone/N-methyl-2-pyrrolidone/water quaternary system, *Journal of Applied Polymer Science* 74 (1999) 2113–2123.
- [60] A. Idris, Z. Man, A.S. Maulud, M.S. Khan, S. Suetsugu, Effects of Phase Separation Behavior on Morphology and Performance of Polycarbonate Membranes, *Membranes* 7 (2017) 21.
- [61] L. Yu, F. Yang, M. Xiang, Phase separation in a PSf/DMF/water system: a proposed mechanism for macrovoid formation, *RSC Advances* 4 (2014) 42391–42402.
- [62] B. Chakrabarty, A.K. Ghoshal, M.K. Purkait, Preparation, characterization and performance studies of polysulfone membranes using PVP as an additive, *Journal of Membrane Science* 315 (2008) 36–47.
- [63] V. Kaiser, C. Stropnik, Membranes from polysulfone/N, N-dimethylacetamide/water system; structure and water flux, *Acta Chimica Slovenica* 47 (2000) 205–214.
- [64] G.R. Guillen, G.Z. Ramon, H.P. Kavehpour, R.B. Kaner, E.M.V. Hoek, Direct microscopic observation of membrane formation by nonsolvent induced phase separation, *Journal of Membrane Science* 431 (2013) 212–220.
- [65] C. Barth, B.A. Wolf, Quick and reliable routes to phase diagrams for polyethersulfone and polysulfone membrane formation, *Macromolecular Chemistry and Physics* 201 (2000) 365–374.
- [66] H.J. Lee, B. Jung, Y.S. Kang, H. Lee, Phase separation of polymer casting solution by nonsolvent vapor, *Journal of Membrane Science* 245 (2004) 103–112.
- [67] E. Drioli, L. Giorno (Eds.), *Encyclopedia of Membranes*, Springer Berlin Heidelberg, Berlin, Heidelberg, 2015.
- [68] L.J. Zeman, A.L. Zydney, *Microfiltration and Ultrafiltration: Principles and Applications*, 1st ed., CRC Press, Boca Raton, 1996.
- [69] J.S. Walker, C.A. Vause, *Wiederkehrende Phasen*, *Spektrum der Wissenschaft* 86 (1987).
- [70] P.W. Atkins, J. de Paula, *Physikalische Chemie*, 4th ed., Wiley-VCH Verlag GmbH & Co. KGaA, Weinheim, 2006.
- [71] L. Keshavarz, M.A. Khansary, S. Shirazian, Phase diagram of ternary polymeric solutions containing nonsolvent/solvent/polymer: Theoretical calculation and experimental validation, *Polymer* 73 (2015) 1–8.
- [72] A. Glowacki, *Berechnung des Flüssigkeits-Flüssigkeits-Gleichgewichtes von Polymerlösungen mit dem UNIFAC-RFVT-Modell*. Dissertation, Halle-Wittenberg, 1999.

- [73] H. Matsuyama, M. Teramoto, T. Uesaka, M. Goto, F. Nakashio, Kinetics of droplet growth in the metastable region in cellulose acetate/acetone/nonsolvent system, *Journal of Membrane Science* 152 (1999) 227–234.
- [74] J.Y. Kim, Y.D. Kim, T. Kanamori, H.K. Lee, K.-J. Baik, S.C. Kim, Vitrification phenomena in polysulfone/NMP/water system, *Journal of Applied Polymer Science* 71 (1999) 431–438.
- [75] S.-G. Li, T. van den Boomgaard, C.A. Smolders, H. Strathmann, Physical Gelation of Amorphous Polymers in a Mixture of Solvent and Nonsolvent, *Macromolecules* 29 (1996) 2053–2059.
- [76] M. Mulder, MEMBRANE PREPARATION | Phase Inversion Membranes, in: I.D. Wilson (Ed.), *Encyclopedia of Separation Science*, Academic Press, Oxford, 2000, pp. 3331–3346.
- [77] X. Tan, D. Rodrigue, A Review on Porous Polymeric Membrane Preparation. Part I: Production Techniques with Polysulfone and Poly (Vinylidene Fluoride), *Polymers* 11 (2019) 1160.
- [78] I.M. Wienk, R.M. Boom, M.A.M. Beerlage, A.M.W. Bulte, C.A. Smolders, H. Strathmann, Recent advances in the formation of phase inversion membranes made from amorphous or semi-crystalline polymers, *Journal of Membrane Science* 113 (1996) 361–371.
- [79] C. Stropnik, L. Germič, B. Žerjal, Morphology variety and formation mechanisms of polymeric membranes prepared by wet phase inversion, *Journal of Applied Polymer Science* 61 (1996) 1821–1830.
- [80] S.T. Bromley, Zwijnenburg Martijn A., *Computational Modeling of Inorganic Nanomaterials*, 1st ed., CRC Press, Boca Raton, 2016.
- [81] Z. Liu, Z. Cui, Y. Zhang, S. Qin, F. Yan, J. Li, Fabrication of polysulfone membrane via thermally induced phase separation process, *Materials Letters* 195 (2017) 190–193.
- [82] S.M. Mousavi, A. Zadhoush, Investigation of the relation between viscoelastic properties of polysulfone solutions, phase inversion process and membrane morphology: The effect of solvent power, *Journal of Membrane Science* 532 (2017) 47–57.
- [83] R. Khanna, N.K. Agnihotri, M. Vashishtha, A. Sharma, P.K. Jaiswal, S. Puri, Kinetics of spinodal phase separation in unstable thin liquid films, *Physical Review E* 82 (2010) 11601.
- [84] H. Chae Park, Y. Po Kim, H. Yong Kim, Y. Soo Kang, Membrane formation by water vapor induced phase inversion, *Journal of Membrane Science* 156 (1999) 169–178.
- [85] P. van de Witte, P.J. Dijkstra, J.W.A. van den Berg, J. Feijen, Phase separation processes in polymer solutions in relation to membrane formation, *Journal of Membrane Science* 117 (1996) 1–31.
- [86] R. Finsy, On the Critical Radius in Ostwald Ripening, *Langmuir* 20 (2004) 2975–2976.
- [87] S. Kasapis, I.T. Norton, J.B. Ubbink (Eds.), *Modern Biopolymer Science*, Academic Press, San Diego, 2009.
- [88] I. Pinnau, B.D. Freeman, Formation and Modification of Polymeric Membranes: Overview, in: *Membrane Formation and Modification*, American Chemical Society, 1999, pp. 1–22.
- [89] J.G. Wijmans, J.P.B. Baaij, C.A. Smolders, The mechanism of formation of microporous or skinned membranes produced by immersion precipitation, *Journal of Membrane Science* 14 (1983) 263–274.
- [90] F.W. Altena, Phase separation phenomena in cellulose acetate solutions in relation to asymmetric membrane formation, 1982.
- [91] H. Wijmans, *Synthetic Membranes: On the mechanisms of formation of membranes and the concentration polarization phenomenon in ultrafiltration*. Dissertation, Enschede, 1984.

- [92] H. Strathmann, K. Kock, P. Amar, R.W. Baker, The formation mechanism of asymmetric membranes, *Desalination* 16 (1975) 179–203.
- [93] C.A. Smolders, A.J. Reuvers, R.M. Boom, I.M. Wienk, Microstructures in phase-inversion membranes. Part 1. Formation of macrovoids, *Journal of Membrane Science* 73 (1992) 259–275.
- [94] M.A. Frommer, R.M. Messalem, Mechanism of Membrane Formation. VI. Convective Flows and Large Void Formation during Membrane Precipitation, *Product R&D* 12 (1973) 328–333.
- [95] H.J. Kim, R.K. Tyagi, A.E. Fouda, K. Jonasson, The kinetic study for asymmetric membrane formation via phase-inversion process, *Journal of Applied Polymer Science* 62 (1996) 621–629.
- [96] T.-H. Young, L.-W. Chen, Pore formation mechanism of membranes from phase inversion process, *Desalination* 103 (1995) 233–247.
- [97] F.P. Byrne, S. Jin, G. Paggiola, T.H.M. Petchey, J.H. Clark, T.J. Farmer, A.J. Hunt, C. Robert McElroy, J. Sherwood, Tools and techniques for solvent selection: green solvent selection guides, *Sustainable Chemical Processes* 4 (2016) 7.
- [98] Á. Botos, J.D. Graham, Z. Illés, Industrial chemical regulation in the European Union and the United States: a comparison of REACH and the amended TSCA, *Journal of Risk Research* 22 (2019) 1187–1204.
- [99] E.S. Williams, J. Panko, D.J. Paustenbach, The European Union's REACH regulation: a review of its history and requirements, *Critical Reviews in Toxicology* 39 (2009) 553–575.
- [100] European Chemicals Agency, Understanding REACH, <https://echa.europa.eu/de/regulations/reach/understanding-reach>, accessed 25 November 2019.
- [101] A. Mohammad, *Green solvents I: Properties and applications in chemistry*, 1st ed., Springer Science & Business Media, 2012.
- [102] P.T. Anastas, J.C. Warner, *Green chemistry: Theory and Practice*, Oxford University Press, New York, 1998.
- [103] A. Ivanković, A. Dronjić, A.M. Bevanda, S. Talić, Review of 12 Principles of Green Chemistry in Practice, *International Journal of Sustainable and Green Energy* 6 (2017) 39–48.
- [104] H.N. Cheng, R.A. Gross, P.B. Smith, *Green polymer chemistry: biobased materials and biocatalysis*, ACS Publications, Washington DC, 2015.
- [105] H.H. Wang, J.T. Jung, J.F. Kim, S. Kim, E. Drioli, Y.M. Lee, A novel green solvent alternative for polymeric membrane preparation via nonsolvent-induced phase separation (NIPS), *Journal of Membrane Science* 574 (2019) 44–54.
- [106] X. Dong, A. Al-Jumaily, I.C. Escobar, Investigation of the Use of a Bio-Derived Solvent for Non-Solvent-Induced Phase Separation (NIPS) Fabrication of Polysulfone Membranes, *Membranes* 8 (2018) 23.
- [107] N. Evenepoel, S. Wen, M. Tilahun Tsehaye, B. van der Bruggen, Potential of DMSO as greener solvent for PES ultra- and nanofiltration membrane preparation, *Journal of Applied Polymer Science* 135 (2018) 46494.
- [108] J. Chang, J. Zuo, L. Zhang, G.S. O'Brien, T.-S. Chung, Using green solvent, triethyl phosphate (TEP), to fabricate highly porous PVDF hollow fiber membranes for membrane distillation, *Journal of Membrane Science* 539 (2017) 295–304.

- [109] X. Dong, H.D. Shannon, I.C. Escobar, Investigation of PolarClean and Gamma-Valerolactone as Solvents for Polysulfone Membrane Fabrication, in: *Green Polymer Chemistry: New Products, Processes, and Applications*, American Chemical Society, 2018, pp. 385–403.
- [110] M.A. Rasool, I.F.J. Vankelecom, Use of  $\gamma$ -valerolactone and glycerol derivatives as bio-based renewable solvents for membrane preparation, *Green Chemistry* 21 (2019) 1054–1064.
- [111] T. Marino, F. Galiano, A. Molino, A. Figoli, New frontiers in sustainable membrane preparation: Cyrene™ as green bioderived solvent, *Journal of Membrane Science* 580 (2019) 224–234.
- [112] M.L. Huggins, Some Properties of Solutions of Long-chain Compounds, *The Journal of Physical Chemistry* 46 (1942) 151–158.
- [113] P.J. Flory, *Principles of polymer chemistry*, Cornell University Press, 1953.
- [114] L. Zeman, G. Tkacik, Thermodynamic analysis of a membrane-forming system water/N-methyl-2-pyrrolidone/polyethersulfone, *Journal of Membrane Science* 36 (1988) 119–140.
- [115] T. Lindvig, M.L. Michelsen, G.M. Kontogeorgis, A Flory–Huggins model based on the Hansen solubility parameters, *Fluid Phase Equilibria* 203 (2002) 247–260.
- [116] J. Barzin, B. Sadatnia, Theoretical phase diagram calculation and membrane morphology evaluation for water/solvent/polyethersulfone systems, *Polymer* 48 (2007) 1620–1631.
- [117] P.T.P. Aryanti, D. Ariono, A.N. Hakim, I.G. Wenten, Flory-Huggins Based Model to Determine Thermodynamic Property of Polymeric Membrane Solution, *Journal of Physics: Conference Series* 1090 (2018) 12074.
- [118] A. Ghasemi, M. Asgarpour Khansary, M.A. Aroon, A comparative theoretical and experimental study on liquid-liquid equilibria of membrane forming polymeric solutions, *Fluid Phase Equilibria* 435 (2017) 60–72.
- [119] M. Metze, *Untersuchungen zur Bildung von porösen Membranen aus Cellulosederivaten nach dem Verdunstungsverfahren*. Dissertation, Hannover, 2014.
- [120] S.A. Al Malek, M.N. Abu Seman, D. Johnson, N. Hilal, Formation and characterization of polyethersulfone membranes using different concentrations of polyvinylpyrrolidone, *Desalination* 288 (2012) 31–39.
- [121] M. Amirilargani, E. Saljoughi, T. Mohammadi, M.R. Moghbeli, Effects of coagulation bath temperature and polyvinylpyrrolidone content on flat sheet asymmetric polyethersulfone membranes, *Polymer Engineering & Science* 50 (2010) 885–893.
- [122] A.F. Ismail, A.R. Hassan, Effect of additive contents on the performances and structural properties of asymmetric polyethersulfone (PES) nanofiltration membranes, *Separation and Purification Technology* 55 (2007) 98–109.
- [123] E. Saljoughi, M. Amirilargani, T. Mohammadi, Effect of poly(vinyl pyrrolidone) concentration and coagulation bath temperature on the morphology, permeability, and thermal stability of asymmetric cellulose acetate membranes, *Journal of Applied Polymer Science* 111 (2009) 2537–2544.
- [124] D.B. Mosqueda-Jimenez, R.M. Narbaitz, T. Matsuura, G. Chowdhury, G. Pleizier, J.P. Santerre, Influence of processing conditions on the properties of ultrafiltration membranes, *Journal of Membrane Science* 231 (2004) 209–224.

- [125] M.-J. Han, S.-T. Nam, Thermodynamic and rheological variation in polysulfone solution by PVP and its effect in the preparation of phase inversion membrane, *Journal of Membrane Science* 202 (2002) 55–61.
- [126] K.-W. Lee, B.-K. Seo, S.-T. Nam, M.-J. Han, Trade-off between thermodynamic enhancement and kinetic hindrance during phase inversion in the preparation of polysulfone membranes, *Desalination* 159 (2003) 289–296.
- [127] J. Abdoul Raguime, G. Arthanareeswaran, P. Thanikaivelan, D. Mohan, M. Raajenthiren, Performance characterization of cellulose acetate and poly(vinylpyrrolidone) blend membranes, *Journal of Applied Polymer Science* 104 (2007) 3042–3049.
- [128] B. Jung, J.K. Yoon, B. Kim, H.-W. Rhee, Effect of molecular weight of polymeric additives on formation, permeation properties and hypochlorite treatment of asymmetric polyacrylonitrile membranes, *Journal of Membrane Science* 243 (2004) 45–57.
- [129] D. Wang, K. Li, W.K. Teo, Preparation and characterization of polyvinylidene fluoride (PVDF) hollow fiber membranes, *Journal of Membrane Science* 163 (1999) 211–220.
- [130] Z. Zhang, Q. An, Y. Ji, J. Qian, C. Gao, Effect of zero shear viscosity of the casting solution on the morphology and permeability of polysulfone membrane prepared via the phase-inversion process, *Desalination* 260 (2010) 43–50.
- [131] Z.-L. Xu, T.-S. Chung, Y. Huang, Effect of polyvinylpyrrolidone molecular weights on morphology, oil/water separation, mechanical and thermal properties of polyetherimide/polyvinylpyrrolidone hollow fiber membranes, *Journal of Applied Polymer Science* 74 (1999) 2220–2233.
- [132] N.A. Ochoa, P. Prádanos, L. Palacio, C. Pagliero, J. Marchese, A. Hernández, Pore size distributions based on AFM imaging and retention of multidisperse polymer solutes: Characterisation of polyethersulfone UF membranes with dopes containing different PVP, *Journal of Membrane Science* 187 (2001) 227–237.
- [133] R.M. Boom, I.M. Wienk, T. van den Boomgaard, C.A. Smolders, Microstructures in phase inversion membranes. Part 2. The role of a polymeric additive, *Journal of Membrane Science* 73 (1992) 277–292.
- [134] J. Barzin, S.S. Madaeni, H. Mirzadeh, M. Mehrabzadeh, Effect of polyvinylpyrrolidone on morphology and performance of hemodialysis membranes prepared from polyether sulfone, *Journal of Applied Polymer Science* 92 (2004) 3804–3813.
- [135] H.-T. Yeo, S.-T. Lee, M.-J. Han, Role of a Polymer Additive in Casting Solution in Preparation of Phase Inversion Polysulfone Membranes, *Journal of Chemical Engineering of Japan* 33 (2000) 180–184.
- [136] J.S. Kang, Y.M. Lee, Effects of molecular weight of polyvinylpyrrolidone on precipitation kinetics during the formation of asymmetric polyacrylonitrile membrane, *Journal of Applied Polymer Science* 85 (2002) 57–68.
- [137] H. Matsuyama, T. Maki, M. Teramoto, K. Kobayashi, Effect of PVP Additive on Porous Polysulfone Membrane Formation by Immersion Precipitation Method, *Separation Science and Technology* 38 (2003) 3449–3458.
- [138] A. Idris, N. Mat Zain, M.Y. Noordin, Synthesis, characterization and performance of asymmetric polyethersulfone (PES) ultrafiltration membranes with polyethylene glycol of different molecular weights as additives, *Desalination* 207 (2007) 324–339.

- [139] Y. Ma, F. Shi, J. Ma, M. Wu, J. Zhang, C. Gao, Effect of PEG additive on the morphology and performance of polysulfone ultrafiltration membranes, *Desalination* 272 (2011) 51–58.
- [140] E. Saljoughi, M. Amirilargani, T. Mohammadi, Effect of PEG additive and coagulation bath temperature on the morphology, permeability and thermal/chemical stability of asymmetric CA membranes, *Desalination* 262 (2010) 72–78.
- [141] E. Saljoughi, M. Sadrzadeh, T. Mohammadi, Effect of preparation variables on morphology and pure water permeation flux through asymmetric cellulose acetate membranes, *Journal of Membrane Science* 326 (2009) 627–634.
- [142] H.-B. Li, W.-Y. Shi, Y.-F. Zhang, D.-Q. Liu, X.-F. Liu, Effects of additives on the morphology and performance of PPTA/PVDF in Situ Blend UF membrane, *Polymers* 6 (2014) 1846–1861.
- [143] J.-H. Kim, K.-H. Lee, Effect of PEG additive on membrane formation by phase inversion, *Journal of Membrane Science* 138 (1998) 153–163.
- [144] B. Chakrabarty, A.K. Ghoshal, M.K. Purkait, Effect of molecular weight of PEG on membrane morphology and transport properties, *Journal of Membrane Science* 309 (2008) 209–221.
- [145] B. Chakrabarty, A.K. Ghoshal, M.K. Purkait, SEM analysis and gas permeability test to characterize polysulfone membrane prepared with polyethylene glycol as additive, *Journal of Colloid and Interface Science* 320 (2008) 245–253.
- [146] Q.-Z. Zheng, P. Wang, Y.-N. Yang, Rheological and thermodynamic variation in polysulfone solution by PEG introduction and its effect on kinetics of membrane formation via phase-inversion process, *Journal of Membrane Science* 279 (2006) 230–237.
- [147] Q.-Z. Zheng, P. Wang, Y.-N. Yang, D.-J. Cui, The relationship between porosity and kinetics parameter of membrane formation in PSF ultrafiltration membrane, *Journal of Membrane Science* 286 (2006) 7–11.
- [148] Y. Liu, G.H. Koops, H. Strathmann, Characterization of morphology controlled polyethersulfone hollow fiber membranes by the addition of polyethylene glycol to the dope and bore liquid solution, *Journal of Membrane Science* 223 (2003) 187–199.
- [149] G. Arthanareeswaran, P. Thanikaivelan, K. Srinivasn, D. Mohan, M. Rajendran, Synthesis, characterization and thermal studies on cellulose acetate membranes with additive, *European Polymer Journal* 40 (2004) 2153–2159.
- [150] Z.-L. Xu, F. Alsahy Qusay, Polyethersulfone (PES) hollow fiber ultrafiltration membranes prepared by PES/non-solvent/NMP solution, *Journal of Membrane Science* 233 (2004) 101–111.
- [151] B.K. Chaturvedi, A.K. Ghosh, V. Ramachandhran, M.K. Trivedi, M.S. Hanra, B.M. Misra, Preparation, characterization and performance of polyethersulfone ultrafiltration membranes, *Desalination* 133 (2001) 31–40.
- [152] W.-L. Hung, D.-M. Wang, J.-Y. Lai, S.-C. Chou, On the initiation of macrovoids in polymeric membranes—effect of polymer chain entanglement, *Journal of Membrane Science* 505 (2016) 70–81.
- [153] J.-F. Li, Z.-L. Xu, H. Yang, Microporous polyethersulfone membranes prepared under the combined precipitation conditions with non-solvent additives, *Polymers for Advanced Technologies* 19 (2008) 251–257.
- [154] J. Peng, Y. Su, W. Chen, Q. Shi, Z. Jiang, Effects of Coagulation Bath Temperature on the Separation Performance and Antifouling Property of Poly(ether sulfone) Ultrafiltration Membranes, *Industrial & Engineering Chemistry Research* 49 (2010) 4858–4864.

- [155] A. Amelio, G. Genduso, S. Vreysen, P. Luis, B. van der Bruggen, Guidelines based on life cycle assessment for solvent selection during the process design and evaluation of treatment alternatives, *Green Chemistry* 16 (2014) 3045–3063.
- [156] C. Capello, U. Fischer, K. Hungerbühler, What is a green solvent? A comprehensive framework for the environmental assessment of solvents, *Green Chemistry* 9 (2007) 927–934.
- [157] T. Marino, F. Galiano, S. Simone, A. Figoli, DMSO EVOL™ as novel non-toxic solvent for polyethersulfone membrane preparation, *Environmental Science and Pollution Research* 26 (2019) 14774–14785.
- [158] G. Arthanareeswaran, V.M. Starov, Effect of solvents on performance of polyethersulfone ultrafiltration membranes: Investigation of metal ion separations, *Desalination* 267 (2011) 57–63.
- [159] D.S. Lakshmi, A. Figoli, M.G. Buonomenna, G. Golemme, E. Drioli, Preparation and characterization of porous and nonporous polymeric microspheres by the phase inversion process, *Advances in Polymer Technology* 31 (2012) 231–241.
- [160] Y.L. Thuyavan, N. Anantharaman, G. Arthanareeswaran, A.F. Ismail, Impact of solvents and process conditions on the formation of polyethersulfone membranes and its fouling behavior in lake water filtration, *Journal of Chemical Technology & Biotechnology* 91 (2016) 2568–2581.
- [161] N.T. Hassankiadeh, Z. Cui, J.H. Kim, D.W. Shin, S.Y. Lee, A. Sanguineti, V. Arcella, Y.M. Lee, E. Drioli, Microporous poly(vinylidene fluoride) hollow fiber membranes fabricated with PolarClean as water-soluble green diluent and additives, *Journal of Membrane Science* 479 (2015) 204–212.
- [162] J. Sherwood, M. de bruyn, A. Constantinou, L. Moity, C.R. McElroy, T.J. Farmer, T. Duncan, W. Raverty, A.J. Hunt, J.H. Clark, Dihydrolevoglucosenone (Cyrene) as a bio-based alternative for dipolar aprotic solvents, *Chemical Communications* 50 (2014) 9650–9652.
- [163] S. Mazinani, S. Darvishmanesh, A. Ehsanzadeh, B. van der Bruggen, Phase separation analysis of Extem/solvent/non-solvent systems and relation with membrane morphology, *Journal of Membrane Science* 526 (2017) 301–314.
- [164] J. Xu, Y. Tang, Y. Wang, B. Shan, L. Yu, C. Gao, Effect of coagulation bath conditions on the morphology and performance of PSf membrane blended with a capsaicin-mimic copolymer, *Journal of Membrane Science* 455 (2014) 121–130.
- [165] C. Kahrs, M. Metze, C. Fricke, J. Schwellenbach, Thermodynamic analysis of polymer solutions for the production of polymeric membranes, *Journal of Molecular Liquids* 291 (2019) 111351.
- [166] C. Kahrs, J. Schwellenbach, Membrane formation via non-solvent induced phase separation using sustainable solvents: A comparative study, *Polymer* 186 (2020) 122071.
- [167] C. Kahrs, T. Gühlstorf, J. Schwellenbach, Influences of different preparation variables on polymeric membrane formation via nonsolvent induced phase separation, *Journal of Applied Polymer Science* (2019) 48852.

## 7 Appendix

### 7.1 List of Abbreviations

°C	<u>C</u> entigrade
μm	<u>M</u> icrom <u>e</u> ter
2P	<u>2</u> - <u>p</u> yrrolidone
Da	<u>D</u> alton <u>s</u>
DMAc	<u>D</u> imethy <u>a</u> cetamide
DMF	<u>D</u> imethy <u>f</u> ormamide
DML	<u>D</u> imethy <u>l</u> actamide
DMSO	<u>D</u> imethy <u>s</u> ulfo <u>o</u> xide
EIPS	<u>E</u> vapora <u>i</u> on i <u>n</u> duced p <u>h</u> ase s <u>e</u> paration
FDA	<u>F</u> ood and <u>D</u> rug <u>A</u> ssocia <u>t</u> ion
kDa	<u>K</u> ilo <u>d</u> alton <u>s</u>
mPa·s	<u>M</u> illi <u>p</u> ascal s <u>e</u> conds
NIPS	<u>N</u> on-solvent i <u>n</u> duced p <u>h</u> ase s <u>e</u> paration
nm	<u>N</u> ano <u>m</u> eter
NMP	<u>N</u> - <u>m</u> ethyl-2- <u>p</u> yrrolidone
PA	<u>P</u> oly <u>a</u> mid <u>e</u>
PEG	<u>P</u> oly <u>e</u> thylene glycol
PES	<u>P</u> oly <u>e</u> ther <u>s</u> ulfone
pH	<i>Potentia hydrogenii</i> (power of hydrogen)
Polarclean	Rhodiasolv® <u>P</u> olar <u>c</u> lean
PSf	<u>P</u> oly <u>s</u> ulfone
PVDF	<u>P</u> oly <u>v</u> inylidene <u>f</u> luoride
PVP	<u>P</u> oly <u>v</u> inyl <u>p</u> yrrolidone
REACH	<u>R</u> egulation, <u>e</u> valuation and <u>a</u> uthorization of <u>c</u> hemicals
TIPS	<u>T</u> emperature i <u>n</u> duced p <u>h</u> ase s <u>e</u> paration
VIPS	<u>V</u> apor i <u>n</u> duced p <u>h</u> ase s <u>e</u> paration
wt. %	<u>W</u> eigh <u>t</u> percent



## 7.2 List of Figures

<b>Figure 1</b> Schematic illustration of a membrane separation process (adapted from Mulder) [1] .....	4
<b>Figure 2</b> Schematic illustration of membrane cross-section morphologies (adapted from Rösler) [18] .....	5
<b>Figure 3</b> Classification of size-exclusion based membrane processes (adapted from van Reis and Zydney) [4] ....	6
<b>Figure 4</b> Scanning electron microscopy image showing the typical structure of an ultrafiltration membrane .....	7
<b>Figure 5</b> Scanning electron microscopy image of an ultrafiltration membrane with a finger-like (a) and a sponge-like (b) morphology .....	7
<b>Figure 6</b> Schematic illustration of the different steps during the immersion precipitation process .....	9
<b>Figure 7</b> Schematic illustration of a membrane casting line for membrane production via immersion precipitation (adapted from Strathmann) [44].....	10
<b>Figure 8</b> Representative phase diagram for the thermodynamic description of a ternary polymeric system at constant pressure and temperature (adapted from Mulder) [1].....	12
<b>Figure 9</b> Free enthalpy of mixing as a function of the substance amount fraction in a phase diagram [72].....	13
<b>Figure 10</b> Schematic illustration of structure forming mechanism in dependence of the point of entry into the heterogeneous region of the ternary phase diagram (adapted from Stropnik et al.) [79] .....	14
<b>Figure 11</b> Schematic illustration of the development of macrovoids (adapted from Mulder) [1] .....	19
<b>Figure 12</b> Depiction of the twelve principles of green chemistry .....	21
<b>Figure 13</b> Graphical abstract of the publication “Thermodynamic analysis of polymer solutions for the production of polymeric membranes” [165] .....	30
<b>Figure 14</b> Graphical abstract of the publication “Membrane formation via non-solvent induced phase separation using green solvents: A comparative study” [166] .....	49
<b>Figure 15</b> Graphical abstract of the publication “Influences of different preparation variables on membrane formation via non-solvent induced phase separation in dependence of the applied solvent system” [167] .....	75

## 8 List of Publications

### 8.1 Journal Articles

C. Kahrs, M. Metze, C. Fricke, J. Schwellenbach, Thermodynamic analysis of polymer solutions for the production of polymeric membranes. *Journal of Molecular Liquids*, **291**, 2019, 111351. DOI: doi.org/10.1016/j.molliq.2019.111351.

- Kahrs (80 %): Method development; Planning, execution and coordination of the experiments; Data analysis and interpretation of the results; Preparation of the manuscript
- Fricke (15 %): Support in the execution of the experiments
- Metze/Schwellenbach (5 % in total): Supervision during method development; Discussion of results; Paper review

C. Kahrs, J. Schwellenbach, Membrane formation via non-solvent induced phase separation using sustainable solvents: A comparative study. *Polymer*, **186**, 2020, 122071. DOI: doi.org/10.1016/j.polymer.2019.122071.

- Kahrs (95 %): Method development; Planning, execution and coordination of the experiments; Data analysis and interpretation of the results; Preparation of the manuscript
- Schwellenbach (5 %): Supervision; Discussion of results; Paper review

C. Kahrs, T. Gühlstorf, J. Schwellenbach, Influences of different preparation variables on polymeric membrane formation via non-solvent induced phase separation. *Journal of Applied Polymer Science*, early view online publication, 2019, 48852. DOI: doi.org/10.1002/app.48852.

- Kahrs (85 %): Method development; Planning, execution and coordination of the experiments; Data analysis and interpretation of the results; Preparation of the manuscript
- Gühlstorf (10 %): Support in the execution of the experiments
- Schwellenbach (5 %): Supervision; Discussion of results; Paper review

## 8.2 Conference Contributions

C. Kahrs, J. Schwellenbach, B. Hansmann, T. Scheper, Herstellung von Polymermembranen mittels Fällbadverfahren: Methoden zur Gießlösungsentwicklung. Poster presentation, Jahrestreffen der ProcessNet-Fachgruppen Fluidverfahrenstechnik, Membrantechnik und Mischvorgänge, Munich, Germany, 27<sup>th</sup> – 28<sup>th</sup> February 2018.

C. Kahrs, Investigations of the formation of porous membranes during the immersion precipitation process. Oral presentation, 16<sup>th</sup> Network Young Membrains, Valencia, Spain, 05<sup>th</sup> – 07<sup>th</sup> July 2018.

C. Kahrs, J. Schwellenbach, M. Metze, B. Hansmann, Polymer solution thermodynamics: Examining the phase separation behavior of polymer solutions for the production of macroporous membranes via NIPS. Poster presentation, Euromembrane, Valencia, Spain, 9<sup>th</sup> – 13<sup>th</sup> July 2018.

C. Kahrs, J. Schwellenbach, B. Hansmann, Membrane formation: Influences of polymeric additives in different solvent systems. Poster presentation, Gordon Research Seminar: Materials and Processes, New London, NH, USA, 11<sup>th</sup> – 12<sup>th</sup> August 2018.

C. Kahrs, J. Schwellenbach, B. Hansmann, Membrane formation: Influences of polymeric additives in different solvent systems. Poster presentation, Gordon Research Conference: Materials and Processes, New London, NH, USA, 12<sup>th</sup> – 17<sup>th</sup> August 2018.

C. Kahrs, J. Schwellenbach, Membrane formation: Influences of polymeric additives in different solvent systems. Poster presentation, Engineering with Membranes Conference, Båstad, Sweden, 8<sup>th</sup> – 10<sup>th</sup> April 2019.

C. Kahrs, J. Schwellenbach, Membrane formation: Influences of polymeric additives in different solvent systems. Poster presentation, North American Membrane Society 28<sup>th</sup> Annual Meeting, Pittsburgh, PA, USA, 11<sup>th</sup> – 15<sup>th</sup> May 2019.

## 9 Curriculum Vitae

---

### Personal Data

Name: Catharina Kahrs  
 Date of birth: 18<sup>th</sup> September 1992  
 Place of birth: Bremen, Germany

### School Education

1998 - 2002 Elementary school Tarmstedt  
 2002 - 2008 Comprehensive school Tarmstedt  
 2008 - 2011 High school Tarmstedt

### Academic Studies

10/2011 - 02/2015 Bachelor of Science, International Degree Program Industrial and Environmental Biology, University of Applied Sciences, Bremen, Germany  
 Thesis: "Production of an active pharmaceutical ingredient against *Candida glabrata* based on a bacterial exoenzyme mixture - Upstream processes"

07/2013 – 11/2013 Semester abroad, University of the Sunshine Coast, Sippy Downs, Australia

03/2015 – 09/2016 Master of Science, International Degree Program Industrial and Environmental Biology, University of Applied Sciences, Bremen, Germany  
 Thesis: "Investigation of the retention mechanisms of virus particles based on model systems applied to mesoporous membranes"

### Professional Experience

02/2014 - 06/2014 Internship, Iron Metabolism Laboratory, QIMR Berghofer Medical Research Institute, Brisbane, Australia

08/2015 - 02/2016 Internship, Development Membrane Technologies: Precipitation Technology, Sartorius Stedim Biotech GmbH, Göttingen, Germany

02/2016 - 09/2016 Master thesis, Development Membrane Technologies: Precipitation Technology, Sartorius Stedim Biotech GmbH, Göttingen, Germany

09/2016 - 12/2016 Student trainee, Development Membrane Technologies: Precipitation Technology, Sartorius Stedim Biotech GmbH, Göttingen, Germany

01/2017 – 01/2020 Doctoral Student, Institute of Technical Chemistry, Gottfried Wilhelm Leibniz University Hannover in cooperation with the Sartorius Stedim Biotech GmbH, Göttingen, Germany